



UNIVERSITÀ DEGLI STUDI DI TRENTO



QUEEN MARY
UNIVERSITY OF LONDON

Erasmus Mundus Joint Doctorate School in Science for Management of Rivers and their Tidal System

Politti Emilio

Investigating and modelling the interaction among vegetation, hydrodynamics and morphology





November, 2017

Doctoral thesis in Science for Management of Rivers and their Tidal System,

IV Cohort

University of Trento - Department of Civil, Environmental and Mechanical Engineering

Queen Mary University of London – School of Geography

Edmund Mach Foundation

Supervisors

Walter, Bertoldy, University of Trento

Alexander J., Henshaw, Queen Mary University of London

Academic year **2016/2017**.



Erasmus Mundus
Joint Doctorate Programme



SMART - Science for Management of Rivers and their Tidal systems

The SMART Joint Doctorate Programme

Research for this thesis was conducted with the support of the Erasmus Mundus Programme¹, within the framework of the Erasmus Mundus Joint Doctorate (EMJD) SMART (Science for Management of Rivers and their Tidal systems). EMJDs aim to foster cooperation between higher education institutions and academic staff in Europe and third countries with a view to creating centres of excellence and providing a highly skilled 21st century workforce enabled to lead social, cultural and economic developments. All EMJDs involve mandatory mobility between the universities in the consortia and lead to the award of recognised joint, double or multiple degrees.

The SMART programme represents a collaboration among the University of Trento, Queen Mary University of London, and Freie Universität Berlin. Each doctoral candidate within the SMART programme has conformed to the following during their 3 years of study:

- (i) Supervision by a minimum of two supervisors in two institutions (their primary and secondary institutions).
- (ii) Study for a minimum period of 6 months at their secondary institution
- (iii) Successful completion of a minimum of 30 ECTS of taught courses
- (iv) Collaboration with an associate partner to develop a particular component / application of their research that is of mutual interest.
- (v) Submission of a thesis within 3 years of commencing the programme.

¹This project has been funded with support from the European Commission. This publication reflects the views only of the author, and the Commission cannot be held responsible for any use which may be made of the information contained therein

Acknowledgements

Thank you to the Edmund Mach Foundation for the training and the instrumentation required in the field work, Angela Gurnell my supervisors and my colleagues for their precious advice and my family and Patty Battistig for the support during these years and particularly during the last months.

Abstract

The dissertation presented in this manuscript contributes to river science by providing a detailed overview on the state of the art on the interaction between riparian vegetation and hydrogeomorphological processes, by devising a novel model encompassing most of such processes and by proposing a field methodology aimed at providing means for improving the modelling of such interactions. The state of the art is summarized in an extensive review describing riparian vegetation and hydrogeomorphological processes mutual feedbacks. Such review did not simply seek to describe these feedbacks but, compiling from a large array of results from field, laboratory and modelling studies, provides a set of physical thresholds that trigger system changes. Therefore, processes are not only described terms but also explained with a quantitative approach. Processes description provided the conceptual foundation for the development of the novel simulation model while model parameterization was based on the quantitative information collected in the review. Such novel model, encompasses the main relationships entwining riparian woody vegetation and hydrogeomorphological processes and is able of replicating long term riparian landscape dynamics considering disturbance events, environmental stressor and riparian woody vegetation establishment from seeds and large wood. The manuscript presents the model structure and its conceptual validation by means of hydrological scenarios aimed at testing the coherence of the simulation results with expected system behaviour. Examples of such coherences are vegetation growth rate in response to hydrological regime, entrainment and establishment of large wood in an unconfined river system and vegetation effect on erosion and deposition patterns.

Analysis of sedimentation patterns from the modelled results suggested that vegetation flow resistance should be modelled with greater detail. These conclusions pointed the dissertation research towards the testing of a novel class of vegetation flow resistance equations, proposed by different authors, able of describing woody vegetation flow resistance on a physical basis. These equations have the advantage of considering flow stage, plants foliation level and species-specific flexibility. However, the use of such equations is limited by the difficulty of measuring the vegetation properties required as equation-inputs. In order to test if these equations could effectively improve sediment dynamics predictions, a field method was formulated and tested. The field method allows to sample vegetation properties that can be used with these novel class of flow resistance equations. In the manuscript, such method is applied and the resulting vegetation properties used in several modelling scenarios. Such scenario proved that hydraulic variables modelled with these novel flow resistance approaches are more realistic and thus that the model developed during the dissertation could benefit from inclusion of such flow resistance equations in its source code.

Contents

Abstract	5
Introduction	13
Background and motivation	13
Riparian vegetation ecological succession and hydrogeomorphological processes	14
Riparian vegetation hydrodynamics and morphology numerical modelling history	19
Thesis objectives	21
Thesis outline	21
1 Mutual feedbacks between the riparian Salicaceae and fluvial processes: a quantitative review	23
1.1 Introduction	23
1.2 Processes conceptual hierarchy	24
1.3 Salicaceae feedbacks to fluvial processes	26
1.3.1 Roots	26
1.3.1.1 Substrate cohesiveness	27
1.3.2 Canopy and stem	29
1.3.2.1 Flow resistance	29
1.3.2.2 Flow deflection	30
1.3.2.3 Effects of flow alteration on sediment transport, erosion and deposition	32
1.4 Fluvial process feedbacks to Salicaceae	33
1.4.1 Water flow	33
1.4.1.1 Groundwater depth	33
1.4.1.2 Waterlogging and submersion	38
1.4.1.3 Drag	40
1.4.2 Sediment transport	44
1.4.2.1 Erosion	44
1.4.2.2 Deposition	45
1.5 Discussion and conclusions	47
2 Fuzzy modelling of riparian vegetation dynamics and fluvial processes feedbacks	60
2.1 Introduction	60
2.2 Methods	62
2.2.1 Caesar Lisflood-Fp	62
2.2.2 Riparian vegetation model component	62
2.2.2.1 Fuzzy logic principles in ecological modeling	63
2.2.3 Integration of physical and biological processes	64
2.2.4 Cumulative disturbance effects	65
2.2.5 RVM submodels	65
2.2.5.1 Fuzzy seed recruitment	65
2.2.5.2 Growth	66
2.2.5.3 Fuzzy erosion and shear stress	66
2.2.5.4 Fuzzy deposition mortality and bending	67
2.2.5.5 Fuzzy hydric stress	68
2.2.5.6 Fuzzy moisture habitat suitability	68
2.2.5.7 Fuzzy flood duration	69
2.2.5.8 LW lifecycle	69
2.2.5.9 Fuzzy roughness	70
2.2.6 Test cases	71

2.2.6.1	Test 1: Groundwater feedback	73
2.2.6.2	Test 2: Vegetation feedback on sediment transport	74
2.2.6.3	Test 3: LW lifecycle	75
2.3	Results	78
2.3.1	Test 1: Water table feedback to biomass increase and distribution	78
2.3.2	Test 2: Vegetation feedback to sediment erosion and deposition	81
2.3.3	Test 3: Large Wood lifecycle and vegetation distribution response to disturbance regime	82
2.3.3.1	LW entrainment and deposition location	82
2.3.3.2	Stranding locations quantification and first year survival locations	86
2.3.3.3	LW stranding elevation	88
2.3.3.4	LW geomorphic interactions	89
2.3.3.5	Simulated landscape evolution	92
2.4	Discussion and conclusions	96
3	Optical field measurement of flexible vegetation properties to derive spatially-variable estimates of flow resistance for use in hydrodynamic models	184
3.1	Introduction	184
3.2	Materials and methods	185
3.2.1	Field measurements and analysis of vegetation properties	185
3.2.1.1	Leaf area measurement	186
3.2.1.2	Frontal area measurement	188
3.2.2	Flow resistance estimation	189
3.2.3	Flow resistance sensitivity	190
3.2.3.1	Sensitivity to empirical parameters set and foliation	190
3.2.3.2	Sensitivity to reference areas measurements	190
3.2.4	Flow resistance modelling	190
3.2.4.1	Hydrodynamic model	190
3.2.4.2	Modelled scenarios	192
3.3	Results	194
3.3.1	Vegetation properties and relationship with height	194
3.3.2	Flow resistance sensitivity	195
3.3.2.1	Empirical parameters set and foliation	195
3.3.2.2	Reference areas	198
3.3.2.3	Flow resistance scenarios	199
3.4	Discussion and conclusions	204
	Conclusions	207
	Bibliography	211

List of Figures

Figure 1-1 Process hierarchy of vegetation feedbacks to fluvial processes ..25	25
Figure 1-2 Process hierarchy of fluvial process feedbacks to vegetation.....25	25
Figure 1-3 Tensile strength per unit area calculated for three species of Salicaceae with Eq. 1. Data sources: (Pollen and Simon, 2005; Polvi et al., 2014; Simon et al., 2006) 26	26
Figure 1-4 Modelled Populus fremontii and Salix nigra increase in soil cohesion in relation to age. Data source: (Pollen-Bankhead and Simon, 2009).29	29
Figure 1-5 Effects of a finite width patch on the flow field horizontal dimension. Adapted from (Nepf, 2012)31	31
Figure 1-6 Effects of a circular patch on the flow field horizontal dimension. Adapted from (Nepf, 2012)31	31
Figure 1-7 Effects on the flow field vertical distribution of a submerged (A) and partially submerged (B) patch. Adapted from (Baptist et al., 2009) and (Nepf and Vivoni, 2000)32	32
Figure 1-8 Scour and deposition measured in a flume experiment, for a channel side and a centre bar with flexible objects simulating flexible submerged vegetation. Scour was measured upstream and on the sides of the bars, deposition was measured downstream from the bars. Plant density is the ratio of the projected area of the flexible objects and the area of each bar. In the charts, a plant density of 1 indicates a solid, non-flexible object with the same bar area and object height as that of the flexible objects. Data source: Chen, Kuo & Yen 2012b33	33
Figure 1-9 Survival of seed-recruited seedlings under different water table decline rates (Data source: Table 1-5)34	34
Figure 1-10 Mean shoot (top) and root (bottom) weight percentage variations in response to inundation (flooding depth and duration varies; see Table 1-6)40	40
Figure 1-11 Mortality of Salix spp. cuttings due to deposition, erosion and shear stress (Pasquale et al., 2014)41	41
Figure 1-12 Relationship between breaking momentum and trunk diameter for S. subfragilis from laboratory experiments. PB: Plastic Bending, TB: Trunk Breakage (adapted from Tanaka and Yagisawa, 2009)43	43
Figure 1-13 Relationship between the dimensionless particle shear stress and dimensionless critical particle shear stress and morphodynamic bending effects (with τ^*_{84} dimensionless shear stress acting on d_{84} particle size, τ^*_{c84} dimensionless critical shear stress for d_{84} particle size motion, τ^*_{50} dimensionless shear stress acting on d_{50} particle size, τ^*_{c50} dimensionless critical shear stress for d_{50} particle size motion). Region A: quasi-clear scour: only particles smaller than d_{50} are mobilized. Region B: bed partial scour: particles in the range of the d_{50} are entrained, possibly causing local armouring. Region C: bed scour: particles in the range of the d_{84} are entrained, thus causing local erosion. Adapted from Tanaka & Yagisawa (2009).45	45
Figure 1-14 Relative burial percentage and survivorship of 1-3 years old seedlings of Populus fremontii with heights ranging from 14 to 69 cm. Data extracted from Kui & Stella (2016)47	47
Figure 1-15 Relevant water stage thresholds and time scales affecting riparian Salicaceae recruitment, growth and survival51	51
Figure 2-1 Fuzzy sets shapes available in RVM. Adapted from (I.E.C., 2000) .63	63

Figure 2-2 CLF and RVM submodels and feedbacks integration schema	64
Figure 2-3 Conceptualization of deposition effect on RDMD and plants' height. RDMD: root density maximum depth, H: plant height, d: deposition, β : bending angle resulting from deposition	68
Figure 2-4 Initial vegetation distribution derived for the simulated reach	73
Figure 2-5 Normal flow regime (A) and Sustained low flows scenarios (B) hydrographs used to test flow regime feedback to vegetation growth performance	74
Figure 2-6 Hydrograph of a Tagliamento 10 year recurrence interval flood used to simulate vegetation feedback to sediment transport processes.....	75
Figure 2-7 Initial vegetation for the LW lifecycle test case.....	77
Figure 2-8 Hydrograph used to simulate LW recruitment and establishment	77
Figure 2-9 Cumulative biomass in the modelling domain pixels vegetated at the beginning of the undrying and drying scenarios	78
Figure 2-10 Total vegetation biomass for the undrying and undrying scenarios	79
Figure 2-11 Vegetated area in the drying and undrying scenarios	79
Figure 2-12 Vegetation age distribution of the last simulated year of the Sustained low flow scenario scenario	80
Figure 2-13 Vegetation age distribution of the last simulated year of the Normal flow regime	80
Figure 2-14 Eroded and deposited sediment volumes in the areas covered by vegetation in the vegetated and unvegetated scenarios	81
Figure 2-15 Erosion, deposition and stable areas of the vegetated areas for the vegetated and unvegetated scenarios	82
Figure 2-16 LW deposition positions after the first simulated year.....	83
Figure 2-17 A: potential LW sources before the 1st year May flood. B: potential LW sources after the 1st year May flood and LW stranding locations.....	84
Figure 2-18 A: potential LW sources before the 1st year November flood. B: potential LW sources after the 1st year November flood and LW stranding locations.	85
Figure 2-19 Erosion and deposition at the stranding locations of the LW entrained during the 1st year floods	86
Figure 2-20 Resprouting wood deposited by the first year flood events	86
Figure 2-21 Stranding elevation above the detrended topography of the first simulated year	89
Figure 2-22 1st year survival elevation above the detrended topography of the first simulated year	89
Figure 2-23 A: Median particle size (D50) of the 2nd simulated year, in the locations where LW deposited in the 1st year resprouted. B: D50 of the 2nd simulated year in locations where LW depositions did not occur.....	91
Figure 2-24 A: histogram of the median particle size (D50) of the second simulated year. B: boxplot of the median particle size (D50) of the second simulated year.	92
Figure 2-25 Vegetation age and LW stranding positions at the end of each simulated year. Red and blue circles in panel A marks two river segments whose development over the years show some similarities with development patterns observed on similar landforms of the Tagliamento	93

Figure 2-26 Side channel filling observed on the Tagliamento upstream from the modelled site. Blue arrow on 2003 image indicates the flow direction	95
Figure 3-1 Graphical representation of the leaf area sampling performed by placing the camera at different heights. On the top rows, examples of resulting HPs in foliated and defoliated conditions. Note how gap fraction increases as camera position heightens.	188
Figure 3-2 Shape and position of the vegetation in the two modelled scenarios. In both scenarios, flow direction goes from the left edge to the right one.	192
Figure 3-3 Measured values of PAI, STAI and FAI, and interpolation lines, as a function of the relative height	194
Figure 3-4 Friction factors modelled and yield from direct measures on fully submerged specimens. Modelled friction factors are computed assuming a complete submersion, using Equation 18 and Equation 19 to compute FAI and LAI and Equation 1 to compute friction factor. SC: Salix Caprea, SR: Salix Rubens, MW: Mountain Willow, HW: Hybrid Willow, SV: Salix Viminalis, SCL: Salix Caprea Low, SCH: Salix Caprea High. Image in colour available online	196
Figure 3-5 Friction factors calculated with Equation 1 assuming foliated and defoliated condition and different flow velocities. Legend entries ending with “F” represent Foliated conditions, while those ending with “D” Defoliated conditions. Empirical parameters acronyms: Salix Caprea (SC), Salix Caprea Low (SCL), Salix Caprea High (SCH), Salix Rubens (SR), Salix Viminalis (SV).	197
Figure 3-6 Sensitivity to LAI and FAI of Equation 1 applied with Salix rubens parameters. Red dotted line represents the friction factor value calculated without any variation	199
Figure 3-7 Chart in the left column depict the ratio between the water depth simulated using Equation 1 and the water depths using fixed Manning’s coefficients. Charts in the left column are instead the value of Manning’s n. In the charts of both columns, the x axis represents the x coordinate on the longitudinal dimension of the vegetated bank. Manning’s n fixed values: 0.045 (VBN0045), 0.062 (VBN0062) and 0.098 (VBN0098). VBSRF: Salix Rubens Foliated, VBSRD: Salix Rubens Defoliated.	201
Figure 3-8 Left column contains boxplots of the ratio between bed shear stress modelled with Equation 1, in foliated conditions and using SR parameters and the bed shear stress modelled in defoliated conditions and with a fixed roughness. X axis entries marked with “IS” represent the bed shear stress values inside the centre island, while those unmarked are yield from the bulk of shear stress values in the analysis reach. Right column contains the boxplots of the Manning’s n coefficients inside the centre island. Manning’s n fixed values: 0.045 (CIN0045), 0.062 (CIN0062) and 0.098 (CIN0098). CISRF: Salix Rubens Foliated, CISRD: Salix Rubens Defoliated.	203
Figure 3-9 Bed shear stress in the analysis reach at full submersion. Flow direction is from left to right, the yellow edge marks the position of the centre island.	204

List of Tables

Table 1-1	Roots reinforcement estimated by RipRoot model for a bank 10 m long and a shear surface length of 1.15 m (Pollen and Simon, 2005)	28
Table 1-2	Maximum groundwater depth for survival of Populus and Salix species (expanded from Lite and Stromberg, 2005)	37
Table 1-3	Groundwater depth thresholds and corresponding timescales affecting Salicaceae processes	38
Table 1-4	Percentiles of the pullout forces measured on seedlings with different root frontal area and rooted in different substrates. Seedlings rooted in finer sediments generally exhibit higher pullout forces because of the higher friction due to the larger roots-substrate contact surface. (Data source: Bywater-Reyes et al., 2015)	44
Table 1-5	Experimental and observed water table decline rates, root elongation, substrates and germinations survival percentages of seedlings and cuttings. * Field observation; ** Controlled experiment; *** Field experiment. W Weight, L Length. s Seedling, c Cutting	52
Table 1-6	Shoot and root growth responses to flooding stress experiments	56
Table 1-7	Factors controlling riparian species asexual reproduction and survival. *Asexual mode: 1flood training, 2: translocated fragments, 3: coppice re-growth, 4: suckering. **Site specific (observed). ***From summer river stage. ****Elevation relative to nearest vegetated surface. ***** Measured with respect to the lower limit of established floodplain forest. a Field study. b Controlled experiment c Field experiment	59
Table 2-1	Initial vegetation properties estimated according to distance from the growing season water table	72
Table 2-2	Allometric relationships relating height and diameter at breast height to Populus Nigra age	73
Table 2-3	Stranding and 1st year survival percentages calculated on the total number of locations and percentage of 1st year survival per location calculated on the total stranding per location	87
Table 2-4	Wood mass storage percentages measured on the Tagliamento in the summer of 1998 on two river reaches located immediately upstream and downstream of the modelled reach. Data extracted from Gurnell, Petts, Harris, et al., (2000)	87
Table 2-5	Percentage of dead and live (resprouting) wood measured on the Tagliamento in the summer of 1998 on two river reaches located immediately upstream and downstream of the modelled reach. Data extracted from: Gurnell et al., (2000a)	88
Table 2-6	CLF and RVM inputs and units of measures. * Mandatory input	1
Table 2-7	CLF parameters. Adapted from Ziliani et al., (2013)	2
Table 2-8	Sediment input grain sizes and distribution (Ziliani, 2011)	2
Table 2-9	Model parameters, their units, description, values applied in the test case and submodels by which parameters are used	3
Table 2-10	Description of the linguistic variables, their units, direction (input or output) and submodels by which the linguistic variables are used	5
Table 2-11	Fuzzy sets linguistic terms, memberships, shapes and literature used for their definition. Shapes: RL: right linear, TRA: trapezoidal, TRI: triangular, LL: left linear,	

SING: singleton. Numbers preceding the shapes shortcut mark the control points of the sets shapes.	8
Table 2-12 Fuzzy rules applied in each submodel	179
Table 3-1 Equation 1 empirical parameters. a Jalonen & Järvelä, (2014), b Västilä & Järvelä (2014)	189
Table 3-2 Scenarios-simulations, flow resistance modelling solution and corresponding acronyms	193
Table 3-3 Regression equations and LAI derived equation relating relative height and reference areas. Note that LAI equation is yield from Eq. 4 and 5 and thus does not have an R².	195

Introduction

Background and motivation

Mankind is depending upon freshwater availability since its early times. In the latest centuries, the dependency went far beyond the simple physiological needs: besides supplying human settlements for civil purposes, freshwater is in fact also used for manufacturing goods, processing staples, intensive agriculture and not less importantly, electricity production. All these uses put a significant pressure on water resources (Dudgeon et al., 2006); when considering rivers, in many cases (e.g. water extraction or hydro-power production) water exploitation require also the construction and operation of hydraulic works which alter the physiognomy and functionality of the riparian landscape (Azami et al., 2004; Braatne et al., 2007; Jamieson and Braatne, 2001). This set of issues raised concerns on the conservation of rivers' good ecological status and the consequent formulation of stringent legal frameworks such as the Water Framework Directive, the Water Blueprint or the Habitat Directive (European Parliament, 2012, 2000, 1992).

In parallel with the evolution of legislative frameworks aimed to ameliorate and protect riparian habitats, also scientists' view toward the rivers has changed. In the latest decades river studies have moved from hydrologists and limnologist approaches that considered lotic and terrestrial zones as distinct entities, to perspectives that acknowledged the tight connection between river and surrounding landscape. This new course was marked by the formulation of the Flood Pulse Concept (FPC) (Junk et al., 1989) which recognized the importance of lateral connectivity over the longitudinal one. FPC was extended by Tockner, Malard & Ward (2000) who considered also theories and concepts relating discharge and biodiversity also for temperate and periglacial rivers. In this re-formulation of the FP concept, also discharges below the bankfull (the "flow pulse") are considered important for the creation and maintenance of the riverscape heterogeneity and biodiversity patterns. This latter work spearheaded the application of landscape ecology approaches to understand patterns and processes occurring within the "riverine landscape" (sensu Church, 2002). Such concepts were further developed in later papers (Ward et al., 2002; Wiens, 2002) where the authors considered spatial patterns, dynamic interactions and functional processes occurring across riparian zones. Riparian landscape perspectives sublimated in the "shifting mosaic concept" (Stanford et al., 2005) which postulates "*...composition and abundance of habitat types do not change over time despite high habitat turnover rates*". Despite the simplicity of the concept, the implications deriving from this statement are manifold. The shifting mosaic formulation acknowledges the importance of periodic disturbance events that re-work the landscape features composition and affect vegetation growth as well as the periodic intervals at which such disturbances occur (Whited et al., 2007). Further implication is the relevance of the temporal scale required to fully characterize riparian zones. Single point observations cannot capture the temporal oscillation of the landscape features abundance since they may greatly differ within relative short periods (Figure 1).

Scientists' view was therefore moving from the observation of the fluxes to the processes occurring between the different landscape units and on different time scales. The shift of perspective corresponded with an increase of studies exploring the quantitative and qualitative relationships entwining riparian vegetation, hydraulics and landform genesis.

This brief review of the recent history of the funding paradigms underpinning the study of riverine landscape ecology is by no mean an extensive review of all the valuable works that contributed to the advancement of science in this field but rather an overview on how the perspectives and approaches toward the study of the riparian zones has changed through time. Contemporary river science paradigms recognize the importance of the multidirectional feedbacks occurring among biotic, physical and geomorphic components of the riparian landscape. Consequently, studying such systems requires looking at riparian ecosystems under a multifocal lens, crafted from different scientific fields. At the same time, studies must take into account the different temporal scales at which feedbacks occur as well as the long term spatio-temporal dynamics (Richards et al., 2002).

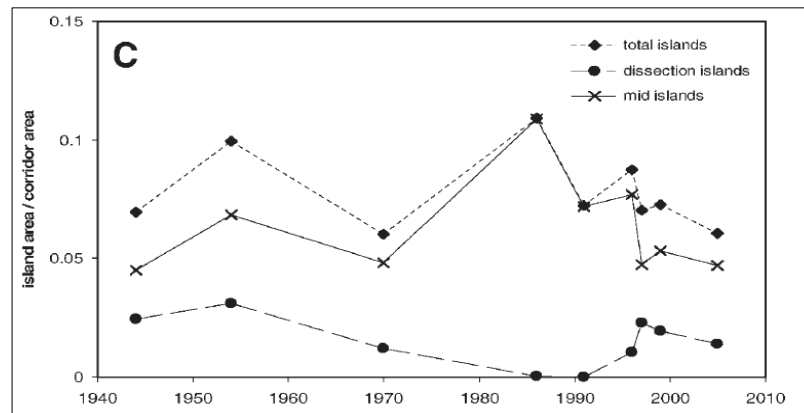


Figure 1 Rate between islands area and corridor area over time at the Tagliamento River (Italy). The periodic fluctuations of the two habitats illustrates the shifting mosaic concept (Arscott et al., 2002)

Riparian vegetation ecological succession and hydrogeomorphological processes

Building upon literature and field experiences, in the latest years several authors have laid the conceptual foundations of a riparian systems conceptualization that gravitates around succession dynamics, hydrogeomorphological processes and disturbance regime. This latter concept is derived from "classic" ecology and was first defined by Pickett & White (1985), the concept states that vegetation communities are shaped by disturbance and that frequency and intensity of the disturbance act as antagonists of vegetation resistance and recovery time. In nature, vegetation communities tend to reach an ideal stage of climax (Clements, 1916). Periodic disturbances halt or reverse this progression; the degree of retrogression depends on the intensity of the disturbance in respect of the vegetation resistance. Conversely, the frequency of the disturbance is counterbalanced by the vegetation recovery time defined as the time required by the vegetation to recover the development stage prior the disturbance occurrence. Under natural settings, riparian ecosystems are frequently disturbed and in the active channel this leads to a frequent and fast turnover of the landscape features and vegetation stands (Corenblit et al., 2010; Tockner et al., 2006; Ward et al., 2002). At the same time, riparian species (e.g. *Salix* sp.) show a very high resistance and short recovery time (Karrenberg et al., 2002). When applied to riparian ecology, the disturbance approach can be classified in three process types (Table I) according to disturbance intensity (I), vegetation resistance to disturbance (R), recovery time (TREC) and disturbance interval (TDIS) (Egger et al., 2013; Formann et al., 2014).

Table I Process types according to Egger et al. 2013, Formann et al. 2013. TRECmat*: Time Recovery mature stage

Process type	Process relationships	Process Characteristics
Metastable	$I = R$; $TDIS \ll TRECmat^*$	Mature stage never reached Oscillatory and gap dynamics are observed but no real successional development takes place Succession sequence interruption causes the biocoenosis to remain at the same early stage
Oscillation	$I > R$; $TDIS < TREC-mat$	Vegetation succession is observed, but maturity is never reached Disturbance severity is high Recovery time is high System is always in an unstable state
Acyclic	$TDIS > TREC-mat$	Succession progress until the mature stage Typical of zones rarely affected by river dynamics

The prevailing disturbance regime, is determined by river energy gradient, aspect (width to depth ratio) and sediment size, therefore they vary according to river type (e.g. braided versus meander) and position within the active channel (Gurnell et al., 2016, 2012). On the other hand, vegetation resistance and recovery time depend on vegetation development stage. However, because of channel migration, process-types spatial arrangement can change over time and thus successional dynamics are not immutably bound to a specific location.

Different authors recognized different riparian zones or development stages characterized by differences in vegetation development stage or dominant hydrogeomorphological processes. Corenblit, Steiger, & Tabacchi (2010) formulated the "biogeomorphologic succession" concept. With the term "biogeomorphologic" the authors synthesized the interdependent relationship between biota and geomorphic processes which lead to characteristic associations between landforms and riparian communities. With the word "succession" instead, the authors acknowledged the progressive change of the dominant hydrogeomorphic and ecological processes occurring within each development phase because of biostabilisation and bioconstruction processes operated by vegetation. The progression or regression between consecutive phases as well as their spatial and temporal distribution is a results of the counterbalance between resisting (sediment cohesion, geometry and vegetation roughness) and destructive agents (Corenblit, Steiger, & Tabacchi, 2010). Extending from this first formulation, Gurnell et al., (2016) devised a conceptual model encompassing five lateral zones lying along the river corridor and characterized by dominant hydrogeomorphological processes (Figure II A). Such zones vary their spatial extent from the headwaters to the mouth in respect of river valley shape and aspects (Figure II B) and, at the reach scale, in response to main channel lateral migration.

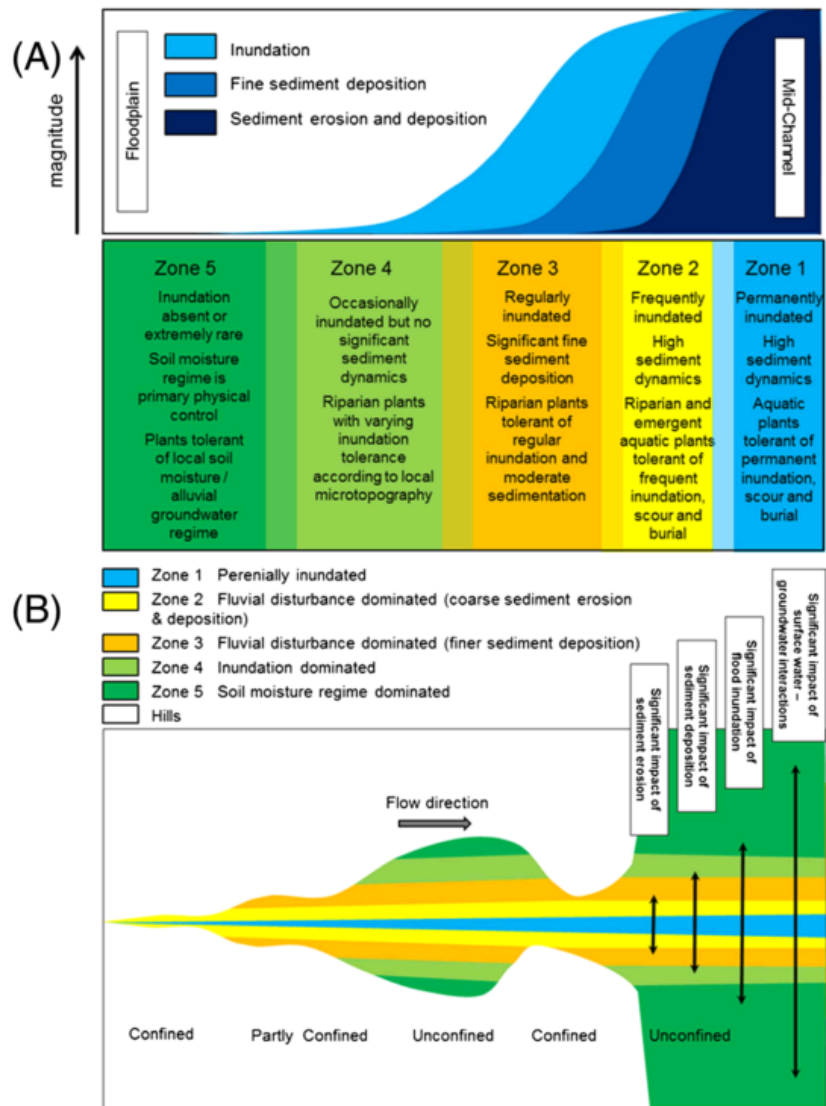


Figure II Characteristics of the river corridor hydromorphological zones according to inundation frequency and sediment dynamics (A) and lateral variation along the longitudinal dimension (B)

According to Egger et al. (2013) and Egger et al. (2015) instead, river corridor zonation can be characterized by the dominant vegetation development stage, succession phase, habitat characteristics and the flow disturbance regime that vegetation have experienced (Table II). In addition to stages and phases, Egger et al. (2013) recognize also three succession series, namely Woodland, Reed and Wetland series (Kovalchik and Clausnitzer, 2004). Woodland series is made up of woody species recruiting in the pioneer phase and later following the trajectory through the shrub, early successional woodland, established forest and mature forest phases. Reed series can be found in constantly water logged habitats as well as on high terraces too dry for the woody species recruitment. The species are mainly herbaceous with high competitiveness and capacity to withstand intense flood disturbances. Finally, the wetland series is mostly found in permanently saturated habitats such as riparian wetland or side arms.

Table II Succession stages and phases characteristics according to Egger et al. 2013

Stage	Phase	Description
Colonization	Initial	Consists of bare soil where few plants are present, and in some instances seedlings only become established for a short time period before the next disturbance
	Pioneer	Relatively sparse, newly recruited vegetation. It consists primarily of species with a ruderal or stress tolerant strategy which are adapted to frequent disturbance and strong hydrological variability
Transitional	Herb	Characterized by short-lived herbaceous species with a ruderal or competitive strategy. In many cases, it may comprise mono-specific vegetation of sedges and/or reeds
	Shrub	Develops directly from the 'Pioneer Phase' or follow the 'Herb Phase'. It comprises woody and long-lived species with stress-tolerant and competitive development strategies
	Early Successional Woodland	Trees replace the shrubs as the dominant life forming the patch. Dominant trees were recruited during the 'Initial Phase'
	Established Forest Phase	Species are recruited to the understory in the Early Successional Woodland Phase. They typically have slow growth rates and many may die before the onset of the next succession phase. Patches are more stable, less prone to disturbance
Mature Stage	Mature Mixed Forest Phase	Includes a combination of woody and long-lived riparian and terrestrial species. Trees regenerate and grow without the influence of external disturbances

Both Gurnell et al., (2016) and Egger et al. (2013) approaches share some similarities and attempt to explain the result of the physical habitat-vegetation interaction as a progression of development stages characterized by the variation of dominant hydrogeomorphological processes, vegetation life stages, disturbance pressure and landforms. Nevertheless, the two theories differ for their fundamental approach: while Gurnell et al., (2016) put more focus on the geomorphic aspects of the subject, in Egger et al. (2013) the approach has a perspective leaning towards plant - ecology. Yet the two can be joined in an attempt to explain with a unifying perspective both geomorphic and vegetation trajectories along river corridors.

Hydrogeomorphological Zone 1 corresponds to the main channel; it is characterized by permanent flooding and high sediment dynamics. Such habitats are too hostile for terrestrial plants although in low energy reaches, vegetation can be present with macrophytes. Hydrogeomorphological Zone 2 lays at the edge of the main channel, it is frequently inundated and exhibit active and frequent sedimentation or erosion events. The interface of these two zones is the habitat for the initial phase: most of the

ground is bare although plants can occasionally establish but frequent inundations and active sediment dynamics promptly resets the succession. The pioneer phases of the woodland and reed series are typically recruited in Zone 2 (Auble and Scott, 1997). In the Northern hemisphere, riparian woody species recruited in the active channel are dominated by the Salicaceae family (Malanson, 1993). The species ascribed to this family (i.e. willows and poplars) bear a set of traits allowing them to withstand the severe fluvial disturbance regime and thus outcompete other species (Karrenberg et al., 2002). In the early life stage, although the woodland and reed series are competing for the future dominance, they do not exhibit relevant distinctive traits in terms of hydraulic and morphological interaction. Thus, hydrogeomorphic processes are dominant over vegetation dynamics (Gurnell et al., 2001) and vegetation succession is easily reset by floods of low magnitude (Asaeda and Rashid, 2012; Bendix, 1999). Zone 3 exhibits a lower disturbance frequency and magnitude than Zone 2, nevertheless it is regularly flooded and the disturbance regime is still relatively high. The succession phases found in this habitat are alternatively the shrub or the herb phase. These two phases progress from the pioneer phase and can reach their state if there is no disturbance able to obliterate newly created vegetation stands. As individuals grow in strength and size, their feedbacks to hydro-morphodynamics increase and trigger habitat autogenic processes. Therefore, transition from Zone 2 to Zone 3 is fostered by the biogeomorphic action of the vegetation. The capacity of vegetation to interact and modify the surrounding physical habitat is expressed by the term “ecosystem engineers” (Jones et al., 1994). Nevertheless, shrub and herb phases behave differently for their morphological traits differ. Reed series maintains an herbaceous aspect, when associated in dense mats, it protects the ground from erosion (Prosser et al., 1995) and favours the accumulation of silt and sand (Corenblit et al., 2009). On the other hand, the woodland series evolves with a shrubby habitus that reduces sediment transport capacity, that thus generates higher accretion rates (Corenblit et al., 2009). Sedimentation is caused by sediment particles interception by plants’ aerial structures and the perturbation of the flow field, which inside vegetated plots, tends to slow down (Anderson et al., 2006; Corenblit et al., 2007; Zong and Nepf, 2010). For both herb and shrub phases net accretion is as well facilitated by the reduction or impeded erosion caused by roots stabilization effect (De Baets et al., 2006; De Baets and Poesen, 2010). Presence of narrow-spaced patches of shrubs reduce channel widening and channel cutoffs (Tal and Paola, 2010) while sparse patches favours bifurcation (Coulthard, 2005) thus contributing to control the transition from multiple to single thread channels.

As accretion proceeds, Zone 3 degrades into Zone 4, the level of disturbance intensity and frequency decreases, because such surfaces are less prone to inundation (Friedman et al., 2006). Reduced disturbance allows the deposition of organic matter, the formation of an organic-soil horizon (Latterell et al., 2006) and conditions suitable for the understory initialization by species not specifically adapted to the active channel disturbance regime. The transition from Zone 3 to Zone 4 favours the establishment of riparian trees species within the herbs. In fact, herbs dead biomass and sediment entrainment tend to fill water logged ponds and create conditions less suitable for reeds and more suitable for ligneous species. Over time, the arboreous life form becomes dominant and the reed series is replaced by softwood shrubs of the woodland series (Girel and Pautou, 1997). In Zone 4, the woodland series develops a young softwood forest (Early successional woodland phase) made by trees with very high disturbance resistance; thus the progression can be reset only by bank erosion (Little et al., 2013). However, this process is actively contrasted for the bank stability is enhanced by the reinforcing action of the roots (Pollen and Simon, 2005) that thus also limit lateral channel migration. When bank erosion occurs, trees falling into the active channel can be transported downstream and deposited on alluvial surfaces in Zone 2 or Zone 3. If moisture conditions on such surfaces are suitable and no floods able of remobilizing the logs occur, trees can resprout, thus creating a new vegetated stand (Mikuš et al., 2013). Plants sprouting from deposited logs grow faster and more vigorously than those originated by seeds (Francis et al., 2006), they quickly transit to the shrub phase, and thus actively promoting local geomorphological changes such as accumulation of fine sediments in the downstream direction and scour on the upstream front (Gurnell et al., 2005). Resprouting trees favour also the accumulation of live material from upstream that in turn can also re-sprout. On the downstream edge instead, the fine materials accumulated and the sheltering effect of the canopy towards flood-

induced strong currencies represents a suitable habitat for establishment of seedlings and smaller propagules. When several of these islands are found on contiguous locations, as they grow they can coalesce thus originating larger islands (Gurnell et al., 2001).

As the distance from the channel margins increases, Zone 4 degrades into Zone 5. In this latter zone, flooding is a very rare event; groundwater dynamics replaces hydrogeomorphic processes as main physical control over vegetation. The absence of disturbance events allows the trees recruited in the pioneer phase to grow to their full potential. Softwood forests species can last for a period of 30-50 years, after that, they begin to reach the maximum physiological age of an average Salicaceae (Egger et al., 2015; Friedman et al., 1996; Johnson et al., 1976). Individuals die back increases the light availability for the understory layer and afford the chance for other hardwood species to emerge to the canopy layer. While more softwood trees die back, the dominant species composition progressively switch to hardwood species such as Coniferous, Oaks, Alder, etc. (Hupp, 2000).

Alternatively, in Zone 4 and Zone 5, where hydric soils are present, the wetland series can replace the woodland. Wetlands are forming in oxbows resulting from meanders cutoff and in abandoned side arms. The first type is more typical in lowland rivers with low energy gradients (Hopkinson, 1992; Mitsch et al., 2012) while the latter can be found in braided and anastomosing rivers. In these locations wetland series can develop somehow similarly to the woodland series. Initial stages begin with submerged or floating sedge grasses (e.g. from the Cyperaceae, Juncaceae or Typhaceae families), as depressions fills with sediments deposited by floods and organic material, succession advances with a woody shrub phase and finally a swamp-bog forest phase (Hansen et al., 1995; Latterell et al., 2006). Alternatively, in abandoned and seldom flooded channels, wetland series can initiate by hydrophilic sedges and rapidly evolve arboreous cover (Hansen et al., 1995). In the wetland series, successional development is less obvious than in the woodland and reed ones and not all the stages are always present.

Riparian vegetation hydrodynamics and morphology numerical modelling history

Concurrently to the development of riparian landscape paradigms, the scientific community developed simulations models attempting to acknowledge the abovementioned multidirectional feedbacks occurring among biotic, physical and geomorphic components of the riparian landscape. In our opinion, spread of simulations models has been promoted also because of the lack of quantitative information and at least partial, lack of empirical laws explaining biotic and physical components feedbacks (see chapter 1). In fact, although a general consensus exists on the development trajectories and feedback direction, for many processes the quantification of the physical drivers' intensity triggering biological responses and the relation between vegetation states and physical habitat response remains in many cases unclear. Examples of such unknowns are, for example, the inundation time required to yield plants damage or mortality, the quantity of deposited sediments that lead to plants extinction and the quantification of roots' stabilizing effect on non-cohesive substrates (Politti et al., 2017). Lack of such information complicates management decisions and process understanding. To this end, the use of models represents a viable solution to explore scenarios or test the importance of riparian systems' control factors.

One of the first attempt is the model from (Pearlistine, McKellar and Kitchens, 1985) which simulated bottomland vegetation establishment, growth and mortality according to hydrological parameters. In later years, many other models based on functional relationships between river hydrology and vegetation species community have been proposed. For example Glenz et al., (2008) modelled vegetation mortality with a fuzzy system accounting for inundation duration, Dixon and Turner, (2006) and Benjankar et al., (2014) focussed instead on riparian woody species seed recruitment. Other models attempted to provide a broader representation of the system by considering not only a single life stage or impact but a larger array of processes. Baptist (2005) proposed a hydraulic model coupled with sediment and vegetation dynamics where vegetation mortality was regulated by sedimentation

rates. Although the results showed satisfactory agreement with observed data, the results of this model show also that the inclusion of morphodynamic disturbance would result in a more realistic outcome. Such impact was somehow included by Benjankar et al., (2011): in this model vegetation mortality is also caused by excess shear stress which is assumed as a proxy for morphodynamic activity. This latter model was extended by Garcia-Arias et al., (2011) with soil moisture dynamics, particularly relevant when modelling rivers in arid and Mediterranean climates. These models mimic vegetation development in response of hydraulic and morphological variables though did not implement any vegetation feedback to hydraulic and morphological processes.

On the other hand, hydraulic models developed at first as 1-D models able of simulating water depth and cross-sectional mean flow velocity by solving, most commonly, the Saint Venant equations. Later 2-D models integrating momentum and continuity equations on the vertical dimension, and thus able of simulating water depth and velocity on two horizontal planes, have been developed. Similarly, more advanced and computational-expensive 3-D models are able of simulating flow depths and velocities on all three dimensions. Flow velocities simulated with hydraulic models can be combined with sediment transport equations, thus allowing simultaneous simulation of river hydraulics and morphodynamics. However, hydraulic and hydrodynamics models typically used in both the industry and academic domains, account for vegetation as a static element, most commonly treated as an additional flow resistance term (Horritt and Bates, 2002).

The lack of true integration between vegetation and hydro-morphodynamic models rises also from the difference in the purpose that lead to the formulation of such models. Natural scientists are in fact, more intrigued by spatio-temporal dynamics spanning longer times than the event-scale dynamics, which is a typical interest promoting the development of hydromorphological models. Nevertheless, in latest years, the two fields are converging towards a more integrated view and several promising vegetation-hydromorphodynamic models emerged. For example, Bertoldi et al., (2014) proposed a model where vegetation growth, in terms of biomass, is controlled by the distance from the water table and its disruption by the shear stress required to mobilize substrate particles. Such critical value is linearly increased with vegetation biomass which controls with the same solution, also vegetation roughness. Presence of vegetation has therefore an effect on erosion processes by reducing flow velocity and increasing substrate cohesion. Similarly the model from Crosato and Saleh, (2011) account for flow resistance but includes also a distinction between submerged and emergent canopies. Such approach is followed also in van Oorschot et al., (2016) but besides submergence condition, vegetation flow resistance depends also on stem density, height and diameter which modelled using a logarithmic growth function. In addition to shear stress mobilization effect, in this latter model, vegetation mortality can occur also by waterlogging, desiccation, burial or scour.

In the seminal work of Camporeale et al. (2013) the authors describe several other quantitative and semi-quantitative models developed with the scope of simulate riparian vegetation and physical habitat interactions. The review points out how, thus far, biological and physical riparian processes are modelled separately and fully coupling of hydraulic, sediment transport and riparian vegetation models is still in its infancy. In their conclusions Camporeale et al. (2013), highlighted the research priorities which shall be addressed to reconcile engineers' and biologists' modelling approaches. Such priorities can be summarized with the need of improving the understanding of the effects of vegetation spacing and flexural properties on flow field and sediment transport dynamics; the quantification of fluvial disturbance thresholds leading to vegetation extinction or disruption; bank structures geotechnical enhancement operated by roots; effects of groundwater on vegetation dynamics; and quantification of ecological successions. A more recent review from Solari et al. (2015) acknowledges the same priorities as Camporeale et al. (2013) with the addition of Large Wood (LW) interaction with geomorphic processes.

Thesis objectives

Among the research priorities highlighted by Solari et al. (2015) and Camporeale et al., (2013) the research carried on within this dissertation did focus on the following topics:

- I. Quantification of fluvial disturbance thresholds leading to vegetation extinction or disruption;
- II. Vegetation dynamics
- III. LW interaction with geomorphic processes
- IV. Improving the understanding of vegetation flexural properties on flow field and sediment transport dynamics

Considering these four research topics, this dissertation developed these three objectives:

1. Quantitative review of riparian Salicaceae and fluvial processes mutual feedback
2. Develop a riparian vegetation dynamic model that simulates vegetation according to fluvial processes and that is able of providing feedback variables to the physical system.
3. Develop a field methodology to characterize riparian vegetation properties, to be used in hydraulic modelling, for vegetation flow resistance parameterization

The research topics represent the overall purposes of the dissertation, the objectives aim at fulfilling these purposes by extensively reviewing literature concerning riparian vegetation responses to fluvial processes, thus including also the quantification of disturbance thresholds leading to vegetation extinction or disruption. Disturbance thresholds can be also investigated with a modelling approach, to this end, the objective of developing an integrated vegetation-hydromorphological model will contribute to this purpose. Moreover, the developed model can be also used to study long term vegetation dynamics and how LW interacts with geomorphic processes. Finally, the field method was developed with the goal of characterize riparian vegetation properties to be used in a novel class of flow resistance equations proposed by other authors. These equations account for vegetation flexural properties and bring the promise of improving the modelling of the flow hydraulic variables which are relevant for sediment transport.

Thesis outline

Fulfilment of the three dissertation objectives are presented in three chapters. The first is a literature review that summarizes the state of the art on the knowledge about interactions between Salicaceae and hydrogeomorphological processes. The review compiles a large array of results from field, laboratory and modelling studies with the scope of providing a set of physical thresholds that trigger system changes. For example, it seeks to frame what are the suitable environmental conditions for vegetation establishment or the intensity of disturbance events leading to vegetation disruption. Therefore, interactions are not explained simply in descriptive terms but rather with a quantitative approach. The notion and the empirical evidences compiled in the review provided the theoretical framework and information for the parameterization of the simulation model described in the second chapter. Such novel model, developed within the dissertation project, was devised to encompass the main relationships entwining riparian woody vegetation and hydrogeomorphological processes. The scope of the model is to replicate long term riparian landscape dynamics. Within this dissertation, the model was developed and conceptually validated by means of hydrological scenarios apt to prove the coherence of the simulation results with expected system behaviour. Examples of such coherences are vegetation growth rate in response to hydrological regime or recruitment and establishment of large wood in an unconfined river system. Although the developed model is very rich in terms of represented processes, vegetation flow resistance is modelled with an almost static approach, i.e. is not responding

to flow depth and velocity but is simply estimated on plants age and density. Such solution, although widely accepted and commonly used in most hydraulic models represents a simplification of the flow-vegetation interaction. Such simplification is partially due to the lack of viable equations able of properly describe vegetation flow resistance behaviour. Viability in this context is not referring to scientifically sound techniques but rather to the difficulty of gathering empirical parameters to be used in equations accounting for vegetation flexural properties or seasonality. The last chapter deals with this limitation by presenting a field method aimed to sample vegetation properties that can be used with a novel class of flow resistance equations proposed by other authors. Such equations rely on measurable plants' properties, model vegetation flow resistance on a physical basis and are able of accounting for plants' reconfiguration and foliation level. The chapter includes also a modelling section that illustrates the implications of the use of physical based equations in hydraulic modelling. The modelling results of this third chapter suggested a possible upgrade of the model presented in the second one, for physically based flow resistance equations allow a more exhaustive representation of woody vegetation and hydrogeomorphological processes. Finally, the last section presents conclusions, possible applications and outlooks stemming from the dissertation project.

1 Mutual feedbacks between the riparian Salicaceae and fluvial processes: a quantitative review

This chapter was published in:

Politti, E., Bertoldi, W., Gurnell, A.M., Henshaw, A., 2017. Feedbacks between the riparian Salicaceae and hydrogeomorphic processes: A quantitative review. *Earth-Science Rev.* in press. doi:10.1016/j.earscirev.2017.07.018

1.1 Introduction

Fluvial processes shape the physical template and habitat gradients for the establishment and development of riparian vegetation species (Auble and Scott, 1997; Friedman and Auble, 2000; Scott et al., 1997). At the same time, riparian vegetation interacts with fluvial processes modifying their local intensity and so contributing to landform development (Corenblit et al., 2011; Tal and Paola, 2007; Wintenberger et al., 2015).

In the temperate zone of the northern hemisphere, pioneer riparian woodlands are dominated by trees and shrubs of the Salicaceae family (Malanson, 1993), which play a central role in the functioning of temperate river systems (Corenblit et al., 2014; Gurnell, 2014). The riparian Salicaceae bear a set of traits that make them particularly suited to the highly dynamic riparian environment including flood tolerance, an ability to survive and regenerate following damage by floods and to colonize exposed bars through opportunistic seed germination and clonal reproduction, and fast growth rates (Lytle and Poff, 2004). Thus, the Salicaceae function as “resisters”, “endurers” and “invaders”, helping them to be a ubiquitous family within riparian zones (Naiman et al., 2005). This set of traits allows the Salicaceae to out-compete other riparian woody genera (e.g. *Alnus*), even sustaining expansion outside their native range (Cremer, 2003; Thomas et al., 2012), and to have a crucial impact on the physical development and dynamics of river channels and their margins.

Although the riparian Salicaceae display between- and within-species differences in, for example, growth rate, seed dispersal time, and flood and drought tolerance (Amlin and Rood, 2002; Guillooy et al., 2011; Stella et al., 2006b), the species ascribed to the riparian *Populus* and *Salix* genera share similar life histories and exhibit a similar set of adaptations and genotypic traits that justify treating them within the same review (Karrenberg et al., 2002). To a large extent, riparian Salicaceae depend upon fluvial processes for regeneration of the riparian forest (Braatne et al., 1996) while at the same time river planforms without woody riparian vegetation develop differently from those bordered by riparian trees (Davies and Gibling, 2010). This complex interdependence has been acknowledged by conceptual models explaining the formation of riparian landscape features mediated by vegetation (Gurnell et al., 2001), associations between landform development and vegetation successional patterns (Corenblit et al., 2010; Egger et al., 2013), the role of fluvial disturbances in maintaining riparian vegetation assemblages (Formann et al., 2014; Gurnell et al., 2016), and ultimately the dynamic equilibrium of the riparian landscape (Stanford et al., 2005; Tockner et al., 2006). These conceptual models have proved to be widely applicable and provide a theoretical basis for making informed decisions concerning river restoration and management (Ward et al., 2001).

Nevertheless, quantification of vegetation responses to fluvial processes remains a research gap. This reflects the widely different environmental settings, species, and natural process variability experienced at the locations of field investigations and the varied experimental designs that have been used to study interactions between vegetation and fluvial processes (see supplementary material). It is also a consequence of the methods of quantification and the mathematical formulation of fluvial processes, which have developed largely from engineering disciplines. Several recent reviews have considered these aspects (Aberle and Järvelä, 2013; Baptist et al., 2009; Gurnell et al., 2012; Nepf, 2012; Schnauder and Moggridge, 2009), illustrating how the classical engineering approach considers

vegetation as a constant parameter rather than a state variable reacting to fluvial process stimuli. Despite this, quantification of Salicaceae responses is needed to predict river-system functioning and aid the parameterization of numerical models attempting to replicate riparian vegetation and fluvial process interactions and longer term riparian landscape development (Camporeale et al., 2013; Glenz et al., 2006; Rogers and Biggs, 1999; Solari et al., 2015).

In this paper, we contribute to filling this research gap by summarising findings from published studies focusing on the Salicaceae and fluvial processes. In particular, we focus on quantification of the physical processes that trigger riparian vegetation responses. Vegetation feedbacks to fluvial forms and processes are treated more briefly, referring to the aforementioned reviews for in depth explanations and mathematical formulations. In contrast to previous research that has conceptualised vegetation-fluvial processes, this review identifies explicit thresholds that determine “when things happen” physically at different temporal scales.

The review is organised to address the following four objectives:

1. Summarise knowledge concerning the feedbacks of riparian Salicaceae individuals and single patches on fluvial processes at the reach scale.
2. Provide river managers and practitioners with a set of figures and timescales that support the identification of “thresholds of probable concern” and suitable environmental conditions that depend on fluvial processes and are relevant for riparian Salicaceae communities.
3. Aid researchers in parameterising numerical simulation models that combine hydrogeomorphological and riparian vegetation coevolution.
4. Highlight knowledge gaps that need to be addressed to homogenise the level of understanding of different processes with respect to different riparian Salicaceae life stages and across different geographical areas.

The feedback processes considered in this review are not exhaustive. Only feedbacks that depend on vegetation as a “physical object” are considered. All processes mediated by biological factors are excluded, such as the increased bank stability deriving from enhanced matric suction (Pollen-Bankhead and Simon, 2010) or the lowering of the water table due to evapotranspiration (Butler et al., 2007). Furthermore, although biological responses to fluvial processes are mediated by processes occurring at molecular and cellular level, this review only considers plant responses to fluvial processes at a macroscopic level that is easily linked to physical measures or “thresholds of probable concern” (sensu Rogers & Biggs 1999) such as water depth, inundation time, amount of eroded sediment.

First, in section 1.2, the conceptual hierarchy of processes that feed (i) from the Salicaceae to fluvial processes and (ii) from fluvial processes to the Salicaceae are presented. These two groups of feedback processes are explained in sections 1.3 and 1.4, with the latter group reviewed in greater detail than the former. In the final concluding section (section 1.5), empirical evidence is synthesised addressing the sensitivity of the Salicaceae to fluvial processes across different time scales.

1.2 Processes conceptual hierarchy

Although many processes are interdependent and thus difficult to disentangle, in this review the bidirectional relationships entwining Salicaceae and fluvial processes are conceptualized in Figure 1-1 and Figure 1-2. The hierarchy of fluvial processes influenced by Salicaceae (Figure 1-1) is partitioned into feedbacks dependent on the canopy and stem and feedbacks dependent on roots. The canopy and stem interact with fluvial processes by deflecting and providing resistance to the flow field thus affecting sediment transport, deposition and erosion patterns (Coulthard, 2005; Murray and Paola, 2003; Tsujimoto, 1999). Deposition patterns are influenced also by the canopy biovolume, which, under submerged or partially submerged conditions, physically intercepts sediment particles (Corenblit et al., 2009). Roots increase substrate cohesion of both streambank and in-channel non cohesive materials, resulting in increased bank stability and reduced in-channel erosion and channel mobility (Abernethy & Rutherford 2000; Perucca, Camporeale & Ridolfi 2007). The processes in Figure 1-1 are relevant during floods or periods of high flow, i.e. periods when there is some geomorphic action.

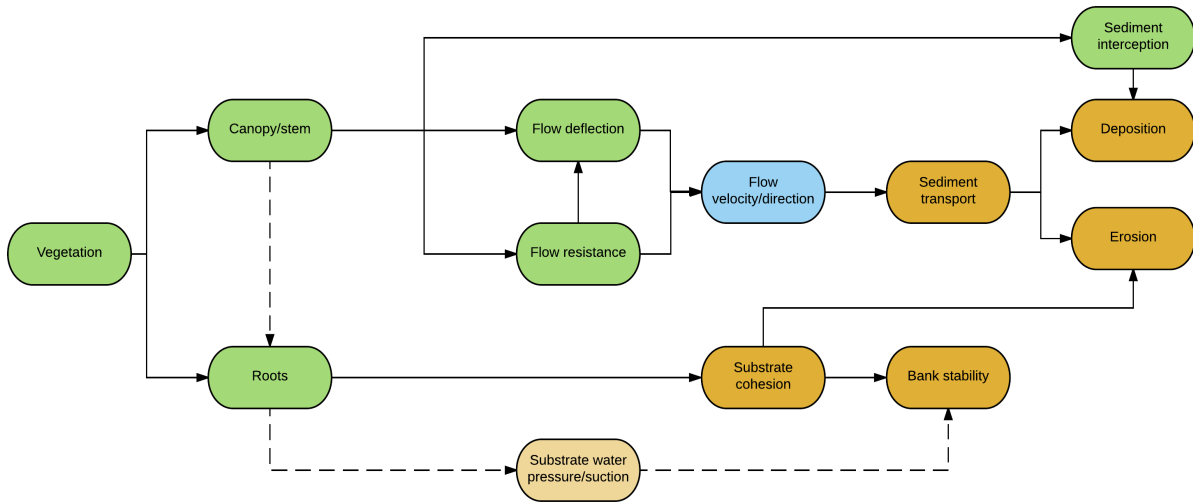


Figure 1-1 Process hierarchy of vegetation feedbacks to fluvial processes

The hierarchy of fluvial processes that affect riparian vegetation (Figure 1-2) is partitioned into sediment transport and water flow, with sediment transport further divided into deposition and erosion and water flow further divided into drag and groundwater depth. Fluvial process feedbacks to vegetation occur at different temporal scales. Drag, erosion and deposition exert their disturbance pressure during floods, when plants can be buried by sediments, broken and bent by flow drag, or toppled and translocated by excessive erosion associated with drag pull (Bendix and Hupp, 2000; Steiger et al., 2005). On a longer time scale, the geomorphic action of floods builds the physical setting, providing the substrate and the hydration conditions for the riparian vegetation life cycle (Hupp and Osterkamp, 1996).

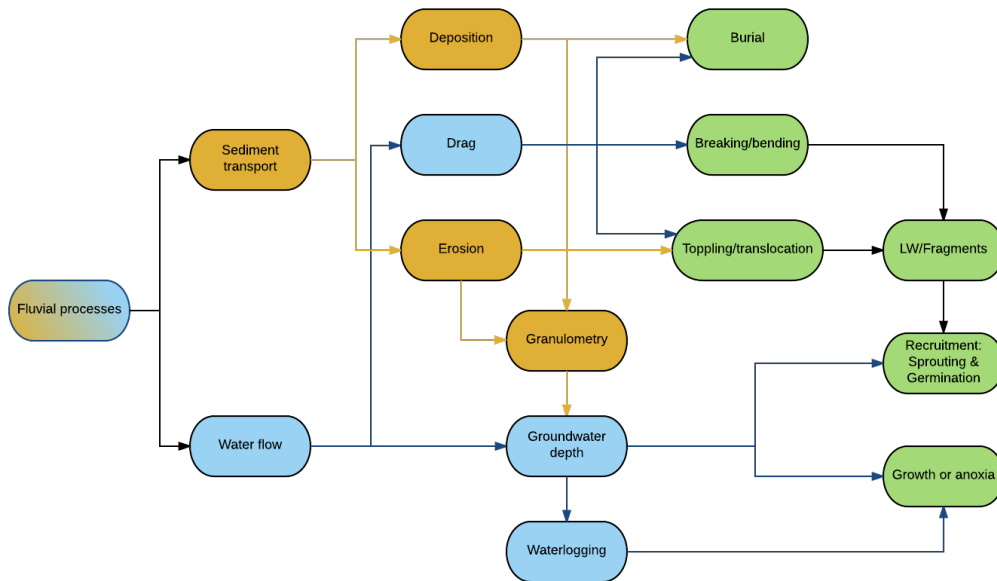


Figure 1-2 Process hierarchy of fluvial process feedbacks to vegetation

1.3 Salicaceae feedbacks to fluvial processes

Many studies concerned with vegetation-fluvial process interaction are not “Salicaceae specific”. However, many of these studies have been included in this review when they have a sufficient degree of generality to make their conclusions applicable to the Salicaceae.

1.3.1 Roots

Roots provide additional substrate cohesion thus increasing the shear load required to mobilize the substrate (Reubens et al., 2007). The shear load can cause failure of a single root either because of breakage or pullout (Coppin and Richards, 2007). Pullout resistance can be seen as a measure of root-soil friction and is a function of root length and diameter. For a single root it can be defined (Ennos, 1990) as:

$$F_p = S L 2\pi r \quad \text{Equation 1-1}$$

where F_p is the pullout force per unit area (kPa), S is the shear strength of the soil (KPa), r is the radius of the root (m) and L is the length of the root (m). If the soil friction holding the root is greater than the root's F_p , the root can also break before the tractive force F_p is reached. The force to break a root was defined by Pollen & Simon (2005) as:

$$F_b = ax^{-b} \quad \text{Equation 1-2}$$

where F_b is the breakage force per unit area (kPa), corresponding to root tensile strength, and a and b are species-specific coefficients estimated from field data (Figure 1-3). Figure 1-3 shows also how finer roots have higher tensile strength per unit area than coarser ones, therefore suggesting that a large number of fine roots have a better stabilization effect than fewer coarse roots with the same root area ratio.

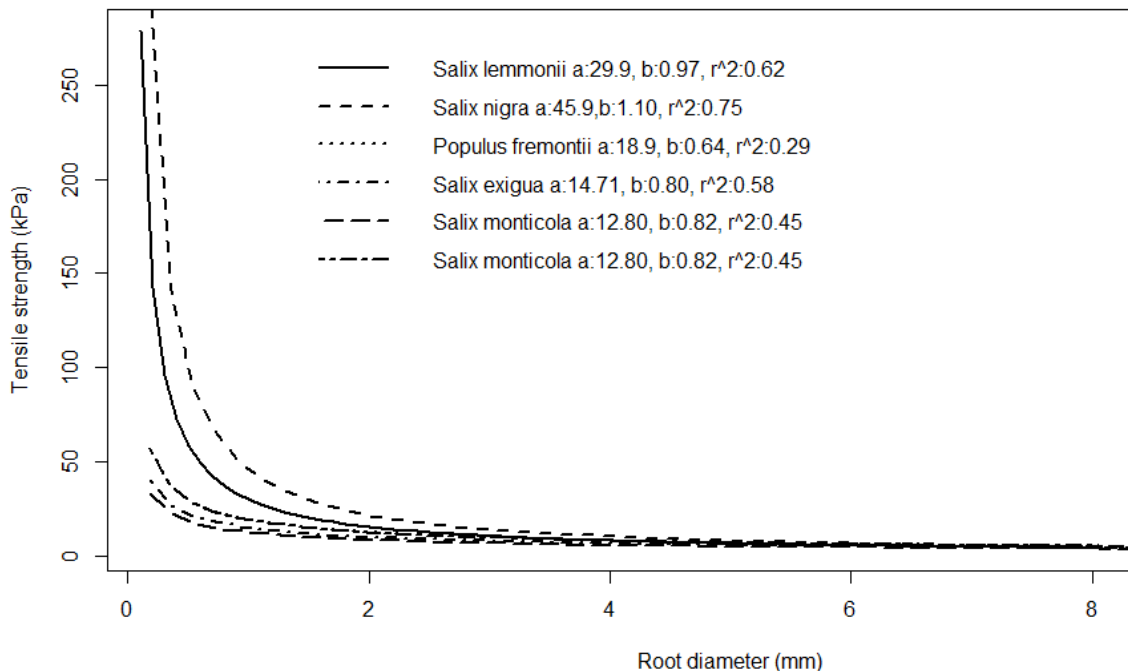


Figure 1-3 Tensile strength per unit area calculated for three species of Salicaceae with Eq. 1. Data sources: (Pollen and Simon, 2005; Polvi et al., 2014; Simon et al., 2006)

Pollen (2007) proved the existence of a threshold diameter above which all roots break and under which most roots are pulled out. Breakage of roots under the threshold is likely due to additional friction

caused by root tortuosity, which increases the root-soil friction. The breakage diameter threshold changes according to substrate type and substrate moisture and, as these two properties change with space and time, respectively (Konsoer et al., 2016; Pollen, 2007), breakage diameter is a dynamic attribute of roots. Increased substrate moisture results in lower root-substrate friction and thus a higher breakage diameter threshold (Pollen, 2007). Different substrate types exhibit different shear strength (term S in Equation 1-1 thus resulting in different friction values for a unit area of roots. Despite the variability, the diameter threshold seems to fall between 2.5 and 3.5 mm with breakage being the dominant failure process below the threshold and pull out above it.

1.3.1.1 Substrate cohesiveness

1.3.1.1.1 Bank stability

The effect of vegetation on bank stability can have deep impacts on the overall planform evolution of a river as vegetation is able to induce a change in river planform style from braiding to single thread / meandering (Gibling and Davies, 2012; Gran and Paola, 2001).

For the sake of completeness, it should be mentioned that bank stability is a multifaceted problem, depending on the gravitational forces acting on the bank and including also plant surcharge effects (Abernethy et al., 2001), hydrostatic confinement, bank geometry, substrate types and pore water pressure (Simon and Collison, 2002). However, as this review focuses on plants as active physical objects, only the effects of roots on bank stability are considered. The presence of roots enhances bank stability by reinforcing the substrate matrix as steel bars reinforce concrete (Abernethy and Rutherford, 2000). When the bank is subject to a shear load, the stress is transferred to the roots which in turn increase the shear strength of the bank (Coppin and Richards, 2007). The additional shear strength provided by plants standing on a bank top is strongly influenced by the number of roots crossing the shear plane (Table 1-1). Quantification of this number is not a trivial task. Pollen-Bankhead & Simon (2009) proposed a set of allometric equations to predict the number of roots crossing the bank wall profile. The method assumes a dependence of root fraction on depth and was fitted to data collected for different tree species, including *Populus fremontii* and *Salix nigra*. The results of these allometric estimations were fed into the RipRoot model (Pollen & Simon, 2005; Pollen 2007), which estimates the additional cohesion provided by roots. The model results, when related to vegetation development, showed that for *Populus fremontii* and *Salix nigra* the estimated plant age required to yield significant bank stabilization is in the order of 3-5 years and reaches an asymptotic maximum around 20-30 years (Figure 1-4).

Table 1-1 Roots reinforcement estimated by RipRoot model for a bank 10 m long and a shear surface length of 1.15 m (Pollen and Simon, 2005)

Species	Number of roots	ΔS (kPa)
<i>P. fremontii</i>	200	0.41
	400	0.82
	600	1.23
	800	1.65
	1000	2.05
<i>S. nigra</i>	200	0.84
	400	1.68
	600	2.52
	800	3.37
	1000	4.2

Similarly, Wiel & Darby (2007) modelled Root Area Ratio with a distribution exponentially declining with depth and applied a mathematical model to evaluate bank stability. Their results indicated that the maximum improvement in bank stability occurs where the shear plane crosses the maximum root density. Surprisingly, the increased stability due to plants, expressed as a safety factor (i.e. the ratio between failure and resisting forces), was less than 5% and although the marginal increase of stability in non-cohesive substrates is high; their overall stability remains very low. At the same time, according to Wiel & Darby (2007), vegetation has a considerable effect only where bank properties already ensure a sufficient level of bank stability because of the nature of the substrate or the moisture content. This conclusion is in line with the correlations between root tensile strength and breakage diameter already described, but the limited bank strengthening predicted by the model of Wiel & Darby (2007) differs from the conclusions derived using the RipRoot model. The discrepancies between the two results might be explained by the fact that while RipRoot returns the additional shear strength due to roots, the model of Wiel & Darby (2007) considers also plant density and surcharge and hydrological conditions (i.e. the confinement effect), that are not accounted for in the RipRoot model (Pollen & Simon, 2005; Pollen, 2007). Nevertheless, Pollen & Simon (2005) and Pollen (2007) consider both of the root failure mechanisms and their spatial and temporal variation. In both solutions, the assumptions are not always justifiable because the root development of Salicaceae is often complex and thus not easily predictable (see section 1.4.1.1) and in some cases may even exhibit root grafting (Holloway, Rillig & Gurnell, 2016b) a feature which is likely to increase bank stability but that, to our knowledge, is not recognized in any bank stability model.

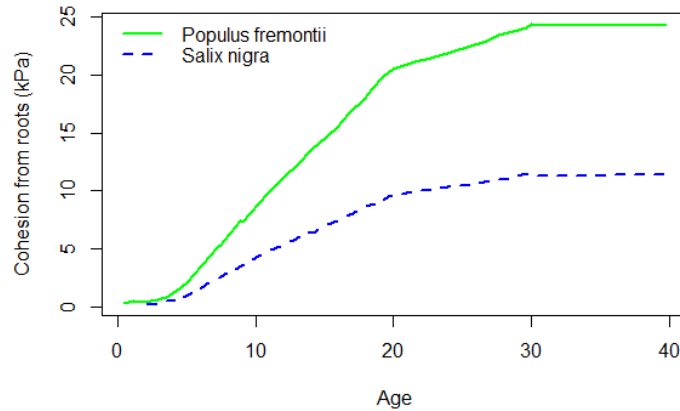


Figure 1-4 Modelled *Populus fremontii* and *Salix nigra* increase in soil cohesion in relation to age. Data source: (Pollen-Bankhead and Simon, 2009).

1.3.1.1.2 Erosion of (in-channel) non-cohesive material

Studies on root enhancement of non-cohesive substrates have received far less attention than bank failure and erosion of cohesive substrates. With respect to bank failure, surface erosion of non-cohesive material does not occur along a preferential failure plane but it rather proceeds by gradual abduction of the substrate. Therefore, root cohesion approaches developed in relation to bank stability fail to capture non cohesive in-channel erosion mechanisms (Pasquale and Perona, 2014). Modelling of such mechanisms has been achieved by increasing the critical shear of the substrate (Bertoldi et al., 2014) or by reducing the eroded quantity by a percentage depending on vegetation cover (Van De Wiel et al., 2007). However, to our knowledge, there is no empirical evidence to support the parameterization of the two methods. Pasquale & Perona (2014) devised and tested a possible strategy for their quantification. The results from their field experiment with *Salix* cuttings revealed a tendency of reduced scour where vegetation was present and increased substrate cohesion in correspondence with root maximum volume. The increase in cohesion was computed to fall within an approximate range of 1.0-2.5 % (Pasquale and Perona, 2014). Such a low increase can be explained by the young age of the cuttings that had not developed extended root systems and by the limited dataset available for analysis.

1.3.2 Canopy and stem

When partly or fully submerged, plant aerial structures affect the flow field by deflecting the water and dissipating energy. The effects include an increase of flow velocity around the plants, while velocity is reduced inside vegetated stands (Schneider and Moggridge, 2009). These processes are particularly relevant when sediment transport occurs.

1.3.2.1 Flow resistance

Water flowing through vegetation encounters form drag and roughness resistance. The former originates from the physical blockage exerted by the plant structures exposed to the flow while the latter accounts for the momentum and energy loss due to surface-flow friction. In hydraulic models, vegetation flow resistance is commonly expressed as a bulk roughness or friction parameter derived from empirical or semi-empirical methods and is the most common parameter used to mimic vegetation feedback to hydraulics. This approach is typical in practical applications even though vegetation flow

resistance varies temporally and spatially. The resistance offered by a single vegetation element to flowing water can be described by the drag force (FD) Equation 1-3:

$$F_D = \frac{1}{2} \rho C_D A_P U^2 \quad \text{Equation 1-3}$$

where ρ is the water density, A_P is the frontal projected area of vegetation exposed to the flow, U is the mean flow velocity and C_D is the drag coefficient, a lumped coefficient that includes friction and form drag. For rigid, tree-shaped individuals with emergent canopies, Equation 1-3 represents a sufficient approximation but for totally or partially submerged flexible plants, such as Salicaceae shrubs, this formulation is difficult to apply (Aberle and Järvelä, 2013). Nevertheless, from a theoretical viewpoint Equation 1-3 is correct and is reported here because it allows a complete consideration of all the key elements of vegetation flow resistance. When flow velocity is sufficiently high, flexible plants streamline in the direction of the flow, thus reducing A_P and C_D (Fathi-Maghadam and Kouwen, 1997; Gosselin and De Langre, 2011; Weissteiner et al., 2015). Streamlining is exacerbated by the presence of leaves (Freeman et al., 2000; Järvelä, 2002a). Therefore, for deciduous species such as those of the Salicaceae, resistance changes seasonally. A_P also varies with water depth. Under partial submergence, as water depth increases more of the plant-area is exposed to the flow, thus increasing flow resistance (Fathi-Maghadam and Kouwen, 1997; Manners et al., 2013). Conversely, under fully submerged conditions, resistance increases linearly with depth until a certain level beyond which resistance decreases until it reaches an asymptotic constant (Manners et al., 2013; Wu et al., 1999). The degree of submersion also has a strong influence on the velocity profile (see section 1.3.2.2), which in turn determines the mean velocity U (Equation 1-3). In the relationship between flow and flexible vegetation, flow resistance is thus a dynamic attribute whose estimation is complicated by continuous interaction between vegetation and flow properties that determines flow resistance.

At the patch scale, flow resistance depends on the longitudinal and lateral distance among individuals (i.e. stem density), with the resistance positively correlated with decreasing distances between stems (Righetti, 2008). In a recent review Aberle & Järvelä (2013) noted how vegetation density and reconfiguration are the main features to be considered in flow resistance equations and that such equations should be based on species specific parameters such as the one developed by Västilä & Järvelä, (2014). This latter method is particularly suited to practical applications because vegetation parameterization relies on measureable plant properties (Antonarakis et al., 2010, 2009, Jalonen et al., 2015, 2013), considers plant reconfiguration, and accounts for different flow depths (Aberle and Järvelä, 2013; Västilä and Järvelä, 2014).

1.3.2.2 Flow deflection

The flow resistance provided by vegetation causes flow field velocity vectors to deviate from their original trajectories. For single, tree-like plants whose canopy is emergent, the flow deflection effect is similar to that of a bridge pier, generating horseshoe vortices on the upstream side of the stem (Unger and Hager, 2007) and creating wakes and local flow acceleration on the downstream side of the stem (Ahmed and Rajaratnam, 1998).

At the patch scale, the effect on the flow field depends on the shape and density of the patch of plants. Nepf (2012b) recognizes two typical shape types: patches with finite width and circular patches with length and diameter smaller than channel width. For the first type, when located at the channel edge (Figure 1-5), the flow approaching the leading edge of the patch with velocity U_0 is decelerated because of the drag imposed by the patch, and is deflected upstream at a distance depending upon the patch width b . Deflection is completed at a distance X_D from the leading edge of the patch. Beyond this distance, the flow inside the patch has a uniform velocity U_1 that is lower than the channel velocity U_2 and the onset of Kelvin-Helmholtz (KH) vortices begins at the edge of the patch. The size of KH vortices increases downstream from X_D and they penetrate the patch up to a maximum distance δL while extending into the channel a distance δo (Figure 1-5). For a patch of similar characteristics but located within the channel, flow deflection and lateral shear layers occur on both sides of the patch (see Nepf 2012b for an in-depth explanation of the mathematical aspects).

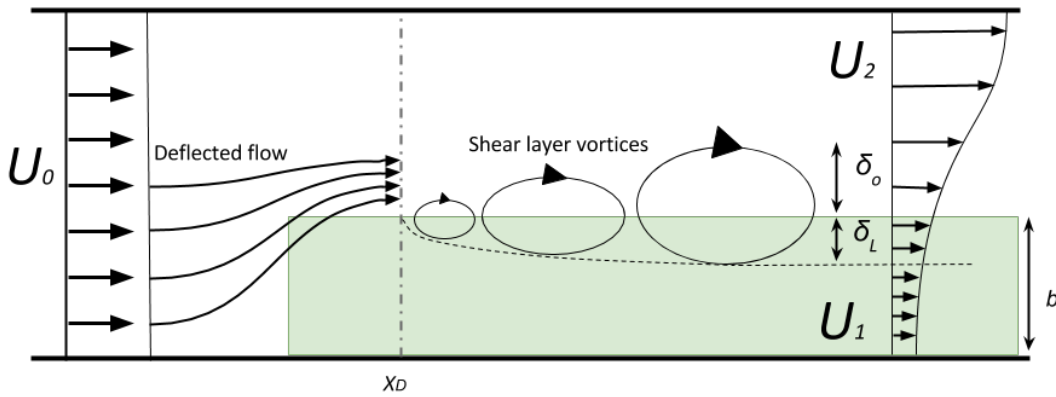


Figure 1-5 Effects of a finite width patch on the flow field horizontal dimension. Adapted from (Nepf, 2012)

In the second case of patches with a circular shape of diameter D_G (Figure 1-6), vegetation drag causes stem scale turbulence that decreases the approaching velocity U_0 to a lower velocity U_1 downstream from the patch (Nepf, 2012). Flow interactions and patch wake characteristics depend on stem densities that can be expressed also as a void fraction (Φ) calculated as:

$$\Phi = N_c (D/D_G)^2 \quad \text{Equation 1-4}$$

where N_c is the number of stems, D_G is the patch diameter and D is the diameter of the stems (Nicolle and Eames, 2011). For $\Phi < 0.05$ the stems behave as isolated entities; when $0.05 < \Phi < 0.15$ a shear layer occurs at the streamwise sides of the patch; and for $\Phi > 0.15$ the patch acts as a solid body of similar diameter. Because the flow downstream from the patch is slower than the flow in the open channel, when the shear layer forms (i.e. $0.05 < \Phi < 0.15$) flow “bleeding” (sensu Schnauder & Moggridge 2009) through the patch interferes with the shear layer and delays the formation of patch-scale Von Karman vortices (VK) (See Nepf 2012b for an in-depth explanation of the mathematical aspects).

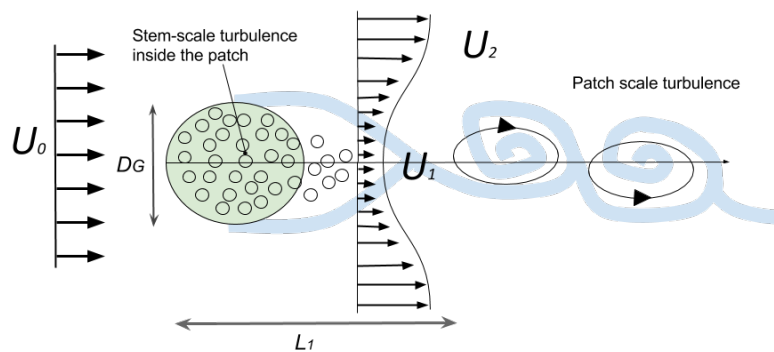


Figure 1-6 Effects of a circular patch on the flow field horizontal dimension. Adapted from (Nepf, 2012)

In the vertical dimension, flow approaching a patch is partly deviated downwards, thus creating a horseshoe vortex zone at the patch front (Chen et al., 2012a), while inside the patch the flow velocity

is reduced (Figure 1-7 B). In the case of submerged vegetation, flow velocity above the vegetated patch displays a logarithmic profile (Figure 1-7 A).

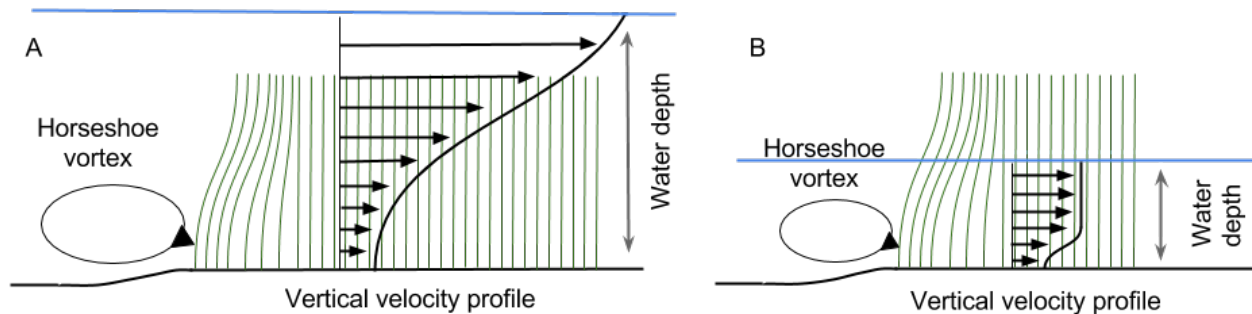


Figure 1-7 Effects on the flow field vertical distribution of a submerged (A) and partially submerged (B) patch. Adapted from (Baptist et al., 2009) and (Nepf and Vivoni, 2000)

1.3.2.3 Effects of flow alteration on sediment transport, erosion and deposition

For a single stemmed plant, the horseshoe vortex on the upstream side of the stem enhances local erosion around the stem's upstream and streamwise sides (Unger and Hager, 2007). A similar situation occurs around densely vegetated patches, as the blockage by the plants resembles that of a single solid bluff body (Nicolle and Eames, 2011; Zong and Nepf, 2010).

For patches with sufficiently high porosity to allow flow to bleed through the patch elements, the flow is deflected downwards and the streamwise shear layers at the edges of the patch entrain sediments and cause local erosion in front and on the streamwise sides of the patch (Chen et al., 2012b). Erosion at the streamwise sides occurs where the vegetation stabilization effect is lower than shear stress exerted by flow velocities accelerated by lateral flow diversion (Rominger et al., 2010). Entrained sediments can enter a patch from the frontal edge by mean flow advection, or by diffusion from the flow along the streamwise edges. The flow resistance imposed by vegetation decreases flow transport capacity thus limiting flow advection transport and causing deposition inside the patch (Chen et al., 2012a). Deposition inside the patch is also enhanced because of sediment interception by the plant canopy.

Sedimentation in patches dominated by Salicaceae is mainly explained by the biovolume defined as vegetation cover (m^2) and plant submerged height (m) (Corenblit et al., 2009). However, the role of biovolume interception remains poorly quantified. Furthermore, since biovolume is also a proxy for plant density and therefore roughness, the relative share of deposition due to biovolume interception or to flow velocity reduction is unclear. However, sediment deposition inside vegetated patches is the crucial process leading to bar accretion and progressive sheltering of standing vegetation from further disturbances (Corenblit et al., 2014). Furthermore, since the region of the patch subject to lateral shear vortices (Figure 1-5) is defined by the distance δL (Zong and Nepf, 2010), when the patch length is larger than flow (frontal) advection penetration and wider than δL , zones where deposition is supply limited will occur inside the patch (Zong and Nepf, 2010). In the wake of a circular patch (Figure 1-6) the delayed onset of VK vortices creates a low velocity flow zone where deposition of fine sediments is enhanced. Central and stream side patches also display quantitative differences in scour and deposition due to the enhanced side wall effect along stream edge patches. This enhances the horseshoe vortex associated with stream edge patches, causing greater scour (Figure 1-8). Figure 1-8 shows also how a slightly denser patch may yield very different amounts of sediment deposition or erosion, confirming the importance of stem density to understanding and properly modelling vegetation - fluvial process interactions.

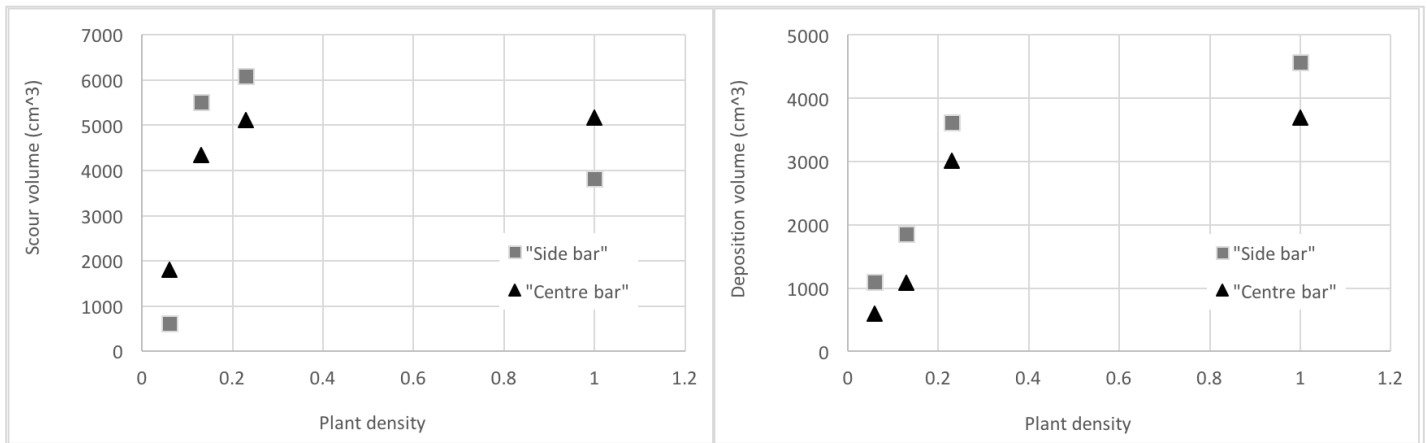


Figure 1-8 Scour and deposition measured in a flume experiment, for a channel side and a centre bar with flexible objects simulating flexible submerged vegetation. Scour was measured upstream and on the sides of the bars, deposition was measured downstream from the bars. Plant density is the ratio of the projected area of the flexible objects and the area of each bar. In the charts, a plant density of 1 indicates a solid, non-flexible object with the same bar area and object height as that of the flexible objects. Data source: Chen, Kuo & Yen 2012b

1.4 Fluvial process feedbacks to Salicaceae

Fluvial processes influence Salicaceae by exerting stresses or disturbances or regulating limiting factors. These three types of influence operate on different time scales. Limiting factors are extremely unlikely to change and therefore are a persistent constraint on plants (e.g. light, nutrients or water). A stressor is an external factor that reduces dry matter production of one or more plant organs during a more limited period of time (Grime, 2002) such as the occurrence of a drought period. A disturbance occurs over a very short period of time, damaging or disrupting an ecosystem and changing its physical condition and its population structure and communities (Pickett & White 1985, p. 7). In the riparian context, disturbances are usually related to the occurrence of floods.

The following sections mainly consider stress and disturbance as impacts on vegetation. Biological responses encompass both resistance and recovery mechanisms where resistance is the set of traits and properties that allow an individual plant to endure a stress or a disturbance while recovery mechanisms are the set of traits and properties that allow plant communities to regain their vigour after a disruptive event, thus forming part of the concept of ecological resilience.

1.4.1 Water flow

1.4.1.1 Groundwater depth

Groundwater depth (GWD) plays a crucial role in the recruitment and growth of Salicaceae. GWD is particularly critical during vegetation establishment by both sexual and asexual reproduction (Johnson, 2000; W. Carter Johnson, 1994). Salicaceae are heliophilous, requiring bare, unshaded, moist sites for their establishment. Examples of such habitats are fine sediments deposited in the lee of islands, accreting bars or other alluvial deposits normally found in the active channel (Barsoum, 2002) and formed by geomorphic restructuring during floods (Polzin and Rood, 2006). Once deposited, seeds or vegetative propagules begin to develop roots to capture water. The depth to the capillary fringe of the water table and the rate of root growth determine the ability of the roots to tap a water supply (Cooper

et al., 1999; Polzin and Rood, 2006). Since propagules are often deposited by declining flood waters, the position of the water table is usually governed by the rate of decline of the falling limb of the flood hydrograph and substrate properties (Mahoney and Rood, 1998). On gravel bars, moisture can be retained by the combined presence of coarse-gravel standing on a finer sediment matrix. The superficial gravel acts as a mulch thus reducing evaporation and maintaining high moisture for weeks even without alluvial or meteoric water inputs (Meier and Hauer, 2010).

Many researchers have investigated experimentally the rate of root growth of seedlings and cuttings subjected to different combinations of substrate granulometry and rates of water table decline (Table 1-5). Decline rates greater than 2.5 to 3 cm day⁻¹ appear to be lethal for the seedlings of most of the Salicaceae (Mahoney and Rood, 1998; Stella et al., 2010) regardless of substrate type. During controlled experiments, the highest survival rates have been observed for water table decline rates of less than 2 cm day⁻¹ (Figure 1-9) and maximum root daily elongation rates of 1.5 and 1.7 cm day⁻¹ have been observed for seedlings and cuttings, respectively (Table 1-5). However, the extremes reported in Table 1-5 should be considered with caution because in natural settings, shallow rooted plants are unlikely to survive the most extreme conditions tested in these experiments (Amlin and Rood, 2002; González et al., 2010).

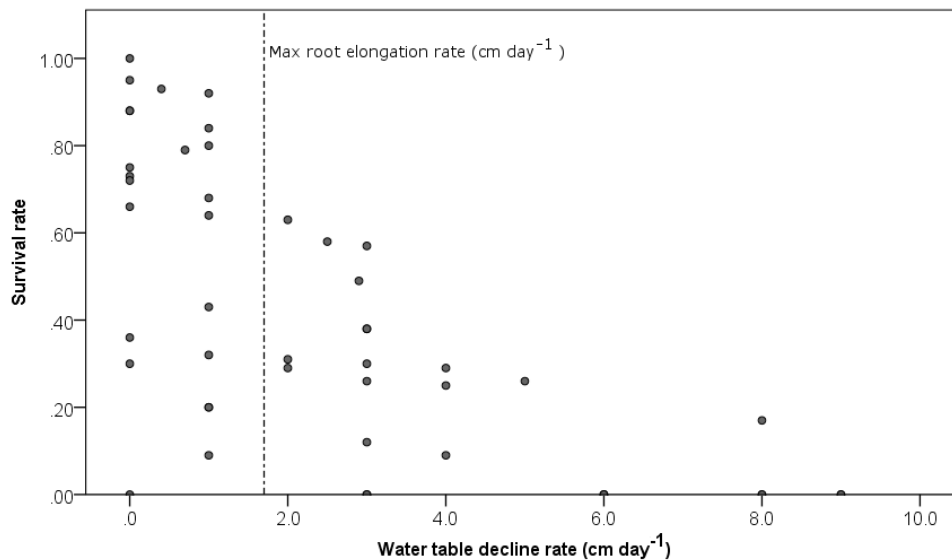


Figure 1-9 Survival of seed-recruited seedlings under different water table decline rates (Data source: Table 1-5)

DGW and granulometry are also of utmost importance for the sprouting of pieces of deposited large wood (LW, > 1 m long and 10 cm diameter) and smaller wood fragments (Francis et al., 2006; Francis and Gurnell, 2006). However, differences in the sampling methods employed in published studies prevent precise quantification of the most suitable quantitative ranges for sprouting (Table 1-7). In general terms, successful sprouting occurs at locations low enough to guarantee sufficient moisture but elevated enough to provide shelter from subsequent floods that would otherwise remobilize the deposited wood. Suitable shelter can also be provided at lower elevations in the lee of obstructions such as islands (Moggridge and Gurnell, 2009).

A decline in DGW can also lead to drought stress causing phytomorphological responses in adult and mature individuals (Amlin and Rood, 2003; Cooper et al., 2003; J. L. Horton et al., 2001). Salicaceae take up water mainly from the capillary fringe although they can also extract water from the unsaturated zone (Cooper et al., 1999; Hultine et al., 2010; Snyder and Williams, 2000). In general terms, the study by Holloway, Rillig & Gurnell (2016a) suggests that roots are distributed vertically where there is water, so they exploit finer sediment layers where water may be retained as well as having deep tap roots.

Drought stress leads to a reduction of the plant water potential with consequent stomatal closure and impaired transpiration (Van Splunder et al., 1996). For the Salicaceae, if the plant water potential decreases below approximately -0.7/-1.7 MPa (Horton et al., 2001; Tyree et al., 1994), xylem cavitation can occur, followed in the most severe cases by senescence and abscission of branches (Rood et al., 2000). Other responses are the reduction in the shoot-to-root ratio, reduced transpiration rates, more efficient use of available water, and a reduction of leaf area (Stella and Battles, 2010; Van Splunder et al., 1996).

For *P. deltoides* subsp. *Monilifera* (Aiton) Eck, sustained GWD declines that are less than or equal to 0.5 – 0.6 m have little or no effect on crown vigour of adult individuals while declines greater than 1 - 1.5 m cause considerable crown dieback, reduced growth and branch abscission (Cooper et al., 2003; Scott et al., 1999). In arid climates, the response time to such GWD decline is shorter than a week (Cooper et al., 2003) and if the stress persists to the following growing season, the vast majority of individuals are likely to die (Scott et al. 1999; Scott, Lines & Auble 2000; Shafroth, Stromberg & Patten 2000). The decrease in annual growth performance in response to GWD lowering was also observed for *Populus fremontii* Watson and *Salix exigua* Nutt. (Hultine et al., 2010). In the first growing season following GWD decline, cottonwood and willow exhibited a radial growth decrease of 22-30% and 32-40%, respectively. Growth rates returned to normal in the growing season after the GWD was reset to the natural range (Hultine et al., 2010).

Fluctuations in GWD are part of natural riparian system functioning and so may not result in adverse consequences for plants and can even promote root elongation in the soil pores vacated by the falling water level (Naumburg et al., 2005). However, the amplitude of such fluctuations appears to be a habitat factor that constrains Salicaceae populations within loosely defined fluctuation boundaries. Along the San Pedro River, Arizona, Lite and Stromberg, (2005) observed that *Populus fremontii* and *Salix goddingii* abundances declined where annual GWD fluctuations exceeded 0.8 m and 0.5 m, respectively, although the absolute value of GWD appears to be less important than the decline rate. Drought effects on Salicaceae ultimately depend on the counterbalance between root elongation and the rate of GWD decline, since root depth is a plastic trait that can change according to water table fluctuations. In a two-year field experiment with *S. alba* and *S. viminalis* cuttings, Pasquale et al. (2014) observed that the depth at which roots achieve maximum density could change during the growing season. Such behaviour is formalized by Equation 1-5 (Pasquale et al., 2012) where Z_r and Z_w are the mode of maximum root density elevation and water table elevation (above sea level), respectively, Z_s is the mean surface elevation during the growing season and η is a scaling parameter corresponding to the site and species tested in Pasquale et al. (2012).

$$Z_r = \frac{\eta Z_s + Z_w}{1 + \eta} \quad \text{Equation 1-5}$$

In a laboratory experiment, Imada et al. (2008) found that most of the total length of fine roots of *Populus Alba* L. is located in soil layers just above (<10 cm) the water table. These studies by Pasquale et al. (2012) and Imada et al. (2008) complement one another, since the former considers maximum density of all roots including the coarser ones that provide anchorage, while the latter considers only fine roots that are responsible for water intake and so normally extend deeper and further laterally than coarser roots. Nevertheless, the validity of Equation 1-5 is untested on other species or life stages. Tron et al. (2015) developed a more sophisticated model validated against measured data including adult individuals of *Populus nigra*. This displayed good agreement with observed root profiles, which appeared to respond to GWD, although the model was unable to explain the presence of shallow roots when the DGW was very deep. However, for the same species of *Populus*, Holloway, Rillig & Gurnell (2016a) found that although root density showed a consistent decline with depth, this variable alone

had low explanatory power. Root density tended to be higher near the surface and to decline more rapidly with depth at wetter sites than at drier sites, illustrating a different distribution of roots depending on moisture availability. Sediment caliber was also important, with the finest sediment layers showing the highest root densities near the surface and the sharpest decline with depth, while coarser sediments showed relatively low root densities than other sediment types regardless of depth. These results suggest that site moisture conditions and depth are the variables that give the most consistent indication of likely root density but that there are strong additional variations driven by the vertical profile of bank sediments. Thus, complex vertical distributions in bank sediment particle size constructed by fluvial processes are reflected in complex vertical distributions of root density. In the same study, Holloway, Rillig & Gurnell (2016a) found that Root Area Ratio (RAR, cm² of roots per m² of bank face area) showed no general variation with depth. Instead, wetter sites showed consistently higher values of RAR than drier sites, indicating that moisture is the most important explanatory variable across the studied profiles, with sediment caliber providing additional explanation of RAR, particularly at wetter sites. The difference in the behaviours observed by Tron et al. (2015) and Holloway, Rillig & Gurnell (2016a) is probably due to differences between the sites of the two datasets. Tron et al. (2015) gathered their samples from undisturbed bank levees and in-channel bars planted with small cuttings with a very short disturbance history (Pasquale et al., 2012, 2011) and a controlled experiment with no disturbance at all (Gorla et al., 2015). In contrast, Holloway, Rillig & Gurnell (2016a) and (Holloway et al., 2017a) made their observations along a highly disturbed river (the braided Tagliamento River, Italy) where riparian vegetation experiences multiple burial and erosion events leading to complex sediment profiles within the banks and highly variable DGW (Tockner et al., 2003). A further difference between the studies by Tron et al. (2015)'s and Holloway, Rillig & Gurnell (2016a) is that while the former took as a reference the DGW, the latter considered depth from the ground surface. Nevertheless, the reviewed studies suggest that the root distribution within river banks and bars may not be easily predicted in highly disturbed habitats. In the presence of moisture from a shallow DGW, Salicaceae tend to develop shallow roots. Moreover, in some documented cases *Populus* sp. developed deep and shallow roots at the same time to intercept water from rain events and supply water from deep DGW at the same time (Rood et al., 2011; Snyder and Williams, 2000). Application of the models proposed by Pasquale et al. (2012) or Tron et al. (2015) should also consider the conclusions from Scott et al. (1999) and Shafroth et al. (2000), who suggest that at least for grown trees, relocation of the roots cannot exceed 1 m in depth within one growing season. In addition, several studies indicate that Salicaceae are normally found where the GWD is less than 4-5 m (Table 1-2), indicating that root growth does not proceed indefinitely.

Table 1-2 Maximum groundwater depth for survival of *Populus* and *Salix* species (expanded from Lite and Stromberg, 2005)

	Species	Groundwater maximum depth (m)	Location	Reference
Sapling survival	<i>P. fremontii</i>	2.91	Bill William River, AZ where water table had regular interannual fluctuations	Shafroth et al., 2000
	<i>S. gooddingii</i>			
	<i>P. fremontii</i>	0.82 and 3.14	Bill William River, AZ where water table were relatively shallow and stable	Shafroth et al., 2000
	<i>S. gooddingii</i>			
	<i>P. fremontii</i>	2.93	Bill William River, AZ	Shafroth et al., 1998 ^a
	<i>S. gooddingii</i>	2.02	Bill William River, AZ	Shafroth et al., 1998 ^a
	<i>P. fremontii</i>	2	San Pedro River, AZ	Stromberg et al., 1996
	<i>S. gooddingii</i>			
<i>P. fremontii</i>	1	Hassayampa River, AZ	Stromberg et al., 1991	
Adult survival	<i>P. fremontii</i>	2.5 – 3	Hassayampa River, AZ	Horton et al., 2001 ^a and Horton et al., 2001 ^a
	<i>S. gooddingii</i>			
	<i>P. fremontii</i>	2.6	Hassayampa River, AZ	Stromberg et al., 1991
	<i>P. fremontii</i>	5.1	San Pedro River, AZ	Stromberg et al., 1996
	<i>S. gooddingii</i>	3.2	San Pedro River, AZ	Stromberg et al., 1996
	<i>P. fremontii</i>	1.5 – 3	Bill Williams River, AZ	Busch and Smith, 1995
	<i>S. gooddingii</i>			
	<i>P. fremontii</i>	3 – 4.5	Lower Colorado River, AZ	Busch and Smith, 1995
	<i>S. gooddingii</i>			
	<i>P. fremontii</i>	1.3 – 3.5	San Pedro River, AZ	Lite and Stromberg, 2005
<i>S. gooddingii</i>				

^a Studies designed to detect threshold values, other values are for observed ranges of occurrence.

GWD and related river discharge also regulate Salicaceae annual growth performances since GWD is strongly dependent on flow stage (Cooper et al., 1999) and annual growth is linearly correlated to streamflow (Stromberg and Patten, 1996; Willms et al., 1998) with growth increasing when annual flows are above the long-term annual mean (Stromberg and Patten, 1996). Within the growing season in glacial fed reaches, late winter and spring flow stages appear to be better growth predictors than late spring and early summer ones, probably because the water table is replenished by peak flows occurring at the end of the winter (Willms et al., 1998).

The geomorphic context is a further control on GWD dynamics that in turn influences plant growth. In wide unconfined valleys, growth exhibits a stronger correlation to streamflow than in narrow, canyon-shaped valleys (Stromberg and Patten, 1996). Growth performances are dependent also upon surface-subsurface flow interactions. For example, increases in the basal area of *Populus trichocarpa* have been shown to be negatively correlated with larger GWD oscillations and greater oscillations have been observed where surface water downwells into the subsurface (i.e. losing or effluent reaches) while more stable GWDs are observed where water from the subsurface upwells into surface waters (i.e. gaining or influent reaches; Harner and Stanford, 2003). Differences in growth linked to hyporheic exchange seem to be relevant only in large gravel bed rivers with expansive aquifers (Mouw et al., 2009), probably reflecting differences in nutrient load between gaining and losing reaches. Differences of growth

performance along a large unconfined reach of the Tagliamento River, Italy were noted also by Gurnell (2016), who observed an almost tenfold variability in annual growth rate of *Populus nigra*, with overall shifts in growth rate displayed across time periods of relatively higher or lower river flows and thus GWD. The effects of upwelling and downwelling on biomass productivity have been found to be more relevant at floodplain scale whereas at local (meso) scale, hydrogeomorphic processes are of greater importance (Mouw et al., 2009).

The linkages between GWD and Salicaceae can be summarized also considering the biogeomorphic co-evolution of vegetation and landforms. Initial Salicaceae stages establish near streambanks where GWD is small and substrate conditions are suitable (Cooper et al., 1999; Francis et al., 2006; Johnson, 2000). As the biogeomorphic succession (Corenblit et al. 2007) progresses, the growth of plants and associated aggradation and channel migration processes lead to an increase in GWD below the aggrading ground surface.

The GWD thresholds and timescales affecting Salicaceae are summarized in Table 1-3. For germinating seedlings or resprouting fragments, fast GWD decline rates in the order of the stress scale can be lethal. For more mature individuals with well-developed root system, temporary GWD declines are relevant on the stress to growing season time scale and negatively affect growth. If the decline persists beyond one growing season, the forest stand will decline. The average GWD level and the amplitude of its within-year fluctuations have an influence at the limiting factor scale, defining the spatial extent of suitable Salicaceae habitat and average growing conditions.

Table 1-3 Groundwater depth thresholds and corresponding timescales affecting Salicaceae processes

Threshold	Threshold value	Process	Time scale
Max water table decline	2.5 – 3 cm/day ⁻¹	Seed recruitment	Stress scale
Seedlings max roots growth	0.15 – 0.17 cm/day ⁻¹	Seed recruitment	Stress scale
Between years max DGW decline	1 – 1.5 m	Growth, canopy health, stand decline	Stress scale to growing season
Within year max DGW fluctuation	0.8 – 0.5 m	Habitat segmentation	Limiting factor
Max DGW	4 – 5 m	Habitat segmentation	Limiting factor

1.4.1.2 Waterlogging and submersion

Flooding can occur with varying magnitude inducing conditions ranging from subsurface waterlogging of the soil to complete submersion of the plant canopy. Thus, in relation to impacts on riparian vegetation, flooding severity can be viewed as a function of both flow depth and plant height. When waterlogging occurs, the exchange of oxygen between the atmosphere and soil is impaired; whereas with complete submersion, photosynthetic activity is also affected, especially when water turbidity is high (Blom and Voesenek, 1996). Since a shortage of oxygen is the main flooding effect, submersions occurring outside the period of vegetation growth when the oxygen demand of plants is negligible, are less stressful than submersions occurring during the growing season (Glenz et al., 2006). For similar reasons, cold and well-oxygenated waters are less damaging than warm waters (Bratkovich et al., 1993). During submersion, the oxygen in the substrate is progressively consumed by metabolic processes; the depletion of oxygen leads to anoxic conditions that are potentially harmful to the plants. Riparian plant species have developed a set of adaptations to cope with extended periods of flooding including the development of aerenchymatous tissues by lysogeny or schyzogeny, and the development of adventitious roots and lenticels (Armstrong et al., 1994; Jackson and Armstrong, 1999; Kuzovkina et al., 2004). Aerenchymatous tissues enhance the atmosphere-soil gas continuum by

transporting oxygen to the rhizosphere and releasing CO₂ into the atmosphere. Adventitious roots are produced in the most superficial layer of the soil where soil compaction is lower and thus oxygen concentration during flooding is relatively higher. Lenticels promote oxygen diffusion through the bark and, in some *Salix* species, the release of toxic compounds to the atmosphere (Glenz et al., 2006).

The impact of flooding on Salicaceae varies greatly with species (Figure 1-10). Negative effects encompass reduced leaf area, reduction of shoot and root mass and metabolic dysfunctions (Nielsen et al., 2010), but relatively short inundation times (i.e. 30 days or less) can promote higher growth rates in some species (Kuzovkina et al., 2004), and *Salix* appear to show better flood tolerance than *Populus* (Amlin and Rood, 2001). Flooding tolerance also varies with gender, with females exhibiting greater flood tolerance than males in both *P. angustifolia* James and the hybrid *P. jackii* Sarg. (*P. deltoides* × *P. balsamifera*) (Nielsen et al., 2010). Differences in genus (Figure 1-10) and gender flooding tolerance have been proposed as one possible reason for the spatial and sexual segregation of *Salix* and *Populus*: *Populus* is found at higher elevations than *Salix* (Amlin and Rood, 2001) and females are found at lower elevations than males (Hughes et al., 2009). Survival of seedlings and cuttings in reviewed studies (Table 1-6) is very high, often above 80% (Cao and Conner, 1999; Higa et al., 2012; Nielsen et al., 2010) and only in the most extreme cases has flooding led to early senescence and death (Amlin and Rood, 2001).

In all the reviewed research, seedlings and cuttings were grown under optimal conditions prior to flooding treatments. Furthermore, as far as we are aware, the establishment of seedlings or cuttings in waterlogged conditions has not been investigated and establishment in fully submerged settings appears a rather unlikely possibility. However, if seedlings or vegetative propagules are able to establish, their flooding tolerance can extend to several months (Amlin and Rood, 2001; Higa et al., 2012; Nielsen et al., 2010). Adult trees can tolerate even longer periods of flooding (Glenz et al., 2006) covering most, if not all, the growing season and, in the case of *S. bebbiana* and *S. discolor*, up to several years (Amlin and Rood, 2001). Nevertheless, survival through such long periods of flooding are exceptional and forest stands will decline when subjected to waterlogged or submerged conditions spanning more than one growing season (Amlin and Rood, 2001). Recovery of cuttings following a short inundation time (1-2 weeks) is rapid, with no differences observed between shoot and root weight of flooded and non-flooded cuttings after one month (Higa et al., 2012). Thus, waterlogging occurring within the disturbance time scale has limited negative effects and growth may even be promoted. However, when flooding stress or chronic waterlogged conditions extend over or beyond an entire growing season, they represent a critical limiting factor.

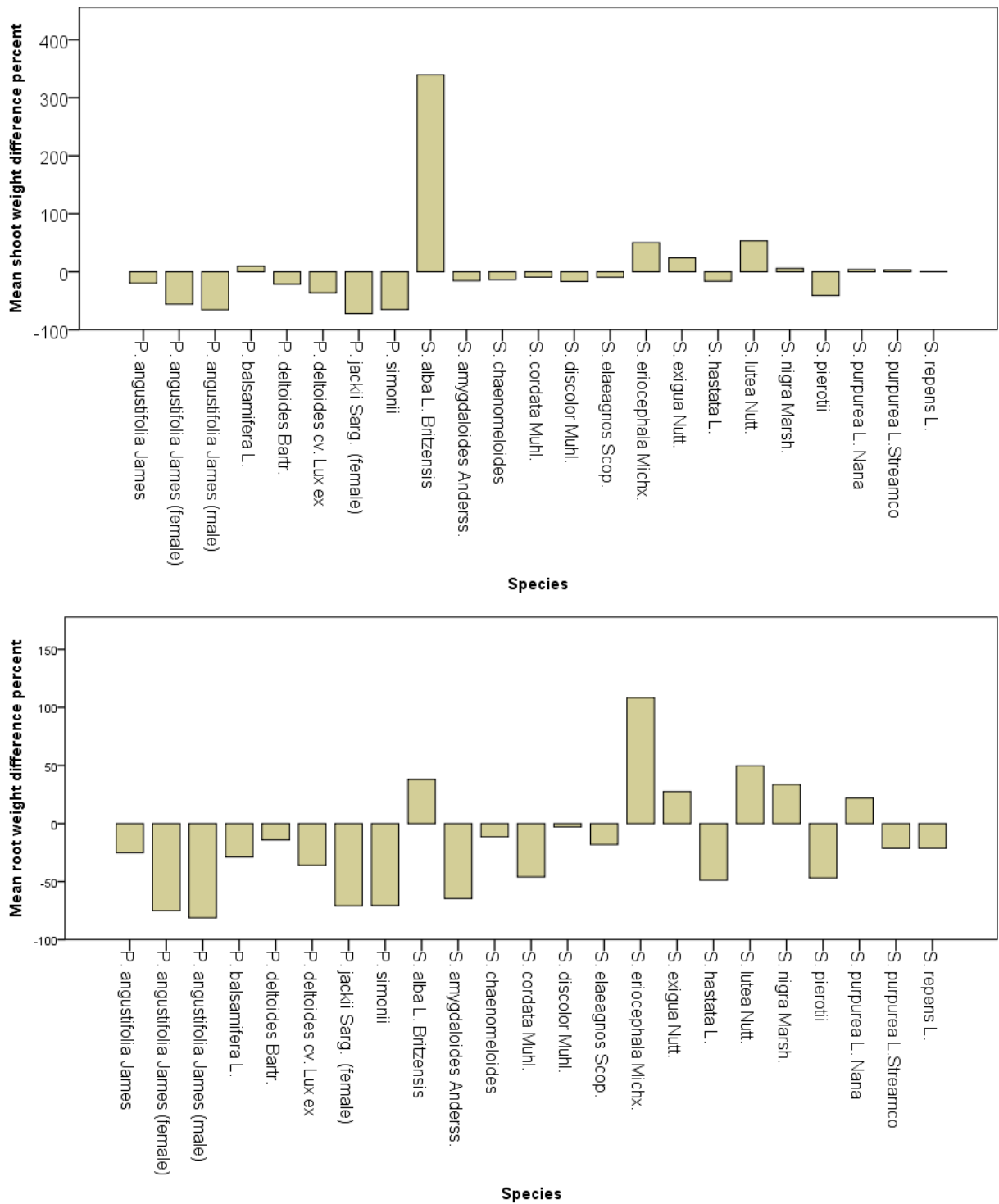


Figure 1-10 Mean shoot (top) and root (bottom) weight percentage variations in response to inundation (flooding depth and duration varies; see Table 1-6)

1.4.1.3 Drag

Flowing water exerts tractive force (i.e. drag) on vegetation during floods and thus at the disturbance time scale. When the canopy is also submerged, leaves and branches assume a more hydrodynamic shape by contracting submerged height and width (Weissteiner et al., 2015). If the drag is greater than the resistance provided by the root system, plants are dislodged and carried away with a mechanism

defined as “Type I” by Edmaier, Burlando & Perona (2011). Failure of the root anchorage system can occur because of root breakage, pullout or a combination of the two (see section 1.3.1 for roots failure mechanisms explanation). Thus the drag dislodgement effect depends on the anchorage strength provided by Salicaceae. In a field experiment on naturally occurring individuals of *P. nigra* L. and *S. elaeagnos* Scopoli aged between 2 and 6 years old, the mean critical shear stress required to pull out the plants was 31.4×10^7 Pa and 50.1×10^7 Pa for *P. nigra* L. and *S. elaeagnos*, respectively, with higher critical shear stress for individuals rooted in sand than for those rooted in gravel (S. Karrenberg et al., 2003). For small cuttings of *S. alba* and *S. viminalis* planted on a gravel bar, Pasquale et al. (2014) observed a 100% mortality with a shear stress 7 orders of magnitude lower (i.e. 27.5-35.0 Pa, Figure 1-11) occurring mainly on eroded plots. Figure 1-11 also displays differences in mortality rates yielded by the same shear stress classes in two different years, suggesting that shear stress is not the only relevant parameter explaining vegetation dislodgement. Further studies have revealed that the measured force required to pull out 1-5 year old seedlings of *Populus fremontii* and *Populus trichocarpa* was best correlated with root frontal area, plant frontal area, height and basal diameter (see Bywater-Reyes et al., 2015 for regression models). In the same study, Bywater-Reyes et al. (2015) calculated that the flow velocities required to exert pullout forces measured on the less resistant individuals were as large as ~6 m/s. Such flow velocities were calculated taking account of a frontal area reduction of approximately 70% and demonstrated that plant removal during floods are unlikely to be achieved without bar-scale or reach-scale erosional processes unless their root structures are poorly developed (Table 1-4). Therefore, the “Type I” mechanism applies only to shallow rooted small individuals or freshly deposited fragments.

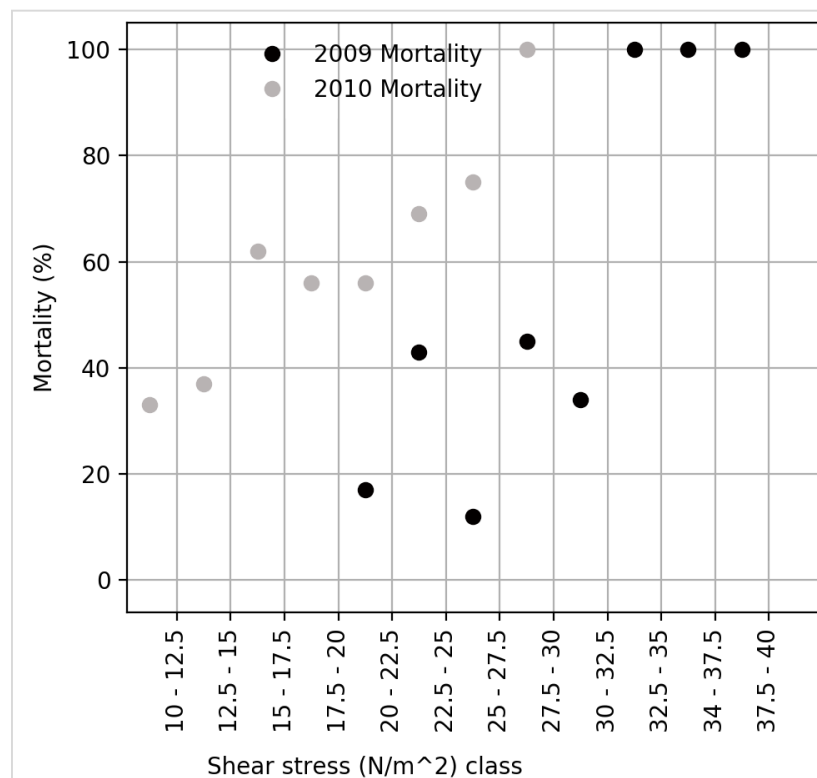


Figure 1-11 Mortality of *Salix* spp. cuttings due to deposition, erosion and shear stress (Pasquale et al., 2014)

Nevertheless, drag can still influence vegetation. The fluid momentum exerted on a trunk can be expressed as (Tanaka et al., 2007):

$$M = \frac{1}{2} \rho C_{d-ref} D_{BH} U^2 \int_0^h z \alpha(z) \beta(z) dz \quad \text{Equation 1-6}$$

Where M is the momentum acting on a tree (Nm), z is a vertical axis from the tree collar (m), Cd-ref is the reference drag coefficient, ρ is the fluid density (Kg/m³), h is water depth (m), DBH is the trunk diameter at breast height (m) and α and β are defined as:

$$\alpha(z) = \frac{d(z)}{D_{BH}} \quad \text{Equation 1-7}$$

$$\beta(z) = \frac{C_d(z)}{C_{d-ref}} \quad \text{Equation 1-8}$$

Where Cd(z) is the drag coefficient, d(z) is the cumulative width of trunk and branches (m) at height z, α(z) is the vertical tree structure coefficient, β(z) is the leaf and branch inclination coefficient. Fluid momentum on trees can cause elastic (EB) or plastic (PB) bending, or in severe cases, trunk breakage (TB). The TB threshold momentum can be expressed by the equation (Gardiner et al., 2000; Tanaka and Yagisawa, 2009):

$$M_{bc} = kd^3 \quad \text{Equation 1-9}$$

Where Mbc is the trunk braking momentum (Nm), k is a species-specific coefficient and d is the diameter of the trunk at the breaking section (m). For *S. subfragilis*, laboratory tests determined that the k coefficient was equal to 3.0 (Figure 1-12).

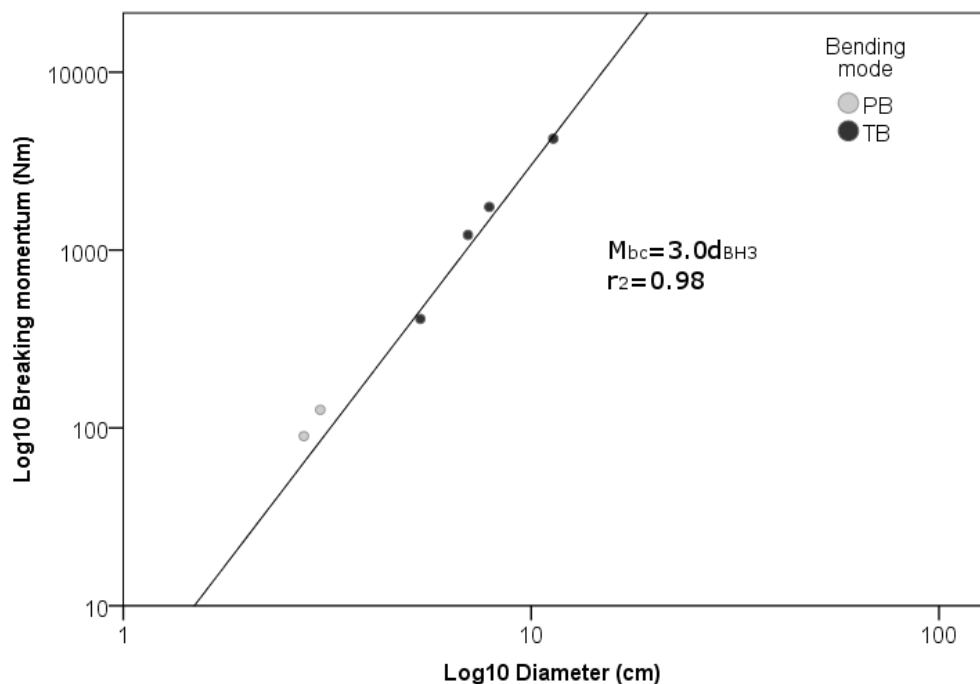


Figure 1-12 Relationship between breaking momentum and trunk diameter for *S. subfragilis* from laboratory experiments. PB: Plastic Bending, TB: Trunk Breakage (adapted from Tanaka and Yagisawa, 2009)

Trunk breaking or bending therefore scales with the plant stem diameter, while pullout is a function of the resistance provided by the root system-substrate friction interface (Table 1-4) and the plant's capacity to reduce drag by reconfiguration.

Table 1-4 Percentiles of the pullout forces measured on seedlings with different root frontal area and rooted in different substrates. Seedlings rooted in finer sediments generally exhibit higher pullout forces because of the higher friction due to the larger roots-substrate contact surface. (Data source: Bywater-Reyes et al., 2015)

Root frontal area class	Substrate	Pullout force (Pa)				
		Percentile 05	Percentile 25	Median	Percentile 75	Percentile 95
Very low (<0.0017 m ²)	Sand
	Sand - fine gravel
	Gravel	8.4	8.4	10.1	11.9	11.9
Low (0.0017 - 0.003 m ²)	Sand
	Sand - fine gravel	64.7	64.7	68.6	72.4	72.4
	Gravel	14.2	15.8	17.5	19.1	38.5
Medium (0.003 - 0.006 m ²)	Sand	282.7	282.7	519.1	585.7	585.7
	Sand - fine gravel	74.7	74.7	74.7	74.7	74.7
	Gravel	41.3	41.3	41.3	41.3	41.3
High (>0.006 m ²)	Sand	96.8	371.6	489.7	550.9	743.1
	Sand - fine gravel	183.8	331.3	877.1	1371.7	2058.3
	Gravel	101.2	101.2	284.2	467.3	467.3

1.4.2 Sediment transport

Sediment transport is associated with flood events and thus is related to the disturbance time scale.

1.4.2.1 Erosion

If flow drag is associated with local scour capable of mobilizing the coarser fraction of the sediments (e.g. d₈₄) most of the substrate is removed, reducing the root-substrate interface, root anchorage and the force required to cause tree toppling (TT) and to dislodge the plant (Figure 1-13). This mechanism was defined as the “Type II” erosion process by Edmaier et al. (2011) and, in its original formulation, it was considered to be the dominant process only for well-developed (i.e. adult) vegetation. However, the results from Bywater-Reyes et al. (2015) and to a lesser extent Rominger, Lightbody & Nepf (2010) suggest that this is the dominant plant dislodgement process-type overall. However, if the scouring process does not last long enough for sufficient root exposure, only partial TT will occur and the plant will not be dislodged.

A further morphodynamic disturbance is the dislodgement of trees standing on streambanks and terraces, where high-energy flood inundation is very infrequent (Egger et al., 2015) and floodplain forest regeneration is mainly due to (lateral) bank erosion (Little et al., 2013). In this latter case, the disturbance effect is instantaneous: the tree falls as the bank collapses. The eroded tree may then be transported away by flood waters or may remain deposited at the toe of the eroded bank. This process is fundamental to LW recruitment and has great geomorphological relevance for initiation of fluvial landforms such as islands and bars (Bertoldi et al., 2013; Lassetre et al., 2009; Little et al., 2013; Rood et al., 2015). The fate of translocated individuals largely depends on the elevation, edaphic and moisture conditions of the surface where the individual is deposited (see section 1.4.1.1).

The impacts of flow momentum and surface erosion can be thus summarized as follows. If the drag force is not sufficient to dislodge the plant, Elastic Bending (EB), Plastic Bending (PB), Trunk Breakage

(TB) or Tree Toppling (TT) can occur. EB and PB occur when the fluid momentum is not sufficient to cause TB. TT requires a degree of morphodynamic activity sufficient to cause local scour that reduces the anchoring strength of the root system (Figure 1-13). In this context, substrate granulometry is of great importance since it determines the threshold for sediment motion. After an erosion event that does not dislodge vegetation and when at least part of the root system embedded in the substrate is maintained, the recovery response is generally positive and individuals readily sprout (Asaeda et al., 2010).

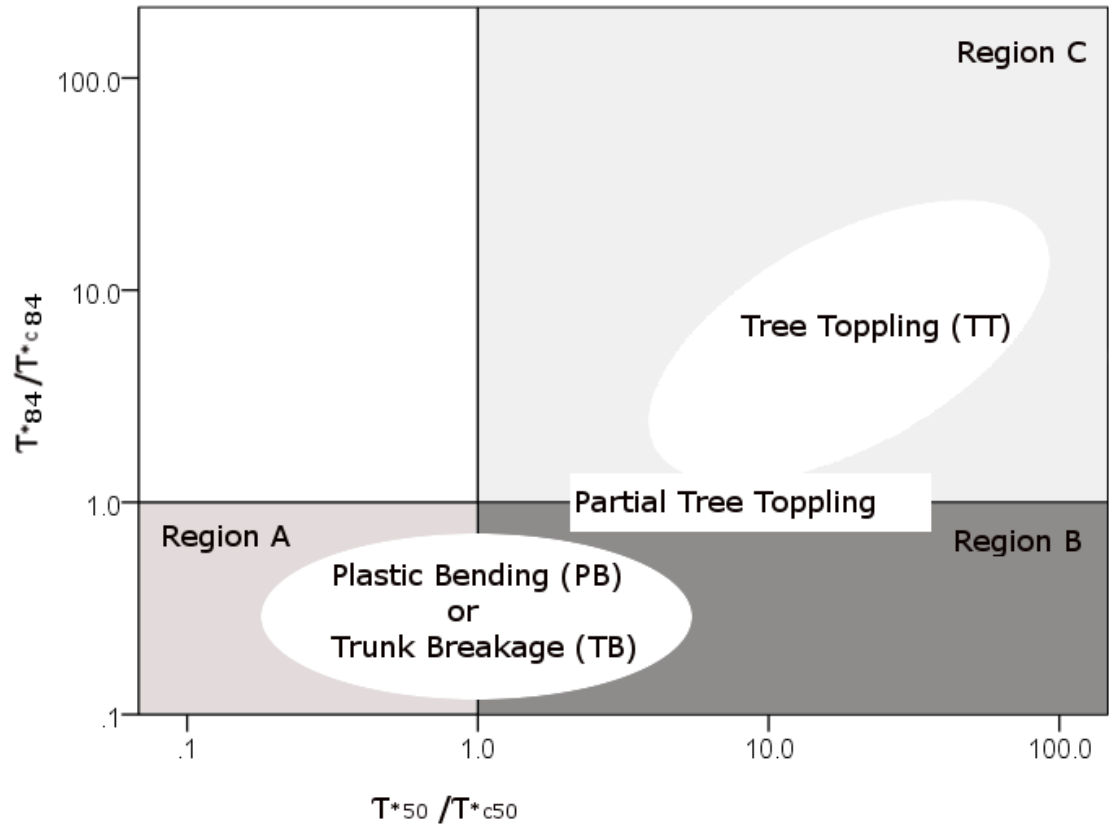


Figure 1-13 Relationship between the dimensionless particle shear stress and dimensionless critical particle shear stress and morphodynamic bending effects (with τ^{*84} dimensionless shear stress acting on d_{84} particle size, τ^{*c84} dimensionless critical shear stress for d_{84} particle size motion, τ^{*50} dimensionless shear stress acting on d_{50} particle size, τ^{*c50} dimensionless critical shear stress for d_{50} particle size motion). Region A: quasi-clear scour: only particles smaller than d_{50} are mobilized. Region B: bed partial scour: particles in the range of the d_{50} are entrained, possibly causing local armouring. Region C: bed scour: particles in the range of the d_{84} are entrained, thus causing local erosion. Adapted from Tanaka & Yagisawa (2009)

1.4.2.2 Deposition

Deposition occurs during floods and is usually accompanied by partial or complete burial of plants. While (re)sprouting is a typical trait of Salicaceae (Radtke et al., 2012), the chances of survival are bound to the quantity and style of sediment deposition. For first-year seedlings and cuttings, the lethal sediment deposition threshold appears to fall within the 40-50 cm range (Polzin and Rood, 2006). However, absolute sedimentation depth is not the only factor controlling burial damage. In a controlled experiment, Levine & Stromberg (2001) observed how small seedlings (14-69 days old) survived up to 2 cm depth of deposited sediment (sediment diameter >2 mm), depending on plant height and style of sediment deposition. Deposition occurring by gradual aggradation resulted in high survival rates of S.

goodingii and *P. fremontii*, and these rates increased as the seedlings grew taller. The Meta-analysis of data by Kui and Stella (2016) suggests an approximate 50% burial threshold. For *Populus fremontii* when relative burial (sediment deposit depth divided by plant height) is below 65 % most of the plants survive but when relative burial exceeds 55% plants begin to die and as relative burial approaches 95% most young seedlings do not survive (Figure 1-14). The key role of the relationship between plant height and burial depth is also documented by Kui and Stella (2016). They exposed 1-3 year-old seedlings of *Populus fremontii* with heights ranging from 14 to 69 cm to 9 burial treatments. The strongest statistical model estimated from their observations of plant height and burial depth indicated an increase of 13% in survival chance per centimetre plant height when burial was 10 cm increasing to 45% per centimetre plant height when burial depth was 30 cm. The second-best model highlighted the importance of the emergent (non-buried) length of the stem, with lengths over ~20 cm being the threshold for almost certain survivorship. Seedling height also has an effect on burial probability (Kui et al., 2014), based on measurements in an outdoor flume, where controlled floods of 283 L/s with a reach-average shear stress of 21 Pa were applied to 1-2 year old seedlings growing on a sand bar. For each centimetre increase in stem height, the burial probability of these *Populus fremontii* seedlings decreased by 3%, falling to 0% at 50 cm.

Seedlings survival rates have also been observed to drop to 0% when the deposited material is accompanied by bending of the seedling prior to the burial (Levine and Stromberg, 2001), even for sedimentation as shallow as 1-2 cm (Kui and Stella, 2016). Deposition alone and concurrent occurrence of deposition and bending resemble what can happen during deposition events occurring in contrasting flow velocity regimes such as in a backwater pool and in an open channel. Deposition and associated bending also confirm the importance of drag as a disturbance factor when it occurs in conjunction with morphodynamic activity.

Responses of taller individuals to burial remain poorly documented. Corenblit et al. (2009) observed that Salicaceae shrubs can thrive with mean deposition rates of 20 cm/year and up to almost 50 cm/year. Schiechl (1992) reported burial tolerances of 3.40 m and 2.20 m, corresponding to 22.7% and 29.4% of total plant height for *S. elaeagnos* and *S. purpurea*, respectively, but data for other species and higher sedimentation events are yet unavailable. Quantification of damage and mortality for older plants is complicated by the fact that is difficult to observe severe sedimentation occurring within forest stands. To our knowledge, the only documented study is by Stromberg et al. (1993) who observed the effect of a 10-year return interval flood on adult trees, pole trees and saplings of *P. fremontii* and *S. goodingii*. Trees experiencing 7.8 ± 8.2 cm deposition did not show any mortality, 93% and 73% of *S. fremontii* and *S. goodingii* pole trees survived up to 14.7 ± 12.5 cm deposition, respectively, while saplings of both species had a survival rate of 35% after deposition of 10.0 ± 6.2 cm. In all cases, survivorship was higher at higher elevations and where flow depth was less than 1.5 m. However, these figures are far from representing a severe sedimentation event. The reason for the lack of such severe sedimentation data reflects floodplain forest successional dynamics, where more advanced successional stages tend to be located at relatively higher elevations where geomorphic disturbance is less frequent and severe (Nakamura & Kikuchi 1996; Egger et al. 2015, 2016; Gurnell et al., 2016) and forest disturbance is mainly driven by other processes (see sections 1.4.1.1 and 1.4.2.1). Buried sections of the stems tend to become part of the root system (Sigafos, 1964) thus complicating roots development history in highly disturbed habitats (Holloway et al., 2017a).

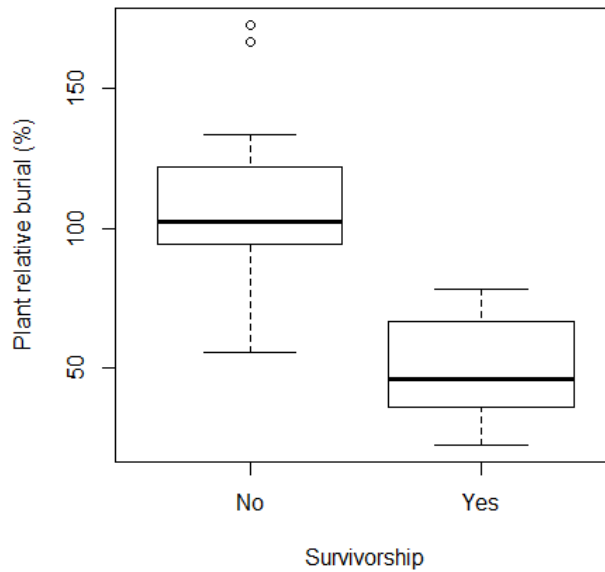


Figure 1-14 Relative burial percentage and survivorship of 1-3 years old seedlings of *Populus fremontii* with heights ranging from 14 to 69 cm. Data extracted from Kui & Stella (2016)

1.5 Discussion and conclusions

As stated in the introduction to this review, if we are to predict natural river-system functioning and aid the parameterization of numerical models attempting to replicate riparian vegetation and fluvial process interactions and long term riparian landscape development, we need to understand and be able to quantify interactions between the riparian Salicaceae and fluvial processes. We have contributed to filling this research gap by summarising current knowledge from published studies concerning the nature, direction and magnitude of Salicaceae interactions with fluvial processes, emphasising fluvial process feedbacks to the Salicaceae. In order to aid modelling, we have presented process descriptions and, where possible, model formulations and quantitative estimates. In this section, we consider uncertainties and gaps in knowledge that need to be addressed in future research so that the magnitude of relevant plant – processes interactions can be estimated more reliably and embedded in the design of management prescriptions. We also propose a framework (Figure 1-15) that incorporates flow stage and DGW as major drivers of riparian woody vegetation and can be used to guide the definition of habitat requirements and how changes in these drivers might affect the vegetation, with consequences for river morphodynamics.

Studies on the effects of plant canopies and stems on flow field and sediment transport processes have a long tradition in engineering and in principle are quite well understood both at individual plant and patch levels (Baptist et al., 2009; Gurnell et al., 2012; Nepf, 2012). However, the quantification of feedbacks from canopies and stems to fluvial processes demonstrate some differences in the level of achieved knowledge. On the one hand, the flow resistance of a rigid, non-submerged plant is similar to a solid cylinder and the quantification of the hydrodynamic effects is merely a mathematical problem (Equation 1-3). On the other hand, the flow resistance of flexible ligneous parts and leaves is a more complex problem due to the reconfiguration abilities of plants (Weissteiner et al., 2015). In this latter case, the approaches that best represent the physical processes occurring at the plant-flow interface are based on species specific parameters (Aberle and Järvelä, 2013). These approaches are relatively new and so there is a need for more studies to provide the parameters for at least the most common

Salicaceae species as well as broad seasonal variation in the properties of these deciduous canopies, thus allowing these approaches to be applicable in common practice.

A greater knowledge gap is the quantification of the additional cohesion provided by roots to alluvial substrates. The stability added to stream banks can be quantified using several models (e.g. Simon et al., 2006; Pollen, 2007; Wiel & Darby, 2007) but because such models rely on slightly different assumptions, they may generate different results and thus there may be significant uncertainty in interpreting their results, particularly when comparing model outputs. Furthermore, quantification of the stabilization of non-cohesive substrate located in the main river channel has received almost no attention. As a result, the mechanisms influencing root development within these channel substrates, a necessary prerequisite for model formulation, are not yet understood (Holloway et al., 2017b).

The greatest number of studies concerning Salicaceae responses to fluvial processes focus on drought, flooding tolerance and to some extent, burial effects on young seedlings and propagules (see Table 1-5 and Table 1-7). As a result, the degree of confidence in estimates of responses to these processes is sufficiently high to allow the formulation of flow prescriptions that will favour seed recruitment (Rood et al., 2005; Stella et al., 2006a). Responses of adult plants to drought and DGW fluctuations are also well documented (see Table 1-2) but flooding tolerance, drag and morphodynamic disturbance effects and impacts on adult vegetation stages have received less attention and rely mainly on opportunistic observations (e.g. Yagisawa & Tanaka; Asaeda et al., 2010). This makes it difficult to accurately quantify these processes although observations from available studies still provide an indication of the possible fluvial processes intensities at which “things happen”.

A further important issue is the disparity in the number of studies performed on different continents and thus focussed on different species. Most research has been conducted within various environmental settings across the United States and has been concerned with two main species, *Populus fremontii* and *Salix goddingii*. There are relatively few studies providing information for European and Asian species and environmental conditions.

Overall, the research priorities that emerge from this review relate to five main themes:

- I. Quantification of root system development in response to environmental factors
- II. Quantification of the durations of waterlogging that result in different levels of plant damage
- III. Quantification of root effects on the erosion of non-cohesive materials
- IV. Quantification of sediment deposition thresholds that impose different levels of plant damage on adult plants
- V. Estimation of species-specific process thresholds critical to colonisation, establishment, growth and survival of riparian Salicaceae species beyond those found in the United States

Beyond these thematic knowledge gaps, an additional crucial issue is the difficulty of comparing results obtained from different studies and experiments because of differences in the environmental conditions and experimental designs that have been employed (e.g. Table 1-6 and Table 1-7). To overcome this limitation our suggestion for future investigations, is to use vegetation-scaled measures (e.g. percent of submerged stem or percent of buried stem) and attempt to correlate them with physical measures (e.g. inundation duration or shear stress) rather than measuring absolute values which are then difficult to compare to other experiments or observations. For future studies, we also recommend the increased adoption of laboratory or field experimental studies because observations of disturbances and stress effects on vegetation in natural settings are complicated by a complex set of factors that are difficult to unravel, including the disturbance history of the observed plots (Wilcox and Shafroth, 2013); the non-linearity of plant responses to the intensity of particular impacting factors; the complex interactions of any such responses with other physical and biological factors that can exacerbate or reduce the effects of an impact (e.g. stem density reduces drag, deposition); and the cumulative effect of subsequent disturbances (Niinemets, 2010; Tockner et al., 2010). Nevertheless, field observations remain of utmost importance because they stimulate the formulation of new hypotheses that can then be tested experimentally and they provide a context for testing the findings of experiments that are conducted in controlled conditions to assess whether they translate into more complex, real world, environmental settings.

Despite the current lack of homogeneity in knowledge of different process-responses and how they function in different geographical settings, scientific understanding based on the existing literature allows the definition of qualitative responses for all the fluvial process feedbacks on the Salicaceae that we have examined. In addition, a set of water levels and time scales have emerged from the literature that can be organized into a framework (Figure 1-15) that can be used as a blueprint for defining habitat requirements (e.g. in a river restoration project) or for assessing qualitatively how changes in a river's hydrology and hydraulics (e.g. because of a dam construction) might affect the local riparian Salicaceae community. The framework (Figure 1-15) recognizes flow stage and DGW as the major drivers of riparian woody vegetation (Merritt et al., 2010; Poff et al., 1997). In accordance with classical disturbance theory (Pickett and White, 1985), flow stage or DGW (Figure 1-15 vertical axis) influence Salicaceae only if they persist at a specific level for a sufficient time (Figure 1-15 horizontal axis). This provides the basis for defining a threshold of probable concern or a set of suitable habitat conditions as a combination of both water level magnitude and duration.

In the proposed framework (Figure 1-15), the vertical axis identifies a range of critical flow stages while the horizontal axis describes the 'disturbance', 'stress', 'growing season' and 'limiting factor' timescales identified in this review. The lowest critical flow stage that is identified is the long-term 'average annual low DGW'. Lowering of this stage by more than 1-1.5 m for longer than a growing season will lead to stand decline (Scott et al., 2000, 1999; Shafroth et al., 2000) while shorter periods, in the order of the growing season, will limit the seasonal stand growth and plant vigour and health (Cooper et al., 2003; Scott et al., 1999). Water availability between the long-term 'average annual low DGW' and the long term 'growing season average flow stage' (Figure 1-15) defines the average hydrological growth conditions experienced by the vegetation. Periods of flow unusually higher than the long term 'growing season average flow stage' that do not extend beyond a single growing season and do not lead to prolonged 'waterlogging' conditions promote biomass growth above the annual average rate (Stromberg and Patten, 1996; Willms et al., 1998). The most suitable establishment positions for seedlings and large wood propagules are just above long term 'growing season average flow stage', where the DGW is small and newly established plants can easily access water (Mahoney and Rood, 1998; Moggridge and Gurnell, 2009). 'Waterlogging' extending for an entire growing season can reduce annual growth (Nielsen et al., 2010). Longer periods of 'waterlogging' are even more detrimental and if submersion of the ground surface (water levels between the 'waterlogging' and 'flood event discharge' stages) extends beyond the length of a growing season, vegetation stands are extremely likely to decline (Amlin and Rood, 2001). Discharges exceeding the 'flood event discharge' threshold stage are confined to the 'disturbance' time scale (Figure 1-15) and involve turbulent flows that exert drag and can cause erosion, potentially leading to trunk bending, breakage, and partial or complete tree toppling. Partial or complete tree toppling is most likely the flow stage and associated flow energy exceed the required level for 'incipient transport of coarser particles' so that the coarser fraction of the sediments become mobilised (Friedman and Auble, 1999; Tanaka and Yagisawa, 2009). When the stage is sufficient for flood waters to move significant quantities of sediment (i.e. the 'incipient transport of coarser particles' stage is exceeded) vegetation can also be damaged by burial and bending when the mobilised sediment is transported and deposited. In the case of burial, vegetation stands begin to decline when only partly buried and are likely to die when completely buried (Kui and Stella, 2016), especially when burial is associated with bending (Levine and Stromberg, 2001). Threshold values (e.g. length of the growing season or flood event discharge) for these various impacts may change accordingly to factors such as climate and river size (Belletti et al., 2013), species and growth stage. However, the extensive body of evidence identified in this review suggests at least some approximations of appropriate values for such thresholds.

The evidence compiled in this review can also aid the parameterization of numerical models that combine hydro-morphological and riparian vegetation interactions. Such models have shown considerable development recently (Solari et al., 2015). The formalization of physical processes in such

models can rely on robust mathematics but the representation of vegetation responses and their feedbacks are often not adequately represented or oversimplified (Camporeale et al., 2013). One reason for this is the difficulty of gathering sufficient information from numerous, diverse publications to parameterize processes and dynamics even though their mathematical structure is quite well understood (Corenblit et al., 2010; Egger et al., 2013; Fierke and Kauffman, 2005). We intended this review to provide a useful synthesis to support such endeavours and to provide reference material for judging model outcomes, for example from those assuming vegetation disruption in response to morphodynamic activity (Bertoldi et al., 2014; Politti et al., 2014) or moisture condition (García-Arias et al., 2013b).

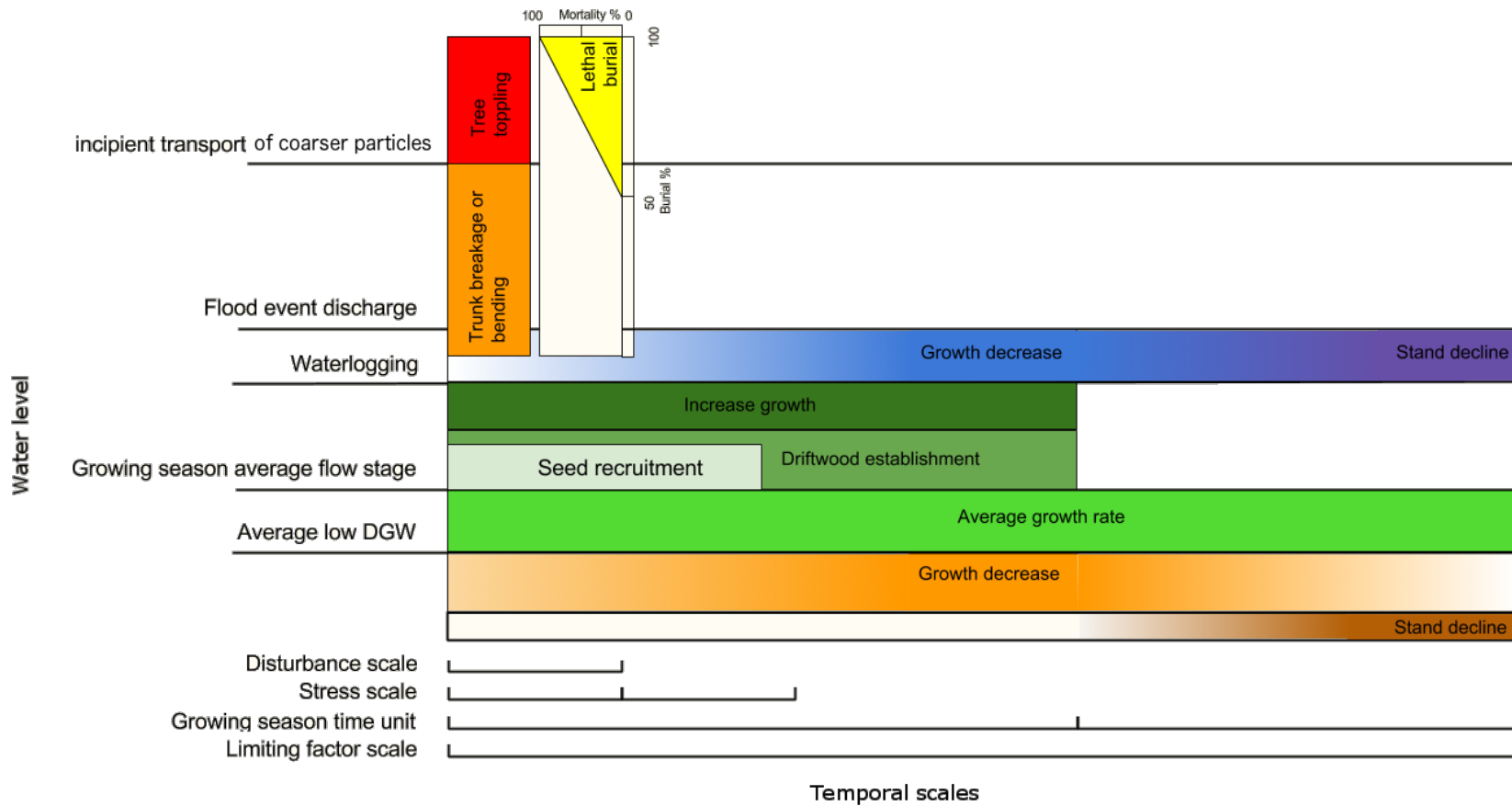


Figure 1-15 Relevant water stage thresholds and time scales affecting riparian Salicaceae recruitment, growth and survival

Table 1-5 Experimental and observed water table decline rates, root elongation, substrates and germinations survival percentages of seedlings and cuttings. * Field observation; ** Controlled experiment; * Field experiment. W Weight, L Length. s Seedling, c Cutting**

Author	Species	Texture	Water table decline rate (cm day-1)	Root elongation (mm day-1)	Shoot: root	Survival rate (1st & 2nd year)
Segelquist et al. 1993 **	<i>P. deltooides</i> subsp. <i>Monilifera</i> s	6% gravel (>2000 µm), 78% sand (>300-2000 µm), 16% fine sand (>75-300 µm), <1% silt & clay	0 (saturated)	2.8 mm day-1	0.73 W, 0.08 L	95%
			0.4	4.0 mm day-1	0.69 W, 0.07 L	93%
			0.7	2.9 mm day-1	0.76 W, 0.08 L	79%
			2.9	3.0 mm day-1	0.67 W, 0.05 L	49%
			Immediate drain.	-	-	0 (not germinated)
Van Splunder et al., 1996***	<i>S. alba</i> L. s	Clay and sand (1:19)	0 (saturated)	7.5 mm day-1	4.89 W	
			Immediate drain.	12.8 mm day-1	3.02 W	
	<i>S. triandra</i> L. s		0 (saturated)	7.0 mm day-1	5.10 W	
			Immediate drain.	14.7 mm day-1	2.96 W	
	<i>S. viminalis</i> L. s		0 (saturated)	5.3 mm day-1	5.74 W	
			Immediate drain.	11.0 mm day-1	3.37 W	
	<i>P. nigra</i> L. s		0 (saturated)	2.4 mm day-1	7.58 W	
			Immediate drain.	8.6 mm day-1	3.51 W	
Amlin & Rood 2002***	<i>P. balsamifera</i> L. s	Medium sand & fine gravel (10:3)	0			75%
			1			92%
			2			63%
			3			38%
			4			25%
			8			17%
	<i>P. deltooides</i> L. s		0			36%
			1			43%
			2			29%
			3			57%
			4			29%
			8			0%

Author	Species	Texture	Water table decline rate (cm day-1)	Root elongation (mm day-1)	Shoot: root	Survival rate (1st & 2nd year)
	<i>S. exigua</i> Nutt. s		0			30%
			1			20%
			2			0%
			3			0%
			4			0%
	<i>S. lutea</i> Nutt. s		8			0%
			0			73%
			1			32%
			2			31%
			3			30%
	<i>P. angustifolia</i> James c	4			9%	
		8			0%	
		0	3.2	0.18 L		
		1	5.9	0.14 L		
		2	4.1	0.2 L		
			3	1.4	0.18 L	
			4	1.6	0.08 L	
			8	1.4	0.06 L	
			0	5.1	0.41 L	
			1	10.5	0.16 L	
	<i>P. balsamifera</i> c		2	12.4	0.07 L	
			3	9.7	0.06 L	
			4	6.8	0.03 L	
			8	4.1	0.05 L	
			0	5.1	0.41 L	
	<i>S. drummondiana</i> Barratt. c		0	4.6	0.35 L	
			1	8.1	0.25 L	
			2	6.5	0.34 L	
			3	4.1	0.26 L	
			4	1.1	0.63 L	
			8	0.8	0.6 L	
	<i>S. exigua</i> Nutt. c		0	4.6	0.35 L	
			0	6.2	0.26 L	
1		11.4	0.18 L			
		2	17	0.11 L		
		3	6.8	0.17 L		

Author	Species	Texture	Water table decline rate (cm day-1)	Root elongation (mm day-1)	Shoot: root	Survival rate (1st & 2nd year)
			4	4.1	0.17 L	
			8	2.7	0.25 L	
Stella and Battles, 2010** Stella et al. 2010 **	<i>P. fremontii</i> S. Watson ssp. <i>fremontii</i> s	Medium and coarse sand (85% 0.25-1mm), d50=0.6mm	0	3.06	1.60 W	72%
			1	3.06	1.65 W	68%
			3	1.61	2.05 W	12%
			6	-	-	0%
			9	-	-	0.03%
			0	6.67	1.32 W	88%
	<i>S. godingii</i> C. Ball s	Medium and coarse sand (85% 0.25-1mm), d50=0.6mm	1	5.16	1.40 W	84%
			3	2.42	1.60 W	38%
			6	-	-	0.05%
			9	-	-	0%
	<i>S. exigua</i> Nutt. s	Medium and coarse sand (85% 0.25-1mm), d50=0.6mm	0	4.43	1.06 W	66%
			1	2.74	1.10 W	64%
3			1.94	1.40 W	26%	
6			3.06	1.60 W	0.02%	
9			-	-	Not tested	
Francis et al. 2004 ***	<i>P. nigra</i> L. c	Sand (d50 = 2.57φ)	0			100%
			1			80%
			3			0%
		Gravel (d50 = -2.79φ)	0			0%
			1			20%
			3			0%
Francis et al. 2005 ***	<i>P. nigra</i> L. c	Sand (~20 mm diameter)	0	0.12	9.6 w , 0.62 L	
			1	0.70	0.32 w , 0.38 L	
			3	0.21	8 w , 0.16 L	
		Gravel (~1mm diameter)	0	-	-	
			1	0.08	4.7 w , 0.08 L	
			3	0.5	12.2 w , 0.04 L	
	<i>S. elaeagnos</i> Scop. c	Sand (~20 mm diameter)	0	0.11	12.2 w , 1.3 L	
			1	0.23	1.8 w , 0.42 L	

Author	Species	Texture	Water table decline rate (cm day-1)	Root elongation (mm day-1)	Shoot: root	Survival rate (1st & 2nd year)
			3	1.29	8.2 w, 0.36 L	
		Gravel (~1mm diameter)	0	0.16	4.2 w, 0.66 L	
			1	0.08	-	
			3	0.94	4.2 w, 0.36 L	
González et al. 2010 **	<i>P. alba L. s</i>	Sand with some gravel (56% >2mm, 32% >63µm, 12% <63 µm)	0 (saturated)	1.9 mm day-1	0.7 w	88 ± 6 %
			1	5.3 mm day-1	1.2 w	90 ± 3 %
			2.5	5 mm day-1	1.21 w	58 ± 10 %
			5	4.6 mm day-1	1.22 w	26 ± 8 %
			Immediate drain.	3.0 mm day-1	1.2 w	22 ± 4 %
		Gravel (d50 = 8.5 mm)	0 (saturated)	2.8	0.6 w	86 ± 4 %
			1	-	-	0%
			2.5	-	-	0%
			5	-	-	0%
			Immediate drain.	-	-	0%

Table 1-6 Shoot and root growth responses to flooding stress experiments

Author	Species	Water depth (cm)	Time (days)	Avg. shoot weight (g)	Avg. root weight (g)	Shoot: root
	<i>S. alba</i> L. 'Britzensis'	0	21	23.1	5.4	4.26
Kuzovkina et al., 2004	<i>S. amygdaloides</i> Anderss.			13.3	4.8	2.79
	<i>S. cordata</i> Muhl.			17.1	2.6	6.50
	<i>S. discolor</i> Muhl.			16.6	4.7	3.55
	<i>S. elaeagnos</i> Scop.			11.4	1.5	7.50
	<i>S. eriocephala</i> Michx.			15.4	5.1	3.03
	<i>S. exigua</i> Nutt.			17.3	3.0	5.71
	<i>S. hastata</i> L.			13.7	2.7	5.13
	<i>S. nigra</i> Marsh.			21.4	5.3	4.06
	<i>S. purpurea</i> L. 'Nana'			11.3	3.4	3.31
	<i>S. purpurea</i> L. 'Streamco'			14.3	5.2	2.76
	<i>S. repens</i> L.			5.7	1.3	4.37
	<i>S. alba</i> L. 'Britzensis'	4	21	25.0	7.5	3.3
	<i>S. amygdaloides</i> Anderss.			11.2	1.7	6.6
	<i>S. cordata</i> Muhl.			15.5	1.4	10.9
	<i>S. discolor</i> Muhl.			17.4	5.6	3.1
	<i>S. elaeagnos</i> Scop.			10.3	1.2	8.3
	<i>S. eriocephala</i> Michx.			23.1	10.6	2.2
	<i>S. exigua</i> Nutt.			18.25	5.46	3.34
	<i>S. hastata</i> L.			11.47	1.36	8.41
	<i>S. nigra</i> Marsh.			22.69	7.05	3.22
	<i>S. purpurea</i> L. 'Nana'			11.81	4.17	2.83
	<i>S. purpurea</i> L. 'Streamco'			14.83	4.09	3.63
	<i>S. repens</i> L.			5.68	1.02	5.56
Vandersande et al., 2001	<i>S. goddingii</i>	submerged	58	51.20	26.90	1.90
	<i>P. fremontii</i>			56.50	25.50	2.22

Author	Species	Water depth (cm)	Time (days)	Avg. shoot weight (g)	Avg. root weight (g)	Shoot: root
Nielsen et al., 2010	<i>P. angustifolia</i> James (male)	11	48-60	3.44	0.26	13.08
	<i>P. angustifolia</i> James (female)			4.85	0.40	12.15
	<i>P. jackii</i> Sarg. (female)			10.39	1.59	6.54
	<i>P. angustifolia</i> James (male)	7	48-60	7.16	1.06	6.77
	<i>P. angustifolia</i> James (female)			7.83	1.04	7.51
	<i>P. jackii</i> Sarg. (female)			28.51	4.86	5.87
	<i>P. angustifolia</i> James (male)	1	48-60	31.96	5.54	5.76
	<i>P. angustifolia</i> James (female)			10.02	1.56	6.43
	<i>P. jackii</i> Sarg. (female)			8.02	1.46	5.48
Du et al., 2012	<i>P. deltoides</i> cv. Lux ex	0	22	39.22	9.91	3.96
	<i>P. simonii</i>			22.46	4.46	5.04
	<i>P. deltoides</i> cv. Lux ex	10	22	29.04	7.20	4.03
	<i>P. simonii</i>			10.01	1.62	6.18
	<i>P. deltoides</i> cv. Lux ex	150	22	21.07	5.50	3.83
	<i>P. simonii</i>			5.61	1.00	5.61
Higa et al., 2011	<i>S. chaenomeloides</i>	control	0/56	0.02	0.03	0.64
	<i>S. pierotii</i>			0.03	0.01	5.99
	<i>S. chaenomeloides</i>	submerged	7/56	0.03	0.04	0.63
	<i>S. pierotii</i>			0.04	0.02	1.51
	<i>S. chaenomeloides</i>	submerged	14/56	0.02	0.03	0.67
	<i>S. pierotii</i>			0.02	0.03	0.87
	<i>S. chaenomeloides</i>	submerged	24/56	0.02	0.03	0.66
	<i>S. pierotii</i>			0.02	0.04	0.44
	<i>S. chaenomeloides</i>	submerged	56/56	0.00	0.01	0.35
	<i>S. pierotii</i>			0.00	0.04	0.08
Cao and Conner, 1999	<i>P. deltoides</i> Marsh.	control	42	24.65	4.80	5.14
		3	42	18.59	1.25	14.85

Author	Species	Water depth (cm)	Time (days)	Avg. shoot weight (g)	Avg. root weight (g)	Shoot: root
		submerged	42	7.80	0.91	8.55
Amlin and Rood, 2001	<i>P. deltoides</i> Bartr.	2.5	152	5.57	1.56	3.58
	<i>P. balsamifera</i>			2.02	2.21	0.91
	<i>P. angustifolia</i> James			0.88	0.55	1.61
	<i>S. discolor</i> Muhl.			3.94	2.67	1.48
	<i>S. exigua</i> Nutt.			2.20	1.51	1.45
	<i>S. lutea</i> Nutt.			1.03	0.93	1.11
	<i>P. deltoides</i> Bartr.	5	152	4.66	2.15	2.17
	<i>P. balsamifera</i>			3.24	2.66	1.22
	<i>P. angustifolia</i> James			0.86	0.72	1.20
	<i>S. discolor</i> Muhl.			3.02	4.29	0.70
	<i>S. exigua</i> Nutt.			3.10	1.99	1.56
	<i>S. lutea</i> Nutt.			1.69	1.88	0.90
	<i>P. deltoides</i> Bartr.	7.5	152	4.22	0.93	4.56
	<i>P. balsamifera</i>			1.74	0.87	2.00
	<i>P. angustifolia</i> James			0.65	0.23	2.88
	<i>S. discolor</i> Muhl.			3.52	1.95	1.80
	<i>S. exigua</i> Nutt.			3.10	1.60	1.94
	<i>S. lutea</i> Nutt.			1.28	0.93	1.38
	<i>P. deltoides</i> Bartr.	10	152	4.28	0.94	4.56
	<i>P. balsamifera</i>			1.65	1.18	1.40
	<i>P. angustifolia</i> James			0.62	0.29	2.15
	<i>S. discolor</i> Muhl.			2.47	0.93	2.66
	<i>S. exigua</i> Nutt.			2.37	1.41	1.69
	<i>S. lutea</i> Nutt.			1.77	1.37	1.30

Table 1-7 Factors controlling riparian species asexual reproduction and survival.

Asexual mode: 1flood training, 2: translocated fragments, 3: coppice re-growth, 4: suckering. **Site specific (observed). ***From summer river stage. *Elevation relative to nearest vegetated surface. ***** Measured with respect to the lower limit of established floodplain forest. a Field study. b Controlled experiment c Field experiment**

Author	Species	Factor	Effect*	Value**
Barsoum, 2002a	<i>Populus nigra L.</i> , <i>Salix alba L. var alba</i>	Low elevation	- records	>0.7 m ***
		High elevation	+	>0.7 m ***
		Gravel bar (LE)	-/+	>0.7 m ***
		Sand bar (LE)	-/+	>0.7 m ***
		Sediment filled depression (LE)	- records	<0.7 m ***
		Fringe around piles of woody debris	++	<>0.7 m ***
		Sand accretion downstream from	+	<0.7 m ***
		Sediment filled depression (HE)	- records	<0.7 m ***
		Erosion areas (HE)	- records	
		Bank scouring sites	++	
		Link to parent plant	1,3,4 +	
		Floods	1,2,3,4 +	
		Cutting relocation (with loss of roots)	No	
		Soil moisture	+	
Waterlogged soil	-			
Francis et al., 2004b,c	<i>Populus nigra L.</i>	Coarse sediment (with subsurface)	+	
		Higher elevation (dry)	-	-84 - 0 cm****
		Lower elevation	+survival	-140 - -108
		Flood duration	-	
		Flood duration	- growth	
		Late summer planting	+	September
		Early summer planting	-	May
		Root inundation	-	5-10 day or
		Coarse sediment (gravel only)	-survival	
Moggridge and Gurnell, 2009c	<i>Populus nigra L.</i> , <i>Salix elaeagnos Scop.</i> <i>Salix alba L.</i>	Late summer planting	+	September
		Early summer planting	-	May
		High elevations	+survival	-0.44 – 0 ****
		Upstream vegetation (far enough to	+survival	
		Sediment organic content	+	
		Soil moisture content	+	
		Fine sediment	+survival	
Coarse sediment	-			

2 Fuzzy modelling of riparian vegetation dynamics and fluvial processes feedbacks

2.1 Introduction

Riparian vegetation and fluvial processes are bound by a relationship of mutual dependency. On one hand, fluvial processes shape the physical template onto which vegetation develops (Polzin and Rood, 2006), regulate essential limiting factors such as water and nutrients (Harner and Stanford, 2003), transport seeds and propagules (Merritt and Wohl, 2006) and account for the disturbance regime regulating vegetation succession (Bornette and Amoros, 1996; Egger et al., 2015). On the other hand, riparian vegetation increases local flow resistance promoting aggradation inside the vegetated areas and scour at their edges (Nepf, 2012); with their roots, vegetation stabilizes in-channel non-cohesive substrate and banks, thus reducing erosion and slope failure (Abernethy and Rutherford, 2000; Pasquale and Perona, 2014).

Given the strong interdependence between riparian vegetation and fluvial processes dynamics, effective modelling of riparian systems calls for integrated modelling of these dynamics (Camporeale et al., 2013; Richards et al., 2002).

In recent years, many numerical, analytical and rule-based models representing fluvial processes and riparian vegetation have been proposed (see Camporeale et al., 2013; Solari et al., 2015; You et al., 2015). Nevertheless, very few of these models incorporate, at least to some extent, the mutual influence of riparian vegetation and fluvial processes. One of these is the model proposed by Bertoldi et al., (2014). This model represents vegetation in terms of dimensionless biomass density and regulates its growth as a function of the distance from the water table. Vegetation disruption occurs when the shear stress exceeds the critical shear stress for particles motion. Where vegetation is present, such critical value is linearly increased in respect of vegetation biomass, at the same time, vegetation roughness is also linearly increased and the drag acting on vegetation is subtracted from the total shear stress acting on the sediments. As a result, the combined cohesion and increased flow resistance provided by vegetation reduces local flow velocity and reduces erosion. Further model accounting for vegetation and fluvial processes interdependence was developed by Crosato and Saleh, (2011). In this model, vegetation establishment is obtained by stopping the model and manually assigning to the cells that became dry after a deposition or channel avulsion event, the same vegetation density as the neighbouring vegetated cells. Vegetation effects on bed shear stress is computed in a similar way as Bertoldi et al., (2014), i.e. by separating the shear stress acting on vegetation and the shear stress acting on the sediments. In addition, Crosato and Saleh, (2011) distinguish vegetation flow resistance due to submerged and emergent vegetation by applying the flow resistance approach proposed by Baptist, (2005). A similar approach is also implemented also in van Oorschot et al., (2016) where vegetation flow resistance is as well parted in emergent and submerged (Baptist et al., 2009). In this model, vegetation flow resistance depends on stem density, height and diameter which are modelled using a logarithmic growth function. Vegetation mortality is computed once per year, it occurs by waterlogging, desiccation, flow velocity (i.e. uprooting), burial or scour. Mortality due to waterlogging, desiccation and flow velocity is modelled with a dose-effect approach consisting in vegetation mortality, in terms of individuals' percent, that is proportional to the intensity of the morphodynamic disturbance. Scour and deposition mortality instead occur respectively when erosion exceeds roots length or the complete

plant is buried. Vegetation establishment considers distance from water level and vegetation seed recruitment window, the model allows for composite vegetation types and age classes per spatial unit. The results of these models with current understanding of river systems, for example: changes in water availability and disturbance regime reflects on vegetation density (Bertoldi et al., 2014). Low vegetation densities resulted in braided channels while higher vegetation densities led to anastomosed or single thread channels (Crosato and Saleh, 2011). These different river styles are the results of vegetation feedback on sediment transport processes and associated morphodynamic activity (van Oorschot et al., 2016). Compliance with current river science paradigms proves the usefulness of these models in the advancement of vegetation-fluvial processes integrated modelling. Nevertheless, several key feedbacks and processes are still underrepresented or not present in all these models. For example, the increased sediment cohesion due to plant's roots is not always considered nor is the additional bank cohesion provided by roots. Vegetation disruption is treated in a simplistic manner or with a timescale that does not reflect the within-year changes in vegetation cover. Furthermore, large wood (LW) dynamics are not considered and vegetation growth rate does not account for the cumulative stress deriving from subsequent disturbances. These feedback and processes can have profound impacts on bank stability (Pollen-Bankhead and Simon, 2009), vegetation renewal from LW in highly dynamic river systems (Kollmann et al., 1999) and cumulative disturbance effects on vegetation growth performance (Niinemets, 2010). To this end, the present work attempts to fill this gap by proposing an integrated vegetation-hydromorphological model that retains several features of the most advanced state of the art vegetation-hydromorphological models but introduces also several innovative aspects. More in detail, the model presented in this paper features a LW dynamics and establishment routine, feedback to both non-cohesive and bank substrate, reconciliation between the timescale at which disturbances and ecological processes are modelled and impacts of vegetation health status on growth performances. In this paper, greater relevance is given to the vegetation component of the model for is the most original contribution being the hydromorphological component the results of previous works (Bates et al., 2010; Coulthard et al., 2013). Moreover, the developed vegetation component is model-neutral, meaning that it can work with any hydromorphological model, provided this latter has the capabilities of supplying the hydromorphological variables required by the vegetation component. The purpose of the proposed model is to replicate reach-scale vegetation dynamics over time scales sufficiently long to capture vegetation and morphology development trajectories. The objective of this chapter, is to present the model concept, structure and test its validity by means of conceptual validation performed by assessment of several simulated scenarios. Validation is intended here as assessment of how well the proposed model replicates riparian systems in respect of the model purposes (Glenz et al., 2006; Rykiel, 1996). Therefore, model results will not be compared with an observed dataset but evaluated to assess whether they comply with expected system behaviour.

2.2 Methods

2.2.1 Caesar Lisflood-Fp

All the fluvial processes necessary to provide the inputs for the Vegetation Model Component (RVM) have been simulated using Caesar Lisflood-Fp (CLF) (Coulthard, 2017; Coulthard et al., 2013, 2002; Van De Wiel et al., 2007). CLF is a reduced complexity model able of simulating hydro-morphological processes at reach and catchment scale. It operates on a temporal-continuous mode, i.e. it does simulate every single hour of the simulated period. CLF differs from other hydro-morphodynamic models for the implementation of a simplified form of the 2D shallow water equations, such simplification results in an execution speed order of magnitude higher than models implementing classical shallow water approaches (Bates et al., 2010). The use of 2D shallow water equations precludes the possibility of modelling secondary currencies that account for meanders formation and migration, therefore, in order to simulate bank migration CLF implements analytical solution similar to the one proposed by Ikeda et al., (1981). Further simplification introduced by CLF is the routing of the sediments to only four neighbouring cells. CLF operates on a regular raster grid; therefore, all the modelling operations occur on a cell basis. CLF implements also a slope failure routing which erodes surfaces having an angle greater than a given threshold (see Table 2-7)

The inputs required by CLF (Table 2-6) are an initial topography and an input file listing the discharge at regular time steps (e.g. hourly discharge). Further optional inputs are the elevation a.s.l. of the bedrock layer, an initial three-dimensional distribution of the substrate grainsizes and the solid discharge for each modelled grainsize. Whenever this last input is not present, it can be replaced by choosing an appropriate option on CLF graphical user interface (GUI). With this option set, all the sediments leaving the modelling domain will be recirculated from the inflow points (Coulthard, 2017). Full listing of the CLF parameters values and the sediment input distribution are listed in Table 2-7 and Table 2-8 respectively.

2.2.2 Riparian vegetation model component

RVM simulates woody vegetation only, the modelled attributes are: age, diameter (D), plant count, roots density maximum depth (RDMD), height (H), fitness, large wood (LW) age, LW count and LW diameter (see Table 2-6 for definitions and units). These properties are optional RVM inputs: if an initial vegetation distribution is not provided, RVM will begin the colonization of the available habitat with the timing and rules described in section 2.2.5.1. Being the RVM based on a cellular spatial model, all vegetation properties are lumped at cell level, i.e. all the plants in a cell are assumed to be equal in size, age, etc. RVM models only one ligneous species, the choice would typically fall on one which has ecological engineering capabilities such those of the species ascribed to the family of Salicaceae. Submodels simulating vegetation establishment by either sexual or asexual reproduction in particular, are tailored to Salicaceae reproductive traits (see section 2.2.5.1 and 2.2.5.8) for these species are the most common ligneous species starting woodland succession in the active channel.

Despite the relative good understanding of many relationships entwining riparian vegetation and fluvial processes (Corenblit et al., 2011; Egger et al., 2015; Gurnell et al.,

2012), many of these are still poorly quantified and lack for mathematical formalization (Camporeale et al., 2013; Politti et al., 2017). Therefore, RVM was developed using a fuzzy logic approach to model all those processes difficult to parameterize because of scarce empirical data or whose mathematical solution is computationally intensive and therefore limits the usability of the model when simulating long time periods.

2.2.2.1 Fuzzy logic principles in ecological modeling

Fuzzy logic (or fuzzy set) theory has a long and well-established tradition in ecological modelling (Barros et al., 2000; Benjankar et al., 2014; Glenz et al., 2008; Roberts, 1996). It stems from conventional set theory but instead of classifying a given value as being a member or not being a member of a set, fuzzy logic assigns weighted partial memberships, thus allowing one to model processes using degrees of truth rather than hard thresholds. Knowledge about the system is modelled using rules (e.g. “If shear stress is strong and root depth is shallow then mortality is high”) instead of algorithms. Partial memberships to the fuzzy sets (e.g. strong and shallow) of the input variables (e.g. shear stress and root depth) are aggregated to produce a single fuzzy set i.e. the fuzzy output (e.g. high mortality). The output of a fuzzy system can be transformed into a scalar value (e.g. a mortality percentage) by the defuzzification process, thus providing an input for decision routines (I.E.C., 2000). Several defuzzification methods exist but for all the fuzzy submodels presented in section 2.2.5, the Centre of Gravity (COG) or centroid method was applied. This method computes the centre of the area of the output fuzzy set and was deemed as most appropriate to represent ecological processes because the defuzzified outputs move smoothly in the solution space, thus allowing to model gradual transitions from one.

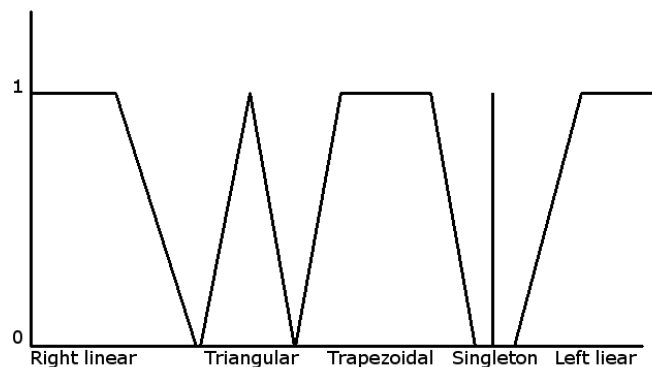


Figure 2-1 Fuzzy sets shapes available in RVM. Adapted from (I.E.C., 2000)

Although there are many possible shapes to describe fuzzy sets, the proposed model implemented only those in Figure 2-1. These shapes are the most commonly used in ecological modelling and represent a good compromise among system representation fidelity, programming complexity and computational efficiency.

Fuzzy logic approach is particularly applicable to situations where system's relationships are mathematically too costly for being solved or to model complex nonlinear relationships such as those found in natural ecosystems (Salski, 1992).

2.2.3 Integration of physical and biological processes

The integration between physical and biological processes occurs through exchange of variables between CLF and RVM. Although developed as a separate and independent package, RVM execution is integrated into CLF, thus featuring a seamless execution flow. CLF computes flow routing, sediment entrainment and transport, slope failure processes and bank erosion. The resulting physical variables delivered to RVM are: grainsize spatial distribution, shear stress, water depth and changes in topography from where erosion and deposition can be derived (blue shapes in Figure 2-2). Water depth and topography are used in RVM to estimate, by inverse distance weighting, the water table elevation over the whole modelling domain. In addition to this set of processes and variables, that are part of CLF standard implementation (Coulthard et al., 2013, 2002; Van De Wiel et al., 2007), CLF has been extended (green-blue gradient shapes in Figure 2-2) with LW routing functionalities simulating LW motion and position within the modelling domain (see section 2.2.5.8.1). On the other hand, RVM (green shapes in Figure 2-2) computes vegetation establishment, disturbances and habitat conditioning effects on vegetation and delivers to CLF vegetation Manning's n (roughness), increases in sediment and bank cohesion (due to vegetation) and LW initial position. Although CLF and RVM represent two distinct entities of the proposed model, in the following sections, for the sake of clarity, the ensemble of these two components will be addressed as CLF-RVM or simply "the model".

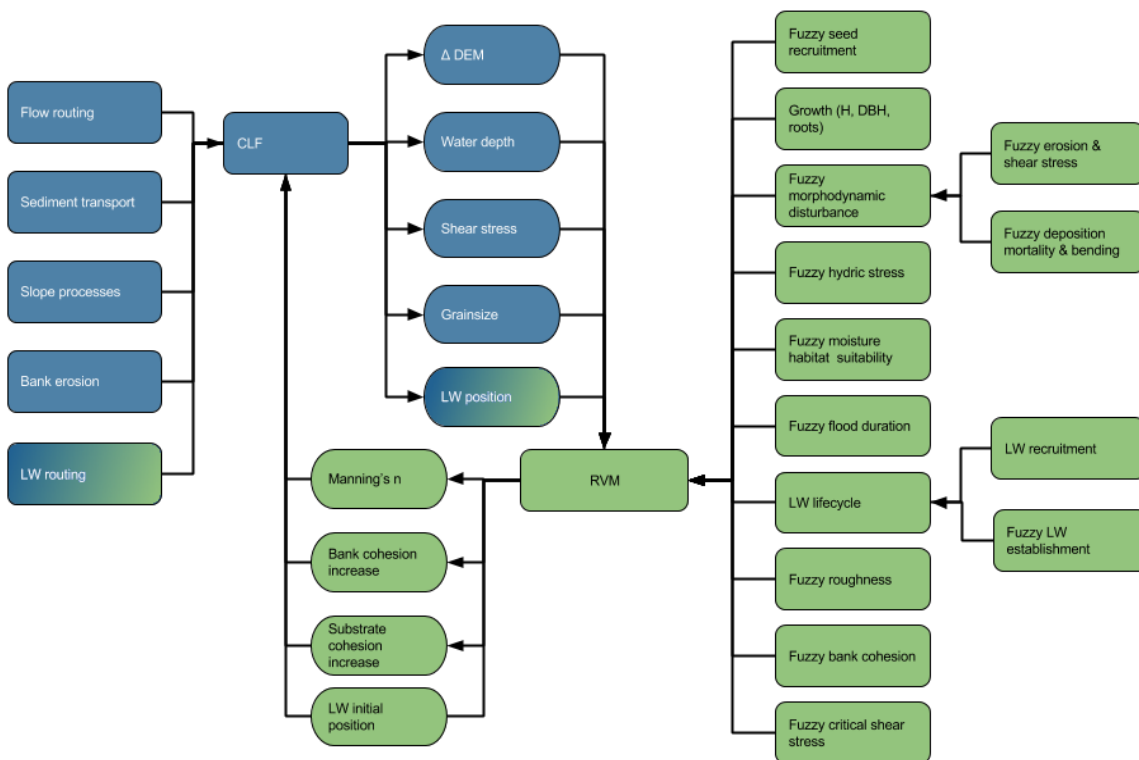


Figure 2-2 CLF and RVM submodels and feedbacks integration schema

2.2.4 Cumulative disturbance effects

A single negative impact such as a flood, might not be lethal for all the plants in a stand but, if sufficiently intense can reduce vegetation's overall health and consequently degrade growth performance and ability to withstand further impacts (Niinemets, 2010). The cumulative effect of consecutive impacts is accounted in the model by the "fitness factor", a value ranging from 1 (maximum fitness) to 0 (extinction). Fitness decreases with each impact the vegetation in a cell must endure. The reduction occurs by a value equal to the percentage of individuals lost because of an impact. For example, if the plants in a cell have a fitness level of 0.7 and are affected by an impact causing 50% mortality, the remaining plants will have fitness equal to 0.35. For each day in which the cell is not flooded (i.e. there is no disturbance), the fitness level increases by 1/365, i.e. a cell with a very low fitness requires approximately one year without any significant impact to regain its full strength.

2.2.5 RVM submodels

Submodels will be described in conceptual terms while parameters' definitions, their values, and fuzzy linguistic variables descriptions are summarized in Table 2-9 and Table 2-10 respectively.

2.2.5.1 Fuzzy seed recruitment

Seed recruitment of riparian Salicaceae occurs typically in correspondence with the late-spring flood waves generated by glacial thaw and snowmelt (Johnson, 2000; Sophie Karrenberg et al., 2003). In this time of the year, Salicaceae produce and abundant seed-rain that is transported by hydrochory or anemochory (Braatne et al., 1996). Seeds are shortly viable because lacking of endosperm, therefore to germinate they need to be deposited on suitable substrates. Being Salicaceae heliophilous, suitable substrates are moist, non-vegetated surfaces typically created by floods' restructuring action on the active-channel (Meier and Hauer, 2010; Polzin and Rood, 2006). According to the literature reviewed in section 1.4.1.1, survival of the germinated seeds depends on their capacity to keep contact with the receding limb of the water table which in turn depends by the flow stage and substrate grainsize (Amlin and Rood, 2002; Mahoney and Rood, 1998). To model this process, the fuzzy seed recruitment submodel has a start and an end month (parameters 2 and 3 in Table 2-9) and it is executed at the end of the recruitment period. The inputs for the submodel are grainsize median size (d_{50}) and distance between the topographic elevation and the elevation a.s.l. of the mean recruitment month's water table (see Table 2-10). The water table elevation is calculated by inverse distance weighting interpolation of the mean monthly water elevation a.s.l. (i.e. topography plus water depth) over the whole modelling domain. Estimation of the parameters values considered the information in Table 1-3 and Table 1-5.

The submodel allows seed recruitment to occur only where neither vegetation nor LW are present. The value resulting from the defuzzification is a natality value representing the number of shoots per square meter. The shoots per meter are then converted to shoots per cell and receive an initial fitness equal to the ratio between the natality value resulting from the defuzzification and the maximum natality. Shoots are also assigned an initial H and D of 50 cm and 0.35 cm respectively.

2.2.5.2 Growth

The growth submodel is the last submodel executed on the last day of the growing season; it increases plants H and D and adjusts RDMD to the mean water table elevation of the growing season. Annual growth of H and D are modelled using Equation 2-1 and Equation 2-2 respectively: a modified version of the JABOWA (Botkin et al., 1972) and FORET (Shugart and West, 1977) models. In their original formulations, JABOWA/FORET modulate growth according to shade tolerance, temperature and soil quality, thus accounting for sub-optimal conditions that decrease plants annual growth performance (Botkin et al., 1972). However, JABOWA and FORET were developed for upland forests and do not consider disturbances or limiting factors that typically affect riparian woody species. A subsequent evolution of JABOWA was the model FORFLO, which includes also a water table optimality criteria (Pearlistine et al., 1985). Similarly to FORFLO, also our growth submodel considers the effect of the water table on growth performance (term *s* in Equation 2-1, see section 2.2.5.6), in addition the growth submodel accounts also for the fitness factor (term *f* Equation 2-1, see section 2.2.4). The *f* and *s* terms in Equation 2-1 range between 0 and 1, thus their effect is to reduce the optimal growth in relation to the degree of disturbance endured and the quality of the habitat occupied by the plants in a cell. Other growth-modulation factors present in JABOWA and further derivations, are assumed to be negligible in riparian systems (Berg et al., 2007) and have not been explicitly modelled with the sole exception of competition which is applied as a fixed yearly mortality rate affecting the number of individuals in a cell (parameter 14 in Table 2-6).

$$\frac{\Delta D}{\Delta t} = \left(\frac{GD \left(1 - \frac{DH}{D_{max}H_{max}} \right)}{2dbh + 3b_2D - 4b_3D^2} \right) f s \quad \text{Equation 2-1}$$

$$H = dbh + b_2D - b_3 D^2 \quad \text{Equation 2-2}$$

Terms in Equation 2-1 and Equation 2-2 are thus defined: D diameter (cm), t: time (typically 1 year), G: growth rate (cm/ t), D_{max} : maximum diameter (cm) the modelled species can reach, H_{max} : maximum height (cm) the modelled species can reach, dbh: height (cm) at which diameter is measured, $b_2: 2(H_{max} - dbh)/D_{max}$, $b_3: (H_{max} - dbh)/D_{max}^2$, *f*: dimensionless vegetation fitness, *s*: dimensionless habitat suitability parameter.

RDMD is modelled with Equation 1-5 (Pasquale et al., 2012) presented in section 1.4.1.1, the scaling parameter η of the equation was set to 1.2 as at the site and for the Salicaceae species tested by Pasquale et al., (2012).

2.2.5.3 Fuzzy erosion and shear stress

This submodel derives from the material reviewed in sections 1.4.1.3, 1.4.2.1. It mimics the combined erosion and pull-out disturbance exerted by floods on plants standing in the active channel and the fell by bank erosion and slope failure, of plants standing on fluvial

terraces. The first process, erosion and pull-out, occurs when floods are sufficiently energetic to mobilize sediments. As the substrate is ablated, roots systems are gradually exposed eventually until a point where the root-substrate friction is no longer sufficient to balance the drag exerted on the plant by flowing water, thus causing plant translocation (Bywater-Reyes et al., 2015; Tanaka and Yagisawa, 2009). In the second case, fall of plants standing on fluvial terraces, erosion occurs by bank migration sustained by bank-toe shear stress or bank slope failure. RDMD and shear stress acting on vegetation (Equation 2-4) are assumed as a proxy for root depth and pull-out force (Edmaier et al., 2011) while terraces erosion is a built-in function of CLF. This submodel is executed at the end of each hour of flooding with flooding defined by a threshold discharge (see parameter 1 in Table 2-9). At the end of each hour, the difference of topographic elevation before and after the hour is computed, where the difference is negative (i.e. erosion has occurred) RDMD is decreased by the eroded amount and the pull-out effect is assessed according to the fuzzy rules of the submodel (see Table 2-12). The fuzzy sets defining RDMD and shear stress strength are shaped considering the data summarized in Table 1-4. The value resulting from the defuzzification is a mortality rate i.e. the percentage of individuals that are translocated from the cell. In case RDMD reaches 0, mortality is assumed to be 100% even if τ_{veg} is null. Such case is the typical one for plants standing on fluvial terraces. The fate of translocated individuals is decided according to the LW lifecycle submodels (see section 2.2.5.8).

2.2.5.4 Fuzzy deposition mortality and bending

As explained by the literature reviewed in section 1.4.2.2, deposition can bend plants because of the momentum exerted by sediments motion (Tanaka and Yagisawa, 2009). Moreover, plants can possibly die because of the anoxic conditions and lack of light (Kui et al., 2014). Individuals with thin stems oppose less resistance to sediments momentum (Tanaka and Yagisawa, 2009) and have less energy resources to sustain post-burial resprouting than individuals with a thicker stem. In consequence of these considerations, the submodel is executed after each flood event. The amount of deposited sediment is computed by difference of the topographic elevation before and after the flood. The buried part of the stem is assumed to become part of the root system (Holloway et al., 2017a; Sigafoos, 1964) therefore such difference is subtracted from H and added to RDMDs' (Figure 2-3). Mortality is assessed considering the relative burial, i.e. the rate between plants' H and the height of the deposition, the fitness status and the age of the plants. The shape and values of the fuzzy sets are drawn from Figure 1-11. Bending is instead assessed considering relative burial and D. Bending defuzzification result is an angle (in degrees) of bending. The angle is used to compute the new height (H') according to Equation 2-3 (see Figure 2-3 for term's explanation). To fit with the new height, also D is re-computed by back-calculation from Equation 2-2.

$$H' = (H - d) \sin(90 - \beta)$$

Equation 2-3

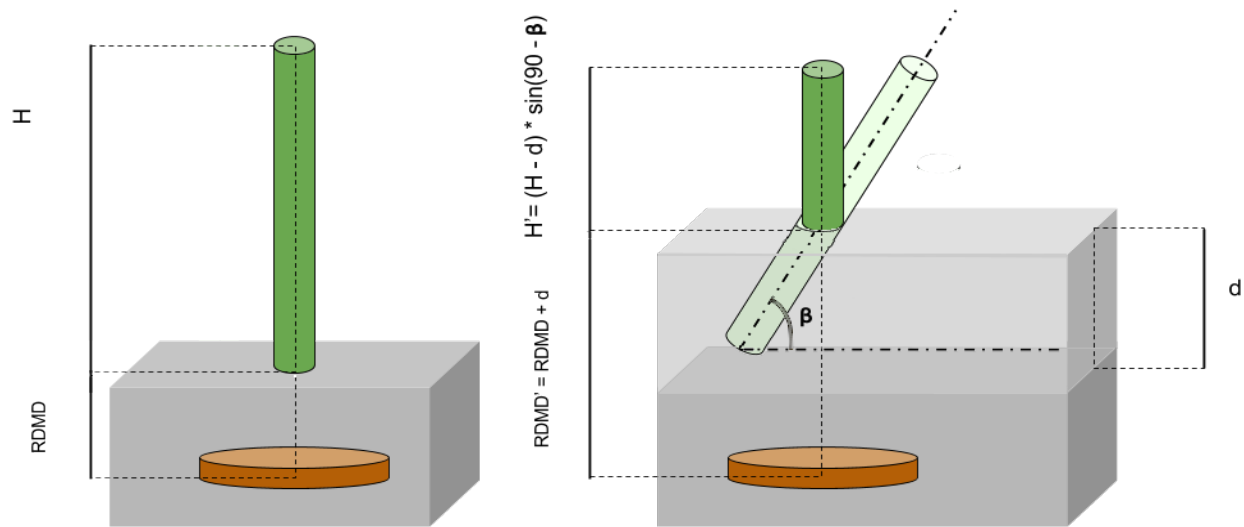


Figure 2-3 Conceptualization of deposition effect on RDMD and plants' height.
RDMD: root density maximum depth, H: plant height, d: deposition, β : bending angle resulting from deposition

2.2.5.5 Fuzzy hydric stress

According to the literature reviewed in section 1.4.1.1, lowering of mean growing-season water table between consecutive years, reduces vegetation stand health and in more severe cases, can even lead to plants' wilting, especially in stands with lower vigour (Cooper et al., 2003; Scott et al., 1999). Therefore, the fuzzy hydric stress submodel takes as inputs the difference between the growing-season mean water table of the current and previous years and the fitness level of the vegetation. Similarly to the fuzzy recruitment submodel, water table is calculated by inverse distance weighting interpolation of the water elevation a.s.l.; this submodel is executed once a year at the end of the growing season but before the growth submodel; the resulting outcome is a mortality rate.

2.2.5.6 Fuzzy moisture habitat suitability

As the previous submodel, also this one found its theoretical ground and parameterization in the literature reviewed in section 1.4.1.1: growth performance of riparian Salicaceae is strongly influenced by the hyporheic exchange between the groundwater and the river. In particular, growth is favoured in gaining reaches while is limited in losing ones (Harner and Stanford, 2003). Moreover, a shallow water table can reduce growth because having the roots in a fully saturated substrate leads to anoxic conditions. In last instance, growth of riparian-adapted species seems to be favoured within a range of water table depths (Table 1-2 and Table 1-3). In RVM, simulations of the hyporheic flow and groundwater dynamics are approximated by the water mean table elevation during the growing season (Stromberg and Patten, 1996; Willms et al., 1998). The position of the water table determines the suitability of the habitat to grow riparian woody species, the submodel is executed before the growth submodel and the defuzzification output is a "habitat suitability factor" (term s in Equation 2-1).

2.2.5.7 *Fuzzy flood duration*

Literature reviewed in section 1.4.1.2 shows how riparian woody species are well adapted to submersion and can endure such condition for time periods extending almost if not all, the growing season (Amlin and Rood, 2001; Higa et al., 2012). Nevertheless, prolonged waterlogged conditions lead to reduced growth and in more severe cases, depending upon species, to plants early senescence and death (Nielsen et al., 2010). Submersion is relevant only during the growing season for in the dormant one, plants have a minimal oxygen consumption and do not suffer the anoxic conditions caused by submersion (Glenz et al., 2006). In the fuzzy flood duration submodel, the only variable considered is the percentage of the growing season a given (vegetated) cell is under water (Glenz et al., 2008). The defuzzification is also in this case a mortality rate and the submodel is executed at the end of the growing season.

2.2.5.8 *LW lifecycle*

2.2.5.8.1 *LW recruitment and routing*

LW recruiting occurs within the “Shear stress and erosion” submodel. When trees whose diameter is beyond a threshold (parameter 8 in Table 2-6) are eroded, they enter the LW lifecycle. LW found in cells where there is water, are assumed to float if the water is sufficiently deep to allow floating (parameter 9 in Table 2-6). LW routing is integrated in CLF code: floating trees are routed from one cell (donor cell) to the next (receiving cell) according to the direction calculated from the sum of the flow velocity vectors in the donor cell. If the receiving cell is vegetated, LW can float over only if water depth in the receiving cell is higher than vegetation height i.e. LW floats above the canopy layer, otherwise it will not move unless velocity direction changes or water depth increases. When LW is deposited, the roughness of the cell is changed to the value set by parameter 10 in Table 2-6.

2.2.5.8.2 *Fuzzy LW establishment*

Log jams created by LW deposition on a single cell are limited to a maximum (parameter 12 in Table 2-6) (Bertoldi et al., 2013), establishment and consequent re-sprouting of deposited LW depend on local moisture conditions and absence of floods for a period sufficiently long to allow LW to grow roots and avoid re-mobilization (Francis et al., 2006; Moggridge and Gurnell, 2009). Moisture conditions are evaluated using as a proxy the water mean table elevation during the growing season (same as in “Growth” submodel). Fuzzy sets of the water mean table elevation are drawn from the reviewed material reported in Table 1-7. The outcome of the defuzzification is a binary value (yes/no) that deems whether the deposited wood survives. All surviving wood is assumed to re-sprout if, for a given number of months (parameter 11 in Table 2-6) wood is not re-mobilized by any flood (Gurnell, personal communication). Re-mobilization occurs when the conditions of relative D submersion are met (see section 2.2.5.8.1). Upon re-sprouting, a random number of stems comprised between 1 and 6 will sprout from each log in a cell. Re-sprouted stems receive an initial H and D of 2.5 m and 0.18 m respectively, roots’ depth is instead assigned in the growth submodel. Survival evaluation is performed just before

the growth submodel while resprouting is evaluated at the end of each month during the growing season.

2.2.5.9 Fuzzy roughness

As explained with greater detail in section 1.3.2.1, vegetation roughness is a measure of the flow resistance opposed by vegetation and as such, is one of the vegetation feedbacks to hydro-morphological processes. Vegetation flow resistance is due to the physical blockage exerted by plants structures exposed to the flow and the momentum and energy loss due to surface-flow friction. Flexible plants, typically the young ones, when attacked by flow, streamline, thus reducing the blockage and surface exposed to friction (Gosselin and De Langre, 2011; Weissteiner et al., 2015). Presence of leaves increases the streamlining (Freeman et al., 2000; Järvelä, 2002b) therefore for deciduous species, flow resistance varies with age and between summer and winter. At patch scale, flow resistance depends on plant density, with higher resistance encountered with higher plant density (Righetti, 2008). In RVM, roughness is assigned to vegetated cells according to degree of plant cover, estimated as percentage, and vegetation age. Degree of cover is a vegetation property calculated using a fuzzy approach that considers the age and number of individuals per cell. Being leaves a major source of flow resistance, RVM uses one fuzzy system for the summer roughness and a second one for winter roughness. Fuzzy sets definition was drawn considering literature values in Chow, (1959). Start and end summer months are set by the parameters 6 and 7 in Table 2-9.

This submodel is executed each time there is a potential change in vegetation cover, i.e. after each time shear stress and erosion disturbance is executed, at the end of the growing season and after the fuzzy seed recruitment submodel. The result of the defuzzification is a Manning's n roughness coefficient which is fed to CLF. In CLF, Manning's n is used to calculate the flow velocity then used to calculate the total shear stress (τ_t). CLF has been modified to use vegetation roughness to calculate the shear stress (N/m^2) acting on vegetation (τ_v) and the shear stress (N/m^2) acting on the river bed (τ_b) (Baptist et al., 2009). Therefore, the higher the vegetation roughness (i.e. vegetation flow resistance) the higher will be τ_v , conversely, τ_b will decrease thus reducing surface erosion. In order to disentangle the shear stress acting on bed shear stress acting on the sediments and stress acting on vegetation, CLF source code has been modified to compute the former according to Equation 2-4 and the latter according to Equation 2-5.

$$\tau_v = \frac{gn^2}{\sqrt[3]{h}} \rho_0 u^2 \quad \text{Equation 2-4}$$

$$\tau_b = \rho_0 g \frac{u^2}{C_b^2} \quad \text{Equation 2-5}$$

With n: vegetation Manning's roughness coefficients ($s/m^{1/3}$), h : water depth (m), τ_b : bed shear stress (N/m^2), ρ_0 : water density C_b : Chezy roughness coefficient for the bed only, u flow velocity (m/s) and g gravity acceleration (m/s^2).

2.2.5.9.1 Fuzzy bank cohesion

The concept for this submodel was derived from the literature in section 1.3.1.1.1, in a nutshell, roots crossing bank's shear plane increase bank's substrate cohesion and stability (Abernethy and Rutherford, 2000; Coppin and Richards, 2007). The strengthening provided by roots is the second vegetation feedback simulated by RVM. Bank cohesion is proportional to the number of roots crossing the shear plane (Pollen and Simon, 2005). For several riparian species, such number was found to increase with age, starting to be significant after 3-5 years and increasing asymptotically upon the age of 20-30 years (Figure 1-4). In RVM the additional cohesion provided by vegetation is computed considering the degree of cover (same as in "Fuzzy roughness" submodel), RDMD and vegetation age. In CLF bank erosion is calculated using Equation 2-6 (Van De Wiel et al., 2007).

$$\zeta = (1/C_a)\tau_b E_{ca} t \quad \text{Equation 2-6}$$

Where ζ is the rate of lowering of bank cell, E_{ca} is a bank erosion coefficient, C_a the bank radius of curvature (in m), τ_b the near bank shear-bed stress (N/m^2) and t time (seconds). The defuzzification results of the fuzzy bank cohesion submodel is a percentage increase in bank cohesion, such value is then used in CLF bank erosion routine by decreasing the term E_{ca} in Equation 2-6. Like Fuzzy roughness, this submodel is executed each time there is a potential change in vegetation cover.

2.2.5.9.2 Fuzzy critical shear stress

Surface erosion of river-bed substrates occurs when the critical shear stress required to mobilize the sediments is exceeded by the shear stress exerted by the flow on the river-bed. The presence of plants reduces the surface scour by interaction with the flow field and by provision of additional substrate cohesion that increases the critical shear stress required to mobilize the sediments (see sections 1.3.1.1.2 and 1.3.2). Being roots binding effect increasing with roots biomass (Gyssels and Poesen, 2003), this submodel considers the degree of cover (same as in "Fuzzy roughness" submodel), RDMD and vegetation age. The result of the defuzzification is a percentage increase in substrate cohesion applied indistinctly to all grainsizes simulated by CLF. Vegetation feedback to substrate critical shear stress is the third vegetation feedback submodel in RVM; as the previous two, also this submodel is executed each time there is a potential change in vegetation cover. As highlighted in section 1.3.1.1.2, there are no empirical data on the additional cohesion provided by roots to non-cohesive substrates, thus, for this submodel, fuzzy sets had to be drawn on an expert knowledge basis.

2.2.6 Test cases

To demonstrate CLF-RVM features and provide means for its conceptual validation, three simulations have been performed. Simulations objectives were to show how RVM simulates: I) the feedback of vegetation on erosion and deposition, II) the effect of water

table decline and water table distance on vegetation growth, III) the LW lifecycle routine and IV) how vegetation responds to the disturbance regime. Simulations are loosely based on a river reach of the Tagliamento River (North-East Italy) but did not aim at replicating any specific observed landscape. This reach is located downstream from Pinzano gorge has a length of approximately 3km and an active channel width ranging from 0.25 to 0.9 km and averaging approximately 0.7 km. Nearby reaches were extensively studied in previous works (e.g. Arscott et al., 2002; Bertoldi et al., 2011; Gurnell et al., 2000b; Kollmann et al., 1999; Surian et al., 2015; Ziliani et al., 2013) thus providing terms of reference to assess some of CLF-RVM simulated results. All simulations were run using as input topography a 5 x 5 m cell Digital Elevation Model (DEM) of the reach in year 2001. Input bedrock elevation (see Table 2-6) was estimated by subtracting 5 m from the DEM elevation while initial grainsize spatial distribution was yield by simulating a 10 years' recurrence interval flood using CLF (Coulthard, 2017). Using CLF, the DEM was used to simulate a discharge of 50 m³/s which is the mean discharge during the growing season, defined as all months between March and October (Tockner et al., 2003). The resulting mean water level was interpolated by inverse distance weighting, over the whole modelling domain as a proxy of the groundwater table (Benjankar et al., 2011). The distance between the DEM and the groundwater table was used to derive an initial vegetation cover at first by classifying the distance in distance-classes and then by assigning a vegetation age to each class (Table 2-1). Age assignment was performed on an expert basis. For display purposes and facilitate results explanation and discussion, vegetation age was classified in succession phases (Egger et al., 2013). Finally height and diameter using where calculated using Equation 2-7 and Equation 2-8, which in turn were derived from a large dataset of poplar trees measured on the Tagliamento River (unpublished data). The results of both equations had to be converted from m to cm to comply with model-inputs requirements (see Table 2-6).

Table 2-1 Initial vegetation properties estimated according to distance from the growing season water table

Succession phase	Min distance (m)	Max distance (m)	Min age (years)	Max age (years)	Plant count (plant/m ²)
Sand-gravel	-2.2	0.3			
Pioneer	0.3	0.7	1	2	10
Pioneer-shrub	0.7	1	3	4	1
Shrub	1	1.5	5	10	0.9
Early successional woodland	1.5	3.5	11	20	0.8
Established forest	3.5	-	21	25	0.7

The number of plants/m² was estimated by expert judgement while RDMD was calculated according to Equation 1-5.

Table 2-2 Allometric relationships relating height and diameter at breast height to *Populus Nigra* age

$$H = -0.0053 \text{ age}^2 + 0.5662 \text{ age} \quad (r^2 = 0.83) \quad \text{Equation 2-7}$$

$$DBH = 0.0095 \text{ age}^2 + 0.5071 \text{ age} \quad (r^2 = 0.73) \quad \text{Equation 2-8}$$

Fuzzy sets definitions, fuzzy rules and CLF-RVM parameters values were derived from an extensive review on Salicaceae (Politti et al., 2017) presented in chapter 1 and a previous CLF modelling exercise performed on the Tagliamento (Ziliani et al., 2013). All CLF-RVM parameters descriptions, values and fuzzy rules used in the simulations are reported in Table 2-6 - Table 2-12.

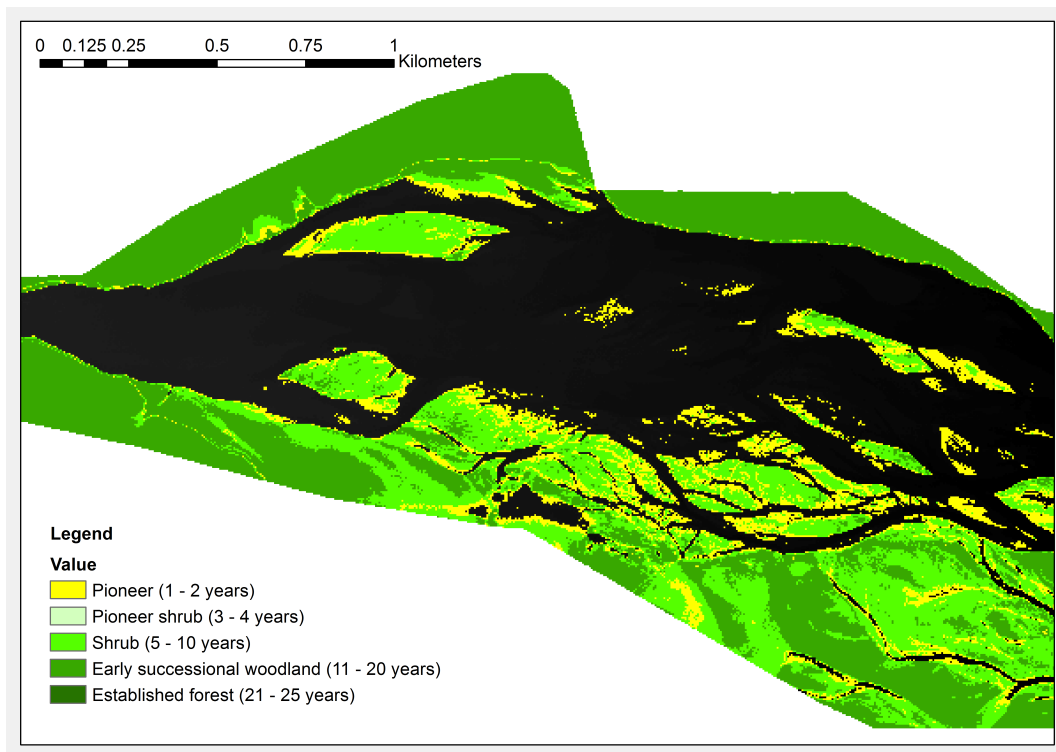


Figure 2-4 Initial vegetation distribution derived for the simulated reach

2.2.6.1 Test 1: Groundwater feedback

Groundwater feedback test aimed at showing how CLF-RVM simulates the effect of between-years lowering of the water table and the effect of a low groundwater on growth performance. To this end, two scenarios spanning 5 years have been performed; in the first one (“Normal flow regime”) each year is simulated with the same discharge (Figure 2-5 A). In the second scenario (“Sustained low flows”) instead, from the second year, growing season discharge is halved (Figure 2-5 B). Both scenarios do not have any disturbance event, therefore vegetation loss can only be due to hydric stress and growth performance be only influenced by habitat moisture. Groundwater effects were evaluated

by comparing the biomass and vegetated area of the two scenarios. For a single cell, biomass (B_s) was calculated using Equation 2-9:

$$B_s = (H\pi (DBH/2)^2) p_c \quad \text{Equation 2-9}$$

i.e. by computing the volume of a plant stem times the plants count (p_c) of a cell.

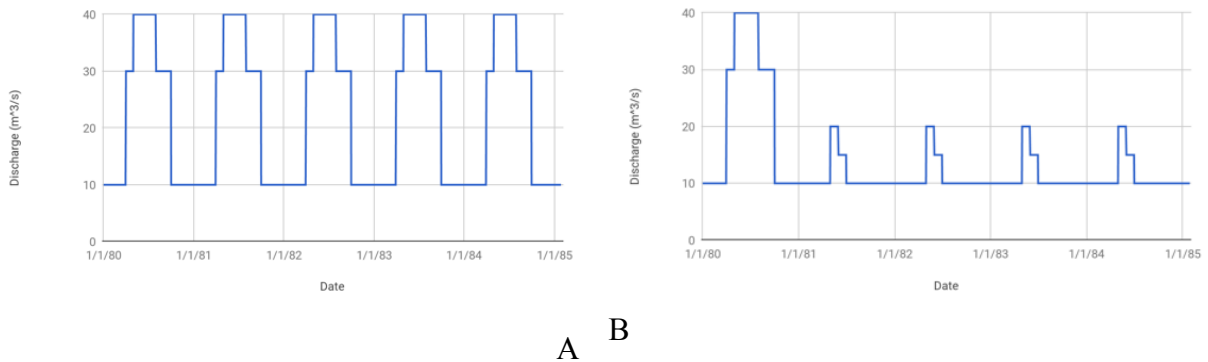


Figure 2-5 Normal flow regime (A) and Sustained low flows scenarios (B) hydrographs used to test flow regime feedback to vegetation growth performance

2.2.6.2 Test 2: Vegetation feedback on sediment transport

This second test demonstrates CLF-RVM vegetation simulated feedback on sediment transport processes. Also in this case, two scenarios were run. The first one using the standard version of CLF (Coulthard, 2017) while the second used CLF-RVM. In both scenarios, a flood corresponding to a Tagliamento 10 year recurrence interval flood was simulated (Figure 2-6). Simulated vegetation feedback could be appreciated by comparing the erosion and deposition volumes and active areas, i.e. areas undergoing either erosion or deposition, in the two scenarios. Having vegetation a stabilizing effect on sediment dynamics (Abernethy and Rutherford, 2000; Prosser et al., 1995), the unvegetated scenario was expected to have an higher degree of morphodynamic activity than the vegetated one.

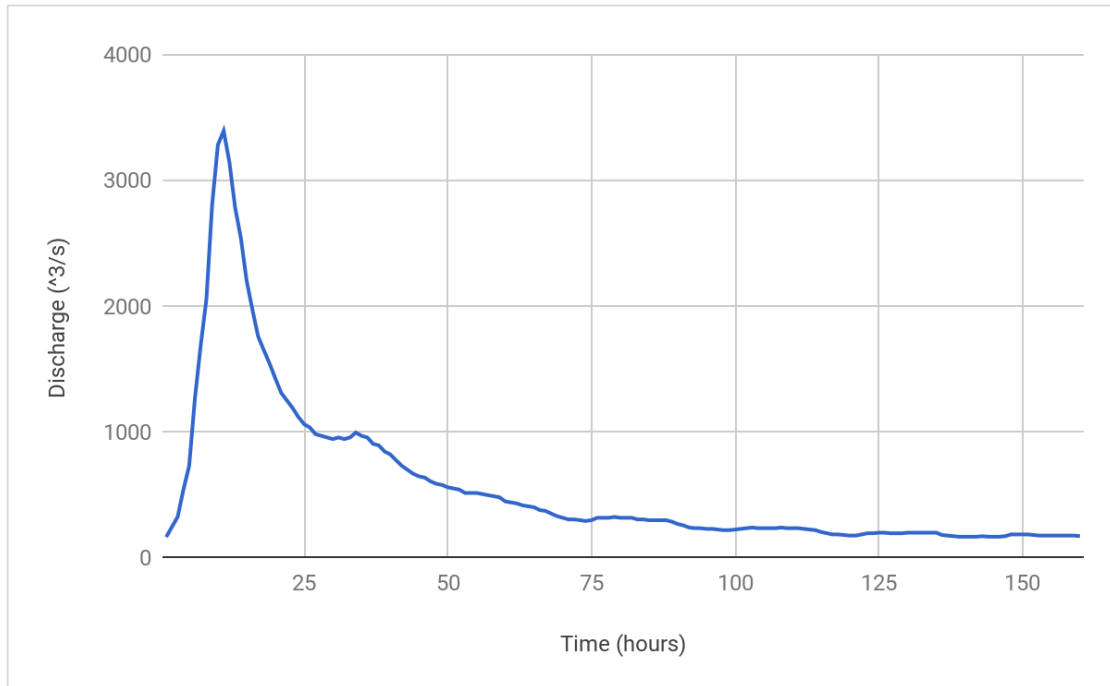


Figure 2-6 Hydrograph of a Tagliamento 10 year recurrence interval flood used to simulate vegetation feedback to sediment transport processes

2.2.6.3 Test 3: LW lifecycle

This last test case had the objective of showing of CLF-RVM entrains and establishes LW. The test case uses a modified initial vegetation map (Figure 2-7). In respect to the input vegetation of Test 1 and Test 2, this map has almost no vegetation in the open channel except for two large islands on the upstream side and several small ones on the downstream side of the modelling domain. Removal of vegetation was aimed at providing room for LW stranding and establishment. Moreover, in order to have vegetation with a diameter sufficiently large to provide a source of LW (parameter 8 in Table 2-9), vegetation having 5 years of age was increased to the age of 15. Increase in age implied also an increase in diameter and height which were calculated using Equation 2-7 and Equation 2-8. The hydrological regime used to simulate this test case was of bimodal type with one flood in May and a larger one in November (Figure 2-8).

For the first simulated year, the first flood, in May, had a discharge of 650 m³/s while the second one, in November, had a discharge of 1300 m³/s. For this reach of the Tagliamento, these two discharges correspond to floods having a return interval of less than one year and one in two years respectively (Ziliani, 2011). Floods of this magnitude on the Tagliamento are sufficient to trigger bank erosion and LW entrainment and retention (Bertoldi et al., 2013; Surian et al., 2015) while higher discharges can transport most of the entrained LW far downstream, thus invalidating the simulation objective (Ruiz-Villanueva et al., 2016). The discharges of the following three years had only minor floods (Figure 2-8), all below the one year discharge threshold while the last simulated year had a May flood with a magnitude in the order the one year return period and a November flood in the order of one in five return period. Such flow regime was aimed at showing how CLF-RVM simulated vegetation expansion and contraction responds to the

hydrological regime. Apart from the floods discharges, the monthly discharge of this test case was the same as in the undrying scenario (Figure 2-5 A), i.e. without droughts or water table decline stresses, disturbances and stresses were therefore due only to flood events.

Performance of simulated LW lifecycle was assessed considering: LW entrainment locations, LW stranding locations, the locations that allowed 1st year survival, i.e. resprouting, and the geomorphic effect of resprouted wood.

Entrainment was assessed looking at the vegetation maps at the beginning and end of the first simulated year, i.e. after the floods generating the first wave of LW deposits.

LW stranding locations were manually classified in four types: Open channel, Open channel forest edge, Side arm and Side arm forest edge, according to the type of channel where LW stranded and proximity to forest edge. For each of these location-types, simulated LW stranding elevation and survival was measured on the detrended topography of the first simulated year, i.e. the topography after 1st year November's flood. Detrended topography was calculated by subtracting, from the topography, a plane interpolated from the topographic elevations. Interpolation used a second order polynomial and, in order to avoid high-leverage effects, neglected the high terraces on the left bank of the modelling domain. For each location type, it was also determined if the stranding LW was deposited on a surface undergoing erosion or deposition. Entrainment, stranding and resprouting locations properties were compared with literature data on studies conducted on LW in nearby reaches of the Tagliamento (Bertoldi et al., 2013; Gurnell et al., 2000a, 2000b).

LW geomorphic effect was assessed looking at how LW, resprouted after the first simulated year, influenced sediment size deposition and then looking at the simulated vegetation patterns in response to the disturbance regime in all simulated years. Simulated LW interaction with sediment deposition was performed by comparing the second-year median grain size (d_{50}) inside the cells where LW resprouted with the sediment size in similar location where LW resprouts were not present. Extracting d_{50} from second year was necessary to provide to LW deposited in the first year, sufficient time to resprout and experience some the inundation events of the second year. Comparison was performed by means of boxplots and non parametric statistical tests. Simulated vegetation patterns were instead visually compared to typical landforms encountered on similar reaches of the Tagliamento and considering how simulated vegetation expands and contracts in response to the disturbance regime.

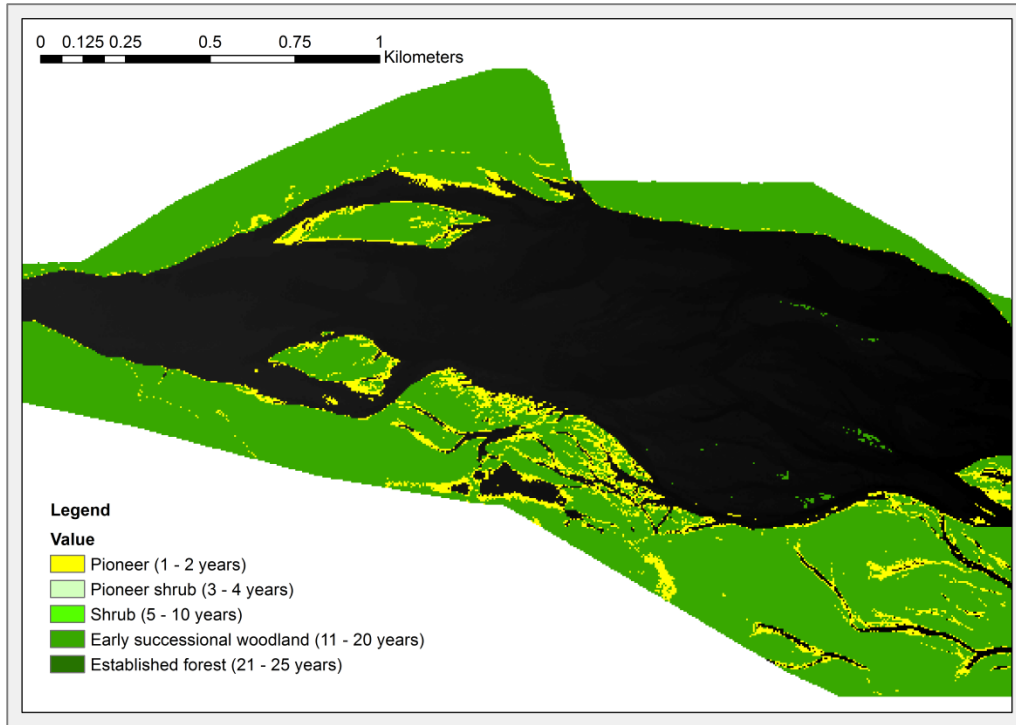


Figure 2-7 Initial vegetation for the LW lifecycle test case

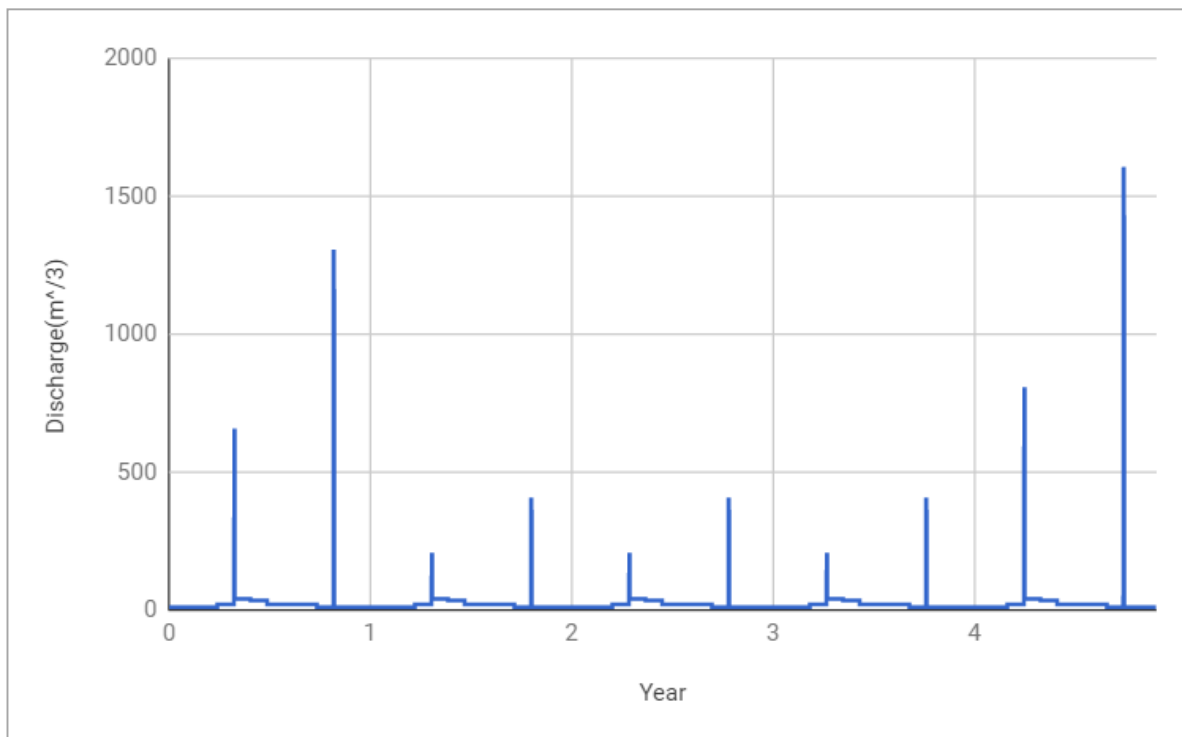


Figure 2-8 Hydrograph used to simulate LW recruitment and establishment

2.3 Results

2.3.1 Test 1: Water table feedback to biomass increase and distribution

Figure 2-9 shows the total biomass of the vegetation at the locations (pixels) that were vegetated at the beginning of the simulations. After the first simulated year, the one with equal hydrological conditions, both scenarios exhibit a slight increase of biomass compared to the initial condition. In the second simulated year, the Sustained low flows scenario suffers a very minor loss of biomass, due to the hydric stress caused by the interannual variation of water table. For this scenario, biomass remains stationary in the third year while fourth and five exhibit minor increases. Conversely, in the Normal flow regime scenario, during the five simulated years, biomass constantly increases until more than doubling the initial biomass.

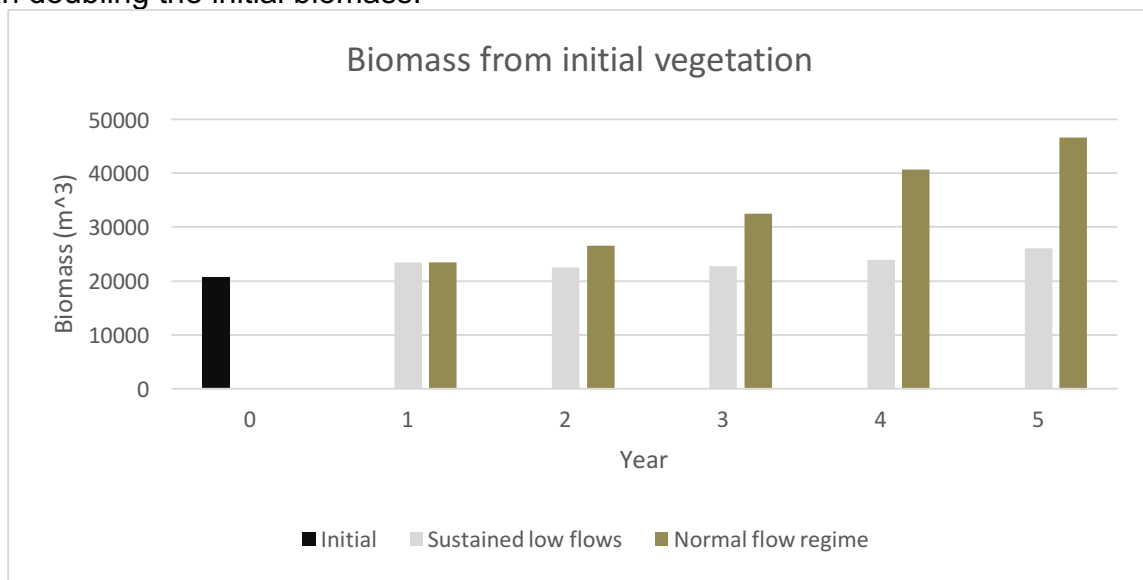


Figure 2-9 Cumulative biomass in the modelling domain pixels vegetated at the beginning of the undrying and drying scenarios

The trend of the two scenarios is confirmed also by the total biomass depicted in Figure 2-10: also in this case, the Sustained low flows scenario grows with a rate that is much slower than the Normal flow regime one. However, looking to the total vegetated area chart (Figure 2-11), the Sustained low flows scenario has a higher vegetated area; this because reduced discharge allows vegetation to colonize the former channel. Nevertheless, the newly established vegetation is in a pioneer stage and grows very little thus is not sufficient to match the Normal flow regime scenario growth performances.

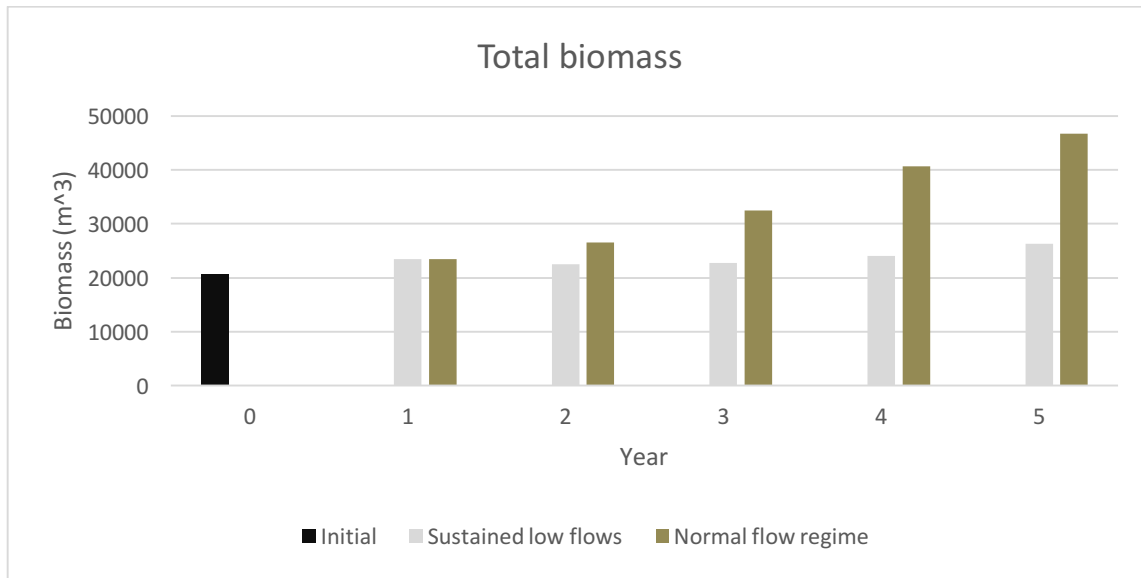


Figure 2-10 Total vegetation biomass for the undrying and undrying scenarios

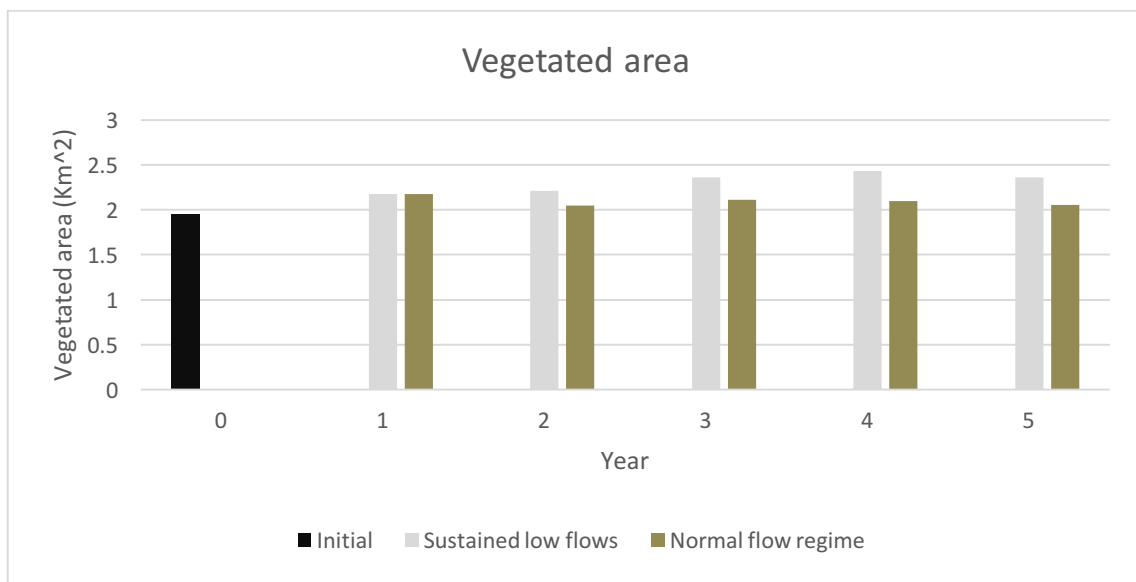


Figure 2-11 Vegetated area in the drying and undrying scenarios

The increase of vegetated area in the Sustained low flow scenario with consequent reduction of the active channel area (Figure 2-12) is consistent with the behaviour observed in river systems impacted by flow regulation (Dolores Bejarano and Sordo-Ward, 2011; Johnson, 1997). Conversely, in the Normal flow regime scenario, only minor sections of the modelled reach are colonised by new vegetation (Figure 2-13).

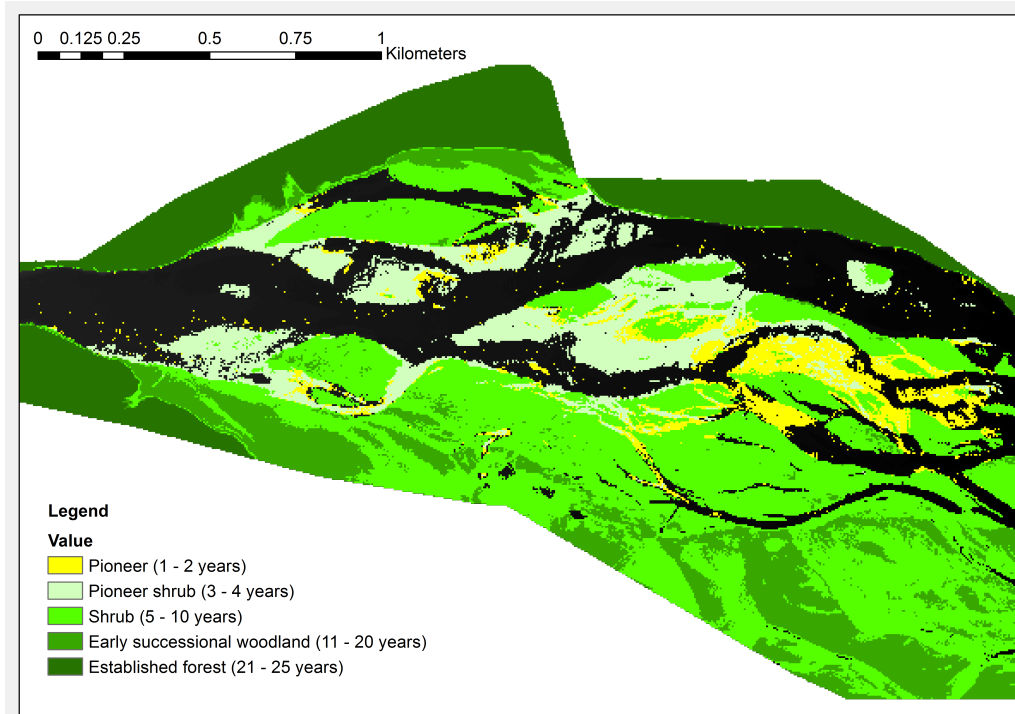


Figure 2-12 Vegetation age distribution of the last simulated year of the Sustained low flow scenario scenario

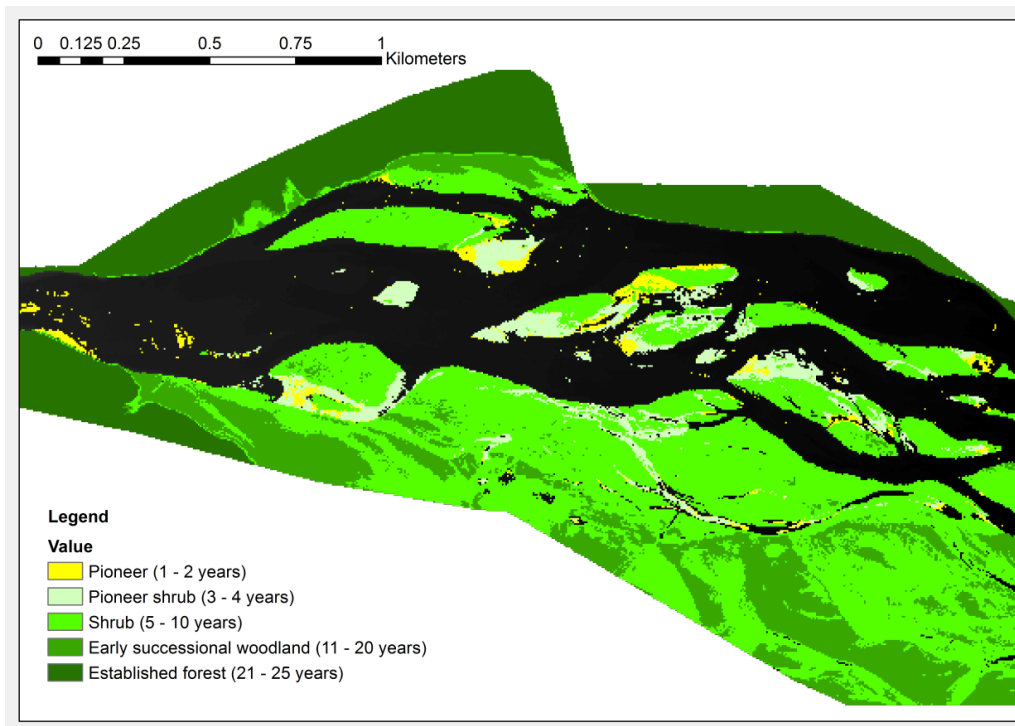


Figure 2-13 Vegetation age distribution of the last simulated year of the Normal flow regime

2.3.2 Test 2: Vegetation feedback to sediment erosion and deposition

The results of the scenarios demonstrating modelled vegetation effect on erosion and deposition processes are shown in Figure 2-14 and Figure 2-15. The two figures compare the results in terms of eroded and deposited volumes and active erosion and deposition areas for two simulations performed with and without vegetation. The datasets of both figures consider the spatial extent of the initial vegetation used in the vegetated scenario (Figure 2-4). From Figure 2-14 is possible to see how in the vegetated scenario, a much smaller volume of sediment is entrained while more deposition occurs in the unvegetated scenario.

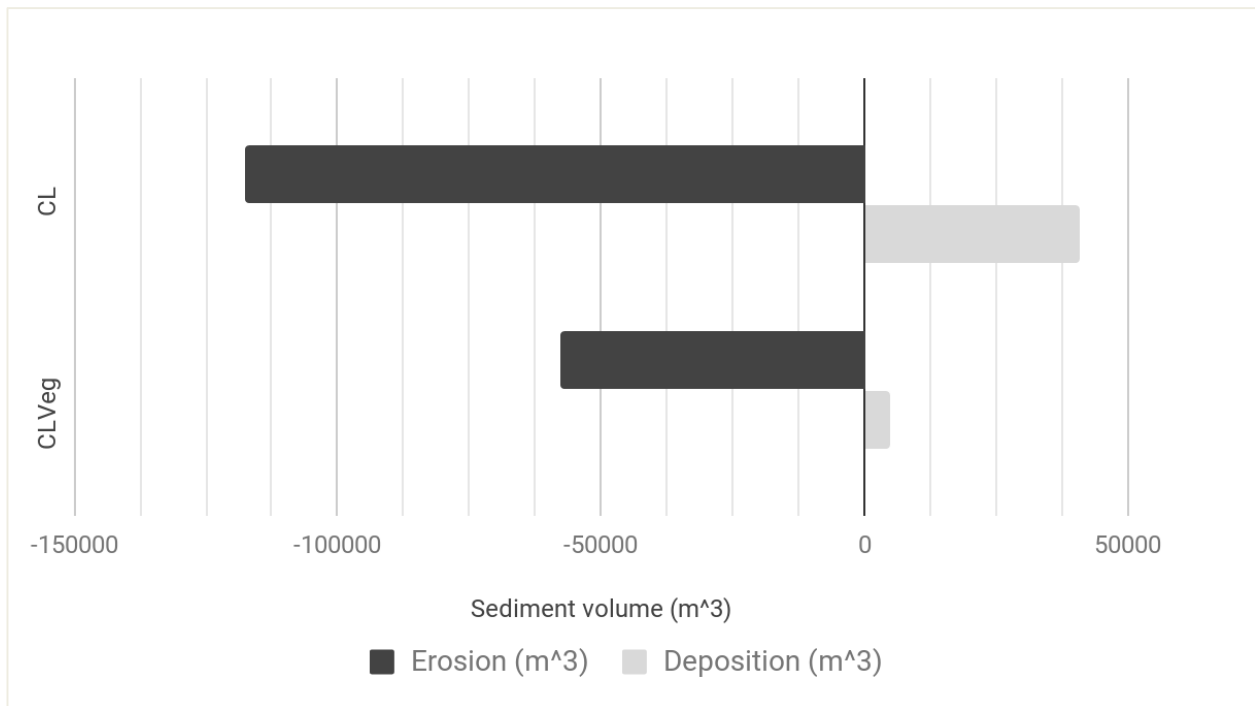


Figure 2-14 Eroded and deposited sediment volumes in the areas covered by vegetation in the vegetated and unvegetated scenarios

In the vegetated scenario, the simulated stabilizing effect of vegetation results also in smaller areas of erosion and much greater stable areas, i.e. where neither erosion nor deposition occurs.

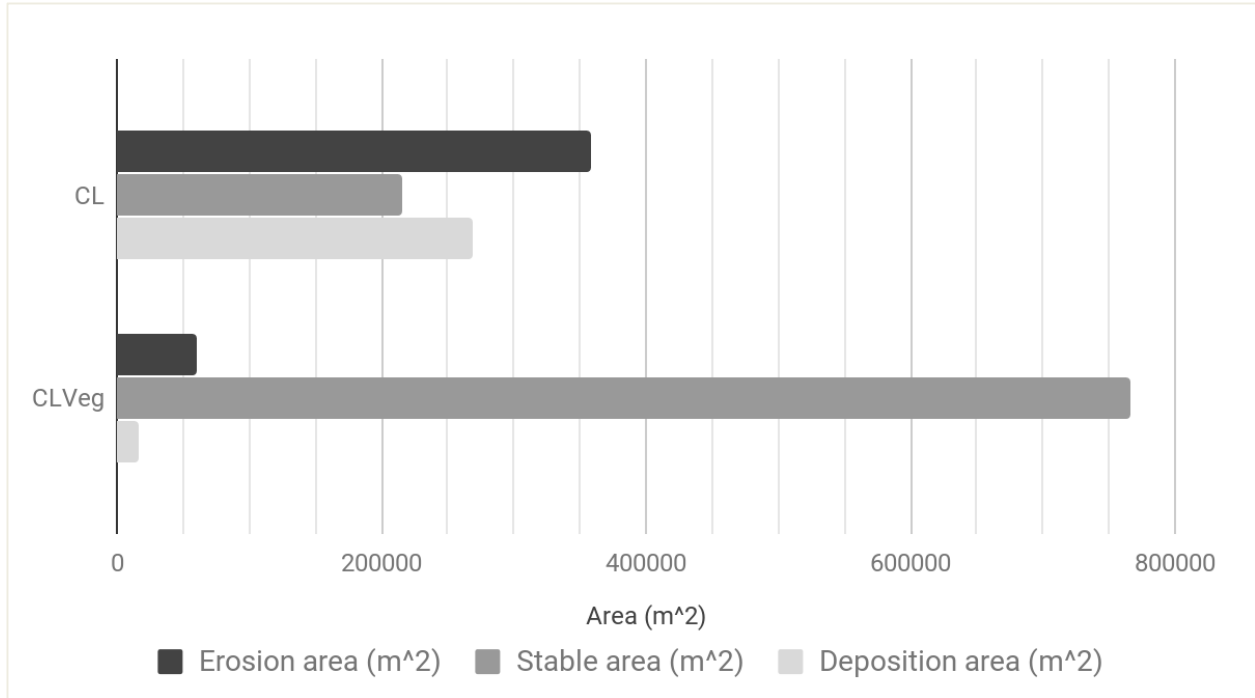


Figure 2-15 Erosion, deposition and stable areas of the vegetated areas for the vegetated and unvegetated scenarios

The reduction of erosion and higher stable areas resulting from the vegetated scenario are explained by the combined effect of simulated sediment cohesion increase due to roots and the flow velocity reduction due to vegetation flow resistance.

2.3.3 Test 3: Large Wood lifecycle and vegetation distribution response to disturbance regime

2.3.3.1 LW entrainment and deposition location

Figure 2-16 shows the position of the LW entrained and deposited after the floods of the first simulated year. Simulated LW deposition occurs on four types of locations: on upstream sides of bars in the open channel, at the edges of the forest in the open channel, on open surfaces inside side arms and near the edges of the forest bordering side arms. From qualitative point of view, these location are in good agreement with literature studies that reported side arms (Piegay, 1993), floodplain woodland edges (Piégay and Gurnell, 1997) and upstream and side edges of vegetated islands (Hickins, 1974) as LW storage preferential locations. Bertoldi, Gurnell and Welber, (2013) observed, on a nearby reach of the Tagliamento, that most of the trees entrained by erosion tend to strand downstream from the eroded site and that these trees tend to strand on surfaces created by deposition during the same flood event. Although from CLF-RVM is not possible to track LW sources, Figure 2-17 and Figure 2-18 show that upstream from LW stranding positions, portions of the forest were eroded during the two simulated floods, thus generating LW. In Figure 2-17 and Figure 2-18, vegetation extent is defined in terms of “potential LW source”

meaning that only vegetation having a diameter sufficiently large to be considered a potential LW (parameter 8 in Table 2-6) is displayed in these two figures. The tendency of having LW stranding on sediment depositional surface is well replicated by the model which places most of the stranding wood on alluvial surfaces undergoing deposition (Figure 2-19).

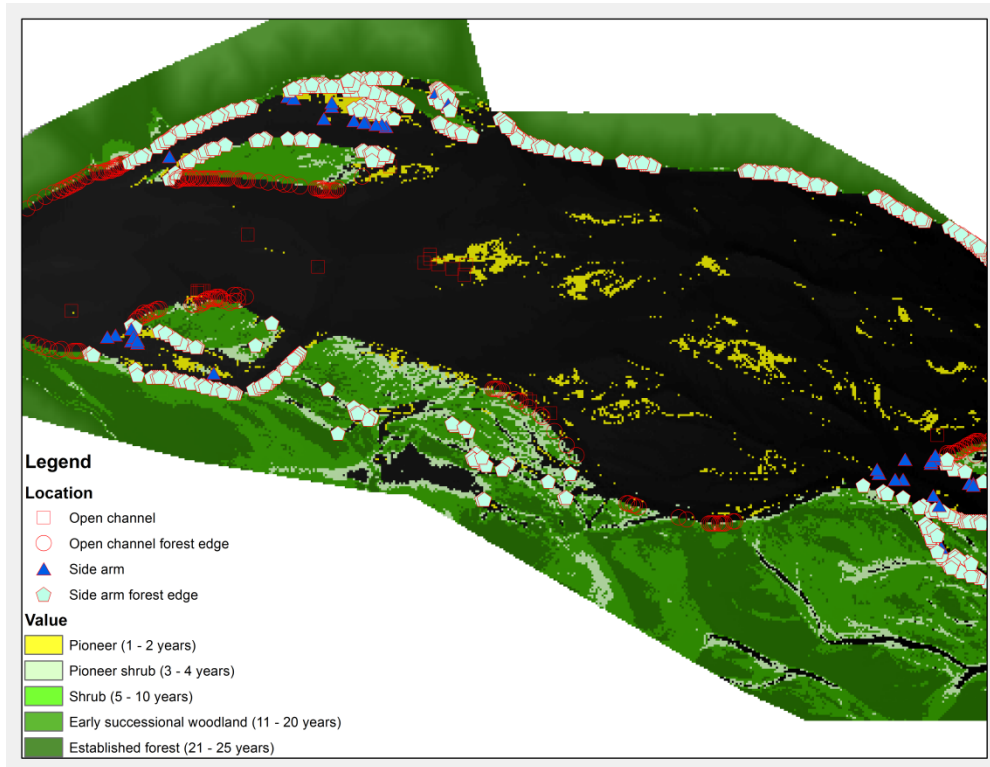


Figure 2-16 LW deposition positions after the first simulated year

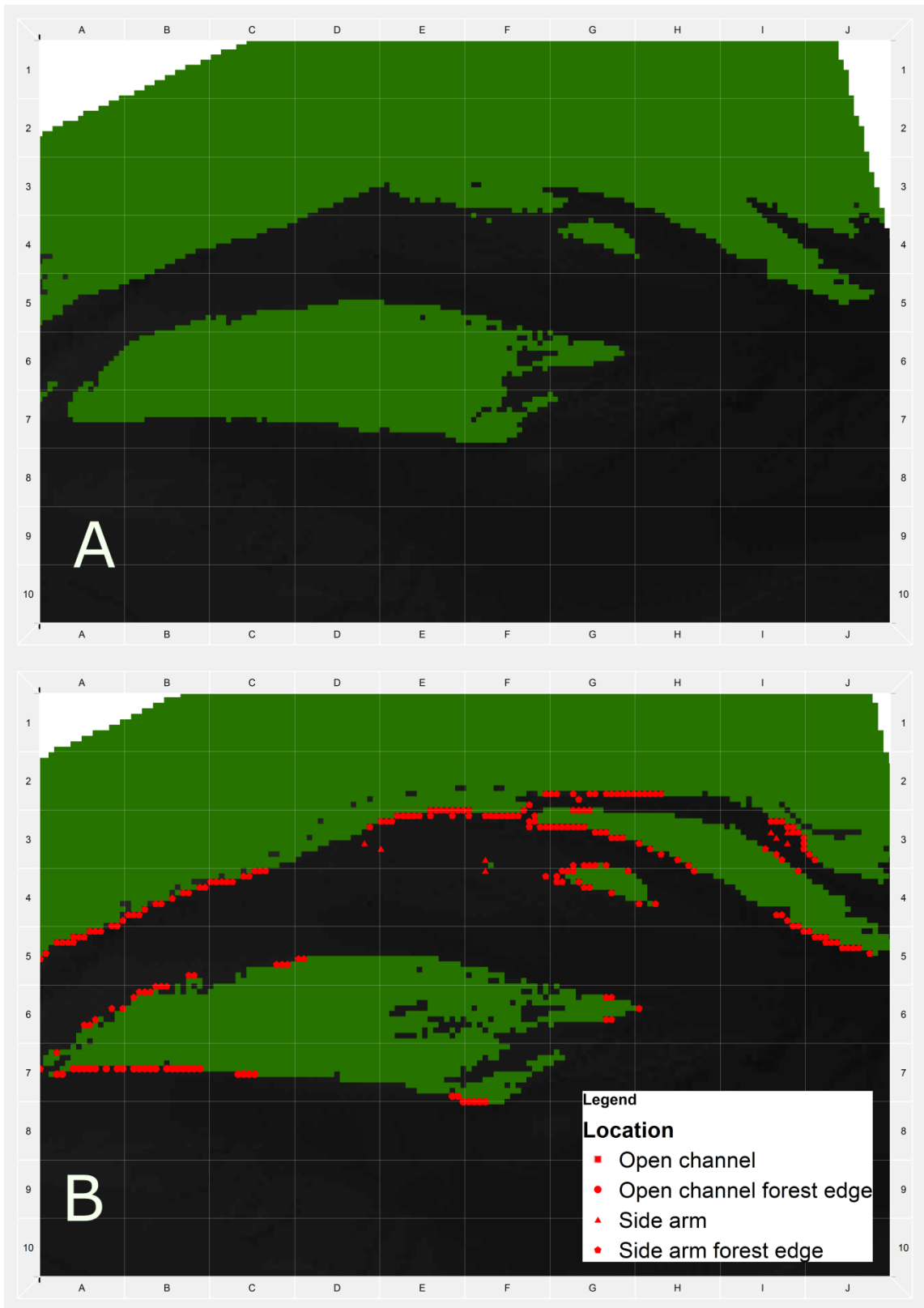


Figure 2-17 A: potential LW sources before the 1st year May flood. B: potential LW sources after the 1st year May flood and LW stranding locations

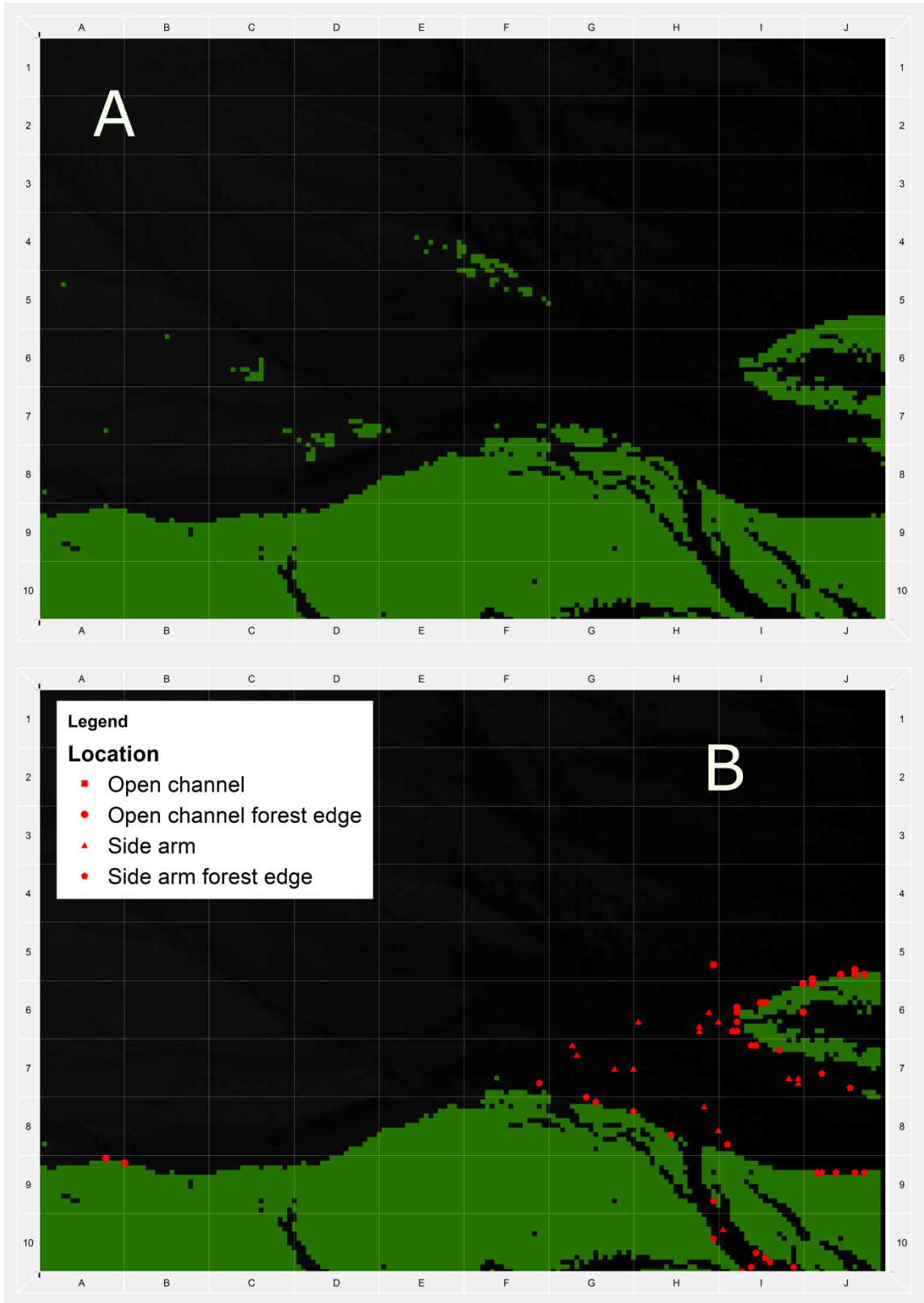


Figure 2-18 A: potential LW sources before the 1st year November flood. B: potential LW sources after the 1st year November flood and LW stranding locations

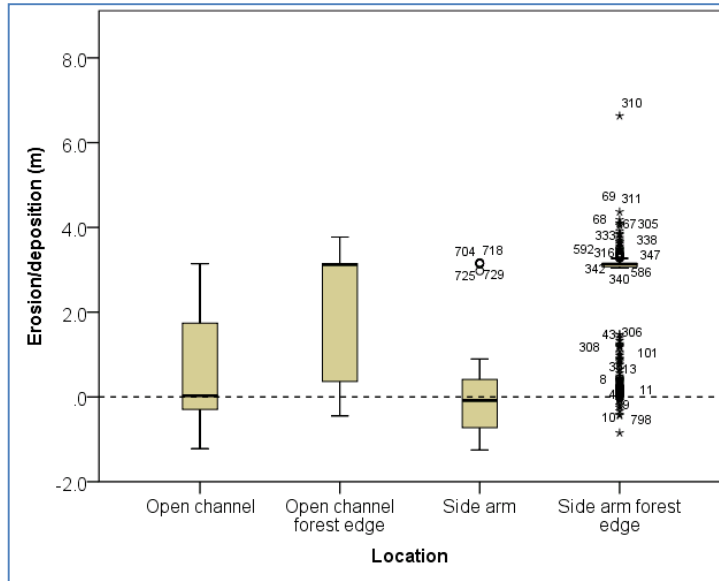


Figure 2-19 Erosion and deposition at the stranding locations of the LW entrained during the 1st year floods

2.3.3.2 Stranding locations quantification and first year survival locations

Figure 2-20 portrays the vegetation after the second growing season, when the LW deposited by the floods of the first simulated year had enough time to resprout (parameter 11 in Table 2-9).

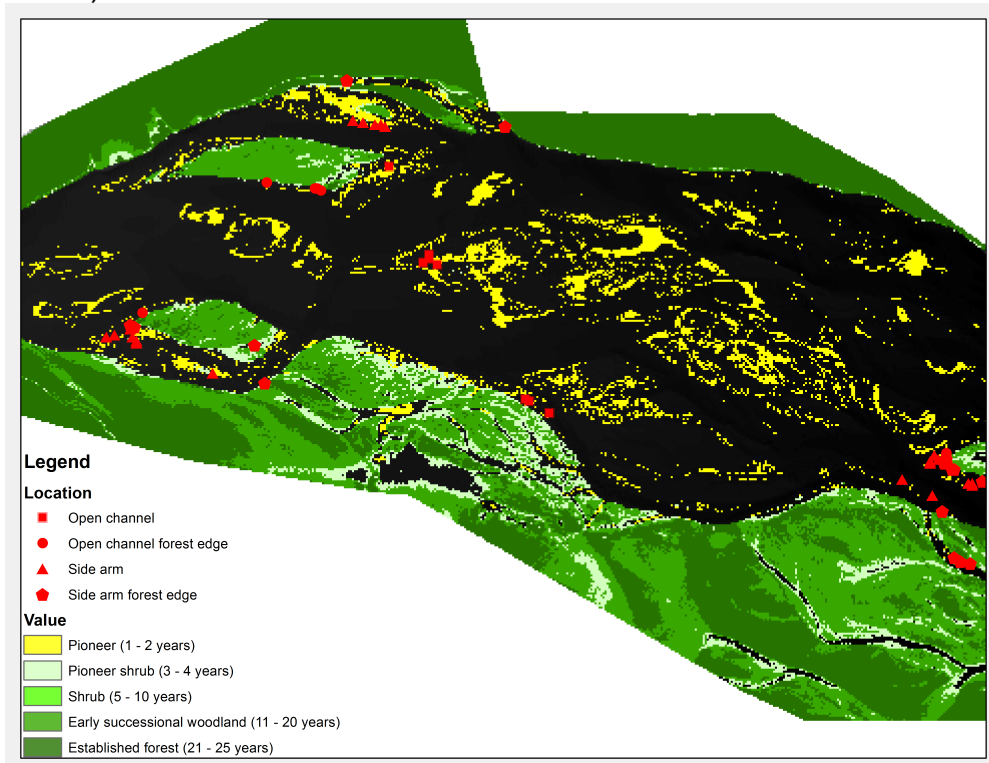


Figure 2-20 Resprouting wood deposited by the first year flood events

Comparing Figure 2-20 with Figure 2-16 is evident that most of the LW deposited in the first year did not resprouted either because local conditions were unsuitable or because re-entrained and transported outside the modelling domain by a subsequent flood. This is particularly likely for the wood deposited by the first flood, this because the LW deposited by the second flood, experienced only one minor disturbance event.

First two columns in Table 2-3 show the percentage of stranding locations and 1st year survival/resprouting, calculated on the total number of stranding sites. Last column of Table 2-3 shows instead the percentage of LW that survives in each type of location. Forested edges of side arms are the preferential stranding location, followed with a much lower percentage, by the forested edges of the open channel (Table 2-3). Open channel and bare surfaces in side channels are the locations with the lower percentages of stranding occurrences (Table 2-3). RVM therefore tends to strand logs near vegetated areas rather than bare ones. Studies on wood storage conducted by Gurnell, Petts, Harris, et al., (2000) on the Tagliamento, measured for two sites located immediately upstream (Cornino) and downstream (Pinzano) from the area modelled in this exercise, that most of the LW is stored near vegetated islands and only very minor quantities in the open channel (Table 2-4).

Table 2-3 Stranding and 1st year survival percentages calculated on the total number of locations and percentage of 1st year survival per location calculated on the total stranding per location

Location	Stranding %	1 st year survival total %	1 st year survival location %
Open channel	2.4	1.0	40.0
Open channel forest edge	24.3	0.8	3.4
Side arm	4.8	2.5	52.5
Side arm forest edge	68.5	2.0	3.0

Similar conclusions can be drawn from (Ruiz-Villanueva et al., 2016) which demonstrated that for a regular flood in the order of the year return period, in a river reach having traits similar to the modelled reach of the Tagliamento, most LW will snag on vegetated surfaces.

Table 2-4 Wood mass storage percentages measured on the Tagliamento in the summer of 1998 on two river reaches located immediately upstream and downstream of the modelled reach. Data extracted from Gurnell, Petts, Harris, et al., (2000)

Site	Gravel & water	Pioneer island	Established island
Cornino	0.7	85.5	13.9
Pinzano	2	85.2	12.8

Most of the positions where LW stranded were deemed by the model-rules unsuitable for resprouting (Table 2-3). The locations with the highest resprouting suitability were the

Side arm and the Open channel. Considering the share of stranding and the 1st year survival location fields in Table 2-3, is possible to argue that, for this simulation setting, stranding of LW on Open channel or Side arm locations is very unlikely, but when it occurs, LW has fair chances of resprouting. Conversely, stranding near vegetated surfaces is very likely but resprouting possibilities are very low. Qualitative comparison of this behaviour with literature data is complicated by a number of factors. Resprouting and survival of LW depends on disturbance history and local moisture conditions that for the literature data are not available. Moreover, the literature data available for the Tagliamento does not show a clear trend (Table 2-5).

Table 2-5 Percentage of dead and live (resprouting) wood measured on the Tagliamento in the summer of 1998 on two river reaches located immediately upstream and downstream of the modelled reach. Data extracted from: Gurnell et al., (2000a)

Site	Location	Dead wood	Live wood
Cornino	Gravel	6	94
	Established island	100	0.00
Pinzano	Gravel	80	20
	Established island	46	54

2.3.3.3 LW stranding elevation

Further qualitative assessment performed on the LW lifecycle model components considered the elevation at which LW was deposited by the floods of the first year and the elevation of the LW resprouting after the first year. Elevation was measured on the detrended topography of the active channel, thus removing the elevation above sea level due to the reach slope and making upstream and downstream deposition elevations comparable. Figure 2-21 shows the boxplots of the elevations at which simulated LW stranded. Side arm forest edge and Open channel forest edge locations show stranding ranges of approximately 12 and 5 m respectively. These ranges are not very realistic for, on the Tagliamento River on reaches near the modelled one, Bertoldi, Gurnell and Welber, (2013) observed deposition range of approximately 0.5 m around the mean elevation of the bed. A slightly wider range was observed by Gurnell, Petts, Hannah, et al., (2000) that reported deposition elevation in the range of 0.8 m at Cornino and 1.5 m at Pinzano. The predicted deposition elevation range for the Open channel and Side arm locations are more in line with the observations on the Tagliamento, although the predictions are still slightly higher than the observations. Nevertheless, for all the simulated locations, 75% of the data (boxplot body in Figure 2-21) falls within a range of 1 m, thus suggesting that at least most the simulated LW is deposited within a feasible range.

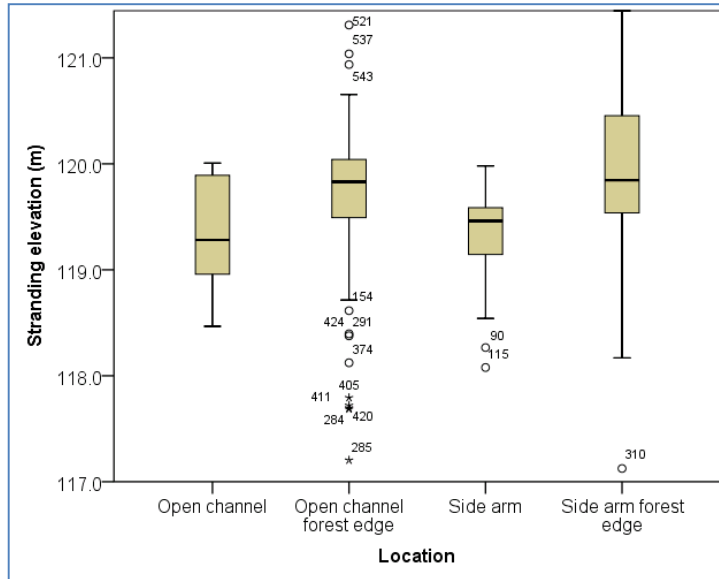


Figure 2-21 Stranding elevation above the detrended topography of the first simulated year

Qualitative assessment of predicted stranding elevations against remote sensed and field measurements from Bertoldi, Gurnell and Welber, (2013) and Gurnell, Petts, Hannah, et al., (2000) improves when considering only resprouting LW (Figure 2-22). In this case, all location but the Side arm have a deposition range of 1 m with this latter having the range extending up to 1.4 m.

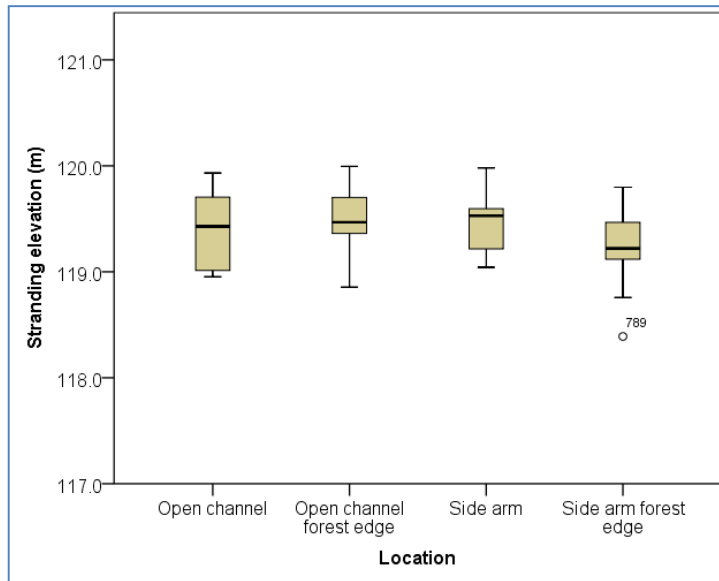


Figure 2-22 1st year survival elevation above the detrended topography of the first simulated year

2.3.3.4 LW geomorphic interactions

Presence of resprouting LW in the active zone of a river triggers fine sediment deposition at the edges, on the downstream side and inside the resprouting position. In order to

assess whether CLF-RVM is able of replicating fine sediment deposition caused by LW resprouts, the median particle size (d_{50}) at the end of the second simulated year was compared between positions in locations where resprouting LW was deposited by the floods of the first year and similar positions where LW deposition did not occur. Similar positions for each location where selected near LW resprouting sites where no vegetation was present. Figure 2-23 A shows the d_{50} distribution on the LW deposition locations. Visual comparison of this distribution with analogous locations where LW was not deposited (Figure 2-23 B) does not show differences. Almost complete lack of difference between resprouting LW and similar locations is confirmed by non-parametric Mann-Whitney U test performed by pair wise comparison of the d_{50} among the different locations. The statistical test revealed a significant difference in the d_{50} distribution only for the Side arm while for all the other locations, d_{50} distribution was deemed not significantly different.

Statistically significant differences of the d_{50} among the different locations, irrespectively of LW resprouting, were also tested with a non parametric Kruskal-Wallis test. The test did not reveal any difference in the sediment distribution of the locations, thus suggesting that d_{50} is probably quite homogenous in the modelling domain. This was confirmed by the histogram and boxplot of the d_{50} extended of the whole modelling domain (Figure 2-24) showing a dominant grainsize in the range of 2.5-3.5 cm.

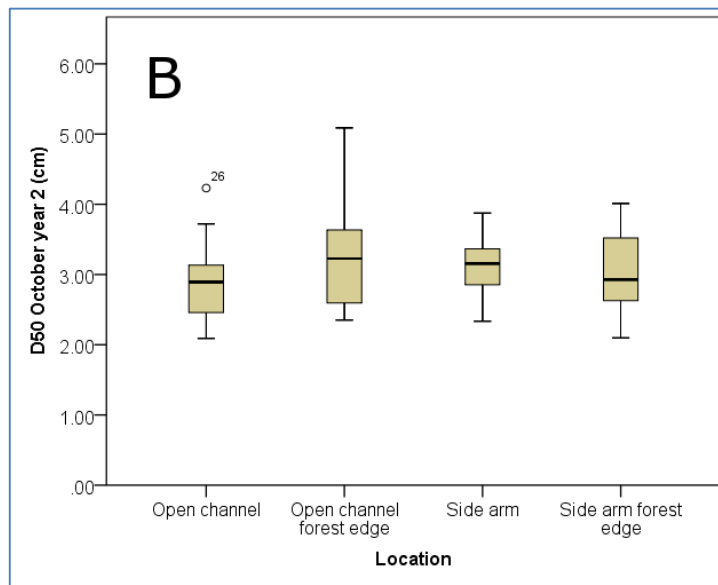
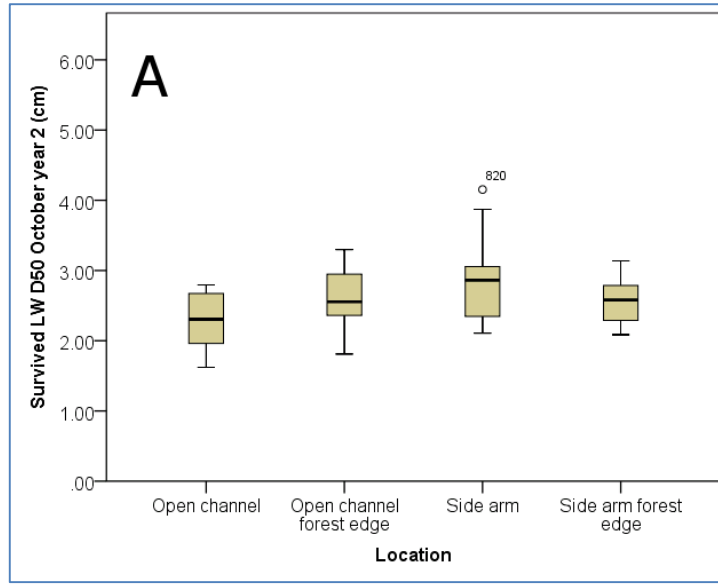


Figure 2-23 A: Median particle size (D50) of the 2nd simulated year, in the locations where LW deposited in the 1st year resprouted. B: D50 of the 2nd simulated year in locations where LW depositions did not occur.

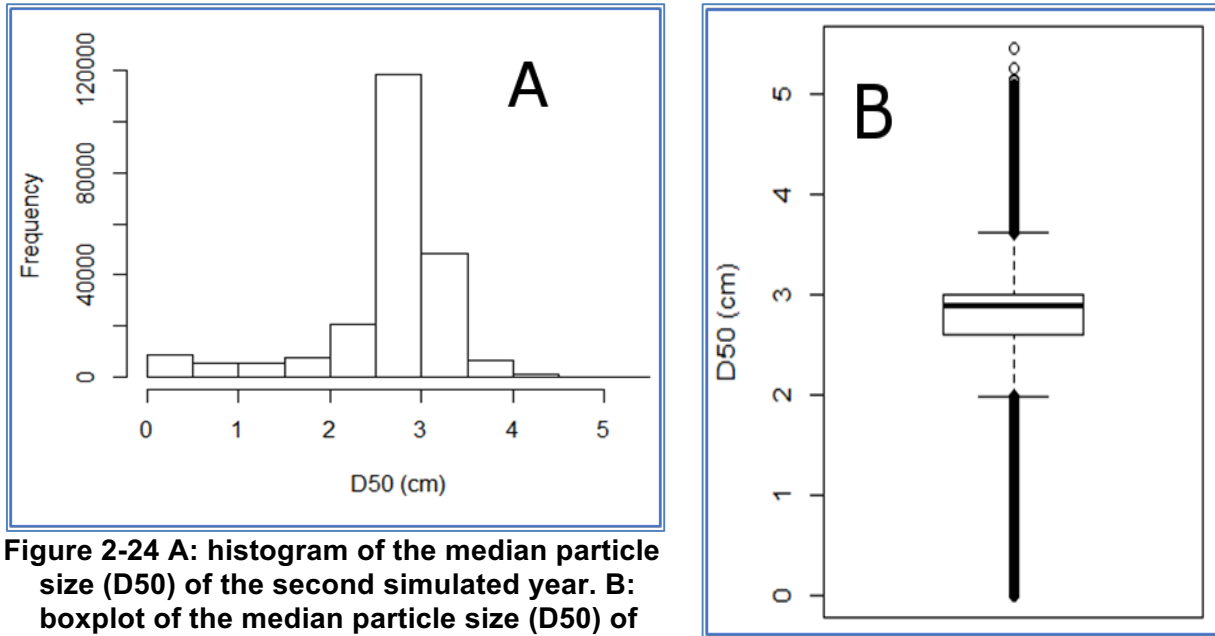


Figure 2-24 A: histogram of the median particle size (D50) of the second simulated year. B: boxplot of the median particle size (D50) of the second simulated year.

2.3.3.5 Simulated landscape evolution

Last qualitative assessment of this test case considered the overall simulated landscape development. The assessment looked to how the vegetation evolved in respect to the hydrological regime of the test case and the degree of similarity between the simulated landforms and typical landforms observed on this reach of the Tagliamento. Figure 2-25 shows the vegetation maps and the stranding positions of the LW at the end of each simulated year. Comparing the initial vegetation map (Figure 2-7) with the vegetation map at the end of the first year (Figure 2-25 A), is possible to see how the floods of the first year eroded most of the pioneer vegetation and dissected the early successional woodland inside of the side arm in the upper side of the map. Further vegetation erosion occurred at the forest margins of the active channel, including the margins of the two islands delimiting the two upstream side arms. Pioneer vegetation that was not eroded transited to the next succession phase (Pioneer shrub), at the same time, new pioneer vegetation established in the innermost sections of the side arms and on the higher surfaces of the open channel. One of the recruited areas stands downstream from several LW resprouting positions (blue circle in year Figure 2-25 A). These pioneers established after the first flood and where able of withstanding the destructive force of the second one. During the second year (Figure 2-25 B), pioneer expansion continued in the open channel and inside the side arms. During this second year, only a small quantity of LW was entrained. In the third and fourth year, no LW was entrained while pioneer expansion continued and the pioneer vegetation recruited in the previous years, progressed towards the pioneer shrub phase (Figure 2-25 C and Figure 2-25 D). The low magnitude of the floods in the second, third and fourth year, was however sufficient to maintain most of the open channel free from vegetation.

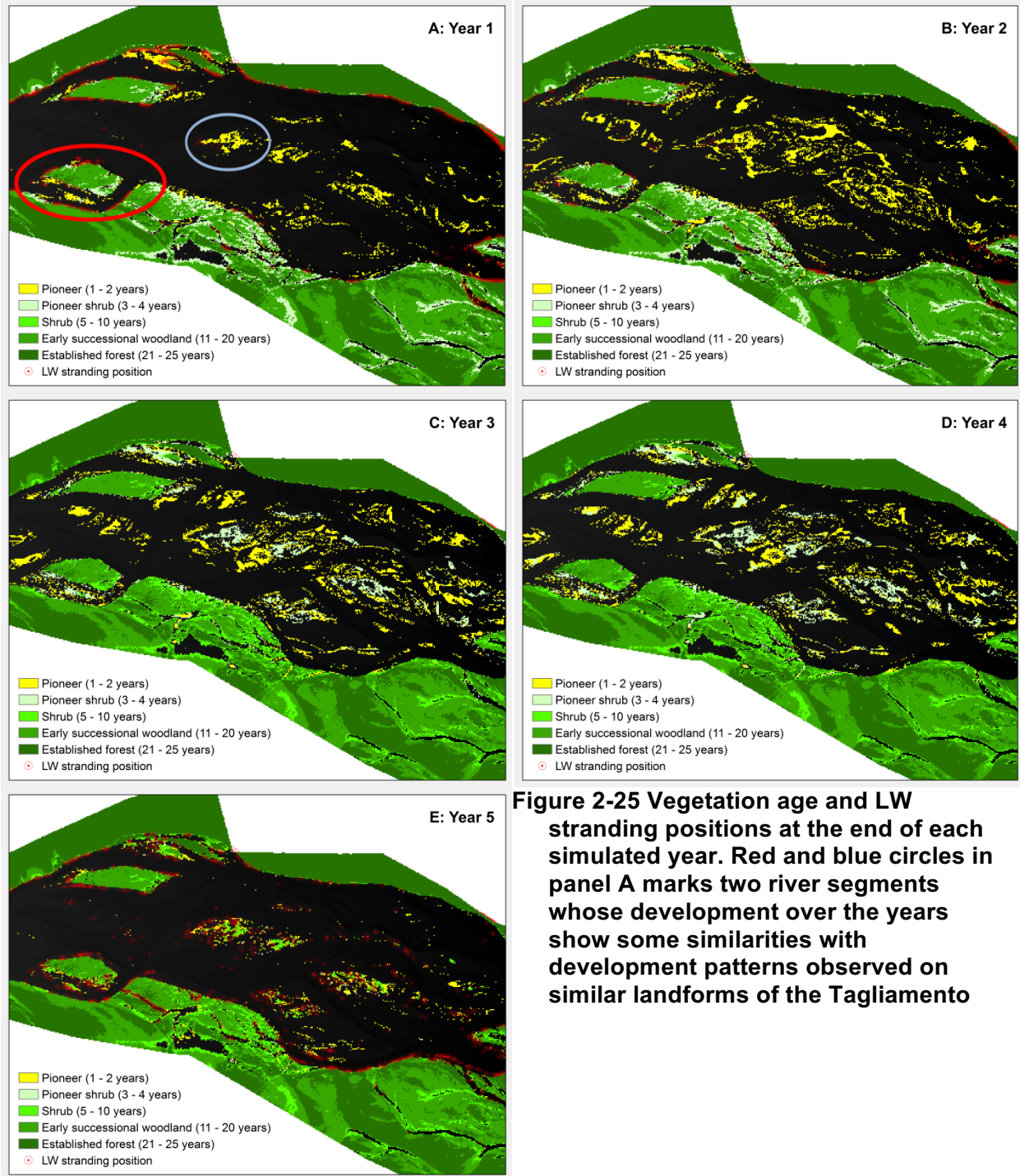


Figure 2-25 Vegetation age and LW stranding positions at the end of each simulated year. Red and blue circles in panel A marks two river segments whose development over the years show some similarities with development patterns observed on similar landforms of the Tagliamento

In the last simulated year, the two floods having one and one in five return period magnitude disrupted most of the vegetation established in the previous three years, especially in the open channel where only the vegetation standing on higher surfaces survives (Figure 2-25 E). Surviving vegetation inside the open channel is made mostly by

shrub phase, fringed by narrow ribbons of pioneer phase. Among the surviving vegetation of the open channel, there are also most of the shrubs originating from LW deposited and established after the first year (blue circle in year Figure 2-25 A) and the shrubs, originated from seed recruitment, growing downstream from LW deposition and resprouting positions. This confirms that the model can replicate the genesis of vegetated islands promoted by LW resprouting. However, during the simulation, similar vegetated islands developed simply from seed recruitment. The presence of vegetation in the open channel favours also LW stranding in the open channel, in fact comparing Figure 2-25 E and Figure 2-16 is possible to see that the former exhibits a much larger quantity of LW in the open channel, especially at the head and edges of vegetated islands. This agrees with the conclusions of section 2.3.3.1 and confirms the capability of the model of replicating this riparian systems behaviour. The floods of the last year have also the effect of shaping, by lateral erosion, the profile of the vegetated islands in the open channel. The shape of the islands after the floods is more hydrodynamic and has a good visual resemblance to in-channel vegetated islands of the Tagliamento.

Figure 2-26 shows the evolution of a vegetated island located on a river reach several kilometres upstream from the modelled one. Over the years, the island edge facing the open channel is progressively eroded while the channel between the island and the floodplain forest is progressively filled with vegetation originating from resprouting wood and seedlings. A similar development pattern can be noted on the maps produced by the model. During the simulated years, the island marked by the red circle in Figure 2-25, is subject to erosion on the edge facing the open channel while vegetation developing from both sprouts and seedlings progressively fills the side arm facing the floodplain forest. The two situations can be compared only on a qualitative level because in the real case, the side arm filling process was probably reset by disturbances having a higher frequency than the simulated case.



2003



2012



2015



2017

Figure 2-26 Side channel filling observed on the Tagliamento upstream from the modelled site. Blue arrow on 2003 image indicates the flow direction

2.4 Discussion and conclusions

The focus of the study was on the conceptual validation of CLF-RVM i.e. by ensuring that the results produced by the model comply with expected riparian ecosystem behaviours. More in detail, CLF-RVM validation assessed simulated vegetation feedback on sediment dynamics, vegetation growth performance in response to water table decline, how vegetation responds to the disturbance regime and how well LW lifecycle is replicated.

The first test, groundwater feedback to growth, showed that modelled growth decreases in response to a decrease in water availability during the growing season, as expected in riparian systems where annual growth of riparian tree species is correlated with streamflow (Stromberg and Patten, 1996; Willms et al., 1998). This first test showed also the decrease in biomass, due to vegetation mortality, caused by large interannual decreases in flow stage (Cooper et al., 2003; Scott et al., 1999). Moreover, vegetation encroachment on the dried channel of the drying scenario, is consistent with the behaviour observed in rivers subject to water withdrawal or flow regulation (Dolores Bejarano and Sordo-Ward, 2011; W Carter Johnson, 1994). Both the drying scenarios and undrying, although in the latter the surface of the active channel is maintained, show also the initiation of vegetation community aging. This behaviour has been observed downstream from dams reservoirs where, due to lack of flood events intercepted by dams, recruited seeds tend to grow and, over time, there is less and less space for new cohorts while pre-existing vegetation is allowed to grow undisturbed (Braatne et al., 2007). Groundwater feedback to growth test case demonstrated how CLF-RVM can consistently model riparian trees growth and how their population responds to changes in the hydrological regime. However, CLF-RVM assumes as proxy for water table the flow stage interpolated over the whole modelling domain. Such assumption is supported by several studies that demonstrated how groundwater in riparian contexts is dependent on flow stage (Cooper et al., 1999; Mahoney and Rood, 1998). Nevertheless, the assumption holds true in unconfined valleys while in narrow shaped canyons groundwater and streamflow stage are less well correlated (Stromberg and Patten, 1996). Moreover being riparian trees growth favoured in gaining reaches and limited in losing ones (Harner and Stanford, 2003) the groundwater assumption made in CLF-RVM allows to model river reaches where groundwater dynamics are homogeneous and there is no need to account for differences in growth due to groundwater upwelling or downwelling.

The second test case, vegetation feedback to sediment dynamics, demonstrated how simulated feedback of CLF-RVM on sediment cohesion and flow resistance is able of reducing the quantity of entrained sediment and the area subject to erosion. Lower quantity of eroded sediments has the effect of reducing also the quantity of deposited material. The simulated sediment feedback is in line from studies that demonstrated how presence of vegetation stabilizes sediments, thus reducing surface and lateral erosion (Abernethy and Rutherford, 2000; Prosser et al., 1995). Nevertheless, model results from the LW lifecycle test case pointed out that presence of vegetation does not favour accumulation of fine sediments (Figure 2-23) in contrast to what reported by field observations (Abbe and Montgomery, 2003; Mikuš et al., 2013). Lack of simulated fine sediment accumulation can also be due to the relative low input of fine sediments used in the simulations (Table 2-8) and therefore, definitive conclusion on this aspect shall be demanded to future studies.

The last test case, LW lifecycle tested the most innovative feature of the presented model: i.e. entrainment and establishment of LW. Simulated LW entrainment and stranding locations assessment criteria were drawn considering that LW tends to strand on high surfaces near the zones from where LW is entrained (Bertoldi et al., 2013). LW deposition occurs preferably on depositional surfaces having narrow elevation ranges (Bertoldi et al., 2013; Gurnell et al., 2000a), depending also on reach characteristics (Gurnell et al., 2000b) and magnitude of the flood entraining the wood (Ruiz-Villanueva et al., 2016). Simulated LW resprouting was assessed considering that, although, it depends on local edaphic conditions, on the Tagliamento resprouting appears to occur preferentially on specific geomorphic units (Gurnell et al., 2000a). Further qualitative assessment regarding LW stranding locations considered that, in descriptive terms, LW stranding preferential location are: side arms (Piegay, 1993), floodplain woodland edges (Piégay and Gurnell, 1997) and upstream and side edges of vegetated islands (Hickins, 1974). The results from this test case simulation showed that CLF-RVM entrains and deposits LW in locations and with proportions that are in line with studies conducted on the Tagliamento. Simulated stranding locations showed also good agreement with elevation profiles and deposition attributes observed on similar reaches of the Tagliamento. In fact, the large elevation range simulated for the Side arm forest edge and Open channel forest edge can be explained by the slope failure mechanism implemented by CLF. CLF simulates slope failure when local slope exceeds a threshold angle. This process is independent from lateral bank migration and is not due to any hydraulic-related variable. Observing the position of the LW stranded on the higher locations, it was possible to see how these trees were not entrained by the erosive action of the floods but rather by slope failure.

Simulated LW sprouts initiate also landforms and vegetation patterns consistent with landforms and patterns that are typical for this river reach. More in detail, LW stranded in the open channel participate to the creation of vegetated islands while those stranded in side arms favour coalescence between the floodplain and the vegetated island delimiting the side arm. However, it should be noted that also vegetation established by seed recruitment initiated vegetated islands. On the Tagliamento, such island genesis is very unlikely because of the relative slow growth rate of seedlings compared to LW resprouts, and the likelihood of being disrupted by fluvial processes (Gurnell, 2016). Creation of this type of island in the simulated landscapes can be explained by four simplifications introduced in this modelled scenario. First, the simulation started with a bare open channel, thus providing an extensive potential recruitment area. Second, the disturbance regime following the first simulated year was very weak and was not sufficient to remove the pioneer vegetation established in the open channel. Such low disturbance frequency and intensity is very unlikely on the Tagliamento and is likely one of the reasons why reproduction from propagules is more successful in this river reach. Third and fourth factors are due to the simplified form of the hydrograph used in the simulation (Figure 2-8). During the recruitment period, only one flood was simulated while in piedmont rivers, during the seed-recruitment period, flash floods from thunderstorms or melting events can be quite frequent and disrupt newly established seed-cohorts (Johnson, 2000). Finally, aside from the floods, mean monthly discharges during the growing season were the same for all simulated years, thus droughts were not accounted although, especially on gravel-bed rivers, lack of water during summer is a cause of seedlings extinction

(Johnson, 2000). However, a simplified hydrograph was a necessary compromise to allow the validation of the model features that simulate LW lifecycle. Consequently, the role of disturbance frequency and intensity on the dominant riparian trees reproductive strategy and emerging vegetated landforms will be subject for further studies.

LW lifecycle and growth test cases showed also that vegetation expansion and contraction in response is consistent with the disturbance regime: during low or no disturbance periods, vegetation tends to encroach into the open channel while flood events disrupt pioneer phase vegetation and erodes the edges of islands and channel margins vegetated with shrubs and trees (Figure 2-25 D and Figure 2-25 E).

Riparian landscapes are dynamic systems undergoing expansion and contraction cycles (Surian et al., 2015) fast landscape units turnover (Zanoni et al., 2008) and successional dynamics that unfold over the course of several years (Egger et al., 2015). This implies that in riparian systems multiple timescales are relevant. For example, vegetation disruption can occur on the flood event time scale (i.e. hours) while establishment and growth occur on seasonal and multiple years time scales respectively (Richards et al., 2002). Therefore, simulations models aimed to replicate landscape evolution of these dynamic systems must include components working on different timescales. The riparian vegetation model component (RVM) proposed in this chapter includes all these timescales, relevant successional and retrogression riparian vegetation processes and feedback to fluvial morphodynamics. Although the proposed RVM relies on Caesar Lisflood-Fp (CLF), any hydromorphodynamic model (HyMo) able of delivering the outputs provided by CLF can be used, provided the HyMo execution speed is compatible with the objective of simulating long time periods (years).

The main innovations introduced by the presented model are an extensive use of fuzzy logic to model complex riparian ecosystem behaviour, inclusion of the most important riparian woody vegetation-hydromorphological processes interaction and, most importantly, the development of a LW entrainment, transport and establishment submodel.

Results from the test cases demonstrated that fuzzy logic can be proficiently used to model complex riparian ecosystem interaction. The use of fuzzy logic in this context is particularly suited because although there is a generic good understanding on riparian systems functioning, many processes-thresholds are unknown or ill defined (Politti et al., 2017) and therefore, knowledge is somehow vague. In this context, fuzzy logic is appropriate for it allows to the take advantage of imprecise information and allows integration of expert knowledge into computer systems aimed at modelling complex system in a deterministic fashion.

In the current version, the RVM can replicate only a single ligneous species, if applied to a real case scenarios, the choice shall fall on the dominant species which has ecological engineering capabilities (e.g. poplars or willows). Although in rivers where one species is dominant such solution is justifiable, in riparian context where more complex species assemblages are present, a single species simplification might not be a satisfactory solution. In alternative, one could resort in translating the “generic fish” concept to “generic tree”, thus considering for the RVM parameterization average ligneous species average (Västilä and Järvelä, 2017). The use of a single species limits also modelling of vegetation succession beyond the “Transitional stage” (sensu Egger et al., 2013) i.e.

when main drivers of vegetation succession are more bound to ecological processes rather than ecological ones (e.g. competition). Nevertheless, RVM source code is designed for scalability and further species, also of herbaceous type could be integrated in future versions.

Extensions of RVM shall consider that, in the current form, the number of parameters is quite large and extending the model will likely extend this number. On the other hand, in a real case scenario one should consider that not all submodels are equally important, for example flood duration is of little relevance in Alpine contexts while morphodynamic disturbance is less important in low land rivers (García-Arias et al., 2013a). Therefore, for the sake of computational efficiency, in a real case scenario less important submodels could be switched off.

Finally, the potential applications of the proposed model can range from scientific studies aiming at testing hypothesis to management applications where the outcome of river management long term decisions shall be evaluated.

Table 2-6 CLF and RVM inputs and units of measures. * Mandatory input

Input	Description	Unit
Topography*	Raster data type, portrays topography of the modelling domain.	m (a.s.l.)
Bedrock	Raster data type, portrays the height of the bedrock layer in the modelling domain.	m (a.s.l.)
Initial grain size	CLF formatted text file, lists the spatial and vertical distribution of the sediments.	m
Discharge file*	CLF formatted text file, list the input discharges (mandatory) and the solid discharge for each grainsize (optional)	m ³ /s, m ³
Vegetation age	Raster data type, portrays topography of the modelling domain.	years
Stems D	Raster data type, portrays the diameter of the initial vegetation.	cm
Plant count	Raster data type, portrays the number of the initial vegetation individuals.	plants/c ell
Roots maximum density	Raster data type, portrays the depth at which is found the maximum density of the initial vegetation roots.	m
Vegetation height	Raster data type, portrays the height of the initial vegetation.	cm
Vegetation fitness	Raster data type, portrays the health status of the initial vegetation.	-
LW age	Raster data type, portrays the age of the initial LW.	days
LW count	Raster data type, portrays the number of the initial LW.	logs/cell
LW diameter	Raster data type, portrays the average diameter of the initial LW logs.	cm

Table 2-7 CLF parameters. Adapted from Ziliani et al., (2013)

Parameter	Value	Unit
Lateral erosion rate	0.0001	
Number of passes for edge smoothing filter	50	
Number of cells to shift lateral erosion downstream	20	
Max difference allowed in cross channel smoothing	0.0001	
Max erode limit	0.075	m
Water depth above which erosion can happen	0.03	m
Min discharge for depth calculation	0.05	m ³ /s
Bare ground Mannings n	0.04	
Erosion equation	Wilcock and Crowe	
Slope failure threshold	60	Degrees
Input output difference allowed	7	m ³
Slope for edge cells	0.003	
Courant number	0.2	
Froude limit	0.8	

Table 2-8 Sediment input grain sizes and distribution (Ziliani, 2011)

Grain size (cm)	Proportion %
0.48	0.3
0.68	1.4
0.97	2
1.37	5.1
1.93	13.1
2.73	22
3.86	28.8
5.46	22.7
7.73	4.6

Table 2-9 Model parameters, their units, description, values applied in the test case and submodels by which parameters are used

Parameter	Description	Value	Unit	Submodels
1. Significant discharge	Discharge above which a flood is assumed to occur and disturbances are simulated	200	m ³ /s	Fuzzy erosion and shear stress, Fuzzy deposition mortality and bending
2. Recruitment start month	First month in which recruitment is simulated	May		Fuzzy seed recruitment
3. Recruitment end month	Last month in which recruitment is simulated	June		Fuzzy seed recruitment
4. Growing season start month	First month of the growing season	April		Growth, fuzzy hydric stress, fuzzy moisture habitat suitability, fuzzy flood duration, LW establishment
5. Growing season end month	Last month of the growing season	September		Growth, fuzzy hydric stress, fuzzy moisture habitat suitability, fuzzy flood duration, LW establishment
6. Leafy time start month	Month in which leafs are assumed to appear	April		Fuzzy roughness feedback
7. Leafy time end month	Month in which leafs are assumed to fall	September		Fuzzy roughness feedback
8. Large wood diameter threshold	D above which a log is assumed to be a LW	10	cm	LW recruitment
9. LW minimum submerged fraction for float	Ratio between water depth and D required for LW to float.	2		LW routing
10. LW roughness	Manning's n roughness coefficient of LW	0.1		LW routing
11. LW establishment required time	Time required by LW to establish and resprout	9	Months	LW establishment
12. Log jam maximum size	Maximum number of logs allowed in a cell	7	Logs	LW routing
13. Roots relative distance from growing season water table	Depth, relative to the distance from the growing season average water table	45%	m	Growth

Parameter	Description	Value	Unit	Submodels
	elevation, at which most of the roots are found			
14. Population annual thinning ratio	Annual mortality occurring to vegetation because of auto-competition and other non-fluvial specific mortality causes	5%		Growth
15. Maximum woody vegetation age	Maximum age reachable by the woody vegetation	300	Years	Growth
16. Maximum woody vegetation D	Maximum D reachable by woody vegetation	120	cm	Growth
17. Maximum woody vegetation height	Maximum height reachable by woody vegetation	4000	cm	Growth
18. D reference height	Height at which D is measured	137	cm	Growth
19. Absolute burial tolerance	maximum depth of sediments that vegetation can endure	1.5	m	Fuzzy deposition

Table 2-10 Description of the linguistic variables, their units, direction (input or output) and submodels by which the linguistic variables are used

Linguistic variable	Description	Unit	Direction	Submodels
Monthly water distance	Distance between the mean water table and the ground surface in the recruitment months	m	Input	Fuzzy seed recruitment
Substrate	Grain size of the substrate	cm	Input	Fuzzy seed recruitment, LW establishment
Natality	Number of seedlings germinating per unit ground	seedlings/m ²	Output	Fuzzy seed recruitment
Deposition	Depth of sediment deposited by a flood	m	Input	Fuzzy deposition mortality & bending
Vegetation age	Age of vegetation	years	Input	Growth, fuzzy deposition mortality & bending, fuzzy roughness, fuzzy bank cohesion, fuzzy critical Shields
Fitness	Health status of the vegetation	-	Input	Fuzzy deposition mortality & bending, fuzzy hydric stress,
Mortality	Percentage of individuals on a cell dying because of an impact	%	Output	Fuzzy erosion & shear stress, fuzzy deposition mortality & bending, fuzzy hydric stress, fuzzy flood duration, fuzzy LW establishment
Stem diameter	Diameter of the plants standing on a cell	cm	Input	Fuzzy deposition mortality & bending
Bending	Bending of plants in response to a deposition event	degrees	Output	Fuzzy deposition mortality & bending
Shear stress	Shear stress acting on vegetation during a flood	N/m ²	Input	Fuzzy erosion and shear stress

Linguistic variable	Description	Unit	Direction	Submodels
Vegetation roots depth	Depth of roots maximum density	m	Input	Fuzzy erosion and shear stress, fuzzy bank cohesion, fuzzy critical Shields
Seasonal water distance	Distance between the average water table of the growing season and the ground surface	m	Input	Fuzzy hydric stress
Habitat moisture suitability	Degree of suitability of the distance between roots maximum density and annual water table	-	Output	Fuzzy moisture habitat suitability,
Interannual water difference	Difference between the average water table of the current growing season and the average water table from the previous growing season	m	Input	Fuzzy moisture habitat suitability,
Seasonal flooding	Percentage of the growing season's days under waterlogged condition		Input	Fuzzy flood duration
Stems count	Number of individual plants per unit ground	m ²	Input	Fuzzy roughness, fuzzy bank cohesion, fuzzy critical Shields
LW vitality	Dichotomic dimension expressing if LW is vital	Yes/No	Output	Fuzzy LW establishment

Linguistic variable	Description	Unit	Direction	Submodels
Relative cover	Percentage of ground covered by vegetation	%	Output/ Input	Fuzzy roughness, fuzzy bank cohesion, fuzzy critical Shields
Manning's n	Manning's roughness coefficient	s/m ^{1/3}	Output/ Input	Fuzzy roughness
Cohesion root depth	RDMD that provides cohesion to substrate	m	Input	Fuzzy bank cohesion, Fuzzy critical shear stress
Bank cohesion increase	Percentage increase in bank cohesion because of roots strengthening effect	%	Output/ Input	Fuzzy bank cohesion
Substrate cohesion increase	Percentage increase in substrate cohesion because of roots strengthening effect	%	Output/ Input	Fuzzy critical shear stress

Table 2-11 Fuzzy sets linguistic terms, memberships, shapes and literature used for their definition. Shapes: RL: right linear, TRA: trapezoidal, TRI: triangular, LL: left linear, SING: singleton. Numbers preceding the shapes shortcut mark the control points of the sets shapes.

Linguistic variable	Linguistic term	Membership & set shape
Monthly water distance	low distance	0.1, 0.4 RL
	medium distance	0.1, 0.75 TRI
	high distance	0.4, 4 LL
Substrate	fine	0.5, 1 RL
	intermediate	0.5, 2, 3 TRA
	coarse	2, 8 LL
Natality	low natality	2, 10 RL
	medium natality	2, 15, 25 TRA
	high natality	15, 25 LL
Deposition	low deposition	0.2, 0.4 RL
	medium deposition	0, 0.7, 1 TRA
	high deposition	0.7, 1.5 LL
Vegetation age	Young	2, 4 RL
	Adult	2, 20, 30 TRA
	Mature	20, 400 LL
Fitness	low fit	0.2, 0.3 RL
	medium fit	0.2, 0.6, 0.7 TRA
	high fit	0.6, 1 LL
Mortality	no mortality	0, 1 SING
	low mortality	15, 35 RL

Linguistic variable	Linguistic term	Membership & set shape
	medium mortality	15, 60, 100 TRA
	high mortality	60, 100 LL
Stem diameter	small	0.5, 1 RL
	medium	0.5, 3, 5 TRA
	large	3, 5 RL
Bending	low bending	10, 25 RL
	medium bending	10, 45, 65 TRA
	high bending	45, 90 LL
Shear stress	low shear	5, 25 RL
	medium shear	5, 30, 45 TRA
	high shear	30, 150 LL
Vegetation roots depth	shallow	0.05, 0.15 RL
	medium	0.05, 0.5, 0.8 TRA
	deep	0.5, 4.5 LL
Interannual water difference	low distance	0.1, 0.5 RL
	medium distance	0.1, 1 TRA
	high distance	0.5, 5 LL
Seasonal flooding	low percent	10, 30 RL
	medium percent	10, 50, 100 TRA
	high percent	50, 100 LL
Seasonal water distance	low distance	0.2, 0.8 RL
	medium distance	0.2, 1.5, 2 TRA
	high distance	1.5, 4.5 LL
Habitat moisture suitability	low suitability	RL
	medium suitability	0.1, 0.75, 1 TRA

Linguistic variable	Linguistic term	Membership & set shape
	high suitability	0.75, 1 LL
LW vitality	survive	1 SING
	die	0 SING
Vegetation age	Young	2, 4 RL
	Adult	2, 20, 30 TRA
	Mature	20, 400 LL
Stems count	low count	0.5, 2 RL
	medium count	0.5, 4, 7 TRA
	high count	4, 100 LL
Relative cover	sparse	RL
	light	15, 60, 100 TRA
	dense	60, 100 LL
Summer Manning's n	young sparse	0.02, 0.03 TRI
	young light	0.025, 0.035 TRI
	young dense	0.03, 0.05 TRI
	adult sparse-mature sparse	0.035, 0.06 TRI
	mature light-adult light	0.05, 0.08 TRI
	mature dense	0.06, 0.1 TRI
	adult dense	0.08, 0.105 TRI
Winter Manning's n	young sparse	0.02, 0.03 TRI
	young light	0.025, 0.035 TRI
	young dense	0.03, 0.04 TRI
	mature sparse	0.035, 0.05 TRI
	adult sparse-adult light-mature light	0.04, 0.06 TRI
	mature dense	0.05, 0.07 TRI

Linguistic variable	Linguistic term	Membership & set shape
	adult dense	0.06, 0.075 TRI
Cohesion root depth	shallow	RL
	medium	0.02, 0.5, 0.8 TRA
	deep	0.5, 4.5 LL
Bank cohesion increase	no increase	0 SING
	low increase	RL
	medium increase	500, 2500, 3500 TRA
	high increase	2500, 5000 LL
Critical shear stress increase	no increase	0 SING
	low increase	50, 300 RL
	medium increase	50, 500, 700 TRA
	high increase	500, 1500 LL

Table 2-12 Fuzzy rules applied in each submodel

Fuzzy submodel	Fuzzy rules
Fuzzy seed recruitment	IF lowDistance AND fine THEN highNatality
	IF lowDistance AND intermediate THEN highNatality
	IF lowDistance AND coarse THEN medNatality
	IF medDistance AND fine THEN highNatality
	IF medDistance AND intermediate THEN medNatality
	IF medDistance AND coarse THEN lowNatality
	IF highDistance AND fine THEN noNatality
	IF highDistance AND intermediate THEN noNatality
	IF medDistance AND coarse THEN noNatality
	Fuzzy deposition mortality
IF lowDeposition AND Adult AND lowFit THEN noMortality	
IF lowDeposition AND Mature AND lowFit THEN noMortality	
IF lowDeposition AND Young AND mediumFit THEN noMortality	
IF lowDeposition AND Adult AND mediumFit THEN noMortality	
IF lowDeposition AND Mature AND mediumFit THEN noMortality	
IF lowDeposition AND Young AND highFit THEN noMortality	
IF lowDeposition AND Adult AND highFit THEN noMortality	
IF lowDeposition AND Mature AND highFit THEN noMortality	
IF medDeposition AND Young AND lowFit THEN highMortality	
IF medDeposition AND Adult AND lowFit THEN medMortality	
IF medDeposition AND Mature AND lowFit THEN noMortality	
IF medDeposition AND Young AND mediumFit THEN highMortality	
IF medDeposition AND Adult AND mediumFit THEN lowMortality	
IF medDeposition AND Mature AND mediumFit THEN noMortality	
IF medDeposition AND Young AND highFit THEN medMortality	
IF medDeposition AND Adult AND highFit THEN noMortality	

	IF medDeposition AND Mature AND highFit THEN noMortality
	IF highDeposition AND Young AND lowFit THEN highMortality
	IF highDeposition AND Adult AND lowFit THEN highMortality
	IF highDeposition AND Mature AND lowFit THEN highMortality
	IF highDeposition AND Young AND mediumFit THEN highMortality
	IF highDeposition AND Adult AND mediumFit THEN highMortality
	IF highDeposition AND Mature AND mediumFit THEN highMortality
	IF highDeposition AND Young AND highFit THEN highMortality
	IF highDeposition AND Adult AND highFit THEN highMortality
	IF highDeposition AND Mature AND highFit THEN medMortality
Fuzzy deposition bending	IF lowDeposition AND Small THEN lowBending
	IF lowDeposition AND Medium THEN noBending
	IF lowDeposition AND Large THEN noBending
	IF medDeposition AND Small THEN highBending
	IF medDeposition AND Medium THEN lowBending
	IF medDeposition AND Large THEN noBending
	IF highDeposition AND Small THEN highBending
	IF highDeposition AND Medium THEN highBending
	IF highDeposition AND Large THEN lowBending
	Fuzzy shear and erosion
	IF lowShear AND Shallow THEN lowMortality
	IF lowShear AND Medium THEN noMortality
	IF lowShear AND Deep THEN noMortality
	IF medShear AND Shallow THEN lowMortality
	IF medShear AND Medium THEN noMortality
	IF medShear AND Deep THEN noMortality
IF highShear AND Shallow THEN highMortality	
IF highShear AND Medium THEN medMortality	
IF highShear AND Deep THEN noMortality	
	IF lowDistance AND lowFit THEN lowMortality

Fuzzy hydric stress	IF lowDistance AND mediumFit THEN noMortality
	IF lowDistance AND highFit THEN noMortality
	IF medDistance AND lowFit THEN medMortality
	IF medDistance AND mediumFit THEN lowMortality
	IF medDistance AND highFit THEN noMortality
	IF highDistance AND lowFit THEN highMortality
	IF highDistance AND mediumFit THEN medMortality
	IF highDistance AND highFit THEN lowMortality
	Fuzzy flooding stress
	IF lowPercent THEN noMortality
	IF medPercent THEN lowMortality
	IF highPercent THEN highMortality
	Fuzzy moisture habitat suitability
	IF lowDistance THEN medSuitability
IF medDistance THEN highSuitability	
IF highDistance THEN lowSuitability	
Fuzzy LW establishment	IF lowDistance AND fine THEN Death
	IF lowDistance AND medium THEN Death
	IF lowDistance AND coarse THEN Death
	IF medDistance AND fine THEN Survival
	IF medDistance AND medium THEN Survival
	IF medDistance AND coarse THEN Death
	IF highDistance AND fine THEN Death
	IF highDistance AND medium THEN Death
IF highDistance AND coarse THEN Death	
Fuzzy relative cover	IF lowDensity AND Young THEN Sparse
	IF lowDensity AND Adult THEN Light
	IF lowDensity AND Mature THEN Sparse
	IF medDensity AND Young THEN Sparse
	IF medDensity AND Adult THEN Dense
	IF medDensity AND Mature THEN Dense
	IF highDensity AND Young THEN Light
	IF highDensity AND Adult THEN Dense
IF highDensity AND Mature THEN Dense	
Fuzzy summer roughness	IF Sparse AND Young THEN YS
	IF Sparse AND Adult THEN ASMS
	IF Sparse AND Mature THEN ASMS

	IF Light AND Young THEN YL
	IF Light AND Adult THEN MLAL
	IF Light AND Mature THEN MLAL
	IF Dense AND Young THEN YD
	IF Dense AND Adult THEN AD
	IF Dense AND Mature THEN MD
	Fuzzy winter roughness
	IF Sparse AND Young THEN YS
	IF Sparse AND Adult THEN ASALML
	IF Sparse AND Mature THEN MS
	IF Light AND Young THEN YL
	IF Light AND Adult THEN ASALML
	IF Light AND Mature THEN ASALML
	IF Dense AND Young THEN YD
	IF Dense AND Adult THEN AD
	IF Dense AND Mature THEN MD
	IF Sparse AND Shallow AND Young THEN noIncrease
	IF Sparse AND Medium AND Young THEN noIncrease
	IF Sparse AND Deep AND Young THEN lowIncrease
	IF Sparse AND Shallow AND Adult THEN lowIncrease
	IF Sparse AND Medium AND Adult THEN medIncrease
	IF Sparse AND Deep AND Adult THEN medIncrease
	IF Sparse AND Shallow AND Mature THEN lowIncrease
	IF Sparse AND Medium AND Mature THEN medIncrease
	IF Sparse AND Deep AND Mature THEN medIncrease
	IF Light AND Shallow AND Young THEN lowIncrease
	IF Light AND Medium AND Young THEN lowIncrease
	IF Light AND Deep AND Young THEN medIncrease
	IF Light AND Shallow AND Adult THEN lowIncrease
	IF Light AND Medium AND Adult THEN medIncrease
	IF Light AND Deep AND Adult THEN highIncrease
	IF Light AND Shallow AND Mature THEN lowIncrease
	IF Light AND Medium AND Mature THEN highIncrease
	IF Light AND Deep AND Mature THEN highIncrease
Fuzzy bank cohesion	

	IF Dense AND Shallow AND Young THEN lowIncrease
	IF Dense AND Medium AND Young THEN lowIncrease
	IF Dense AND Deep AND Young THEN medIncrease
	IF Dense AND Shallow AND Adult THEN medIncrease
	IF Dense AND Medium AND Adult THEN medIncrease
	IF Dense AND Deep AND Adult THEN highIncrease
	IF Dense AND Shallow AND Mature THEN lowIncrease
	IF Dense AND Medium AND Mature THEN medIncrease
	IF Dense AND Deep AND Mature THEN medIncrease
Fuzzy critical shear stress	IF Sparse AND Shallow AND Young THEN highIncrease
	IF Sparse AND Medium AND Young THEN highIncrease
	IF Sparse AND Deep AND Young THEN highIncrease
	IF Sparse AND Shallow AND Adult THEN highIncrease
	IF Sparse AND Medium AND Adult THEN highIncrease
	IF Sparse AND Deep AND Adult THEN highIncrease
	IF Sparse AND Shallow AND Mature THEN highIncrease
	IF Sparse AND Medium AND Mature THEN highIncrease
	IF Sparse AND Deep AND Mature THEN highIncrease
	IF Light AND Shallow AND Young THEN highIncrease
	IF Light AND Medium AND Young THEN highIncrease
	IF Light AND Deep AND Young THEN highIncrease
	IF Light AND Shallow AND Adult THEN highIncrease
	IF Light AND Medium AND Adult THEN highIncrease
	IF Light AND Deep AND Adult THEN highIncrease
	IF Light AND Shallow AND Mature THEN highIncrease
	IF Light AND Medium AND Mature THEN highIncrease
	IF Light AND Deep AND Mature THEN highIncrease
	IF Dense AND Shallow AND Young THEN highIncrease
	IF Dense AND Medium AND Young THEN highIncrease
	IF Dense AND Deep AND Young THEN highIncrease
	IF Dense AND Shallow AND Adult THEN highIncrease
	IF Dense AND Medium AND Adult THEN highIncrease
	IF Dense AND Deep AND Adult THEN highIncrease
	IF Dense AND Shallow AND Mature THEN highIncrease
	IF Dense AND Medium AND Mature THEN highIncrease
	IF Dense AND Deep AND Mature THEN highIncrease

3 Optical field measurement of flexible vegetation properties to derive spatially-variable estimates of flow resistance for use in hydrodynamic models

3.1 Introduction

Vegetation flow resistance reduces flow velocity and decreases floods waves celerity. Thus, during floods, vegetation flow resistance can promote water levels higher than those caused by the same discharge flowing through a vegetation-free channel and having the same geometry and substrate (Anderson et al., 2006). Changes in flow velocity reflect on sedimentation spatial patterns and geomorphic heterogeneity which in turn affect habitat diversity and biodiversity (Nichols et al., 1998). Sound estimation of vegetation flow resistance is therefore relevant for both flood-risk management and nature conservation purposes. The effect of vegetation on flow resistance depends on a number of factors including the total area of vegetation exposed to the flow, its density, its flexural properties, the presence or absence of leaves, and also the flow velocity (Politti et al., 2017). For example, as flow velocity increases, flexible shrubs reduce their exposed area by streamlining (Gosselin and De Langre, 2011; Weissteiner et al., 2015; Wunder et al., 2011). The presence of leaves amplifies streamlining (Freeman et al., 2000; Järvelä, 2002a) ensuring that flow resistance varies on a seasonal basis. Furthermore, the exposed area tends to increase with flow depth thus increasing the plant-water surface and associated flow resistance (Fathi-Maghadam and Kouwen, 1997; Manners et al., 2013).

Despite the dynamic nature of flow-vegetation interactions, flow resistance associated with vegetation is typically represented in hydrodynamic simulations using a coefficient that remains constant irrespective of flow velocity and/or depth (Horritt and Bates, 2002). Many methods have been proposed to better account for flow resistance associated with vegetation (see Baptist et al., 2009; Vargas-Luna et al., 2015 for in-depth reviews) but most involve parameterising vegetation using results from laboratory studies in which the spatial configuration and flexural properties of natural vegetation was not replicated (Aberle and Järvelä, 2013; Vargas-Luna et al., 2015). Methods based on measurable properties of natural vegetation are preferable (Aberle and Järvelä, 2013) and several that account for plant streamlining, species-specific biomechanical properties and varying levels of foliation have recently been proposed (Järvelä, 2004; Västilä and Järvelä, 2014; Whittaker et al., 2015). Some of these approaches have proved to be particularly effective in predicting suspended sediment deposition in low energy streams (Västilä and Järvelä, 2017). However, it remains unclear whether these physically-based

approaches can significantly improve the results of hydrodynamic simulations in comparison to traditional static representations of flow resistance.

From a practical perspective, the main barrier to the use of physically-based approaches is their additional data requirements. Spatial and structural properties of vegetation can be described by means of reference areas such as leaf area index (LAI), defined as the one side leaf area per unit ground, and the frontal area index (FAI), defined as the area of the ligneous plant organs exposed to the main flow direction (Västilä et al., 2013). Such reference areas can be measured using airborne or terrestrial laser technology (Antonarakis et al., 2010, 2009, 2008; Jalonen et al., 2012), satellite imagery and data fusion techniques (Forzieri et al., 2011). However, these data types are expensive to obtain and processing requires technical skill and significant time investment. (Warmink, 2007). In addition, airborne and terrestrial laser scanning has not been extensively tested on vegetation with a shrubby habitus, and woody riparian vegetation in the active channel typically assumes this form, especially in the early development stages. These constraints limit de facto the spread of physically-based flow resistance estimation approaches for practical engineering purposes.

In this chapter, we seek to overcome this problem by developing a cost-effective alternative method for reference area measurement based on established optical techniques. Hemispherical (Chianucci and Cutini, 2012; Thimonier et al., 2010) and frontal area photography (Bankhead et al., 2017) have previously been used to derive bulk reference area measurements but are adapted here to derive regression curves based on field data that can be used to estimate flow resistance at different submersion levels. We then explore the sensitivity of flow resistance to errors in reference area measurements. Finally, we assess the effects of spatial and temporal variability in flow resistance associated with vegetation on flow at the reach-scale in comparison to predictions based on a static representation of flow resistance. This final objective is achieved through the modification of a 2D hydrodynamic model to represent vegetation-related flow resistance using an equation proposed by Västilä & Järvelä (2014).

3.2 Materials and methods

3.2.1 Field measurements and analysis of vegetation properties

Fieldwork was undertaken in August 2016 along the Mareta River, an Alpine glacial-fed gravel-bed river located near the village of Racines-Ratschings (Italy) at approximately 1000 m a.s.l. Woody vegetation in the river's active channel is dominated by hybridized *Salix* sp. The site was subject to a restoration in 2009,

consisting of in-channel widening and vegetation removal. Due to a lack of competent flow events capable of causing erosion, the size and density of woody vegetation is relatively homogeneous throughout the reach. Characteristic vegetation reference areas were measured using optical methods at five sampling locations. Plot area and vegetation height were also measured at each sampling location. The sampled plots were composed exclusively by *Salix* sp. and randomly selected along the channel edge. To reduce false readings from nearby vegetation, other shrubs adjacent to the sampled plots were cleared, ground-covering grass was folded or cut, and dead wood removed.

3.2.1.1 Leaf area measurement

Leaf reference areas were measured using hemispherical photography (HP) and a gap-fraction analysis technique. Vegetation properties were computed taking into account the proportion of gaps, i.e. the fraction of sky visible from underneath the canopy that was unobstructed by vegetation. This technique is unable to differentiate between the photosynthetic and woody elements of plants. For this reason, several authors proposed the term “Plant Area Index” (PAI) (see Jonckheere et al. 2004 for an exhaustive review) to define the sum of LAI and stem area index (STAI) returned by gap-fraction techniques. To overcome this limitation, sampled plots were first photographed and then, on the same day, manually defoliated and re-photographed. Post-processed HPs were then used to compute LAI by difference of their vertical distribution in foliated and defoliated conditions. Camera settings were set to over-expose images by two f-stops on the automatic settings (Thimonier et al., 2010; Zhang et al., 2005) and sampling followed the protocol defined by Chianucci & Cutini (2012). The device used was a Nikon Coolpix 4500 equipped with a Nikon FC-E8 fisheye lens, mounted on a levelling tripod. This camera’s lens can be rotated by 180°, thus allowing pictures with accurate zenithal orientation to be taken. For every photograph, the camera was placed at the centre of the plot, so that the entire plot’s gap fraction could be recorded. The camera was adjusted for perfect zenithal orientation using a spirit level and the tripod levellers, and oriented towards north using a compass. Zenithal orientation is required to yield accurate gap fraction measures, while north-wise orientation facilitates the post processing. Three photographs were taken at different heights at each sampling location (Figure 3-1). The photographs were taken at heights ranging from 0.7 to 1.5 m in accordance with the height at which leaves stemmed from branches, the size of the tripod and the maximum height reachable by the operator to set the camera. Photographs were taken on a cloudy day or early in the morning or late in the afternoon, i.e. under diffuse light conditions, in order to minimize light scattering. The HPs were processed

using the algorithm of Thimonier et al., (2010) available from the software Hemisfer® (Swiss Federal Institute for Forest). The software provides also a set of functionalities to reduce possible bias due to canopy clumping, camera gamma corrections, and to remove operator subjectivity through automatic thresholding between sky and vegetation.

Flow resistance estimation with Equation 3-1 requires information on the submerged area of the plants. Since the camera pointed toward the sky, photographed PAI and STAI do not represent the portion of the plants that would be submerged by flow stages having the height of the pictures but represent rather the emergent plant portions (darker plants sections in Figure 3-1). Therefore, PAI and STAI measured with HP needed to be transformed to derive equivalent PAI and STAI that would be exposed to the flow. Considering that Picture 1 (Figure 3-1) captures the whole foliated PAI and STAI of the plot, PAI and STAI at the height of Picture 2 had to be calculated as the difference between PAI/STAI 1 and PAI/STAI 2. Similarly, PAI and STAI at the height of Picture 3 were calculated as the difference between PAI/STAI 1 and PAI/STAI 3. Finally considering that below the height of Picture 1 there are no leaves, PAI and STAI at that height was set to 0. Ultimately, for each plot, a total of four data points was obtained: three from HP and one from observation on lower foliation limit. PAI and STAI thus yield from image analysis were regressed against picture height and relative picture height (i.e. picture height divided by patch height) to find a predictor readily linkable to flow depth. The PAI and STAI curves were then used to statistically model PAI and STAI vertical distribution and yield, by algebraic difference, LAI vertical distribution.

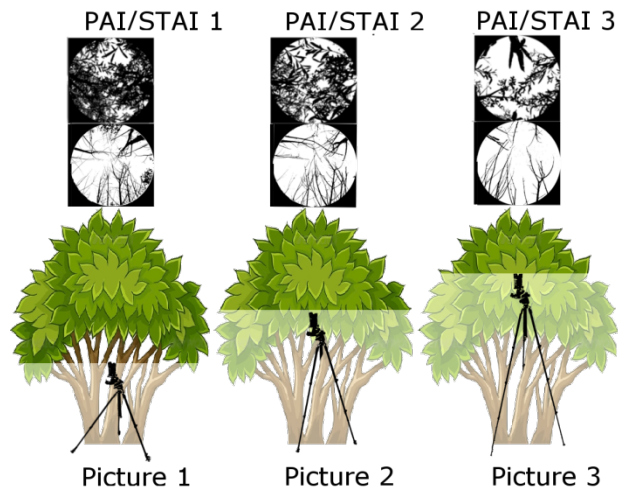


Figure 3-1 Graphical representation of the leaf area sampling performed by placing the camera at different heights. On the top rows, examples of resulting HPs in foliated and defoliated conditions. Note how gap fraction increases as camera position heightens.

3.2.1.2 Frontal area measurement

Frontal area was measured under defoliated conditions by taking a photograph of the upstream face of the plot along the main flow direction. For this set of photographs, the camera was a Nikon D3500 equipped with a Nikon 18-105 mm lenses. The camera was mounted a tripod placed in line with the centre of the sampling location and photographs taken approximately 5-10 m from the patch, depending on local terrain conditions. To enhance the contrast between the stems and the background, a white screen marked near the corners with four black segments of known length, was placed behind each plot. Frontal photographs were analysed using Image J. Image J is a software platform that provides image analysis capabilities, among which measuring areas and distances by providing a reference distance in the analysed pictures. In the post-processing phase, RGB images were converted to binary black and white bitmaps through manual thresholding. Frontal area was measured at different heights by varying the vertical portion of the picture. Derived frontal area was then divided by the plot area so that the frontal area index (FAI) was obtained. As with PAI and STAI, FAI was regressed against patch height and relative height, however in this case, the regression line was forced to originate from 0, i.e. FAI extinguishes at ground level.

3.2.2 Flow resistance estimation

Västilä & Järvelä (2014) flow resistance calculation approach is formalized in Equation 3-1:

$$f_{tot} = 4 \left[LAI \cdot C_{D\chi,F} \left(\frac{u}{u_{\chi,F}} \right)^{\chi_F} + FAI \cdot C_{D\chi,S} \left(\frac{u}{u_{\chi,S}} \right)^{\chi_S} \right] \quad \text{Equation 3-1}$$

where f_{tot} : dimensionless vegetative friction factor, $C_{D\chi,F}$, $C_{D\chi,S}$: species specific foliage and stem drag coefficients, χ_F , χ_S : foliage and stem reconfiguration parameters, u : flow velocity (m/s), $u_{\chi,F}$ and $u_{\chi,S}$: lowest velocities (m/s) used to determine the empirical parameters χ_F and χ_S . Equation 3-1 calculates the friction factor and separates the resistance due to ligneous parts (herein simply stem) and foliage. Thus, by reducing the term LAI to 0, Equation 3-1 allows to consistently model flow resistance of deciduous species also in winter. Flow resistance at different submersion levels can be computed provided the vertical distribution of LAI and FAI are known. Equation 3-1 is applicable to plants of different size (Jalonen and Järvelä, 2014), and to both individual plants and patches, as plant density is implicitly lumped in the LAI and FAI parameters (Järvelä, 2004). Nevertheless, application of Equation 3-1 is subject to the availability of species-specific empirical coefficients and information on vegetation reference areas for the plants that are to be modelled. Although the novelty of the method implies a paucity of empirical parameters, a set of parameters determined for several typical riparian species already exist (Table 3-1) and are readily applicable in modelling (Jalonen and Järvelä, 2014; Västilä and Järvelä, 2014).

Table 3-1 Equation 1 empirical parameters. a Jalonen & Järvelä, (2014), b Västilä & Järvelä (2014)

Species	$C_{D\chi,S}$	χ_S	$C_{D\chi,F}$	χ_F	$u_{\chi,F}$	$u_{\chi,S}$
^a <i>Salix caprea</i>	0.34	-0.66	0.019	-0.98	0.1	0.1
^a <i>Salix caprea</i> low velocity (<0.6 m/s)	0.36	-0.22	0.019	-0.98	0.1	0.1
^a <i>Salix caprea</i> high velocity (>0.6 m/s)	0.59	-1.05	0.019	-0.98	0.1	0.1
^b <i>Salix viminalis</i>	1.03	-0.2	0.11	-1.21	0.2	0.2
^b <i>Salix rubens</i>	0.96	-0.25	0.19	-1.21	0.2	0.2

3.2.3 Flow resistance sensitivity

3.2.3.1 Sensitivity to empirical parameters set and foliation

In this work, the empirical parameters for *Salix rubens* were used on the basis that it is a hybrid (*Salix alba* x *Salix fragilis*) that is common along perennial streams and, thus, most similar to the *Salix* encountered at the Mareta River. Equation 3-1 was applied using velocities of 0.25, 0.5 and 1 m/s, assuming full plants submersion. To assess how the predicted flow resistance would vary in response to reference areas measurement errors and, thus, how sensitive Equation 3-1 is to reference area, the obtained allometric relationships for LAI and FAI were independently (i.e. one reference area at a time) changed by the following percentages: -50, -25, -10, 10, 25, 50.

To understand how the choice of different parameters set would influence friction factor prediction under foliated and defoliated conditions, Equation 3-1 was applied using all the species-specific parameters. Both foliated and defoliated (i.e. LAI set to 0) conditions were computed for different submersion levels and for flow velocities of 0.25, 0.5 and 1 m/s.

3.2.3.2 Sensitivity to reference areas measurements

To assess how the predicted flow resistance would vary in response of eventual reference areas measure errors and thus how sensitive is Equation 3-1 to reference areas, Equation 3-1 was applied using velocities of 0.25, 0.5 and 1 m/s, assuming full plants submersion and using *Salix rubens* empirical parameters set. The choice of applying *Salix rubens* parameters is justified by the fact that at the Mareta River *Salix* in the active channel are mostly hybrids and that *Salix rubens*, among the *Salix* species for whom parameters exist, is as well a hybrid (*Salix alba* x *Salix fragilis*) and is typical along perennial streams. The reference areas resulting from the allometric relationships (see section 3.3.1) were independently (i.e. one reference area a time) changed by the following percentages: -50, -25, -10, 10, 25, 50.

3.2.4 Flow resistance modelling

3.2.4.1 Hydrodynamic model

Västilä & Järvelä (2014)'s method was tested in 2D modelling by implementing Equation 3-1 in the hydrodynamic model Lisflood-FP (Bates et al., 2010). Lisflood-FP is a two-dimensional hydrodynamic model working on a regular grid (raster), it solves the flow (Q) between two cells using Equation 3-2:

$$Q = \frac{q - gh_{flow}\Delta t \frac{\Delta(h+z)}{\Delta x}}{(1 + gh_{flow}\Delta t n^2 |q|/h_{flow}^{10/3}) \Delta x} \quad \text{Equation 3-2}$$

With q : flow between cells from the previous iteration (m^3/s), g : gravity acceleration (m/s), n : Manning's roughness coefficient ($m^{1/3}/s$), h : flow depth (m), z : elevation (m), h_{flow} : maximum depth between two cells, Δt : time step and x : cell width. After the flow from the four boundaries of a cell has been computed, the water depth (h) in the cell, having i and j coordinates, is updated according to Equation 3-4:

$$\frac{\Delta h^{i,j}}{\Delta t} = \frac{Q_x^{i-1,j} - Q_x^{i,j} + Q_y^{i,j-1} - Q_y^{i,j}}{\Delta x^2} \quad \text{Equation 3-3}$$

Lisflood-FP is available in the Caesar Lisflood-FP (CL) landscape evolution model (Coulthard et al., 2013). In this work CL version 1.9 was used (Coulthard, 2017). CL has been modified to accept an additional input, several additional parameters, compute vegetation roughness according to Equation 3-1 and compute bed shear stress according to Equation 3-4:

$$\tau_b = \rho_0 g \frac{u^2}{C_b^2} \quad \text{Equation 3-4}$$

With τ_b : bed shear stress (N/m^2), ρ_0 : water density and C_b : Chezy roughness coefficient. The additional input is a raster map representing vegetation height (m) while the additional parameters are the empirical parameters of Equation 1 listed in Table 3-1. In the modified CL, vegetation roughness is calculated with an iterative routine that computes LAI and FAI according to the equations derived from field data (see section 3.3.1). The routine considers the water depth in a vegetated cell and computes the relative submersion as the ration between plant height and water depth. Relative submersion is used as predictor variable to compute LAI and FAI then used in the flow resistance Equation 3-1. Calculated flow resistance is fed back to CL to re-compute flow depth and consequently, re-compute flow resistance. The iteration proceeds until flow depth is constant. In CL, flow calculations (e.g. Equation 3-2) make use of Manning's flow resistance coefficient. For this reason, the friction factors (f_{tot}) estimated using Equation 3-1 is converted to Manning's n roughness coefficients ($s/m^{1/3}$) using Equation 3-5 (Fathi-Maghadam and Kouwen, 1997).

$$n = \sqrt{f} \left(\sqrt{\frac{1}{8g} h^3} \right) \quad \text{Equation 3-5}$$

3.2.4.2 Modelled scenarios

3.2.4.2.1 General settings

All scenarios were run with fixed bed on a trapezoid isosceles-shaped geometry with the short base of 24 m, walls inclined at 45° and slope of 0.003. The data model used by CL is a regular cell, for the presented scenarios, the cell-size was set to 3x3 m. In all scenarios, *Salix rubens* empirical parameters (Table 3-1) were applied. Vegetated cells had a fixed vegetation height of 2.8 m, corresponding to the average height of the patches sampled at the Mareta River. Where vegetation was not present; bed roughness was set to 0.022 s/m^{1/3} which is a typical roughness value for gravelly channels with uniform section (Chow, 1959). Modified CL was used to simulate several discharges in foliated and defoliated conditions. The results were compared against results yield from an unmodified version of CL having vegetation roughness set to one of the following three values of Manning's n: 0.045 s/m^{1/3} (N0045), 0.062 s/m^{1/3} (N0062) and 0.098 s/m^{1/3} (0098). These values were drawn from Chow, (1959) and reflect possible choices of flow resistance for shrubs in the active channel. A summary of the different scenarios settings and acronyms is displayed in Table 3-2.

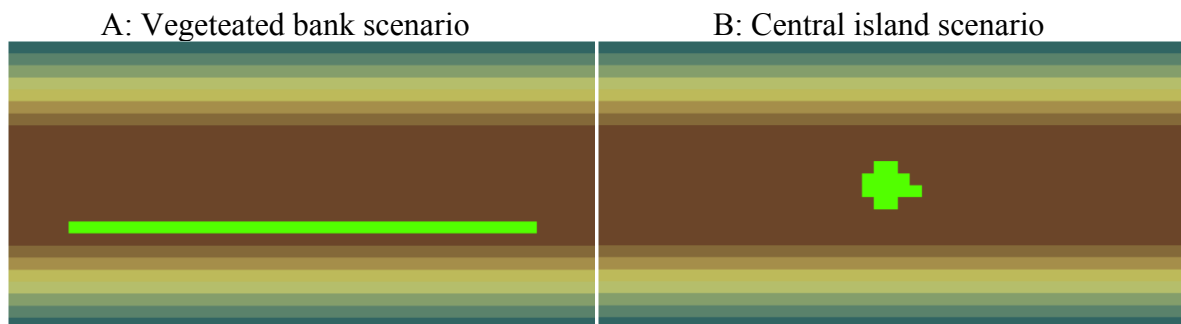


Figure 3-2 Shape and position of the vegetation in the two modelled scenarios. In both scenarios, flow direction goes from the left edge to the right one.

3.2.4.2.2 Vegetated bank

In the vegetated bank scenario, vegetated cells were placed on the left bank of a 220 m long modelling domain. Vegetation strip was 139 m in length and 3 m in width (Figure 3-2). The discharges fed to CL were of 13, 40 and 80 m³/s corresponding to water depths along the bank of approximately 1, 2 and 3 m respectively. The objective of this scenario was to assess how the water depth predicted with the

modified CL differed from the water depths modelled using a single, fixed Manning's n coefficient. Assessment was performed by calculating the ration between water depth computed in simulation VBSRF and the other simulations.

3.2.4.2.3 Central island

In the centre island scenario, discharges were instead of 14, 40, 70 m³/s and did yield all the same, water depths of 1, 2 and 3 m respectively. Vegetation was placed on an almost central position inside a 147 m long channel (Figure 3-2), vegetation had a maximum width of 12 m and length of 15 m. This scenario was run to compare how the bed shear stress computed with the modified CL differs from the bed shear stress computed using a single, fixed Manning's n coefficient. Comparison was performed considering bed shear stress in the portion of the modelling domain stretching one length of the island in both the down and upstream direction. Comparison consisted in considering the rate of difference between simulation CISRF bed shear stress and the other simulations as well as a qualitative spatial arrangement of simulations' shear stress.

Table 3-2 Scenarios-simulations, flow resistance modelling solution and corresponding acronyms

Scenario	Flow resistance method	Parameters	Foliated	Simulation acronym
Vegetated bank	Equation 3-1	<i>Salix rubens</i>	Yes	VBSRF
			No	VBSRD
	Fixed Manning's n (s/m ^{1/3})	0.045	-	VBN0045
		0.062	-	VBN0062
0.098		-	VBN0098	
Central island	Equation 1	<i>Salix rubens</i>	Yes	CISRF
			No	CISRD
	Fixed Manning's n (s/m ^{1/3})	0.045	-	CIN0045
		0.062	-	CIN0062
		0.098	-	CIN0098
			-	

3.3 Results

3.3.1 Vegetation properties and relationship with height

Vegetation references areas measured through the photographic survey are reported in Figure 2-4 as a function of the relative height, defined as the ratio between HP height and vegetation height, which showed to be a better predictor than picture height. In a scenario where Equation 3-1 is used to model vegetation flow resistance, relative height corresponds to the ratio between patch or plant height and flow depth. Regression models were fitted to the data using a linear regression. For PAI and STAI the line was forced to return zero for a relative height equal to 0.2, corresponding to the observation that there were no leaves in the first 50 cm above the ground. For FAI the line was forced to pass through the origin.

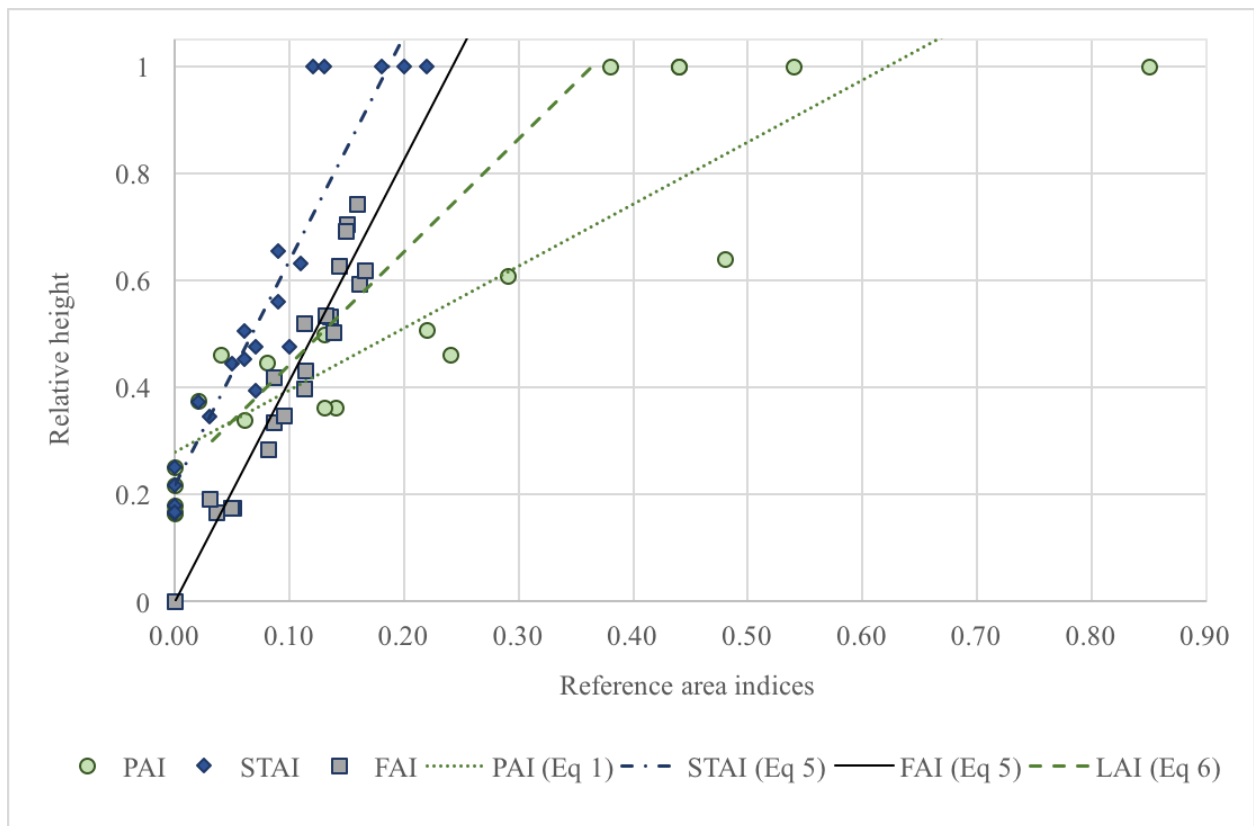


Figure 3-3 Measured values of PAI, STAI and FAI, and interpolation lines, as a function of the relative height

Table 3-3 Regression equations and LAI derived equation relating relative height and reference areas. Note that LAI equation is yield from Eq. 4 and 5 and thus does not have an R².

Reference area	Regression equation	R ²	
PAI	$y = 0.6648 x - 0.133$	0.75	Equation 3-6
STAI	$y = 0.219 x - 0.0438$	0.96	Equation 3-7
FAI	$y = 0.2395 x$	0.92	Equation 3-8
LAI	$y = 0.4458x - 0.0892$		Equation 3-9

Equation 3-9 describes LAI vertical distribution and is yield by algebraic difference between PAI and STAI regression equations. In Equation 3-1, LAI is assumed equal to 0 if the relative flow depth is lower than 0.2. At the same time, for flow depths higher than vegetation (relative height >1), LAI and FAI must be assumed as the maximum achievable value. FAI for one of the plots was not processed because of poor quality of the image.

3.3.2 Flow resistance sensitivity

3.3.2.1 Empirical parameters set and foliation

The empirical parameters set in Table 3-1 show a certain degree of variability and this is reflected in the variability of friction factors values predicted (data series drawn with markers in Figure 3-4) using Equation 3-1 fed by LAI and FAI from Equation 3-8 and Equation 3-9 regression curves and flow velocities from published studies. Nevertheless, simulated friction factor values fall within the range of measured ones, thus indicating that the use Equation 3-8 and Equation 3-9 to compute reference areas can return realistic flow resistance values to be fed to Equation 3-1. Figure 3-4 shows also that, where species are present both as modelled, and measured, the two never quite fit. The reason is to be found in the different LAI-FAI ratio of the specimens used in the referenced studies and the ratio typical for the Mareta specimens.

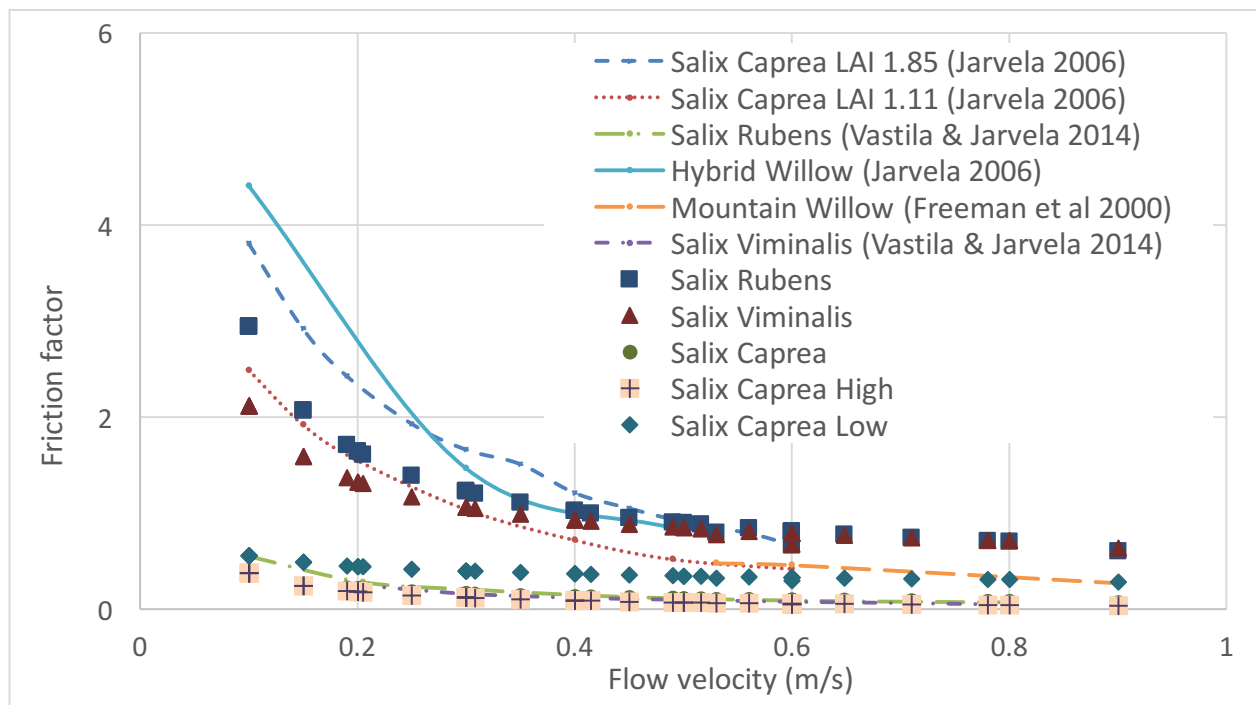


Figure 3-4 Friction factors modelled and yield from direct measures on fully submerged specimens. Modelled friction factors are computed assuming a complete submersion, using Equation 3-8 and Equation 3-9 to compute FAI and LAI and Equation 1 to compute friction factor. SC: Salix Caprea, SR: Salix Rubens, MW: Mountain Willow, HW: Hybrid Willow, SV: Salix Viminalis, SCL: Salix Caprea Low, SCH: Salix Caprea High. Image in colour available online

Figure 3-5 A-C shows friction factors for different submersion levels computed using Equation 3-1 applied to flow velocities of 0.25, 0.5 and 1 m/s in both foliated and defoliated conditions. From Figure 3-5 A-C is possible to understand which parameters are more suitable to model vegetation with different reconfiguration properties. The small differences in friction factor computed with the different velocities, when using parameters from Salix caprea, Salix caprea high and Salix caprea low, indicate that these parameters, at least with the reference areas derived from the field data, result in little reconfiguration thus reflecting the behaviour of less flexible species. For these less flexible species, friction is mainly due to stem for, even at the lowest velocity (Figure 3-5 A), there is almost no difference between friction calculated in foliated and defoliated conditions. On the other hand, friction factors computed using the parameters from Salix rubens and Salix viminalis exhibit large intra-velocities differences, suggesting that the parameters from these species allow to model plants with high reconfiguration capabilities. For these species, at least at the two lowest velocities (Figure 3-5 B and Figure 3-5 C), leaves contribution

to flow resistance is considerable as shown by the difference between the friction factors computed in foliated and defoliated conditions. However, also for this set of more flexible species, contribution of leaves to friction at 1 m/s velocity is relatively small.

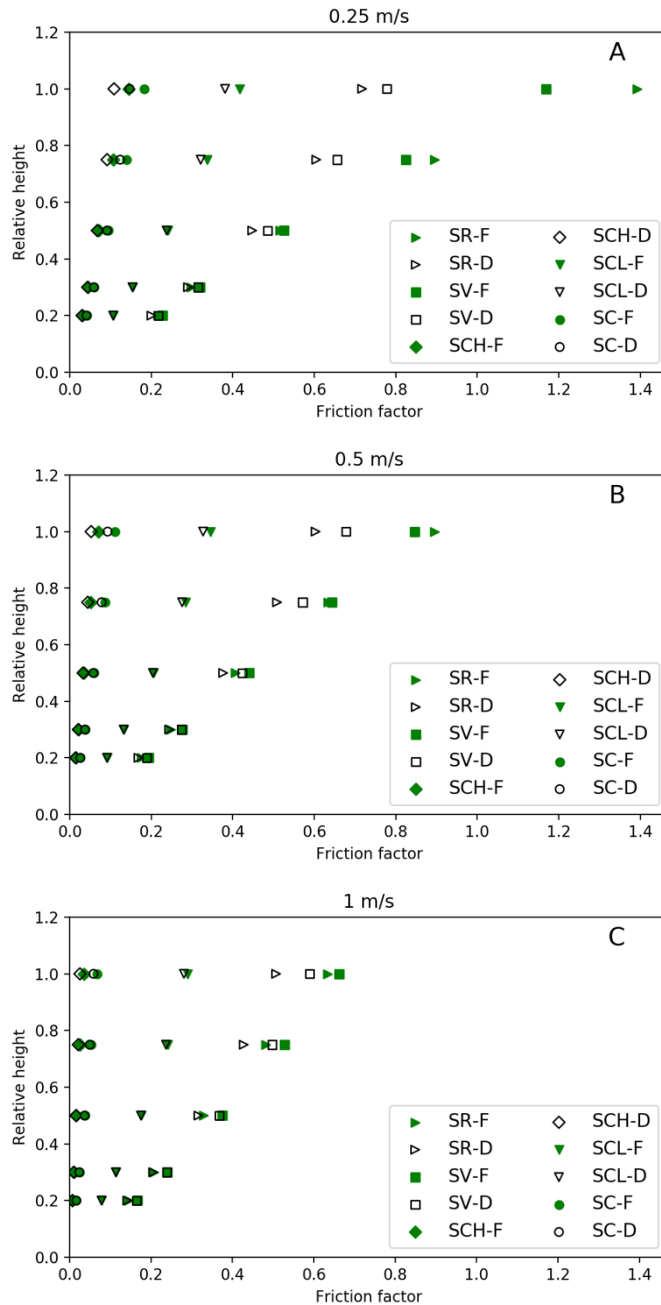


Figure 3-5 Friction factors calculated with Equation 1 assuming foliated and defoliated condition and different flow velocities. Legend entries ending with “F” represent Foliated conditions, while those ending with “D” Defoliated conditions. Empirical parameters acronyms: Salix Caprea (SC), Salix Caprea Low (SCL), Salix Caprea High (SCH), Salix Rubens (SR), Salix Viminalis (SV).

3.3.2.2 Reference areas

Figure 3-6 illustrates the sensitivity of the friction factor, calculated using Equation 3-1, to variations in LAI and FAI independently increased and decreased by 10%, 25% and 50%, using *Salix rubens* parameters and flow velocities of 0.25, 0.5 and 1 m/s. In Figure 3-6, the dotted line marks friction factors calculated using the regression equations reported in Table 3-3. For both FAI and LAI, deviations from unaltered friction are higher at low velocity. This is due to the higher flow resistance exerted by the plant at lower velocities. For flow velocities higher than 0.25 m/s (Figure 3-6 B and Figure 3-6 C), calculated friction factor is more sensitive to variation in FAI than LAI. This because the FAI reconfiguration parameter, in Equation 3-1, is less negative than the foliage reconfiguration parameter (for *Salix rubens*, $\chi_s = -0.25$ while $\chi_f = -1.21$) while at the same time, FAI has a higher drag coefficient (for *S. rubens*: $C_{D\chi,S} = 0.96$, $C_{D\chi,F} = 0.19$). This implies that FAI is the main source of flow resistance, unless LAI is much larger than FAI. Moreover, maintaining the same quantity of leaves for a higher quantity of stems reduces the capacity of the leaves to streamline the stems towards a more hydrodynamic configuration.

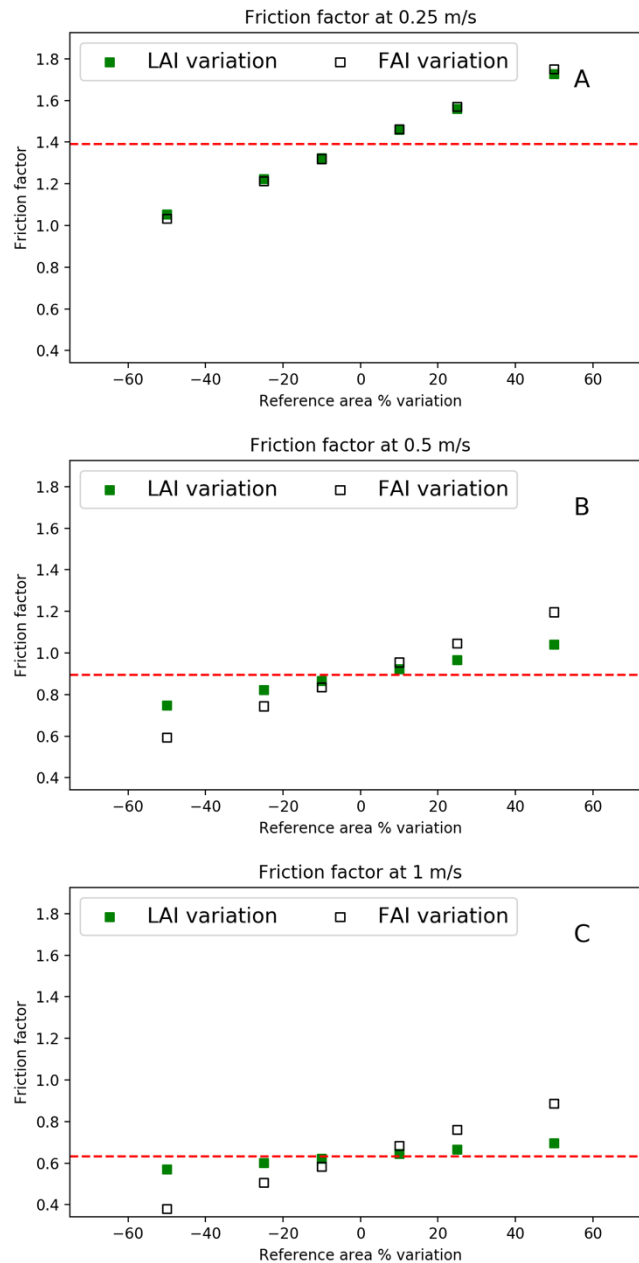


Figure 3-6 Sensitivity to LAI and FAI of Equation 1 applied with *Salix rubens* parameters. Red dotted line represents the friction factor value calculated without any variation

3.3.2.3 Flow resistance scenarios

This section reports the analysis of the scenarios modelled using Lisflood-FP, Equation 3-1 and *Salix rubens* parameters. The simulations modelled using variable

roughness in foliated conditions have been compared against the simulations in defoliated conditions and with fixed roughness using

3.3.2.3.1 Vegetated bank

Figure 3-7 displays the results of the vegetated bank scenario for the three reference discharges of 13, 40 and 80 m³/s corresponding to flow depths of approximately 1, 2 and 3 m, respectively. Panels A-1, B-1, and C-1 report the ratio between the water depth of the simulations VBN0045, VBN0062, VBN0098 (fixed roughness), and VBSRD (defoliated variable roughness) and the water depth of simulation VBSRF (foliated variable roughness). Here, values close to unity mean little difference and values lower than unity mean that water depth of simulation VBSRF was lower than water depths modelled in the other simulation. Differences are limited to 5% in all cases, showing that, in this configuration, the benefits of a detailed roughness parameterization are limited. Moreover, with *Salix rubens* parameters and the computed LAI distribution, the effect of seasonal variability (VBSRD run) is also minimal. The main advantage is the possibility to take into account the variation of the roughness for increasing flow depths and velocities. This is better shown in panels A-2, B-2, and C-2 that report the Manning's n values from the inlet to the outlet of the modelling domain (i.e. the x raster coordinate axis), for all the simulations. The best fixed value of Manning roughness increases from about 0.06

or the lower discharge Figure 3-7 A-2 and increases up to 0.12 for the higher discharge Figure 3-7 C-2.

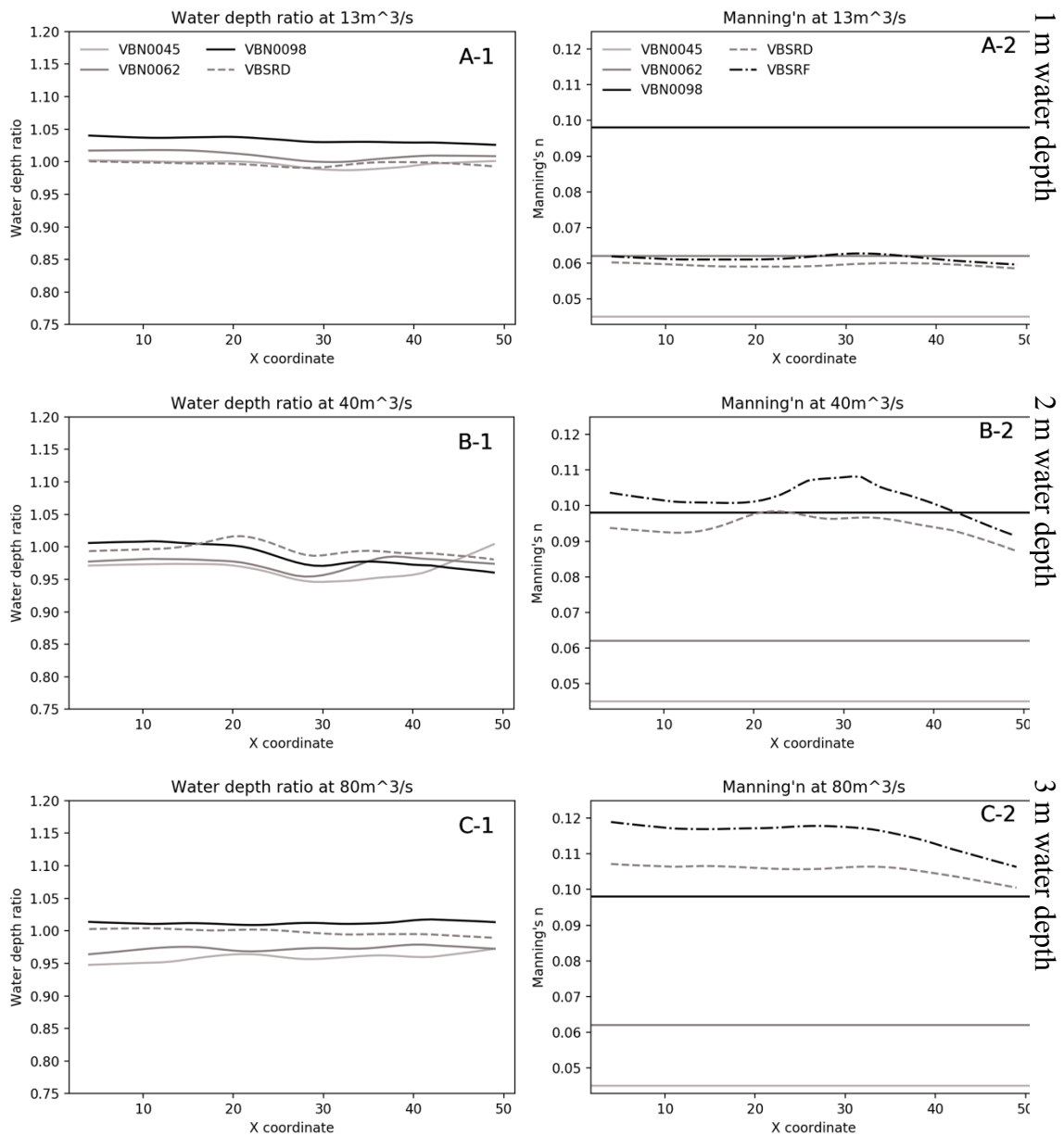


Figure 3-7 Chart in the left column depict the ratio between the water depth simulated using Equation 1 and the water depths using fixed Manning's coefficients. Charts in the left column are instead the value of Manning's n. In the charts of both columns, the x axis represents the x coordinate on the longitudinal dimension of the vegetated bank. Manning's n fixed values: 0.045 (VBN0045), 0.062 (VBN0062) and 0.098 (VBN0098). VBSRF: Salix Rubens Foliated, VBSRD: Salix Rubens Defoliated.

3.3.2.3.2 *Central island*

In this case, the runs were used to assess the effect of varying flow resistance on bed shear stress inside and around the vegetated patch. Figure 3-8 In these three panels, boxplots labels marked with the “.IS” suffix indicate shear stress distributions computed inside the area of the vegetated island, while those without suffix visualize the shear stress in the whole reach. The red dashed lines mark the identity between the bed shear stress values of simulation CISRF and the other simulations. Computed bed shear stress shows large differences, increasing at higher discharges and are particularly high inside the island. Shear stress is higher where vegetation resistance is lower, because lower resistance translates into a reduction in the amount of energy dissipated by vegetation and thus more energy is directed towards the bed. All simulations modelled with a fixed roughness present, at least for a flow rate, some large shear stress differences from CISRF. Also the simulation with defoliated conditions (CISRD) is significantly different from the foliated CISRF run (last two boxplots in Figure 3-8, A-1, B-1, C-1). Panels A-2, B-2, and C-2 plot the distribution of the Manning’s n values inside the vegetated patch for simulations CISRF and CISRD.

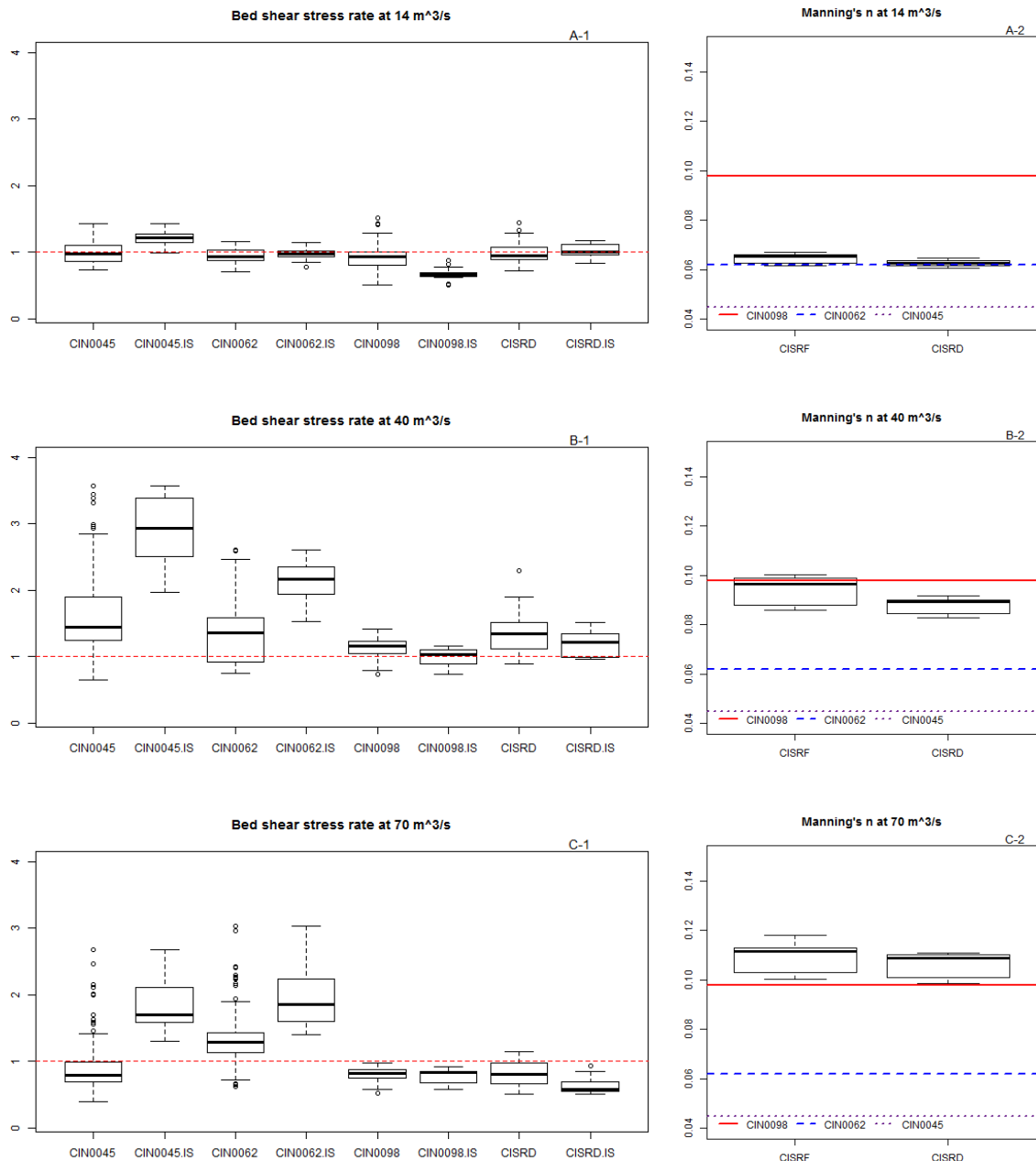


Figure 3-8 Left column contains boxplots of the rate between bed shear stress modelled with Equation 1, in foliated conditions and using SR parameters and the bed shear stress modelled in defoliated conditions and with a fixed roughness. X axis entries marked with “IS” represent the bed shear stress values inside the centre island, while those unmarked are yield from the bulk of shear stress values in the analysis reach. Right column contains the boxplots of the Manning’s n coefficients inside the centre island. Manning’s n fixed values: 0.045 (CIN0045), 0.062 (CIN0062) and 0.098 (CIN0098). CISRF: Salix Rubens Foliated, CISRD: Salix Rubens Defoliated.

Figure 3-9 provides visual context to the quantitative information in Figure 3-8 It shows the spatial distribution of bed shear stress in the different simulations for the 70 m³/s discharge (full plant submersion). The most evident aspects are the low shear stress inside the island and high shear stress at the island sides. However,

the magnitude of bed shear stress, as seen in Figure 3-8, largely differs between simulations CIN0045, CIN0062 (panels C and D), and the other three (CIN0098, CISRF and CISRD). In particular, the two runs with the spatially variable roughness (panels A and B) show larger differences between the vegetated patch and the sides, thus affecting the sediment dynamics.

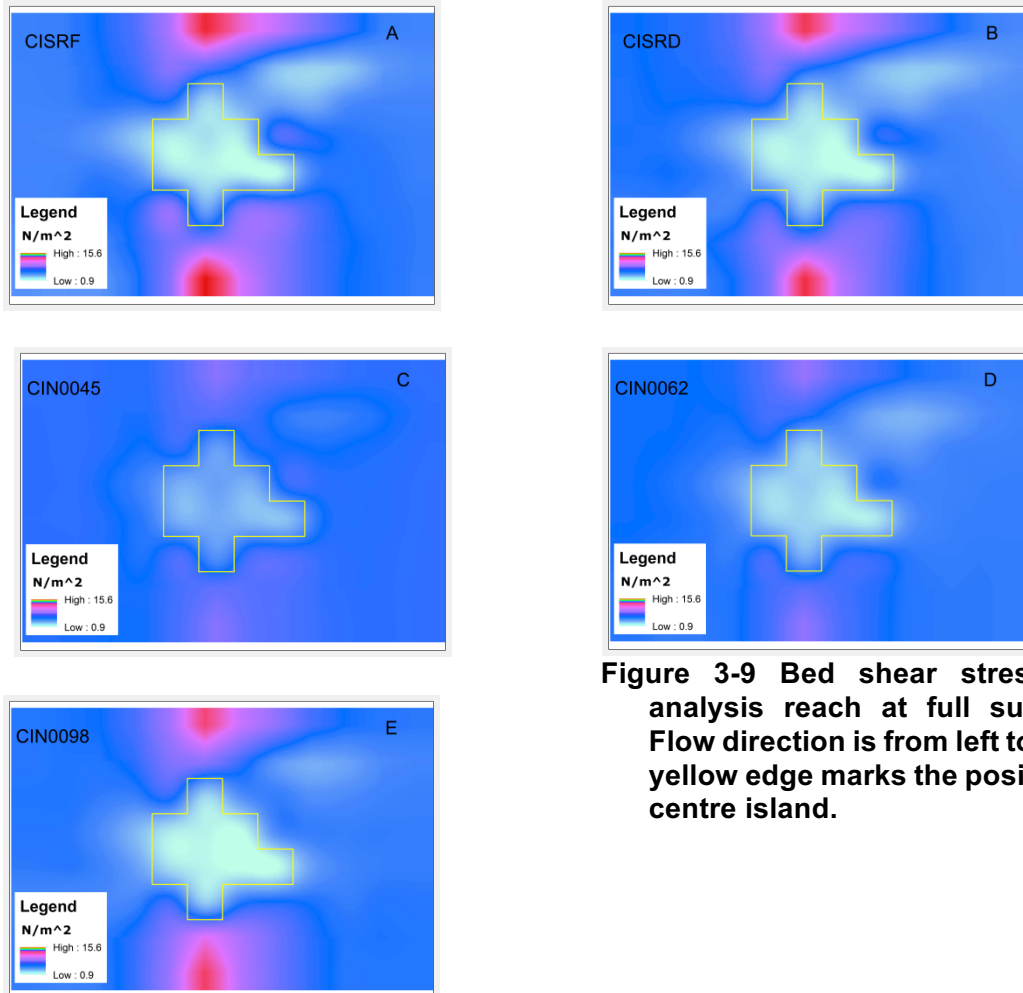


Figure 3-9 Bed shear stress in the analysis reach at full submersion. Flow direction is from left to right, the yellow edge marks the position of the centre island.

3.4 Discussion and conclusions

The use of digital hemispherical and frontal area photography to compute vegetation reference areas proved to be successful provided optimal collection protocols were applied. Digital hemispherical photography precision depends mostly on the quality of the images, which in turn depends on the exposure settings (Thimonier et al., 2010; Zhang et al., 2005). Frontal area photography can produce biased results when the photographed trees stand very close to the camera (≤ 20 cm) and depending on the manual thresholding applied by the operator in the post processing phase (Warmink, 2007). In respect to remote sensing techniques such as terrestrial

and airborne laser scanner, early studies on forest structure sampling using laser technology found that HP and laser scanning have a disagreement of about 8% for broadleaf species (Lovell et al., 2003). A lack of literature data on LAI and FAI vertical distribution for *Salix* species, makes it difficult to assess our field data against published data from other studies and, moreover, vegetation properties are site specific, further complicating comparison.

The configuration of vegetation at the field site on the Mareta River (dominated by *Salix* species of a relatively uniform size) meant it was relatively easy to characterize using the techniques presented in this paper. However, such a situation is rarely encountered along natural rivers, where periodic disturbances lead to the formation of patchier riverine landscapes and an assemblage of different species. Further developments of this approach should therefore consider variations in plant age and whether field measured properties can be upscaled to the reach scale by examining correlations between field measure properties and those computed using remotely sensed data (Forzieri et al., 2011; Manners et al., 2013). Dealing with multi-species composition is probably a more complex task that involves estimation of flow resistance by different assemblages. Given the paucity of theoretical studies on this matter, modelers may decide to consider only the dominant species, or attempting to detect whether LAI and FAI distributions show a statistically predictable behavior in a multi-species scenario. In this case, empirical parameter choice could resort to species average (Västilä and Järvelä (2017).

Empirical parameters reflect species-specific characteristics however it remains unclear how local growing conditions shape the values of such parameters. Results from “Empirical parameters set and foliation” suggest that other factors than species are relevant for the choice of an empirical parameter set over another. To this end, more lab measures on more species are certainly desirable. Nevertheless, field data results fed to Equation 3-1 show that reference areas sampled with this method can return feasible friction factors. Moreover, the wide range of friction factors that can be modeled using the existing parameter shall be considered an advantage for it allows covering a wide spectrum of plants flexural properties, from less to more flexible ones.

Using LAI and FAI distributions to model flow resistance with Equation 3-1 allows modelling a spatially variable and flow-dependent resistance with a single vegetation parameterization. Depth and velocity variations induced by a flood wave translate therefore into variations of vegetation-related flow resistance. Results of the modelling scenarios show that the use of this more accurate and physically-based representation of vegetation roughness can have important effects on the computed hydrodynamics. In particular, the first modelled scenario highlights that the main

effect is not related to the computation of the free surface level, which depends more on the reach-averaged parameters. The “Central island” scenario demonstrates that locally variable vegetation roughness significantly affects the flow velocity pattern and consequently the bed shear stress distribution, both within the vegetation patch and in the nearby channel. It is important to note that the vegetation spatial arrangements presented in this work are very simple and neglects effect of interacting vegetation patches. Such effects can considerably affect the flow pattern and associated deposition dynamics (de Lima et al., 2015) and therefore should be considered when modelling more complex cases.

Recently, numerical models combining hydromorphological processes and riparian vegetation interactions improved considerably (Solari et al., 2016), although vegetation processes and parameterization are often oversimplified (Camporeale et al., 2013). Our results suggest that approaches like the one proposed here should be considered for applications where prediction of sediment dynamics is a major focus. The research presented in this chapter provides both data and a cost-effective method to support the improved representation of vegetation-related flow resistance in hydrodynamic modelling.

Conclusion

The PhD effort was undertaken with the general purposes of: I) Improving the understanding of vegetation flexural properties on flow field and sediment transport dynamics; II) quantify fluvial disturbance thresholds leading to vegetation extinction or disruption; III) explore riparian vegetation dynamics and IV) explore Large Wood (LW) interaction with geomorphic processes. Following these purposes, the dissertation unfolded around three objectives: 1) A Quantitative review of riparian Salicaceae and fluvial processes mutual feedback aimed to contribute to the purpose of quantify fluvial disturbance thresholds leading to vegetation extinction or disruption. 2) Develop a field methodology to characterize riparian vegetation properties for vegetation flow resistance parameterization in hydraulic modelling, thus contributing to the understanding of vegetation flexural properties on flow field and sediment transport dynamics. 3) Develop a riparian vegetation dynamic model that simulates vegetation according to fluvial processes and that is able of providing feedback variables to the physical system. This latter objective was functional to the purposes of exploring riparian vegetation dynamics and LW interactions with geomorphic processes. Moreover, the model can be also used to test hypothesis on fluvial disturbances thresholds causing vegetation damage or fostering growth.

Considering the work carried on with greater detail, this dissertation presented an in-depth review of hydromorphological and vegetation processes interaction, a novel riparian vegetation-hydromorphodynamic model and a field technique for sampling vegetation properties to be used as input parameters in vegetation flow resistance equations. The review did not seek to simply describe the relationships entwining riparian vegetation and hydrogeomorphological processes but most of all to draw, from the large array of consulted studies, a set of thresholds that determine plants' responses to physical drivers. The review highlighted how several processes and associated physical threshold (e.g. plant mortality induced by burial) received far less attention than others (e.g. seeds germination dependence on water table depth) and that typical riparian species are more studied in Northern America than Europe and Asia. Moreover, the review presents also a novel schema of relevant physical habitat drivers, associated thresholds and timescales that yield an effect on riparian Salicaceae. Being the review a collection of research results, it provides a useful database for the parameterization of simulation models. Furthermore, it highlights research priorities while the schema of relevant physical habitat drivers, associated

thresholds and timescales, can find its application in river-management oriented domains, for example for qualitative assessment of relevant flow-dependent variables effects on riparian Salicaceae. Notions and concepts summarized in the review provided the theoretical basis and parameterization for the dynamic simulation model presented in the second chapter. This novel tool mimics the most important vegetation-hydrogeomorphology processes and feedback and although it incorporates several features somehow present in models proposed by other authors, it represents a step forward in riparian system modelling for it bears a set of innovative solutions. For example, it uses fuzzy logic to model vegetation responses and feedback and includes a LW lifecycle routine. The use of fuzzy logic is particularly suited in context where process understanding is sound but physical thresholds are ill defined. As highlighted by the review, riparian systems enlist among these contexts and although the use of fuzzy logic is not completely novel in riparian modelling and ecological modelling in general, thus far fuzzy logic has never been so extensively adopted for riparian systems or for their dynamic modelling. LW reproductive strategy is instead relevant in large, unconfined and frequently disturbed river systems where seeds' establishment is complicated by active sediment dynamics. The capabilities of the model to consistently replicate riparian systems expected behaviour were tested by means of simulated scenarios that proved, for example how modelled vegetation growth and spatial arrangement responds to the hydrological and disturbance regimes, the feedback of vegetation to erosion and sedimentation processes and how LW is recruited and established on typical locations consistent with field observations. Such capabilities are due to the large number of processes and feedback included in the model, this makes it a suitable research tool to test processes hypothesis or, within a river management context, a decision support tool to explore the outcome of different management options. Nevertheless, such rich representation of riparian systems results in a considerable wealth of parameters. In a real-world scenario though, one shall remind that not all of them might be equally important for a specific case. For example, flood duration physiological stress is likely negligible in high energy Alpine rivers where flood retention time is low, in such case, sedimentation and erosion are likely the main vegetation disruption causes. Conversely in a low land river, these latter might not be of essence while flood duration has a larger influence on vegetation mortality. Following these considerations, one could simply focus on the most relevant parameters for a specific case and exclude the drivers having less importance by assigning no-effect fuzzy decision rules (i.e. rules whose outcome do not change the state variables of the systems). As it is now, the model is set to work for only one ligneous species/generic tree, although for Alpine rivers this might represent an

acceptable simplification, for less energetic streams this might limit the model applicability. For such reason one of the future upgrades of the model will be the inclusion of other species, also with herbaceous aspect. The source code of the model is designed for scalability and already bears the slots for such upgrade. A further simplification introduced by the model is the use of a static flow vegetation flow resistance. Currently, vegetation flow resistance is estimated considering vegetation age, density and season (i.e. presence or absence of leaves). The results from the third chapter highlighted how neglecting the stage-dependent nature of vegetation flow resistance leads to inaccuracies in the calculation of the flow field velocities and thus on sediment transport dynamics. Furthermore, one of the test cases used to validate the model showed poor performances in predicting fine sediment accumulation inside vegetated patches. Such poor performance could be due to the sediment input set as model input or the over-simplification of the flow resistance estimation. Such inconsistency should be investigated in future studies. At the same time, a further upgrade of the model could be therefore the inclusion of the experience learned from chapter three. In this latter chapter, a novel field technique for measurements of vegetation physical properties was presented. The technique measures Leaf Area Index (LAI) and Stem Area Index (STAI). The former is defined as the total leaf area per unit area while the latter is defined as the total frontal area of the ligneous parts per unit area. These two plants' properties can be used in a set of physically based vegetation flow resistance equations recently proposed by different authors. These equations have the advantage of considering flow stage, plants foliation level and species-specific flexibility. In the second chapter, one of these equations (Västilä and Järvelä, 2014) was implemented in an hydraulic model to test how the use of such solution affects flow stage and bottom shear stress, thus revealing if the effort required to measure plant properties is justified by improvements in the modelled hydraulic variables. Improvements were judged by comparing hydraulic variables simulated with the physically based equation, with hydraulic variables simulated using typical fixed vegetation flow resistance coefficients. The modelling results highlighted how the use of physically based flow resistance equations that use LAI and STAI as input parameters have negligible effects on flow depth estimation while larger effects were observed for the bottom shear stress.

Ultimately the work described in three chapters provided a firm state of the art overview, suggested future research topics and provided novel tools that can be used in both real-world and scientific domains. The three chapters represent an interconnected and linear research project whose outcomes, although susceptible of

improvements and updates, we hope will represent a contribution to river science and management.

Bibliography

- Abbe, T., Montgomery, D., 2003. Patterns and processes of wood debris accumulation in the Queets river basin, Washington. *Geomorphology* 51, 81–107. doi:10.1016/S0169-555X(02)00326-4
- Aberle, J., Järvelä, J., 2013. Flow resistance of emergent rigid and flexible floodplain vegetation. *J. Hydraul. Res.* 51, 33–45. doi:10.1080/00221686.2012.754795
- Abernethy, B., Rutherford, I.D., 2000. The effect of riparian tree roots on the mass-stability of riverbanks. *Earth Surf. Process. Landforms* 25, 921–937. doi:10.1002/1096-9837(200008)25:9<921::AID-ESP93>3.0.CO;2-7
- Abernethy, B., Rutherford, I.D., Collison, A.J.C., 2001. The distribution and strength of riparian tree roots in relation to riverbank reinforcement. *Hydrol. Process.* 15, 63–79. doi:10.1002/hyp.152
- Ahmed, F., Rajaratnam, N., 1998. Flow around Bridge Piers. *J. Hydraul. Eng.* 124, 288–300. doi:10.1061/(ASCE)0733-9429(1998)124:3(288)
- Amlin, N.A., Rood, S.B., 2001. Inundation Tolerance of Riparian Willows and Cottonwoods. *J. Am. Water Resour. Assoc.* 37, 1709–1720.
- Amlin, N.M., Rood, S.B., 2003. Drought stress and recovery of riparian cottonwoods due to water table alteration along Willow Creek, Alberta. *Trees-Structure Funct.* 17, 351–358. doi:10.1007/s00468-003-0245-3
- Amlin, N.M., Rood, S.B., 2002. Comparative tolerances of riparian willows and cottonwoods to water-table decline. *Wetlands* 22, 338–346. doi:10.1672/0277-5212(2002)022[0338:CTORWA]2.0.CO;2

Anderson, B.G., Rutherford, I.D., Western, A.W., 2006. An analysis of the influence of riparian vegetation on the propagation of flood waves. *Environ. Model. Softw.* 21, 1290–1296. doi:10.1016/j.envsoft.2005.04.027

Antonarakis, A.S., Richards, K.S., Brasington, J., Bithell, M., 2009. Leafless roughness of complex tree morphology using terrestrial lidar. *Water Resour. Res.* 45, 1–14. doi:10.1029/2008WR007666

Antonarakis, A.S., Richards, K.S., Brasington, J., Bithell, M., Muller, E., 2008. Retrieval of vegetative fluid resistance terms for rigid stems using airborne lidar. *J. Geophys. Res. Biogeosciences* 113, 1–16. doi:10.1029/2007JG000543

Antonarakis, A.S., Richards, K.S., Brasington, J., Muller, E., 2010. Determining leaf area index and leafy tree roughness using terrestrial laser scanning. *Water Resour. Res.* 46, n/a-n/a. doi:10.1029/2009WR008318

Armstrong, W., Braendle, R., Jackson, M.B., 1994. Mechanisms of flood tolerance in plants. *Acta Bot. Neerl.* 43, 307–358.

Arcott, D.B., Tockner, K., van der Nat, D., Ward, J. V., 2002. Aquatic Habitat Dynamics along a Braided Alpine River Ecosystem (Tagliamento River, Northeast Italy). *Ecosystems* 5, 0802–0814. doi:10.1007/s10021-002-0192-7

Asaeda, T., Gomes, P.I.A., Takeda, E., 2010. Spatial and Temporal Tree Colonization in a Midstream Sediment Bar and the Mechanism Governing Tree Mortality During a Flood Event. *River Res. Appl.* 26, 960–976. doi:10.1002/rra

Asaeda, T., Rashid, M.H., 2012. The impacts of sediment released from dams on downstream sediment bar vegetation. *J. Hydrol.* 430–431, 25–38. doi:10.1016/j.jhydrol.2012.01.040

- Auble, G.T., Scott, M.L., 1997. Fluvial Disturbance Patches And Cottonwood Recruitment. *Wetlands* 18, 546–556.
- Azami, K., Suzuki, H., Toki, S., 2004. Changes in riparian vegetation communities below a large dam in a monsoonal region: Futase Dam, Japan. *River Res. Appl.* 20, 549–563. doi:10.1002/rra.763
- Bankhead, N.L., Thomas, R.E., Simon, A., 2017. A combined field, laboratory and numerical study of the forces applied to, and the potential for removal of, bar top vegetation in a braided river. *Earth Surf. Process. Landforms* 42, 439–459. doi:10.1002/esp.3997
- Baptist, M.J., 2005. Modelling floodplain biogeomorphology. Delft University of Technology. doi:ISBN 90-407-2582-9
- Baptist, M.J., Babovic, V., Uthurburu, J.R., Keijzer, M., Uittenbogaard, R.E., Mynett, A., Verwey, A., Hoffmann, M.R., 2009. On inducing equations for vegetation resistance. *J. Hydraul. Res.* 45, 435–450. doi:10.1080/00221686.2007.9521778
- Barros, L.C., Bassanezi, R.C., Tonelli, P. a., 2000. Fuzzy modelling in population dynamics. *Ecol. Modell.* 128, 27–33. doi:10.1016/S0304-3800(99)00223-9
- Barsoum, N., 2002. Relative contributions of sexual and asexual regeneration strategies in *Populus nigra* and *Salix alba* during the first years of establishment on a braided gravel bed river. *Evol. Ecol.* 15, 255–279.
- Bates, P.D., Horritt, M.S., Fewtrell, T.J., 2010. A simple inertial formulation of the shallow water equations for efficient two-dimensional flood inundation modelling. *J. Hydrol.* 387, 33–45. doi:10.1016/j.jhydrol.2010.03.027
- Belletti, B., Dufour, S., Piégay, H., 2013. What Is The Relative Effect Of Space And Time To Explain The Braided River Width And Island Patterns At A Regional

Scale? River Res. Appl. 1535–1467. doi:10.1002/rra

Bendix, J., 1999. Stream Power Influence on Southern California Riparian Vegetation. *J. Veg. Sci.* 10, 243–252.

Bendix, J., Hupp, C.R., 2000. Hydrological and geomorphological impacts on riparian plant communities. *Hydrol. Process.* 14, 2977–2990.
doi:10.1002/1099-1085(200011/12)14:16/17<2977::AID-HYP130>3.0.CO;2-4

Benjankar, R., Egger, G., Jorde, K., Goodwin, P., Glenn, N.F., 2011. Dynamic floodplain vegetation model development for the Kootenai River, USA. *J. Environ. Manage.* 92, 3058–3070. doi:10.1016/j.jenvman.2011.07.017

Benjankar, R.M., Burke, M., Yager, E.M., Tonina, D., Egger, G.G., Rood, S.B., Merz, N., 2014. Development of a spatially-distributed hydroecological model to simulate cottonwood seedling recruitment along rivers. *J. Environ. Manage.* 145, 277–288. doi:10.1016/j.jenvman.2014.06.027

Berg, K.J., Samuelson, G.M., Willms, C.R., Pearce, D.W., Rood, S.B., 2007. Consistent growth of black cottonwoods despite temperature variation across elevational ecoregions in the Rocky Mountains. *Trees* 21, 161–169.
doi:10.1007/s00468-006-0108-9

Bertoldi, W., Drake, N. a., Gurnell, A.M., 2011. Interactions between river flows and colonizing vegetation on a braided river: exploring spatial and temporal dynamics in riparian vegetation cover using satellite data. *Earth Surf. Process. Landforms* 36, 1474–1486. doi:10.1002/esp.2166

Bertoldi, W., Gurnell, A.M., Welber, M., 2013. Wood recruitment and retention: The fate of eroded trees on a braided river explored using a combination of field and remotely-sensed data sources. *Geomorphology* 180–181, 146–155.
doi:10.1016/j.geomorph.2012.10.003

- Bertoldi, W., Siviglia, A., Tettamanti, S., Toffolon, M., Vetsch, D., Francalanci, S., 2014. Modeling vegetation controls on fluvial morphological trajectories. *Geophys. Res. Lett.* 41, 7167–7175. doi:10.1002/2014GL061666
- Blom, C.W.P.M., Voeselek, L. a C.J., 1996. Flooding: The survival strategies of plants. *Trends Ecol. Evol.* 11, 290–295. doi:10.1016/0169-5347(96)10034-3
- Bornette, G., Amoros, C., 1996. Disturbance Regimes and Vegetation Dynamics: Role of Floods in Riverine Wetlands. *Jouranl Veg. Sci.* 7, 615–622.
- Botkin, D.B., Janak, J.F., Wallis, J.R., 1972. Some Ecological Consequences of a Computer Model of Forest Growth. *J. Ecol.* 60, 849–872. doi:10.2307/2258570
- Braatne, J.H., Jamieson, R., Gill, M., Rood, S.B., 2007. Instream flows and the decline of riparian cottonwoods along the Yakima river, Washington , USA. *River Res. Appl.* 267, 247–267. doi:10.1002/rra
- Braatne, J.H., Rood, S.B., Heilman, P.E., 1996. Life history, ecology, and conservation of riparian cottonwoods in North America, in: Stettler, R.F., Bradshaw, H.D., Heilman, P.E., Hinckley, T.M. (Eds.), *Biology of Populus and Its Implications for Management and Conservation*. NRC Research Press, Ottawa, pp. 57–86.
- Bratkovich, S., Burban, L., Katovich, S., Locey, C., Pokorny, J., Wiest, R., 1993. Flooding and its effects on trees, in: *Forest Resources Management and Forest Health Protection*, USDA Forest Service. Northeastern Area State and Private Forestry, St. Paul, MN.
- Busch, D.E., Smith, S.D., 1995. Mechanisms associated with decline of woody species in riparian ecosystems of the southwestern U.S. *Ecol. Monogr.* 65, 347–370. doi:10.2307/2937064
- Butler, J.J., Kluitenberg, G.J., Whittemore, D.O., Loheide, S.P., Jin, W., Billinger,

- M.A., Zhan, X., 2007. A field investigation of phreatophyte-induced fluctuations in the water table. *Water Resour. Res.* 43, 1–12. doi:10.1029/2005WR004627
- Bywater-Reyes, S., Wilcox, A.C., Stella, J.C., Lightbody, A.F., 2015. Flow and scour constraints of pioneer woody seedlings. *Water Resour. Res.* 51, 1–17. doi:10.1002/2014WR016259
- Camporeale, C., Perucca, E., Ridolfi, L., Gurnell, A.M., 2013. Modeling The Interactions Between River Morphodynamics And Riparian Vegetation. *Rev. Geophys.* 51, 1–36. doi:10.1002/rog.20014.1.INTRODUCTION
- Cao, F.L., Conner, W.H., 1999. Selection of flood-tolerant *Populus deltoides* clones for reforestation projects in China. *For. Ecol. Manage.* 117, 211–220. doi:10.1016/S0378-1127(98)00465-4
- Chen, S.C., Chan, H.C., Li, Y.H., 2012a. Observations on flow and local scour around submerged flexible vegetation. *Adv. Water Resour.* 43, 28–37. doi:10.1016/j.advwatres.2012.03.017
- Chen, S.C., Kuo, Y.M., Yen, H.C., 2012b. Effects of submerged flexible vegetation and solid structure bars on channel bed scour. *Int. J. Sediment Res.* 27, 323–336. doi:10.1016/S1001-6279(12)60038-9
- Chianucci, F., Cutini, A., 2012. Digital hemispherical photography for estimating forest canopy properties: Current controversies and opportunities. *IForest* 5, 290–295. doi:10.3832/ifor0775-005
- Chow, V. Te, 1959. *Open-channel hydraulics*. McGraw-Hill B. Co. 728. doi:ISBN 07-010776-9
- Church, M., 2002. Geomorphic thresholds in riverine landscapes. *Freshw. Biol.* 47, 541–557. doi:10.1046/j.1365-2427.2002.00919.x

- Clements, F.E., 1916. Plant succession an analysis of the development of vegetation, Library. Carnegie Institution of Washington, Washington.
- Cooper, D.J., D'Amico, D.R., Scott, M.L., 2003. Physiological and morphological response patterns of *Populus deltoides* to alluvial groundwater pumping. *Environ. Manage.* 31, 215–226. doi:10.1007/s00267-002-2808-2
- Cooper, D.J., Merritt, D.M., Andersen, D.C., Chimner, R. a., 1999. Factors controlling the establishment of Fremont cottonwood seedlings on the Upper Green River, USA. *Regul. Rivers Res. Manag.* 15, 419–440. doi:10.1002/(SICI)1099-1646(199909/10)15:5<419::AID-RRR555>3.0.CO;2-Y
- Coppin, N.J., Richards, I.G., 2007. Use of vegetation in civil engineering. CIRIA. LONDON.
- Corenblit, D., Baas, A.C.W., Bornette, G., Darrozes, J., Delmotte, S., Francis, R.A., Gurnell, A.M., Julien, F., Naiman, R.J., Steiger, J., 2011. Feedbacks between geomorphology and biota controlling Earth surface processes and landforms: A review of foundation concepts and current understandings. *Earth-Science Rev.* 106, 307–331. doi:10.1016/j.earscirev.2011.03.002
- Corenblit, D., Steiger, J., González, E., Gurnell, a. M., Charrier, G., Darrozes, J., Dousseau, J., Julien, F., Lambs, L., Larrue, S., Roussel, E., Vautier, F., Voltaire, O., 2014. The biogeomorphological life cycle of poplars during the fluvial biogeomorphological succession: a special focus on *Populus nigra* L. *Earth Surf. Process. Landforms* 39, 546–563. doi:10.1002/esp.3515
- Corenblit, D., Steiger, J., Gurnell, A.M., Tabacchi, E., Roques, L., 2009. Control of sediment dynamics by vegetation as a key function driving biogeomorphic succession within fluvial corridors. *Earth Surf. Landforms* 34, 1790–1810. doi:10.1002/esp
- Corenblit, D., Steiger, J., Tabacchi, E., 2010. Biogeomorphologic succession dynamics in a Mediterranean river system. *Ecography (Cop.)*. 33, 1136–1148.

doi:10.1111/j.1600-0587.2010.05894.x

Corenblit, D., Tabacchi, E., Steiger, J., Gurnell, A.M., 2007. Reciprocal interactions and adjustments between fluvial landforms and vegetation dynamics in river corridors: A review of complementary approaches. *Earth-Science Rev.* 84, 56–86. doi:10.1016/j.earscirev.2007.05.004

Coulthard, T.J., 2017. CAESAR-Lisflood 1.9b.
doi:http://doi.org/10.5281/zenodo.321820

Coulthard, T.J., 2005. Effects of vegetation on braided stream pattern and dynamics. *Water Resour. Res.* 41, n/a-n/a. doi:10.1029/2004WR003201

Coulthard, T.J., Macklin, M.G., Kirkby, M.J., 2002. A cellular model of Holocene upland river basin and alluvial fan evolution. *Earth Surf. Process. Landforms* 27, 269–288. doi:10.1002/esp.318

Coulthard, T.J., Neal, J.C., Bates, P.D., Ramirez, J., de Almeida, G. a. M., Hancock, G.R., 2013. Integrating the LISFLOOD-FP 2D hydrodynamic model with the CAESAR model: implications for modelling landscape evolution. *Earth Surf. Process. Landforms* 38, 1897–1906. doi:10.1002/esp.3478

Cremer, K.W., 2003. Introduced willows can become invasive pests in Australia. *Biodiversity* 4, 17–24. doi:10.1080/14888386.2003.9712705

Crosato, A., Saleh, M.S., 2011. Numerical study on the effects of floodplain vegetation on river planform style. *Earth Surf. Process. Landforms* 36, 711–720. doi:10.1002/esp.2088

Davies, N.S., Gibling, M.R., 2010. Cambrian to Devonian evolution of alluvial systems: The sedimentological impact of the earliest land plants. *Earth-Science Rev.* 98, 171–200. doi:10.1016/j.earscirev.2009.11.002

- De Baets, S., Poesen, J., 2010. Empirical models for predicting the erosion-reducing effects of plant roots during concentrated flow erosion. *Geomorphology* 118, 425–432. doi:10.1016/j.geomorph.2010.02.011
- De Baets, S., Poesen, J., Gysels, G., Knapen, a., 2006. Effects of grass roots on the erodibility of topsoils during concentrated flow. *Geomorphology* 76, 54–67. doi:10.1016/j.geomorph.2005.10.002
- de Lima, P.H.S., Janzen, J.G., Nepf, H.M., 2015. Flow patterns around two neighboring patches of emergent vegetation and possible implications for deposition and vegetation growth. *Environ. Fluid Mech.* 15, 881–898. doi:10.1007/s10652-015-9395-2
- Dixon, M.D., Turner, M.G., 2006. Simulated Recruitment Of Riparian Trees And Shrubs Under Natural And Regulated Flow Regimes On The Wisconsin River, USA. *River Res. Appl.* 22, 1057–1083.
- Dolores Bejarano, M., Sordo-Ward, Á., 2011. Riparian woodland encroachment following flow regulation: a comparative study of Mediterranean and Boreal streams. *Knowl. Manag. Aquat. Ecosyst.* 20. doi:10.1051/kmae/2011059
- Du, K., Xu, L., Wu, H., Tu, B., Zheng, B., 2012. Ecophysiological and morphological adaption to soil flooding of two poplar clones differing in flood-tolerance. *Flora Morphol. Distrib. Funct. Ecol. Plants* 207, 96–106. doi:10.1016/j.flora.2011.11.002
- Dudgeon, D., Arthington, A.H., Gessner, M.O., Kawabata, Z.-I., Knowler, D.J., Lévêque, C., Naiman, R.J., Prieur-Richard, A.-H., Soto, D., Stiassny, M.L.J., Sullivan, C. a, 2006. Freshwater biodiversity: importance, threats, status and conservation challenges. *Biol. Rev. Camb. Philos. Soc.* 81, 163–82. doi:10.1017/S1464793105006950
- Edmaier, K., Burlando, P., Perona, P., 2011. Mechanisms of vegetation uprooting by flow in alluvial non-cohesive sediment. *Hydrol. Earth Syst. Sci.* 15, 1615–

1627. doi:10.5194/hess-15-1615-2011

Egger, G., Politti, E., Garófano-Gómez, V., Blamauer, B., Ferreira, M.T., Rivaes, R., Benjankar, R., Habersack, H., 2013. Embodying interactions of riparian vegetation and fluvial processes into a dynamic floodplain model: concepts and applications, in: Maddock, I., Harby, A., Kemp, P., Wood, P. (Eds.), *Ecohydraulics: An Integrated Approach*. John Wiley & Sons Ltd, Chichester, UK, pp. 407–427. doi:10.1002/9781118526576

Egger, G., Politti, E., Lautsch, E., Benjankar, R., Gill, K.M., Rood, S.B., 2015. Floodplain forest succession reveals fluvial processes: A hydrogeomorphic model for temperate riparian woodlands. *J. Environ. Manage.* 161, 72–82. doi:10.1016/j.jenvman.2015.06.018

Egger, G.G., Politti, E., Lautsch, E., Benjankar, R.M., Rood, S.B., Benjankar, R.M., Rood, S.B., Benjankar, R.M., Rood, S.B., 2017. Time and Intensity Weighted Indices Of Fluvial Processes: A Case Study From The Kootenai River, USA. *River Res. Appl.* 33, 224–232. doi:10.1002/rra.2997

Einstein, H.A., 1950. The Bed-Load Function for Sediment Transportation in Open Channel Flows. *Soil Conserv. Serv.* 1–31.

Ennos, A.R., 1990. The Anchorage of Leek Seedlings: The Effect of Root Length and Soil Strength. *Ann. Bot.* 65, 409–416.

European Parliament, C., 2012. *A Blueprint to Safeguard Europe's Water Resources*.

European Parliament, C., 2000. Directive 2000/60/EC of the European Parliament and of the Council of 23 October 2000 establishing a framework for Community action in the field of water policy.

European Parliament, C., 1992. Council Directive 92/43/EEC on the Conservation

of natural habitats and of wild fauna and flora.

- Fathi-Maghadam, Kouwen, N., 1997. Nonrigid, nonsubmerged, vegetative roughness on floodplains. *J. Hydraul. Eng.* 123, 51–57. doi:doi:
[http://dx.doi.org/10.1061/\(ASCE\)0733-9429\(1997\)123:1\(51\)](http://dx.doi.org/10.1061/(ASCE)0733-9429(1997)123:1(51))
- Fierke, M.K., Kauffman, J.B., 2005. Structural dynamics of riparian forests along a black cottonwood successional gradient. *For. Ecol. Manage.* 215, 149–162.
doi:10.1016/j.foreco.2005.06.014
- Formann, E., Hauer, C., Egger, G., Habersack, H., Hauer, C., Habersack, H., 2014. The Dynamic Disturbance Regime Approach In River Restoration: Concept Development And Application. *Landsc. Ecol. Eng.* 10, 323–337.
doi:10.1007/s11355-013-0228-5
- Forzieri, G., Guarnieri, L., Vivoni, E.R., Castelli, F., Preti, F., 2011. Spectral-ALS Data Fusion For Different Roughness Parametrizations Of Forested Floodplains. *River Res. Appl.* 27, 826–840. doi:10.1002/rra.1398
- Francis, R.A., Gurnell, A.M., Petts, G.E., 2004. The survival and growth response of *Populus nigra* fragments to differing hydrogeomorphological conditions. *Hydrol. Sci. Pract.* 21st Century II, 80–89.
- Francis, R.A., Gurnell, A.M., Petts, G.E., Edwards, P.J., 2006. Riparian tree establishment on gravel bars: interactions between plant growth strategy and the physical environment. *Braided Rivers* 361–380.
doi:10.1002/9781444304374.ch18
- Francis, R. a., Gurnell, A.M., 2006. Initial establishment of vegetative fragments within the active zone of a braided gravel-bed river (River Tagliamento, NE Italy). *Wetlands* 26, 641–648. doi:10.1672/0277-5212(2006)26[641:IEOVFW]2.0.CO;2

Francis, R. a., Gurnell, A.M., Petts, G.E., Edwards, P.J., 2005. Survival and growth responses of *Populus nigra*, *Salix elaeagnos* and *Alnus incana* cuttings to varying levels of hydric stress. *For. Ecol. Manage.* 210, 291–301.
doi:10.1016/j.foreco.2005.02.045

Freeman, G.E., Rahmeyer, W.J., Copeland, R.R., 2000. Determination of Resistance Due to Shrubs and Woody Vegetation 62.

Friedman, J.M., Auble, G.T., 2000. Floods , Flood Control , and Bottomland Vegetation, in: Wohl, E. by E.E. (Ed.), *Inland Flood Hazards. Human, Riparian, and Aquatic Communities*. Cambridge University Press, pp. 219–237.
doi:http://dx.doi.org/10.1017/CBO9780511529412.009

Friedman, J.M., Auble, G.T., 1999. MORTALITY OF RIPARIAN BOX ELDER FROM SEDIMENT MOBILIZATION AND EXTENDED INUNDATION. *Regul. Rivers Res. Manag.* 476, 463–476.

Friedman, J.M., Auble, G.T., Andrews, E.D., Kittel, G., Madole, R.F., Griffin, E.R., Allred, T.M., 2006. Transverse and Longitudinal Variation in Woody Riparian Vegetation Along a Montane River. *West. North Am. Nat.* 66, 78–91.
doi:10.3398/1527-0904(2006)66[78:TALVIW]2.0.CO;2

Friedman, J.M., Osterkamp, W.R., Lewis, W.M.J., 1996. Channel Narrowing and Vegetation Development Following a Great Plains Flood. *Ecology* 77, 2167–2181.

Garcia-Arias, A., Francés, F., Andres-Domenech, I., Vallés, F., Garofano-Gomez, V., Martinez-capel, F., 2011. Modelling the spatial distribution and temporal dynamics of Mediterranean riparian vegetation in a reach of the Mijares River (Spain), in: *EUROMECH. Ecohydraulics: Linkages between Hydraulics, Morphodynamics and Ecological Processes in Rivers*.

García-Arias, A., Francés, F., Ferreira, T., Egger, G., Martínez-Capel, F., Garófano-Gómez, V., Andrés-Doménech, I., Politti, E., Rivaes, R., Rodríguez-

- González, P.M., 2013a. Implementing a dynamic riparian vegetation model in three European river systems. *Ecohydrology* 6, 635–651.
doi:10.1002/eco.1331
- García-Arias, A., Francés, F., Morales-de la Cruz, M., Real, J., Vallés-Morán, F., Garófano-Gómez, V., Martínez-Capel, F., 2013b. Riparian evapotranspiration modelling: model description and implementation for predicting vegetation spatial distribution in semi-arid environments. *Ecohydrology* 7, 659–677.
doi:10.1002/eco.1387
- Gardiner, B., Peltola, H., Kellomäki, S., 2000. Comparison of two models for predicting the critical wind speeds required to damage coniferous trees. *Ecol. Modell.* 129, 1–23. doi:10.1016/S0304-3800(00)00220-9
- Gibling, M.R., Davies, N.S., 2012. Palaeozoic landscapes shaped by plant evolution. *Nat. Geosci.* 5, 99–105. doi:10.1038/ngeo1376
- Girel, J., Pautou, G., 1997. The influence of sediment on vegetation structure, in: Haycock, N., Burt, T., Goulding, K., Pinay, G. (Eds.), *Buffer Zones: Their Processes and Potential in Water Protection*. Haycock Associated Limited, Harpenden, Hertfordshire, AL5 5LJ, UK, pp. 92–112.
- Glenz, C., Iorgulescu, I., Kienast, F., Schlaepfer, R., 2008. Modelling the impact of flooding stress on the growth performance of woody species using fuzzy logic. *Ecol. Modell.* 218, 18–28. doi:10.1016/j.ecolmodel.2008.06.008
- Glenz, C., Schlaepfer, R., Iorgulescu, I., Kienast, F., 2006. Flooding tolerance of Central European tree and shrub species. *For. Ecol. Manage.* 235, 1–13.
doi:10.1016/j.foreco.2006.05.065
- González, E., Comín, F.A., Muller, E., 2010. Seed dispersal, germination and early seedling establishment of *Populus alba* L. under simulated water table declines in different substrates. *Trees* 24, 151–163. doi:10.1007/s00468-009-0388-y

- Gorla, L., Signarbieux, C., Tuberg, P., Buttler, A., Perona, P., 2015. Transient response of *Salix* cuttings to changing water level regimes. *Water Resour. Res.* 51, 1758–1774. doi:10.1002/2014WR015543
- Gosselin, F.P., De Langre, E., 2011. Drag reduction by reconfiguration of a poroelastic system. *J. Fluids Struct.* 27, 1111–1123. doi:10.1016/j.jfluidstructs.2011.05.007
- Gran, K., Paola, C., 2001. Riparian vegetation controls on braided stream dynamics. *Water Resour. Res.* 37, 3275–3283. doi:10.1029/2000WR000203
- Grime, J.P., 2002. *Plant strategies and vegetation processes*, 2nd ed. John Wiley & Sons, Ltd, New York.
- Guilloy, H., González, E., Muller, E., Hughes, F.M.R., Barsoum, N., 2011. Abrupt Drops in Water Table Level Influence the Development of *Populus nigra* and *Salix alba* Seedlings of Different Ages. *Wetlands* 31, 1249–1261. doi:10.1007/s13157-011-0238-8
- Gurnell, A., Tockner, K., Edwards, P., Petts, G., 2005. Effects of deposited wood on biocomplexity of river corridors. *Front. Ecol. Environ.* 3, 377–382.
- Gurnell, A.M., 2016. Trees, wood and river morphodynamics : results from 15 years research on the Tagliamento River, Italy, in: Gilvear, D.J., Greenwood, M.T., Thoms, M.C., Wood, P.J. (Eds.), *River Science: Research and Management for the 21st Century*. John Wiley & Sons Ltd., Chichester, UK, pp. 132–155. doi:10.1002/9781118643525.ch7
- Gurnell, A.M., 2014. Plants as river system engineers. *Earth Surf. Process. Landforms* 39, 4–25. doi:10.1002/esp.3397
- Gurnell, A.M., Bertoldi, W., Corenblit, D., 2012. Changing river channels: The roles of hydrological processes, plants and pioneer fluvial landforms in humid

temperate, mixed load, gravel bed rivers. *Earth-Science Rev.* 111, 129–141.
doi:10.1016/j.earscirev.2011.11.005

Gurnell, A.M., Corenblit, D., García De Jalón, D., González Del Tánago, M., Grabowski, R.C., O'hare, M.T., Szewczyk, M., 2016. A Conceptual Model of Vegetation-Hydrogeomorphology Interactions within River Corridors. *River Res. Appl.* 32, 142–163. doi:10.1002/rra

Gurnell, A.M., Petts, G.E., Hannah, D.M., Smith, B.P., Edwards, P.J., Kollmann, J., Ward, J., Tockner, K., 2001. Riparian vegetation and island formation along the gravel-bed Fiume Tagliamento, Italy. *Earth Surf. Process. Landforms* 26, 31–62.

Gurnell, A.M., Petts, G.E., Hannah, D.M., Smith, B.P.G., Edwards, P.J., Kollmann, J., Ward, J. V., Tockner, K., 2000a. Wood storage within the active zone of a large European gravel- bed river. *Geomorphology* 34, 55–72.

Gurnell, A.M., Petts, G.E., Harris, N., Ward, J. V., Tockner, K., Edwards, P.J., Kollmann, J., 2000b. Large wood retention in river channels: The case of the Fiume Tagliamento, Italy. *Earth Surf. Process. Landforms* 25, 255–275.
doi:10.1002/(SICI)1096-9837(200003)25:3<255::AID-ESP56>3.0.CO;2-H

Gyssels, G., Poesen, J., 2003. The importance of plant root characteristics in controlling concentrated flow erosion rates. *Earth Surf. Process. Landforms* 28, 371–384. doi:10.1002/esp.447

Hansen, P.L., Pfister, R.D., Boggs, K., Cook, B.J., Joy, J., Hinckley, D.K., 1995. Classification and Management of Montanas Riparian and Wetland Sites. *Misc. Publ.* 54, 496.

Harner, M.J., Stanford, J.A., 2003. Differences in Cottonwood Growth between a Losing and a Gaining Reach of an Alluvial Floodplain. *Ecology* 84, 1453–1458.

Hickins, E.J., 1974. The Development of Meanders in Natural River Channels. *Am. J. Sci.* 274, 414–442.

Higa, M., Moriyama, T., Ishikawa, S., 2012. Effects of complete submergence on seedling growth and survival of five riparian tree species in the warm-temperate regions of Japan. *J. For. Res.* 17, 129–136. doi:10.1007/s10310-011-0277-2

Holloway, J. V., Rillig, M.C., Gurnell, A.M., 2017a. Underground riparian wood: Buried stem and coarse root structures of Black Poplar (*Populus nigra* L.). *Geomorphology* 279, 188–198. doi:10.1016/j.geomorph.2016.07.027

Holloway, J. V., Rillig, M.C., Gurnell, A.M., 2017b. Physical Environmental Controls on Riparian Root Profiles associated with Black Poplar (*Populus nigra* L.) along the Tagliamento River, Italy. *Earth Surf. Process. Landforms* 42, 1262–1273. doi:10.1002/esp.4076

Hopkinson, C.S.J., 1992. A Comparison of Ecosystem Dynamics in Freshwater Wetlands. *Estuaries* 15, 549–562.

Horritt, M.S., Bates, P.D., 2002. Evaluation of 1D and 2D numerical models for predicting river flood inundation. *J. Hydrol.* 268, 87–99. doi:10.1016/S0022-1694(02)00121-X

Horton, J.L., Kolb, T.E., Hart, S.C., 2001. Responses of riparian trees to interannual variation in ground water depth in a semi-arid river basin. *Plant. Cell Environ.* 24, 293–304. doi:10.1046/j.1365-3040.2001.00681.x

Horton, J.L., Kolb, T.E., Hart, S.C., 2001. Physiological Response to Groundwater Depth Varies Among Species And With River Flow Regulation. *Ecol. Appl.* 11, 1046–1059. doi:doi: 10.1890/1051-0761(2001)011%5B1046:PRTGDV%5D2.0.CO;2

- Hughes, F.M.R., Johansson, M., Xiong, S., Carlborg, E., Hawkins, D., Svedmark, M., Hayes, A., Goodall, A., Richards, K.S., Nilsson, C., 2009. The influence of hydrological regimes on sex ratios and spatial segregation of the sexes in two dioecious riparian shrub species in northern Sweden. *Plant Ecol.* 208, 77–92. doi:10.1007/s11258-009-9689-x
- Hultine, A.K.R., Bush, S.E., Ehleringer, J.R., Url, S., 2010. Ecophysiology of riparian cottonwood and willow before , during , and after two years of soil water removal. *Ecol. Apl.* 20, 347–361. doi:10.1890/09-0492.1
- Hupp, C.R., 2000. Hydrology , geomorphology and vegetation of Coastal Plain rivers in the south-eastern USA. *Hydrol. Process.* 3010, 2991–3010.
- Hupp, C.R., Osterkamp, W.R., 1996. Riparian vegetation and fluvial geomorphic processes. *Geomorphology.* doi:10.1016/0169-555X(95)00042-4
- I.E.C., 2000. IEC 61131-7 - Fuzzy control programming.
- Ikeda, S., Parker, G., Sawai, K., 1981. Bend theory of river meanders. Part 1. Linear development. *J. Fluid Mech.* 112, 363. doi:10.1017/S0022112081000451
- Imada, S., Yamanaka, N., Tamai, S., 2008. Water table depth affects *Populus alba* fine root growth and whole plant biomass. *Funct. Ecol.* 22, 1018–1026. doi:10.1111/j.1365-2435.2008.01454.x
- Jackson, M.B., Armstrong, W., 1999. Formation of Aerenchyma and the Processes of Plant Ventilation in Relation to Soil Flooding and Submergence. *Plant Biol.* 1, 274–287. doi:10.1111/j.1438-8677.1999.tb00253.x
- Jalonen, J., Järvelä, J., 2014. Estimation of drag forces caused by natural woody vegetation of different scales. *J. Hydrodyn.* 26, 608–623. doi:10.1016/S1001-6058(14)60068-8

- Jalonen, J., Järvelä, J., Aberle, J., 2013. Leaf Area Index as vegetation density measure for hydraulic analyses. *J. Hydraul. Eng.* 139, 461–469. doi:10.1061/(ASCE)HY.1943-7900.0000700
- Jalonen, J., Järvelä, J., Koivusalo, H., Hyyppä, H., 2012. Deriving floodplain topography and vegetation characteristics for hydraulic engineering applications by means of terrestrial laser scanning. *ASCE J. Hydraul. Eng.* 138, 642–652. doi:10.1061/(ASCE)HY.1943-7900
- Jalonen, J., Järvelä, J., Virtanen, J.-P., Vaaja, M., Kurkela, M., Hyyppä, H., 2015. Determining Characteristic Vegetation Areas by Terrestrial Laser Scanning for Floodplain Flow Modeling. *Water* 7, 420–437. doi:10.3390/w7020420
- Jamieson, B., Braatne, J.H., 2001. Riparian Cottonwood Ecosystems and Regulated Flows in Kootenai and Yakima Subbasins Impact of Flow Regulation on Riparian Cottonwood Forests Along the Kootenai River in Idaho, Montana and British Columbia, Contract. Portland, OR 97208. doi:BPA Report DOE/BP-00000005-3
- Järvelä, J., 2006. Vegetative Flow Resistance: Characterization of Woody Plants for Modeling Applications, in: *World Environmental and Water Resource Congress 2006*. pp. 1–10. doi:10.1061/40856(200)418
- Järvelä, J., 2004. Determination of flow resistance caused by non-submerged woody vegetation. *Int. J. River Basin Manag.* 2, 61–70. doi:10.1080/15715124.2004.9635222
- Järvelä, J., 2002a. Determination of flow resistance of vegetated channel banks and floodplains, in: D. Bousmar, D., Zech, Y. (Eds.), *River Flow*. Swets & Zeitlinger, Lisse, pp. 311–318.
- Järvelä, J., 2002b. Flow resistance of flexible and stiff vegetation: a flume study with natural plants. *J. Hydrol.* 269, 44–54.

- Johnson, W.C., 2000. Tree recruitment and survival in rivers : influence of hydrological processes. *Hydrol. Process.* 14, 3051–3074.
- Johnson, W.C., 1997. Equilibrium response of riparian vegetation to flow regulation in the Platte river, Nebraska. *Regul. Rivers Res. Manag.* 13, 403–415. doi:10.1002/(SICI)1099-1646(199709/10)13:5<403::AID-RRR465>3.0.CO;2-U
- Johnson, W.C., 1994. Woodland Expansion in the Platte River, Nebraska: Patterns and Causes. *Ecol. Monogr.* 64, 45–84.
- Johnson, W.C., 1994. Woodland Expansion in the Platte River, Nebraska: Pattern and Causes. *Ecol. Monogr.* 64, 45–84.
- Johnson, W.C., Burgess, R.L., Keammerer, W.R., 1976. Forest Overstory Vegetation and Environment on the Missouri River Floodplain in North Dakota. *Ecol. Mono* 46, 59–84.
- Jonckheere, I., Fleck, S., Nackaerts, K., Muys, B., Coppin, P., Weiss, M., Baret, F., 2004. Review of methods for in situ leaf area index determination Part I. Theories, sensors and hemispherical photography. *Agric. For. Meteorol.* 121, 19–35. doi:10.1016/j.agrformet.2003.08.027
- Jones, C.G., Lawton, J.H., Shachak, M., 1994. Organisms as ecosystem engineers. *Oikos* 69, 373–386.
- Junk, W.J., Bayley, P.B., Sparks, R.E., 1989. The Flood Pulse Concept in River-Floodplain Systems. *Can. Spec. Publ. Fish. Aquat. Sc* 106, 110–127. doi:10.1371/journal.pone.0028909
- Karrenberg, S., Blaser, S., Kollmann, J., Speck, T., Edwards, P.J., 2003. Root anchorage of saplings and cuttings of woody pioneer species in a riparian environment. *Funct. Ecol.* 17, 170–177. doi:10.1046/j.1365-2435.2003.00709.x

- Karrenberg, S., Edwards, P.J., Kollmann, J., 2002. The life history of Salicaceae living in the active zone of floodplains. *Freshw. Biol.* 47, 733–748.
doi:10.1046/j.1365-2427.2002.00894.x
- Karrenberg, S., Suter, M., Kollmann, J., Edwards, P.J., 2003. Phenotypic Trade-Offs in the Sexual Reproduction of Salicaceae From Flood Plains. *Am. J. Bot.* 90, 749–754.
- Kollmann, J., Vieli, M., Edwards, P.J., Tockener, K., Ward, J. V., 1999. Interactions between vegetation development and island formation in the Alpine river Tagliamento. *Appl. Veg. Sci.* 2, 25–36. doi:10.2307/1478878
- Konsoer, K.M., Rhoads, B.L., Langendoen, E.J., Best, J.L., Ursic, M.E., Abad, J.D., Garcia, M.H., 2016. Spatial variability in bank resistance to erosion on a large meandering, mixed bedrock-alluvial river. *Geomorphology* 252, 80–97.
doi:10.1016/j.geomorph.2015.08.002
- Kovalchik, B.L., Clausnitzer, R.R., 2004. Classification and Management of Aquatic , Riparian , and Wetland Sites on the National Forests of Eastern Washington : Series Description. U.S. Departmento of Agriculture, Forest Service, Gen. Tech. Rep. PNW-GTR-593. Portland,Portland, OR (USA).
- Kui, L., Stella, J.C., 2016. Fluvial sediment burial increases mortality of young riparian trees but induces compensatory growth response in survivors. *For. Ecol. Manage.* 366, 32–40. doi:10.1016/j.foreco.2016.02.001
- Kui, L., Stella, J.C., Lightbody, A.F., Wilcox, A.C., 2014. Ecogeomorphic feedbacks and flood loss of riparian tree seedlings in meandering channel experiments. *Water Resour. Res.* 50. doi:10.1002/2012WR013085.Received
- Kuzovkina, Y.A., Knee, M., Quigley, M.F., 2004. Effects of soil compaction and flooding on the growth of 12 willow (*Salix L.*) species. *Eff. soil Compact. flooding growth 12 willow (*Salix L.*) species.*

- Lassette, N.S., Piégay, H., Dufour, S., Rollet, A.-J., 2009. Decadal changes in distribution and frequency of wood in a free meandering river, the Ain River, France. *Earth Surf. Process. Landforms* 33, 1098–1112. doi:10.1002/esp
- Latterell, J.J., Scott Bechtold, J., O'Keefe, T.C., Pelt, R., Naiman, R.J., 2006. Dynamic patch mosaics and channel movement in an unconfined river valley of the Olympic Mountains. *Freshw. Biol.* 51, 523–544. doi:10.1111/j.1365-2427.2006.01513.x
- Levine, C.M., Stromberg, J.C., 2001. Effects of flooding on native and exotic plant seedlings: implications for restoring south-western riparian forests by manipulating water and sediment flows. *J. Arid Environ.* 49, 111–131. doi:10.1006/jare.2001.0837
- Lite, S.J., Stromberg, J.C., 2005. Surface water and ground-water thresholds for maintaining *Populus*–*Salix* forests, San Pedro River, Arizona. *Biol. Conserv.* 125, 153–167. doi:10.1016/j.biocon.2005.01.020
- Little, P.J., Richardson, J.S., Alila, Y., 2013. Channel and landscape dynamics in the alluvial forest mosaic of the Carmanah River valley, British Columbia, Canada. *Geomorphology* 202, 86–100.
- Lovell, J.L., Jupp, D.L.B., Culvenor, D.S., Coops, N.C., 2003. Using airborne and ground-based ranging lidar to measure canopy structure in Australia forests. *Can. J. Remote Sens.* 29, 607–622.
- Lytle, D. a, Poff, N.L., 2004. Adaptation to natural flow regimes. *Trends Ecol. Evol.* 19, 94–100. doi:10.1016/j.tree.2003.10.002
- Mahoney, J.M., Rood, S.B., 1998. Streamflow Requirements for Cottonwood Seedling Recruitment An Integrative Model. *Wetlands* 18, 634–645.
- Malanson, G.P., 1993. *Riparian landscapes*, May 27 199. ed. Cambridge

University Press.

Manners, R., Schmidt, J., Wheaton, J.M., 2013. Multiscalar model for the determination of spatially explicit riparian vegetation roughness. *J. Geophys. Res. Earth Surf.* 118, 65–83. doi:10.1029/2011JF002188

Meier, C.I., Hauer, F.R., 2010. Strong effect of coarse surface layer on moisture within gravel bars: Results from an outdoor experiment. *Water Resour. Res.* 46, W05507. doi:10.1029/2008WR007250

Merritt, D.M., Scott, M.L., LeROY POFF, N., Auble, G.T., Lytle, D.A., Poff, N.L., Auble, G.T., Lytle, D.A., 2010. Theory, methods and tools for determining environmental flows for riparian vegetation: riparian vegetation-flow response guilds. *Freshw. Biol.* 55, 206–225. doi:10.1111/j.1365-2427.2009.02206.x

Merritt, D.M., Wohl, E.E., 2006. Plant dispersal along rivers fragmented by dams. *River Res. Appl.* 22, 1–26. doi:10.1002/rra.890

Mikuś, P., Wyzga, B., Kaczka, R.J., Walusiak, E., Zawiejska, J., 2013. Islands in a European mountain river: Linkages with large wood deposition, flood flows and plant diversity. *Geomorphology* 202, 115–127. doi:10.1016/j.geomorph.2012.09.016

Mitsch, W.J., Zhang, L., Stefanik, K.C., Nahlik, A.M., Anderson, C.J., Bernal, B., Hernandez, M., Song, K., 2012. Creating Wetlands: Primary Succession, Water Quality Changes, and Self-Design over 15 Years. *Bioscience* 62, 237–250. doi:10.1525/bio.2012.62.3.5

Moggridge, H.L., Gurnell, A.M., 2009. Controls on the sexual and asexual regeneration of Salicaceae along a highly dynamic, braided river system. *Aquat. Sci.* 71, 305–317. doi:10.1007/s00027-009-9193-3

Mouw, J.E.B., Stanford, J.A., Alaback, P.B., 2009. Influences of flooding and

- hyporheic exchange on floodplain plant richness and productivity. *River Res. Appl.* 25, 929–945. doi:10.1002/rra.1196
- Murray, A.B., Paola, C., 2003. Modelling the effect of vegetation on channel pattern in bedload rivers. *Earth Surf. Process. Landforms* 28, 131–143. doi:10.1002/esp.428
- Naiman, R.J., Décamps, H., McClain, M.E., 2005. *Riparia*, Gene. Elsevier Academic Press, San Diego, California, USA.
- Nakamura, F., Kikuchi, S., 1996. Some methodological developments in the analysis of sediment transport processes using age distribution of floodplain deposits. *Geomorphology* 16, 139–145.
- Naumburg, E., Mata-Gonzalez, R., Hunter, R.G., McLendon, T., Martin, D.W., 2005. Phreatophytic vegetation and groundwater fluctuations: A review of current research and application of ecosystem response modeling with an emphasis on great basin vegetation. *Environ. Manage.* 35, 726–740. doi:10.1007/s00267-004-0194-7
- Nepf, H.M., 2012. Hydrodynamics of vegetated channels. *J. Hydraul. Res.* 50, 262–279. doi:10.1080/00221686.2012.696559
- Nepf, H.M., Vivoni, E.R., 2000. Flow structure in depth-limited, vegetated flow. *J. Geophys. Res.* 105, 28547–28557. doi:10.1029/2000JC900145
- Nichols, W.F., Killingbeck, K.T., August, P. V., 1998. The influence of geomorphological heterogeneity on biodiversity II. A landscape perspective. *Conserv. Biol.* 12, 371–379. doi:10.1046/j.1523-1739.1998.96238.x
- Nicolle, A., Eames, I., 2011. Numerical study of flow through and around a circular array of cylinders. *J. Fluid Mech.* 679, 1–31. doi:Doi 10.1017/Jfm.2011.77

Nielsen, J.L., Rood, S.B., Pearce, D.W., Letts, M.G., Jiskoot, H., 2010. Streamside trees: Responses of male, female and hybrid cottonwoods to flooding. *Tree Physiol.* 30, 1479–1488. doi:10.1093/treephys/tpq089

Niinemets, Ü., 2010. Responses of forest trees to single and multiple environmental stresses from seedlings to mature plants: Past stress history, stress interactions, tolerance and acclimation. *For. Ecol. Manage.* 260, 1623–1639. doi:10.1016/j.foreco.2010.07.054

Pasquale, N., Perona, P., 2014. Experimental assessment of riverbed sediment reinforcement by vegetation roots, in: Schleiss, A., Decesare, G., Franca, M., Pfister, M. (Eds.), *River Flow 2014*. Press-Taylor & Francis Group, Lausanne, pp. 553–561.

Pasquale, N., Perona, P., Francis, R., Burlando, P., 2014. Above-ground and below-ground *Salix* dynamics in response to river processes. *Hydrol. Process.* 28, 5189–5203. doi:10.1002/hyp.9993

Pasquale, N., Perona, P., Francis, R., Burlando, P., 2012. Effects of streamflow variability on the vertical root density distribution of willow cutting experiments. *Ecol. Eng.* 40, 167–172. doi:10.1016/j.ecoleng.2011.12.002

Pasquale, N., Perona, P., Schneider, P., Shrestha, J., Wombacher, A., Burlando, P., 2011. Modern comprehensive approach to monitor the morphodynamic evolution of a restored river corridor. *Hydrol. Earth Syst. Sci.* 15, 1197–1212. doi:10.5194/hess-15-1197-2011

Pearlistine, L., McKellar, H., Kitchens, W., 1985. Modelling the impacts of a river diversion on bottomland forest communities in the Santee River floodplain, South Carolina. *Ecol. Modell.* 29, 283–302. doi:10.1016/0304-3800(85)90057-2

Perucca, E., Camporeale, C., Ridolfi, L., 2007. Significance of the riparian vegetation dynamics on meandering river morphodynamics. *Water Resour.*

Res. 43, 1–10. doi:10.1029/2006WR005234

Pickett, S.T.A., White, P.S., 1985. Patch dynamics: A synthesis, in: Pickett, S.T.A., White, P.S. (Eds.), *The Ecology of Natural Disturbance and Patch Dynamics*. Academic Press, pp. 371–384.

Piegay, H., 1993. Nature, mass and preferential sites of coarse woody debris deposits in the lower ain valley (Mollon reach), France. *Regul. Rivers Res. Manag.* 8, 359–372. doi:10.1002/rrr.3450080406

Piégay, H., Gurnell, A.M., 1997. Large woody debris and river geomorphological pattern: examples from S . E . France and S . England. *Geomorphology* 19, 99–116. doi:http://dx.doi.org/10.1016/S0169-555X(96)00045-1

Poff, N.L., Allan, J.D., Bain, M.B., Karr, J.R., Prestegard, K.L., Richter, B.D., Sparks, R.E., Stromberg, J.C., 1997. *The Natural Flow Regime*. *Bioscience* 47, 769–784.

Politti, E., Bertoldi, W., Gurnell, A.M., Henshaw, A., 2017. Feedbacks between the riparian Salicaceae and hydrogeomorphic processes: A quantitative review. *Earth-Science Rev.* in press. doi:10.1016/j.earscirev.2017.07.018

Politti, E., Egger, G., Angermann, K., Rivaes, R., Blamauer, B., Klösch, M., Tritthart, M., Habersack, H., 2014. Evaluating climate change impacts on Alpine floodplain vegetation. *Hydrobiologia* 737, 225–243. doi:10.1007/s10750-013-1801-5

Pollen-Bankhead, N., Simon, A., 2010. Hydrologic and hydraulic effects of riparian root networks on streambank stability: Is mechanical root-reinforcement the whole story? *Geomorphology* 116, 353–362. doi:10.1016/j.geomorph.2009.11.013

Pollen-Bankhead, N., Simon, A., 2009. Enhanced application of root-reinforcement

algorithms for bank-stability modeling. *Earth Surf. Landforms* 34, 471–480.
doi:10.1002/esp

Pollen, N., 2007. Temporal and spatial variability in root reinforcement of streambanks: Accounting for soil shear strength and moisture. *Catena* 69, 197–205. doi:10.1016/j.catena.2006.05.004

Pollen, N., Simon, A., 2005. Estimating the mechanical effects of riparian vegetation on stream bank stability using a fiber bundle model. *Water Resour. Res.* 41, 1–11. doi:10.1029/2004WR003801

Polvi, L.E., Wohl, E., Merritt, D.M., 2014. Modeling the functional influence of vegetation type on streambank cohesion. *Earth Surf. Process. Landforms* 39, 1245–1258. doi:10.1002/esp.3577

Polzin, M.L., Rood, S.B., 2006. Effective Disturbance : Seedling Safe Sites And Patch Recruitment Of Riparian Cottonwoods After A Major Flood Of A Mountain River. *Wetlands* 26, 965–980.

Prosser, I.P., Dietrich, W.E., Stevenson, J., 1995. Flow resistance and sediment transport by concentrated overland flow in a grassland valley. *Geomorphology* 13, 71–86. doi:10.1016/0169-555X(95)00020-6

Radtke, A., Mosner, E., Leyer, I., 2012. Vegetative reproduction capacities of floodplain willows--cutting response to competition and biomass loss. *Plant Biol. (Stuttg)*. 14, 257–64. doi:10.1111/j.1438-8677.2011.00509.x

Reubens, B., Poesen, J., Danjon, F., Geudens, G., Muys, B., 2007. The role of fine and coarse roots in shallow slope stability and soil erosion control with a focus on root system architecture: A review. *Trees - Struct. Funct.* 21, 385–402. doi:10.1007/s00468-007-0132-4

Richards, K., Brasington, J., Hughes, F., 2002. Geomorphic dynamics of

floodplains: ecological implications and a potential modelling strategy. *Freshw. Biol.* 47, 559–579. doi:10.1046/j.1365-2427.2002.00920.x

Righetti, M., 2008. Flow analysis in a channel with flexible vegetation using double-averaging method. *Acta Geophys.* 56, 801–823. doi:10.2478/s11600-008-0032-z

Roberts, D.W., 1996. Modelling forest dynamics with vital attributes and fuzzy systems theory. *Ecol. Modell.* 90, 161–173. doi:10.1016/0304-3800(95)00163-8

Rogers, K., Biggs, H., 1999. Integrating indicators , endpoints and value systems in strategic management of the rivers of the Kruger National Park. *Freshw. Biol.* 41, 439–451.

Rominger, J.T., Lightbody, A.F., Nepf, H.M., 2010. Effects of Added Vegetation on Sand Bar Stability and Stream Hydrodynamics. *J. Hydraul. Eng.* 136, 994–1002. doi:10.1061/ASCEHY.1943-7900.0000215

Rood, S.B., Bigelow, S.G., Hall, A.A., 2011. Root architecture of riparian trees: River cut-banks provide natural hydraulic excavation, revealing that cottonwoods are facultative phreatophytes. *Trees - Struct. Funct.* 25, 907–917. doi:10.1007/s00468-011-0565-7

Rood, S.B., Bigelow, S.G., Polzin, M.L., Gill, K.M., Coburn, C.A., 2015. Biological bank protection: trees are more effective than grasses at resisting erosion from major river floods. *Ecohydrology* 8, 772–779. doi:10.1002/eco.1544

Rood, S.B., Patino, S., Coombs, K., Tyree, M.T., 2000. Branch sacrifice: cavitation-associated drought adaptation of riparian cottonwoods. *Trees* 14, 248–257. doi:10.1007/s004680050010

Rood, S.B., Samuelson, G.M., Braatne, J.H., Gourley, C.R., Hughes, F.M.R.,

- Mahoney, J.M., 2005. Managing river flows to restore floodplain forests. *Front. Ecol. Environ.* 3, 193–201. doi:10.1890/1540-9295(2005)003[0193:MRFTRF]2.0.CO;2
- Ruiz-Villanueva, V., Wyzga, B., Hajdukiewicz, H., Stoffel, M., 2016. Exploring large wood retention and deposition in contrasting river morphologies linking numerical modelling and field observations. *Earth Surf. Process. Landforms* 41, 446–459. doi:10.1002/esp.3832
- Rykiel, E.J., 1996. Testing ecological models : the meaning of validation. *Ecol. Modell.* 90, 229–244.
- Salski, A., 1992. Fuzzy knowledge-based models in ecological research. *Ecol. Modell.* 63, 103–112. doi:10.1016/0304-3800(92)90064-L
- Schiechtl, H.M., 1992. *Weiden in der Praxis: Die Weiden Mitteleuropas, ihre Verwendung und Bestimmung.* Patzer, Berlin.
- Schnauder, I., Moggridge, H.L., 2009. Vegetation and hydraulic-morphological interactions at the individual plant, patch and channel scale. *Aquat. Sci.* 71, 318–330. doi:10.1007/s00027-009-9202-6
- Scott, M.L., Auble, G.T., Friedman, J.M., 1997. Flood Dependency of Cottonwood Establishment Along the Missouri River, Montana, Usa. *Ecol. Appl.* 7, 677–690. doi:10.1890/1051-0761(1997)007[0677:FDOCEA]2.0.CO;2
- Scott, M.L., Lines, G.C., Auble, G.T., 2000. Channel incision and patterns of cottonwood stress and mortality along the Mojave River, California. *J. Arid Environ.* 44, 399–414. doi:10.1006/jare.1999.0614
- Scott, M.L., Shafroth, P.B., Auble, G.T., 1999. Responses of riparian cottonwoods to alluvial water table declines. *Environ. Manage.* 23, 347–358. doi:10.1007/s002679900191

- Segelquist, C. a, Scott, M.L., Auble, G.T., 1993. Establishment of *Populus deltoides* under simulated alluvial groundwater declines. *Am. Midl. Nat.* 130, 274–285. doi:10.2307/2426127
- Shafroth, P.B., Auble, G.T., Stromberg, J.C., Patten, D.T., 1998. Establishment of woody riparian vegetation in relation to annual patterns of streamflow, Bill Williams River, Arizona. *Wetlands* 18, 577–590.
- Shafroth, P.B., Stromberg, J.C., Patten, D.T., 2000. Woody Riparian Vegetation Response to Different Alluvial Water Table Regimes. *West. North Am. Nat.* 60, 66–76.
- Shugart, H., West, D., 1977. Development of an Appalachian deciduous forest succession model and its application to assessment of the impact of the chestnut blight. *J. Environ. Manage.*
- Sigafoos, R.S., 1964. *Botanical Evidence of Floods and Flood-Plain Deposition.* Washington D.C.
- Simon, A., Collison, A.J.C., 2002. Quantifying the mechanical and hydrologic effects of riparian vegetation on streambank stability. *Earth Surf. Process. Landforms* 27, 527–546. doi:10.1002/esp.325
- Simon, A., Pollen, N., Langendoen, E., 2006. Influence of two woody riparian species on critical conditions for streambank stability: upper Truckee river, California. *J. Am. Water Resour. Assoc.* 42, 99–113. doi:10.1111/j.1752-1688.2006.tb03826.x
- Snyder, K.A., Williams, D.G., 2000. Water sources used by riparian trees varies among stream types on the San Pedro River, Arizona. *Agric. For. Meteorol.* 105, 227–240. doi:10.1016/S0168-1923(00)00193-3
- Solari, L., Van Oorschot, M., Belletti, B., Hendriks, D., Rinaldi, M., Vargas-Luna, A.,

2015. Advances on Modelling Riparian Vegetation-Hydromorphology Interactions. *River Res. Appl.* in press. doi:10.1002/rra.2910

Stanford, J.A., Lorang, M.S., Hauer, F.R., 2005. The shifting mosaic of river ecosystems. *Int. Vereinigung fur Theor. und Angew. Limnol. Verhandlungen* 29, 123–136.

Steiger, J., Tabacchi, E., Dufour, S., Corenblit, D., Peiry, J.-L., 2005. Hydrogeomorphic processes affecting riparian habitat within alluvial channel-floodplain river systems: a review for the temperate zone. *River Res. Appl.* 21, 719–737. doi:10.1002/rra.879

Stella, J.C., Battles, J., McBride, J., 2006a. Restoring recruitment processes for riparian cottonwoods and willows: a field-calibrated predictive model for the lower San Joaquin Basin, University of California, Berkeley. Sacramento, California.

Stella, J.C., Battles, J.J., 2010. How do riparian woody seedlings survive seasonal drought? *Oecologia* 164, 579–90. doi:10.1007/s00442-010-1657-6

Stella, J.C., Battles, J.J., McBride, J.R., Orr, B.K., 2010. Riparian Seedling Mortality from Simulated Water Table Recession, and the Design of Sustainable Flow Regimes on Regulated Rivers. *Restor. Ecol.* 18, 284–294. doi:10.1111/j.1526-100X.2010.00651.x

Stella, J.C., Battles, J.J., Orr, B.K., McBride, J.R., 2006b. Synchrony of Seed Dispersal, Hydrology and Local Climate in a Semi-arid River Reach in California. *Ecosystems* 9, 1200–1214. doi:10.1007/s10021-005-0138-y

Stromberg, J. C., Richter, B.D., Patten, D.T., Wolden, L.G., 1993. Response of a sonoran riparian forest to a 10-year return flood. *West. North Am. Nat.* 53, 118–130.

Stromberg, J.C., Patten, D.T., 1996. Instream flow and cottonwood growth in the eastern Sierra Nevada of California, USA. *Regul. Rivers Res. Manag.* 12, 1–12. doi:10.1002/(Sici)1099-1646(199601)12:1<1::Aid-Rrr347>3.0.Co;2-D

Stromberg, J.C., Patten, D.T., Richter, B.D., 1991. Flood flows and dynamics of Sonoran riparian forests. *Rivers*.

Stromberg, J.C., Tiller, R., Richter, B., 1996. Effects of groundwater decline on riparian vegetation of semiarid regions: the San Pedro, Arizona. *Ecol. Appl.* 6, 113–131. doi:10.2307/2269558

Surian, N., Barban, M., Ziliani, L., Monegato, G., Bertoldi, W., Comiti, F., 2015. Vegetation turnover in a braided river: Frequency and effectiveness of floods of different magnitude. *Earth Surf. Process. Landforms* 40, 542–558. doi:10.1002/esp.3660

Swiss Federal Institute for Forest, S. and L.R.W., n.d. Hemisphere.

Tal, M., Paola, C., 2010. Effects of vegetation on channel morphodynamics : results and insights from laboratory experiments 1028, 1014–1028. doi:10.1002/esp.1908

Tal, M., Paola, C., 2007. Dynamic single-thread channels maintained by the interaction of flow and vegetation. *Geology* 35, 347–350. doi:10.1130/G23260A.1

Tanaka, N., Sasaki, Y., Mowjood, M.I.M., Jinadasa, K.B.S.N., Homchuen, S., 2007. Coastal vegetation structures and their functions in tsunami protection: Experience of the recent Indian Ocean tsunami. *Landsc. Ecol. Eng.* 3, 33–45. doi:10.1007/s11355-006-0013-9

Tanaka, N., Yagisawa, J., 2009. Effects of tree characteristics and substrate

condition on critical breaking moment of trees due to heavy flooding. *Landsc. Ecol. Eng.* 5, 59–70. doi:10.1007/s11355-008-0060-5

Thimonier, A., Sedivy, I., Schleppi, P., 2010. Estimating leaf area index in different types of mature forest stands in Switzerland : a comparison of methods. *Eur J For. Res* 129, 543–562. doi:10.1007/s10342-009-0353-8

Thomas, L.K., Tölle, L., Ziegenhagen, B., Leyer, I., 2012. Are vegetative reproduction capacities the cause of widespread invasion of Eurasian Salicaceae in Patagonian river landscapes? *PLoS One* 7, e50652. doi:10.1371/journal.pone.0050652

Tockner, K., Malard, F., Ward, J. V., 2000. An extension of the flood pulse concept. *Hydrol. Process.* 14, 2861–2883.

Tockner, K., Paetzold, A., Karaus, U.T.E., Claret, C., 2006. Ecology of braided rivers, in: Sambrook Smith, G.H., Best, J.L., Bristow, C.S., Petts, G.E. (Eds.), *Braided Rivers*. Blackwell Publishing L.t.d., pp. 339–359.

Tockner, K., Pusch, M., Borchardt, D., Lorang, M.S., 2010. Multiple stressors in coupled river-floodplain ecosystems. *Freshw. Biol.* 55, 135–151. doi:10.1111/j.1365-2427.2009.02371.x

Tockner, K., Ward, J. V., Arscott, D.B., Edwards, P.J., Kollmann, J., Gurnell, A.M., Petts, G.E., Maiolini, B., 2003. The Tagliamento River: A model ecosystem of European importance. *Aquat. Sci.* 65, 239–253. doi:10.1007/s00027-003-0699-9

Tron, S., Perona, P., Gorla, L., Schwarz, M., Laio, F., Ridolfi, L., 2015. The signature of randomness in riparian plant root distributions. *Geophys. Res. Lett.* 42, 7098–7106. doi:10.1002/2015GL064857

Tsujiimoto, T., 1999. Fluvial processes in streams with vegetation. *J. Hydraul. Res.*

37, 789–803.

- Tyree, M.T., Kolb, K.J., Rood, S.B., Patino, S., 1994. Vulnerability to drought-induced cavitation of riparian cottonwoods in Alberta: a possible factor in the decline of the ecosystem? *Tree Physiol.* 14, 455–466.
- Unger, J., Hager, W.H., 2007. Down-flow and horseshoe vortex characteristics of sediment embedded bridge piers. *Exp. Fluids* 42, 1–19. doi:DOI 10.1007/s00348-006-0209-7
- Van De Wiel, M.J., Coulthard, T.J., Macklin, M.G., Lewin, J., 2007. Embedding reach-scale fluvial dynamics within the CAESAR cellular automaton landscape evolution model. *Geomorphology* 90, 283–301. doi:10.1016/j.geomorph.2006.10.024
- van Oorschot, M., Kleinhans, M., Geerling, G., Middelkoop, H., 2016. Distinct patterns of interaction between vegetation and morphodynamics. *Earth Surf. Process. Landforms* 41, n/a-n/a. doi:10.1002/esp.3864
- Van Splunder, I., Voesenek, L.A.C.J., Coops, H., De Vries, X.J.A., Blom, C.W.P.M., 1996. Morphological responses of seedlings of four species of Salicaceae to drought. *Can. J. Bot.* 74, 1988–1995. doi:10.1139/b96-238
- Vandersande, M.W., Glenn, E.P., Walworth, J.L., 2001. Tolerance of five riparian plants from the lower Colorado River to salinity drought and inundation. *J. Arid Environ.* 49, 147–159. doi:10.1006/jare.2001.0839
- Vargas-Luna, A., Crosato, A., Uijttewaal, W.S.J., 2015. Effects of vegetation on flow and sediment transport: Comparative analyses and validation of predicting models. *Earth Surf. Process. Landforms* 40, 157–176. doi:10.1002/esp.3633
- Västilä, K., Järvelä, J., 2017. Characterizing natural riparian plant stands for

modeling of flow and suspended sediment transport. *J. Soil Sediments* 943–952. doi:10.1007/s11368-017-1776-3

Västilä, K., Järvelä, J., 2014. Modeling the flow resistance of woody vegetation using physically based properties of the foliage and stem. *Water Resour. Res.* 50, 229–245. doi:10.1002/2013WR013819

Västilä, K., Järvelä, J., Aberle, J., 2013. Characteristic reference areas for estimating flow resistance of natural foliated vegetation. *J. Hydrol.* 492, 49–60. doi:10.1016/j.jhydrol.2013.04.015

Ward, J. V., Malard, F., Tockner, K., 2002. Landscape ecology : a framework for integrating pattern and process in river corridors. *Landsc. Ecol.* 17, 35–45.

Ward, J. V, Tockner, K., Uehlinger, U., Malard, F., 2001. Understanding Natural Patterns and Processes in River Corridors as the Basis for Effective River Restoration. *Regul. Rivers Res. Manag.* 17, 311–323. doi:10.1002/rrr.679

Warmink, J., 2007. Vegetation Density Measurements using Parallel Photography and Terrestrial Laser Scanning. Utrecht University.

Weissteiner, C., Jalonen, J., Järvelä, J., Rauch, H.P., 2015. Spatial-structural properties of woody riparian vegetation with a view to reconfiguration under hydrodynamic loading. *Ecol. Eng.* 85, 85–94. doi:10.1016/j.ecoleng.2015.09.053

Whited, D.C., Lorang, M.S., Harner, M.J., Hauer, F.R., Kimball, J.S., Stanford, J.A., 2007. Climate, hydrologic disturbance, and succession: drivers of floodplain pattern. *Ecology* 88, 940–53.

Whittaker, P., Wilson, C. a. M.E., Aberle, J., 2015. An improved Cauchy number approach for predicting the drag and reconfiguration of flexible vegetation. *Adv. Water Resour.* 83, 28–35. doi:10.1016/j.advwatres.2015.05.005

- Wiel, M.J. Van De, Darby, S.E., 2007. A new model to analyse the impact of woody riparian vegetation on the geotechnical stability of riverbanks. *Earth Surf. Process. Landforms* 32, 2185–2198. doi:10.1002/esp.1522
- Wiens, J. a., 2002. Riverine landscapes: taking landscape ecology into the water. *Freshw. Biol.* 47, 501–515. doi:10.1046/j.1365-2427.2002.00887.x
- Wilcock, P.R., Crowe, J.C., 2003. Surface-based Transport Model for Mixed-Size Sediment. *J. Hydraul. Eng.* 129, 120–128. doi:10.1061/(ASCE)0733-9429(2003)129:2(120)
- Wilcox, A.C., Shafroth, P.B., 2013. Coupled hydrogeomorphic and woody-seedling responses to controlled flood releases in a dryland river. *Water Resour. Res.* 49, 2843–2860. doi:10.1002/wrcr.20256
- Willms, J., Rood, S.B., Willms, W., Tyree, M., 1998. Branch growth of riparian cottonwoods: A hydrologically sensitive dendrochronological tool. *Trees* 12, 215–223. doi:10.1007/s004680050143
- Wintenberger, C.L., Rodrigues, S., Bréhéret, J.-G., Villar, M., 2015. Fluvial islands: First stage of development from nonmigrating (forced) bars and woody-vegetation interactions. *Geomorphology* 246, 305–320. doi:10.1016/j.geomorph.2015.06.026
- Wu, F.-C., Shen, H.W., Chou, Y.-J., 1999. Variation Of Roughness Coefficients For Unsubmerged And Submerged Vegetation. *J. Hydraul. Eng.* 125, 934–942.
- Wunder, S., Lehmann, B., Nestmann, F., 2011. Determination of the drag coefficients of emergent and just submerged willows. *Int. J. River Basin Manag.* 9, 231–236. doi:10.1080/15715124.2011.637499
- Yagisawa, J., Tanaka, N., n.d. Washout conditions of plants growing on islands by floods.

You, X., Liu, J., Zhang, L., 2015. Ecological modeling of riparian vegetation under disturbances: A review. *Ecol. Modell.* 318, 293–300.
doi:10.1016/j.ecolmodel.2015.07.002

Zanoni, L., Gurnell, A., Drake, N., Surian, N., 2008. Island Dynamics in a Braided River From Analysis of Historical Maps and Air Photographs. *River Res. Appl.* 24, 1141–1159. doi:10.1002/rra

Zhang, Y., Chen, J.M., Miller, J.R., 2005. Determining digital hemispherical photograph exposure for leaf area index estimation. *Agric. For. Meteorol.* 133, 166–181. doi:10.1016/j.agrformet.2005.09.009

Ziliani, L., 2011. Ricostruzione e previsione dell'evoluzione morfologica Di un alveo a fondo ghiaioso (f. Tagliamento): Integrazione di modellazione numerica, analisi gis e Rilievi di terreno. University of Padua.

Ziliani, L., Surian, N., Coulthard, T.J., Tarantola, S., 2013. Reduced-complexity modeling of braided rivers: Assessing model performance by sensitivity analysis, calibration, and validation. *J. Geophys. Res. Earth Surf.* 118, 2243–2262. doi:10.1002/jgrf.20154

Zong, L., Nepf, H., 2010. Flow and deposition in and around a finite patch of vegetation. *Geomorphology* 116, 363–372.
doi:10.1016/j.geomorph.2009.11.020